

2010-05-21

Modeling the Transmission Dynamics of the Dengue Virus

Patricia Katri

University of Miami, patriciakatri@yahoo.com

Follow this and additional works at: https://scholarlyrepository.miami.edu/oa_dissertations

Recommended Citation

Katri, Patricia, "Modeling the Transmission Dynamics of the Dengue Virus" (2010). *Open Access Dissertations*. 417.
https://scholarlyrepository.miami.edu/oa_dissertations/417

This Open access is brought to you for free and open access by the Electronic Theses and Dissertations at Scholarly Repository. It has been accepted for inclusion in Open Access Dissertations by an authorized administrator of Scholarly Repository. For more information, please contact repository.library@miami.edu.

UNIVERSITY OF MIAMI

MODELING THE TRANSMISSION DYNAMICS
OF THE DENGUE VIRUS

By

Patricia Katri

A DISSERTATION

Submitted to the Faculty
of the University of Miami
in partial fulfillment of the requirements for
the degree of Doctor of Philosophy

Coral Gables, Florida

June 2010

©2010
Patricia Katri
All Rights Reserved

UNIVERSITY OF MIAMI

A dissertation submitted in partial fulfillment of
the requirements for the degree of
Doctor of Philosophy

MODELING THE TRANSMISSION DYNAMICS
OF THE DENGUE VIRUS

Patricia Katri

Approved:

Shigui Ruan, Ph.D.
Professor of Mathematics

Terri A. Scandura, Ph.D.
Dean of the Graduate School

Robert Stephen Cantrell, Ph.D.
Professor of Mathematics

Chris Cosner, Ph.D.
Professor of Mathematics

John Beier, Sc.D.
Professor of Epidemiology and Public Health

KATRI, PATRICIA
Modeling the Transmission
Dynamics of the Dengue Virus

(Ph.D., Mathematics)
(June 2010)

Abstract of a dissertation at the University of Miami.

Dissertation supervised by Professor Shigui Ruan.
No. of pages in text. (169)

Dengue (pronounced den'guee) **Fever** (DF) and **Dengue Hemorrhagic Fever** (DHF), collectively known as “dengue,” are mosquito-borne, potentially mortal, flu-like viral diseases that affect humans worldwide ([51], [4], [1]). Transmitted to humans by the bite of an infected mosquito, dengue is caused by any one of four serotypes, or antigen-specific viruses. In this thesis, both the spatial and temporal dynamics of dengue transmission are investigated. Different chapters present new models while building on themes of previous chapters. In Chapter 2, we explore the temporal dynamics of dengue viral transmission by presenting and analyzing an ODE model that combines an SIR human host- with a multi-stage SI mosquito vector transmission system. In the case where the juvenile populations are at carrying capacity, juvenile mosquito mortality rates are sufficiently small to be absorbed by juvenile maturation rates, and no humans die from dengue, both the analysis and numerical simulations demonstrate that an epidemic will persist if the oviposition rate is greater than the adult mosquito death rate. In Chapter 3, we present and analyze a non-autonomous, non-linear ODE system that incorporates seasonality into the modeling of the transmission of the dengue virus. We derive conditions for the existence of a threshold parameter, the basic reproductive ratio, \mathcal{R}_0 , denoting the expected number of secondary cases produced by a typically infective individual. In Chapter 4, we present

and analyze a non-linear system of coupled reaction-diffusion equations modeling the virus' spatial spread. In formulating our model, we seek to establish the existence of traveling wave solutions and calculate spread rates for the spatial dissemination of the disease. We determine that the epidemic wave speed increases as average annual, and in our case, winter, temperatures increase. In Chapter 5, we present and analyze an ODE model that incorporates two serotypes of the dengue virus and allows for the possibility of both primary and secondary infections with each serotype. We obtain an analytical expression for the basic reproductive number, \mathcal{R}_0 , that defines it as the maximum of the reproduction numbers for each strain/serotype of the virus. In each chapter, numerical simulations are conducted to support the analytical conclusions.

Acknowledgements

I would first like to thank Dr. Shigui Ruan, my advisor, for introducing me to mathematical biology, for suggesting and overseeing this project, and for his general enthusiasm, encouragement, and expertise throughout the years. I would also like to thank Drs. Cosner, Cantrell, and Beier for serving on my dissertation committee, and thank all four members for their invaluable input. In addition, I would like to thank Dr. Cosner for many productive conversations about the project and the mathematical profession; and Dr. Cantrell for an excellent course in functional analysis, after which, after many years, I began to grasp more serious math. I would like to thank Toni Taylor, Julieta Garcia, Sylvia Bacallao, and especially, Dania Puerto, for their great patience and emotional support throughout my years as a student. Additionally, I thank the math department in general, and specifically, Drs. Zame, Mielke, Pestien, the late Dr. Kelley, Shareshian, Galloway, Wachs, Koçak, Oropesa, Kaliman, and especially, Ramakrishnan and Jennifer Morse for their kindness and advice. I thank David Harden for being a great friend, and for teaching me a lot of math. I also thank Julian Moorehead, Tassos and Sophia Constantinou, Matthew Hyatt, Doug Scheib, Dahlia Zohar, and Richard Colea.

Finally, and most importantly, I would like to thank my family, Joseph, Judith, and Karen Katri (and Hillary, the late Eddie, and Sandy), and Yolanda Rojas-Bravo, without whom I could not have achieved anything in general. Words cannot express my love and gratitude. I dedicate this work to them.

Contents

LIST OF FIGURES	vi
LIST OF TABLES	viii
1 INTRODUCTION	1
1.1 Basic Facts about Dengue	1
1.2 History of the Dengue Epidemic	4
1.3 Review of the Epidemiological and Scientific Literature	6
1.4 Outline of the Thesis	8
2 THE MAIN ODE MODEL AND ANALYSIS OF THE ASEA- SONAL MODEL	9
2.1 Introduction and Assumptions	9
2.2 The Main ODE Model	13
2.3 Analysis of the Aseasonal Model	16
2.3.1 \mathcal{R}_0 for an Autonomous ODE System	21
2.3.2 Compartmentalized Modeling and Threshold Analysis	22
2.3.3 Analysis of the Endemic Equilibria	33
2.4 Numerical Simulations	37
2.5 Discussion	39
3 THE SEASONAL ODE MODEL	46
3.1 Introduction and Assumptions	46
3.2 The Seasonal ODE Model	49
3.3 Analysis of the Seasonal Model	52
3.3.1 The Basic Reproductive Ratio for a Non-Autonomous ODE System	56
3.3.2 The Compartmentalized Seasonal Model and Analysis of Threshold Parameters	57
3.4 Numerical Simulations	75
3.5 Discussion	78

4	TRAVELING WAVES AND SPREAD RATES FOR THE PDE MODEL	87
4.1	Introduction and Assumptions	87
4.2	The New ODE Model	91
4.2.1	Analysis of System (4.2.5)	94
4.3	Spread Rates and Traveling Waves	96
4.4	Spatially-Dependent Model	98
4.5	Traveling Wave Solutions	99
4.6	Spread-Rate Analysis	103
4.7	Case: Advection $\bar{v} \neq 0$	108
4.8	Numerical Simulations	110
4.9	Discussion	115
5	A MULTI-SEROTYPE ODE MODEL FOR DENGUE VIRAL TRANSMISSION	118
5.1	Introductory Remarks	118
5.2	Presentation of the Model and Assumptions	120
5.3	Analysis of Model (5.2.1)	124
5.4	An Alternative Interpretation of Model (5.3.2)	142
5.5	Numerical Simulations	149
5.6	Discussion	152
	APPENDIX I	164
	BIBLIOGRAPHY	166

List of Figures

2.1	Compartmentalized model for dengue.	17
2.2	Solutions of system (2.3.7), $gr_m < u_m, \mathcal{R}_0 > 1, \alpha_H, u_q, u_e = 0$	27
2.3	Solutions of system (2.3.7), $gr_m < u_m, \mathcal{R}_0 < 1$	29
2.4	Solutions of system (2.3.7), $gr_m < u_m, \mathcal{R}_0 > 1$	33
2.5	Solutions of system (2.3.7), $gr_m > u_m, a_H, u_q, u_e = 0$	41
2.6	Solutions of system (2.3.7), $gr_m < u_m, \mathcal{R}_0 < 1, a_H, u_q, u_e = 0$	42
2.7	Solutions of system (2.3.7), $gr_m < u_m, \mathcal{R}_0 > 1, \alpha_H, u_q, u_e = 0$	43
2.8	Solutions of system (2.3.7), $gr_m < u_m, \mathcal{R}_0 < 1$	44
2.9	Solutions of system (2.3.7), $gr_m < u_m, \mathcal{R}_0 > 1$	45
3.1	Climatic index as function of time, $c = .5, d = 1.5, \sigma = 90, w = 1/365$	51
3.2	\mathcal{R}_0 and $\mathcal{R}_{0_{max}}$ when λ_H varies.	60
3.3	Solutions of system (3.3.6), $d < c, \mathcal{R}_0 > 1, \sigma = 0$	63
3.4	Solutions of system (3.3.6), $d < c, \mathcal{R}_0 < 1, \sigma = 0$	64
3.5	Solutions of system (3.3.6), $d > c, \mathcal{R}_0 > 1, \sigma = 0$	66
3.6	Solutions of system (3.3.6), $d > c, \mathcal{R}_0 < 1, \sigma = 0$	68
3.7	Solutions of system (3.3.6), $d > c, \mathcal{R}_0 > 1, \sigma = -90$	71
3.8	Solutions of system (3.3.6), $d > c, \mathcal{R}_0 < 1, \sigma = -90$	78
3.9	\mathcal{R}_0 and $\mathcal{R}_{0_{max}}$ when λ_H varies.	80
3.10	Solutions of system (3.3.6), $d < c, \mathcal{R}_0 > 1, \sigma = 0$	81
3.11	Solutions of system (3.3.6), $d < c, \mathcal{R}_0 < 1, \sigma = 0$	82
3.12	Solutions of system (3.3.6), $d > c, \mathcal{R}_0 > 1, \sigma = 0$	83
3.13	Solutions of system (3.3.6), $d > c, \mathcal{R}_0 < 1, \sigma = 0$	84
3.14	Solutions of system (3.3.6), $d > c, \mathcal{R}_0 > 1, \sigma = -90$	85
3.15	Solutions of system (3.3.6), $d > c, \mathcal{R}_0 < 1, \sigma = -90$	86
4.1	Phase portrait for I_M, I_H	95
4.2	Traveling waves for system (4.5.2), $\gamma = 1$	100
4.3	Traveling waves for system (4.5.2), $\gamma = 1$	101
4.4	Traveling waves for system (4.5.2), $\gamma = .5$	102
4.5	Traveling waves for system (4.5.2), $\gamma = .5$	103
4.6	Traveling waves for system (4.5.2), $\gamma = 2$	105

4.7	Traveling waves for system (4.5.2), $\gamma = 2$	107
4.8	Spread rate for the system (4.5.2) when $\epsilon = 0, \gamma = 1$	112
4.9	Spread rate for the system (4.5.2) when $\epsilon = 0, \gamma = .5$	113
4.10	Spread rate for the system (4.5.2) when $\epsilon = 0, \gamma = 2$	114
5.1	Solutions of system (5.3.2) when $\mathcal{R}_0 < 1$	128
5.2	Solutions of system (5.3.2) when $\mathcal{R}_0 < 1$	130
5.3	Solutions of system (5.3.2) when $\mathcal{R}_1 > 1, \mathcal{R}_2 < 1$	132
5.4	Solutions of system (5.3.2) when $\mathcal{R}_1 > 1, \mathcal{R}_2 < 1$	137
5.5	Solutions of system (5.3.2) when $\mathcal{R}_1 > 1, \mathcal{R}_2 > 1$	138
5.6	Solutions of system (5.3.2) when $\mathcal{R}_1 > 1, \mathcal{R}_2 > 1, \beta_1 = \beta_2 = .5$	142
5.7	Solutions of system (5.3.2) when $\mathcal{R}_1 > 1, \mathcal{R}_2 > 1, \beta_1 = \beta_2 = 5$	150
5.8	Solutions of system (5.3.2) when $\mathcal{R}_1 > 1, \mathcal{R}_2 > 1, \beta_1 = 5, \beta_2 = .5$. .	151
5.9	Solutions of system (5.3.2) when $\mathcal{R}_1 > 1, \mathcal{R}_2 > 1, \beta_1 = 5, \beta_2 = .5$. .	153
5.10	Solutions of system (5.3.2) when $\mathcal{R}_0 < 1$	156
5.11	Solutions of system (5.3.2) when $\mathcal{R}_0 < 1$	157
5.12	Solutions of system (5.3.2) when $\mathcal{R}_1 > 1, \mathcal{R}_2 < 1$	158
5.13	Solutions of system (5.3.2) when $\mathcal{R}_1 > 1, \mathcal{R}_2 < 1$	159
5.14	Solutions of system (5.3.2) when $\mathcal{R}_1 > 1, \mathcal{R}_2 > 1$	160
5.15	Solutions of system (5.3.2) when $\mathcal{R}_1 > 1, \mathcal{R}_2 > 1, \beta_1 = \beta_2 = .5$	161
5.16	Solutions of system (5.3.2) when $\mathcal{R}_1 > 1, \mathcal{R}_2 > 1, \beta_1 = 5, \beta_2 = .5$. .	162
5.17	Solutions of system (5.3.2) when $\mathcal{R}_1 > 1, \mathcal{R}_2 > 1, \beta_1 = 5, \beta_2 = .5$. .	163

List of Tables

Table 2.1	Parameters for Model (2.2.1)	15
Table 2.2	Values for parameters and variables of Model (2.3.7)	38
Table 3.1	Values for parameters and variables of Model (3.3.6) with units explained in Table (2.1).	75
Table 4.1	Values for parameters and variables of Model (4.4.1), ϵ and D are given in $\frac{km^2}{day}$, other units explained in Table (2.1).	111
Table 5.1	Parameters for Model (5.2.1)	125
Table 5.2	Values for parameters and variables of Model (5.3.2)	155

Chapter 1

INTRODUCTION

1.1 Basic Facts about Dengue

Dengue (pronounced den'gueue) **Fever** (DF) and **Dengue Hemorrhagic Fever** (DHF), collectively known as “dengue,” are mosquito-borne, potentially mortal, flu-like viral diseases that affect humans of all ages worldwide [1, 4, 51]. Transmitted to humans by the bite of an infected mosquito, dengue is caused by any one of four serotypes, or antigen-specific viruses, of the genus *Flavivirus*, family *Flaviridae*: DENV 1, DENV 2, DENV 3, and DENV 4 [1, 6, 41, 51]. The *Flavivirus* genus derives its name for the Latin for “yellow,” or “flavus,” and includes the dengue, West Nile, Tick-borne Encephalitis, and Yellow Fever viruses, the latter of which are febrile and jaundice-causing [43].

The *Aedes aegypti* mosquito, the primary vector for the dengue virus, was first classified by Linnaeus in 1762 and originated in Africa. Due to travel by humans, of whom it is a parasite, the mosquito is now found worldwide [58]. Also a transmitter of yellow fever, female *Aedes aegypti* feed primarily on human blood to fortify eggs, at which time a contaminated (uninfected) mosquito may transmit (contract) the virus to (from) an uninfected (infected) human (see Section 2.1 in Chapter 2 for a

more extensive discussion of the life cycle of the mosquito and the specifics of dengue transmission). Because the mosquito lays its eggs in warm, still water and inhabits containers such as unused flower pots and spare tires, it is not surprising that it thrives in impoverished, tropical urban areas that lack piped water [58].

Though the *Aedes aegypti* bite is the primary mode of contagion, rare cases due to organ transplantation, blood transfusion, and mother-fetus transmission have been documented [1]. Additionally, the mosquito *Aedes albopictus*, originating in tropical and subtropical Southeast Asia, has been implicated in outbreaks of dengue epidemics [27].

After a human is bitten by a mosquito carrying the dengue virus, symptoms appear in 3-14 days (average 4-7 days) [4]. Those caused by DF, which is rarely fatal and associated with DENV 1, vary from individual to individual. Symptoms include a fever and rash in infants, and classic flu-like symptoms such as high fever, severe headache, myalgia, and arthralgia (which gives dengue its alternate names, *breakbone fever* or *bonecrusher disease*) in adults [4,41]. Additionally, patients may experience gastritis and other gastro-intestinal disturbances [3]. Mild cases of DF may be mistaken for influenza [3]. DF symptoms generally last between 2-7 days, after which most patients recover [3,4]. Humans may only transmit the virus during the febrile stage, characterized by a biphasic pattern: the main phase, a trough, and a minor peak toward the end of the infection [3]. DHF initially exhibits a similar, if more severe pathology as DF, but deviates from the classic pattern at the end of the febrile stage [1]. At this time, patients experience a 24-48 hour period of extreme capillary permeability, which allows fluid to escape from the capillaries and leak into the peritoneum and pleural cavity. This leads to a low platelet count and possible internal bleeding and circulatory failure [1].

These in turn can lead to **Dengue Shock Syndrome** (DSS), which has a high mortality rate [1, 3].

No dengue-specific medical treatment exists; the CDC recommends that persons who suspect they have dengue consult a physician, as diagnoses are made clinically [1]. Additionally, analgesics with acetaminophen, rest, adequate fluid intake, and avoidance of contact with the mosquito and its habitats are recommended; ibuprofen is contraindicated [1]. Once recovered from dengue, patients are immune to that particular serotype but not to the others; in fact, studies suggests that susceptibility to a secondary infection is enhanced by a primary infection [12].

At present, there is no vaccine against dengue, so prevention centers around mosquito control and eradication efforts [10]. The CDC advises that individuals living in or traveling to regions where the disease is endemic be mindful of the mosquito's domestic habitat by cleaning water containers, water storage barrels, vases, and other places in and around the house [1]. Personal protection also involves the use of mosquito repellent, long-sleeved clothing, window and door screens, and air-conditioning [1]. Persons in the house who have contracted dengue must avoid mosquito contact so as not to spread the disease. Because *Aedes aegypti* eggs exhibit remarkable resilience to adverse weather and environmental effects, governmental efforts on the part of individual nations to eradicate the mosquito have not been successful [10].

1.2 History of the Dengue Epidemic

Though the etymology of the word “dengue” is unclear, one theory suggests that the term is derived from a Swahili phrase which attributes the disease to evil spirits [2]. Known as a human malady, dengue is believed to have evolved as a parasite of subhuman primates in Southeast Asia [24]. As the *Aedes aegypti* mosquito spread out of Africa, accompanying human movement, the virus acquired a vector for contagion in developing urban centers [24]. The first written account of dengue dates to the third century CE, when a Chinese encyclopedia of disease symptoms and remedies, first published during the Chin Dynasty (265 to 420 CE), described the association between a disease known as “water poison” and water-dependent flying insects [21]. Possible dengue outbreaks include epidemics in the French West Indies in 1635 and in Panama in 1699 [21]. Among slaves in the West Indies, the disease was known as “dandy fever,” due to the gait and posture adopted by those suffering from its fever-induced bone pain [25]. Though it is possible that the Cairo (1799) and likely that the Philadelphia (1780) epidemics were dengue, the first confirmed case report, by Benjamin Rush, dates from 1789 [21]. Rush coined the term “breakbone fever,” while Sir John Burton Cleland discovered dengue’s viral etiology and mode of transmission in the 20th century [45]. Between 1780 and 1940, large if infrequent epidemics broke out in several urban tropical centers, where dengue likely became endemic [21]. Notable outbreaks, including ones etiologically consistent with DHF/DSS, occurred in Australia (1897) and in Greece (1928) [24].

During World War II, the combat in the Pacific provided the staging ground for a worldwide dengue pandemic [21]. Infections, common in combatants on both sides of the Pacific War, spread to Hawaii, Japan, and the Pacific Islands [24]. In the

1940s and 50s, Sabin isolated DENV 1 and 2. During this period, Thailand and other Southeast Asian countries experienced outbreaks featuring multiple serotypes [21, 24]. DHF was identified and described, leading to its association with hyperendemicity by Halstead in the 1970s and Gubler in the 1980s and 1990s [21]. Between the 1950s and the 1970s, dengue spread westward from Southeast Asia to India, Sri Lanka, Pakistan, and the Maldives; and on eastward to China [21].

Meanwhile, intensive *Aedes aegypti* eradication efforts in Central and South America successfully prevented epidemic outbreaks; these reappeared, however, when economic instability in the region led to the abandonment of these efforts [21]. In the 1980s and 1990s, dengue reappeared throughout the region. Further, countries where the virus had been either non- or hypo-endemic, that is, producing epidemics of a single serotype, became hyperendemic [21]. Additionally, DHF epidemics emerged. Notable outbreaks include the first nationwide Brazilian pandemic of 1998 (see Section 3.1 in Chapter 3). Curiously, when dengue viruses recovered from outbreaks in Cuba (1981) and Venezuela (1988-89) were topotyped, they were shown to have originated in Southeast Asia [24].

In the last two decades, dengue has become endemic in more than 100 countries in Africa, the Americas, the Eastern Mediterranean, Southeast Asia, and the Western Pacific [4]. Today, it is the most common human mosquito-borne viral disease [4]. Urbanization, poor sanitation in newly urbanized areas, climatic changes, and air travel are all implicated in dengue's rapid spread. It is estimated that 2.5 billion people are at risk, with as many as 50 million cases worldwide each year [4]. While Southeast Asia and the Western Pacific are most heavily hit, the disease is quickly spreading to previously unaffected regions [4]. In 2007, more than 890,000 cases were reported in the Americas [4].

About 500,000 cases of DHF require hospitalization each year, of which 2.5 percent result in fatalities [4].

1.3 Review of the Epidemiological and Scientific Literature

Taking the epidemiological and etiological factors into consideration, various mathematical models for the transmission of the dengue virus have been proposed. In this section, we consider some of these models while identifying the general aims of modeling the dengue epidemic.

Some of the first dengue models attempt to capture the complexity of its transmission dynamics. Among the most important is that of Feng and Velasco-Hernandez, which incorporates vector-host dynamics in a two-strain epidemiological system [15]. Feng and Velasco-Hernandez derive the model's basic reproduction number, or number of secondary infections that a single infectious individual produces in a population where all hosts are susceptible [15]. Analysis of the model yields interesting results: an interior endemic equilibrium, found to exist only when the basic reproduction numbers of each strain are greater than one, is always unstable (see Discussion in [15]). Feng and Velasco-Hernandez conclude that the system's long-term behavior, under these circumstances, is unpredictable. Initially, both strains coexist; eventually, however, one strain prevails and the other dies out (see Discussion in [15]).

Interestingly, in obtaining a precise definition of the basic reproduction number for a general compartmental disease transmission model based on an ODE system, van Driessche and Watmough simplify Feng and Velasco-Hernandez' model into a single-strain vector-host system. Their reproduction number for this simplified model seems

consistent with the one obtained by Feng and Velasco-Hernandez. Van Driessche and Watmough further point out that their calculation of the reproduction number reflects the two generations necessary for the host or vector to “reproduce” itself, which in turn reflects the crucial assumption that human-mosquito contact is the only possible mode of dengue transmission (see Section 4.5 in [52]).

More recent efforts at modeling dengue transmission dynamics have taken various directions. In discussing the goals and challenges of dengue modeling, Favier et al. argue that it should ultimately aim to guide intervention and prevention policies [13]. In so doing, models must “relate the epidemic variables to both climatic and environmental parameters” (see Introduction in [13]). Because these parameters vary regionally, dengue modeling itself has acquired distinct regional orientations. Various studies, some of which feature non-deterministic models, use data from specific dengue hot spots. One model associates weekly El Niño Southern Oscillation sea-surface temperature observations with DF/DHF outbreaks in Costa Rica [19]. Another focuses on the transmission dynamics specific to subtropical regions [8]. Studies based in Brazil and Thailand have been conducted [8, 36, 50]. Spatial dynamics have also been investigated [9, 14, 36, 47, 48].

Given the breadth of dengue studies, one goal should be a comprehensive yet comparative approach to mathematical modeling, analysis, and numerical simulation. This is what we attempt here.

1.4 Outline of the Thesis

In this thesis, both the spatial and temporal dynamics of dengue transmission are investigated. Different chapters present new models while building on themes of previous chapters. In Chapter 2, we explore the temporal dynamics of dengue viral transmission by presenting and analyzing an ODE model that combines an SIR human host- with a multi-stage SI mosquito vector transmission system. In Chapter 3, we present and analyze a non-autonomous, non-linear ODE system that incorporates seasonality into the modeling of the transmission of the dengue virus. In Chapter 4, we present and analyze a non-linear system of coupled reaction-diffusion equations modeling the virus' spatial spread. In formulating our model, we seek to establish the existence of traveling wave solutions and calculate spread rates for the spatial dissemination of the disease. In Chapter 5, we present and analyze an ODE model that incorporates two serotypes of the dengue virus and allows for the possibility of both primary and secondary infections with each serotype. In each chapter, numerical simulations are conducted to support the analytical conclusions.

Chapter 2

THE MAIN ODE MODEL AND ANALYSIS OF THE ASEASONAL MODEL

2.1 Introduction and Assumptions

In this chapter, we introduce the main ODE model for the transmission of the dengue virus between humans and mosquitoes, with the goal of deriving conditions under which the dengue virus will coexist with the human and/ or mosquito populations. We start by stating the main assumptions concerning the modes of transmission of the dengue virus, the life-cycle of the mosquito, and the seasonality of oviposition.

The dengue virus presents two main modes of transmission: human to mosquito and mosquito to human. Additionally, adult, infected female mosquitoes may lay infected eggs. Susceptible humans cannot contract the virus by coming into contact with infected humans. Transmission of dengue from a human to a mosquito can occur when an adult, impregnated female *Aedes aegypti* feeds on human blood, which it does so to fortify its eggs [36]. If the human is infected with the dengue virus, he/she may pass it on to the mosquito, who remains infected throughout its life-cycle [2]. Infected mosquitoes may lay infected eggs, which hatch and undergo infantile, noninfectious

stages in warm, standing water before leaving for dry land as adult mosquitoes [8]. Humans may become infected only if bitten by infected adult mosquitoes. Presently there are four serotypes of the virus, which present low cross-immunity but high serotypic-specific immunity [6, 41, 51] (see Chapter 5 for a more extensive discussion of serotypes).

The life-cycle of the mosquito, which consists of four physically distinct, seasonally-correlated stages- egg, larval, pupa, and adult- plays a crucial role in determining the outbreak of an epidemic. Eggs are laid in water at the end of autumn and, for the most part, do not begin hatching until the beginning of spring, as larvae. Larval mosquitoes mature into pupa and then into adults, at which time they may reproduce and spread the dengue virus. The reproductive stage takes place from spring until the end of autumn, when the cycle restarts. As a whole, the *Aedes aegypti*'s population density undergoes seasonal fluctuation, peaking in the summer and bottoming in the winter (see *Remark* at the end of this section for a clarification of references to seasons).

The duration of each of the four stages is, however, variable and determined by such factors as parasitism and susceptibility to infection. The literature provides some evidence for the intuition that, at the larval stage, for example, the mosquito is more susceptible to certain viral and bacterial infections than at the adult stage. In one example, larvae infected by the aquatic microsporidia *Vavraia culicis* were shown to have fewer metabolic resources throughout their life-cycle and lower pupation rates than their uninfected counterparts [39]. Because infection occurs in an aquatic medium, adults, having left this environment, are not as susceptible to the parasite.

As a result, the death rate of the mosquito at the adult phase is governed by factors different from those that influence the death rates of the immature populations.

Several important studies propose models that take these elements into consideration. Among them, we emphasize that of Coutinho *et al.*, who formulate a non-autonomous, nonlinear system of differential equations that combines an SIR model for disease transmission in the human host with a corresponding multi-stage SEI model in the mosquito vector, whose population is divided into adult (mature) and egg (immature) components [8]. In this paper, the authors investigate the effect of seasonal anomalies on the evolution of the dengue epidemic in both human and mosquito populations. Coutinho *et al.* do this by modulating the maturation from the egg into the adult phase by a periodic seasonal factor (for a more extensive discussion of seasonality, see Chapter 3 and [8]). Another important study for the dynamics of dengue transmission, that of Esteva and Vargas [11], presents a complete analysis of the threshold dynamics of a system for dengue transmission that incorporates a variable human population size.

In this study, we modify the models presented by Esteva and Vargas [11] and Coutinho *et al.* [8] to introduce a new model that combines an SIR system for disease transmission in the human host with a multi-stage SI model for disease transmission in the mosquito vector, which, unlike Coutinho *et al.*'s model, is divided into adult (mature), egg, and larval (immature) populations. By introducing a larval stage, we are able to avoid assuming that the mosquito's intermediate life-cycle phases take place in the winter and that mosquitoes emerge in the spring full-grown. Accordingly, in our model, we introduce a climatic factor that affects the maturation of eggs into larvae, posing advantages from a strategic, intervention-minded point of view. Like Esteva and Vargas in [11], we do not assume that the human or mosquito populations

observe logistic growth, keeping in mind that, ultimately, we want to observe change in the percentages of infected humans and mosquitoes. We show these changes are independent of their respective population sizes. As in Coutinho *et al.*'s study, we assume that the life-cycle of the mosquito takes place in 365 days [8]. Finally, we incorporate an element of vertical transmission; that is, we assume that infected adult mosquitoes can lay infected eggs. These, in turn, can only mature into infected larvae/pupae, which can only grow into infected adults.

In this chapter, we introduce the main ODE model and assume that the emergence from the egg into the larval phase is not affected by seasonal variation. We then analyze the aseasonal model. We derive the basic reproductive number, \mathcal{R}_0 , the threshold parameter denoting the expected number of secondary cases produced by a typically infective individual. Numerical simulations follow.

Remark: Because four distinct seasons are not necessarily observed in most tropical regions where the dengue virus is endemic, here we extend the concept of “season” so that “autumn” and “winter” refer to the beginning and end of the dry season, respectively, and the beginning and end of the “rainy” season are referred to as “spring” and “summer,” respectively. World climatic disruptions may disrupt the dry-rainy tropical cycle as well (see Section 3.1 in Chapter 3).

2.2 The Main ODE Model

In this section, we formulate and discuss the model, which depicts dengue transmission in 4 components: human hosts, adult mosquitoes, larvae, and eggs. One time t unit denotes a day. The human population is broken down into susceptible (\bar{S}_H), infected (\bar{I}_H), and recovered (\bar{R}_H) classes. The total human population is $N_H = \bar{S}_H + \bar{I}_H + \bar{R}_H$. The total adult mosquito population is constant and is denoted by N_M . The infected mosquito population is broken down into adult (\bar{I}_M), larval (\bar{I}_P), and egg (\bar{I}_E) classes. We assume that the total number of individuals in each juvenile stage does not exceed N_M . This is justified by the fact that at every phase of its development, the mosquito loses individuals to death and/or maturation and gains only a fraction of the ones that matured from the previous stage. Since the number of infectives in each stage of mosquito development cannot exceed the total number of individuals in each such stage, N_M is an upper bound for \bar{I}_E and \bar{I}_P . The human population assumes exponential growth without disease, an assumption that is justifiable once we make variable substitutions to analyze change in the proportion of infected humans. The vector populations remain constant in the absence of disease. Since we do not distinguish between serotypes, our model depicts the transmission of a single strain of the dengue virus, from which recovered individuals are immune. The climatic factor is given by S , a function of time.

The model is as follows:

$$\begin{aligned}
\frac{d\bar{S}_H}{dt} &= v_H N_H - u_H \bar{S}_H - \lambda_H \bar{S}_H \frac{\bar{I}_M}{N_M} \\
\frac{d\bar{I}_H}{dt} &= \lambda_H \bar{S}_H \frac{\bar{I}_M}{N_M} - (y_H + \alpha_H + u_H) \bar{I}_H \\
\frac{d\bar{R}_H}{dt} &= y_H \bar{I}_H - u_H \bar{R}_H \\
\frac{d\bar{I}_M}{dt} &= p_1 \left(\frac{N_M - \bar{I}_M}{N_M} \right) \bar{I}_P - u_m \bar{I}_M + \lambda_V (N_M - \bar{I}_M) \frac{\bar{I}_H}{N_H} \\
\frac{d\bar{I}_P}{dt} &= \tau_1 S(t) \left(\frac{N_M - \bar{I}_P}{N_M} \right) \bar{I}_E - p_1 \left(\frac{N_M - \bar{I}_P}{N_M} \right) \bar{I}_P - u_q \bar{I}_P \\
\frac{d\bar{I}_E}{dt} &= gr_m \left(\frac{N_M - \bar{I}_E}{N_M} \right) \bar{I}_M - \tau_1 S(t) \left(\frac{N_M - \bar{I}_P}{N_M} \right) \bar{I}_E - u_e \bar{I}_E
\end{aligned} \tag{2.2.1}$$

with $N_M \geq \bar{I}_M(0)$, $N_M \geq \bar{I}_P(0)$, $N_M \geq \bar{I}_E(0)$, $N_M > 0$, $N_H(0) > 0$, $v_H \geq u_H > 0$.

The parameters in Model (2.2.1) can be understood by referring to Table 2.1. In this chapter, we will henceforth assume all parameters are nonnegative. We will also assume seasonality does not influence egg maturation by setting $S(t) = 1$ for all $t \geq 0$.

The first three equations of Model (2.2.1) describe the transmission of the dengue virus with a variable human population size. As already mentioned, these coincide with the first three equations of the model proposed by Esteva and Vargas [11]. It is assumed that once recovered, humans are immune. Infected adult mosquitoes do not recover.

<i>Parameter</i>	<i>Definition</i>	<i>Unit and/or Range</i>
v_H	natural human birth rate	(births/ 10^3 humans) day^{-1}
u_H	natural human mortality rate	$\frac{\text{deaths}}{10^3 \text{ humans}} \text{ day}^{-1}$
λ_H	effective contact rate between susceptible humans and mosquitoes	bite/susceptible humans
γ_H	human recovery rate from dengue	$\frac{\text{recovered humans}}{10^3 \text{ infected humans}} \text{ day}^{-1}$
α_H	human mortality rate from dengue	$\frac{\text{deaths}}{10^3 \text{ mosquitoes}} \text{ day}^{-1}$
u_q	natural larval mortality rate	$\frac{\text{deaths}}{10^3 \text{ larvae}} \text{ day}^{-1}$
u_m	natural adult mosquito mortality rate	$\frac{\text{deaths}}{10^3 \text{ larvae}} \text{ day}^{-1}$
λ_V	effective contact rate between uninfected mosquitoes and humans	bites/uninfected mosquito
c	winter mildness index: average winter temperature, as compared to previous years' mean of $c = 1$	between 0 and 2
d	season length index: summer and winter length, as compared to previous years' mean of $d = 1$	between 0 and 2
w	length of reproductive cycle unit	day^{-1}
σ	phase shift describing onset of wintering phase	days, between -365 and 365
r_m	oviposition rate	$\frac{\text{eggs}}{10^3 \text{ mosquitoes}} \text{ day}^{-1}$
g	proportion of mosquito eggs laid by an infected female that is infected and female	eggs
u_e	natural egg mortality rate	$\frac{\text{deaths}}{10^3 \text{ eggs}} \text{ day}^{-1}$
τ_1	proportion of infected eggs that proceeds to the larval stage	infected eggs
p_1	proportion of infected larvae that proceeds to the adult stage	infected larvae

Table 2.1: *Parameters for Model (2.2.1)*

Equations 4-6 of Model (2.2.1) reflect the fact that only a fraction of juvenile infectives mature into the next stage. The fact that $u_q \neq 1 - p_1$, for example, implies that at any given time t , not all surviving juveniles progress to the next phase; they may remain in their present state. Further, as already discussed, total mosquito, larval, and egg populations, respectively, remain constant in the absence of seasonality and disease. The last three equations incorporate saturation terms, $\left(\frac{N_M - \bar{I}_P}{N_M}\right)$, $\left(\frac{N_M - \bar{I}_M}{N_M}\right)$, $\left(\frac{N_M - \bar{I}_E}{N_M}\right)$, that take into account the fact that the maturation rate into the next phase of mosquito development is stifled if the population in the next phase is reaching N_M . This ensures that infected populations remain below a threshold, N_M , for the adult, larval, and egg population densities.

2.3 Analysis of the Aseasonal Model

We now analyze Model (2.2.1).

Note that $\frac{dN_H}{dt} = \frac{d\bar{S}_H}{dt} + \frac{d\bar{I}_H}{dt} + \frac{d\bar{R}_H}{dt}$. So if we add the RHS (right-hand side) of equations 1 - 3 of Model (2.2.1) we obtain the following equation:

$$\frac{dN_H}{dt} = (v_H - u_H)N_H - \alpha_H \bar{I}_H. \quad (2.3.1)$$

We now add this equation to Model (2.2.1).

Define $f : R_+^7 \rightarrow R^7$ by $f(y) = (f_1(y), \dots, f_7(y))$, where $f_i : R_+^7 \rightarrow R$ is defined by $f_i(y) = \frac{dy_i}{dt}$ for each i with $1 \leq i \leq 7$.

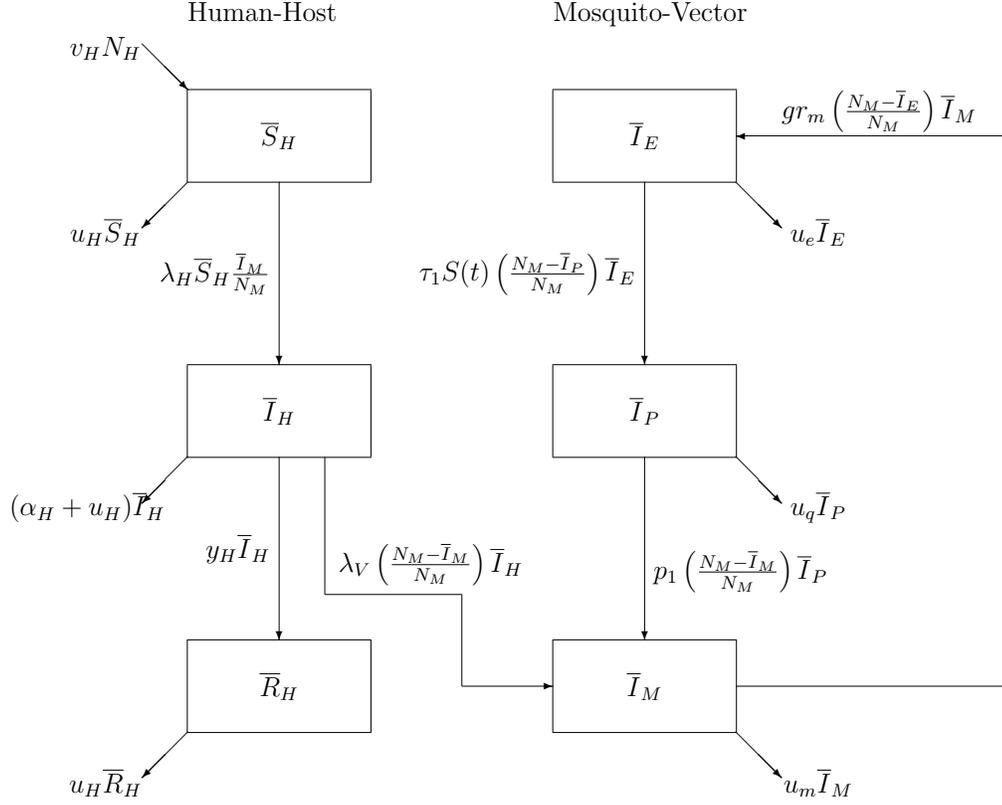


Figure 2.1: *Compartmentalized model for dengue. See Table 2.1 for parameter descriptions.*

System (2.2.1) then allows us to define an initial value problem

$$\begin{aligned} \dot{y} &= f(y) \\ y(t_0) &= y_{t_0} \end{aligned} \tag{2.3.2}$$

where $y = (\bar{S}_H, \bar{I}_H, \bar{R}_H, \bar{I}_M, \bar{I}_P, \bar{I}_E, N_H)$.

As all functions on the RHS of Model (2.2.1) are continuously differentiable on R_+^7 , we know that if $y_{t_0} \in R_+^7$, IVP (2.3.2) possesses a unique solution.

Additionally, we have

Theorem 2.1. *Let $y_0 \in R_+^7$. Any solution $y(t)$ of IVP (2.3.2) through y_0 is defined for all $t \geq 0$, and the positive cone R_+^7 is positively invariant.*

Proof. Let $(\bar{S}_H^*(t), \dots, N_H^*(t))$ with $\bar{S}_H^*(0) > 0, \dots, N_H^*(0) > 0$ be a fixed solution of IVP (2.3.2) through $(\bar{S}_{H_0}^*, \dots, N_{H_0}^*)$ on $[0, \beta)$, with β real.

By the continuity of the solution on $[0, \beta)$, there exists a δ with $0 < \delta < \beta$ such that $\bar{S}_H^*(t') > 0, \dots, N_H^*(t') > 0$ for any $t' \in [0, \delta]$.

Now $\bar{I}_M^*(0) \leq N_M$. Further, if $N_M = \bar{I}_M^*(t')$ for some t' in $[0, \delta]$, $\frac{d\bar{I}_M^*}{dt}|_{t=t'} \leq 0$. The previous two statements also hold for $\bar{I}_P^*(t), \bar{I}_E^*(t)$. The continuity of $\bar{I}_M^*(t)$ on $[0, \delta]$ implies that $\frac{\bar{I}_M^*(t)}{N_M} \leq 1$ on $[0, \delta]$. The latter also holds for $\bar{I}_P^*(t), \bar{I}_E^*(t)$. (*)

So on $[0, \delta]$,

$$\begin{aligned} \frac{d\bar{S}_H^*}{dt} &= v_H N_H^* - u_H \bar{S}_H^* - \lambda_H \bar{S}_H^* \frac{\bar{I}_M^*}{N_M} \\ &\geq -u_H \bar{S}_H^* - \lambda_H \bar{S}_H^* \frac{\bar{I}_M^*}{N_M} \\ &\geq (-u_H \bar{S}_H^* - \lambda_H \bar{S}_H^*), \text{ by } (*) \\ &= \bar{S}_H^* (-u_H - \lambda_H). \end{aligned}$$

So,

$$\bar{S}_H^*(t) \geq e^{(-u_H - \lambda_H)t} \bar{S}_H^*(0) > 0. \quad (2.3.3)$$

The positivity of the other components on $[0, \delta]$ can be shown similarly. By the continuity of $\bar{S}_H^*(t)$ on $[0, \beta)$, equation (2.3.3) holds on $[0, \beta)$. So $\bar{S}_H^*(t)$ is bounded below by a positive number on $[0, \beta)$. The same holds for the other components on $[0, \beta)$.

So $\lim_{t \rightarrow \beta^-} (\bar{S}_H^*(t), \dots, N_H^*(t)) > 0$. Therefore, $(\bar{S}_H^*(t), \dots, N_H^*(t))$ can be continuously extended to $[0, \beta]$ and R_+^7 is invariant with respect to the semiflow defined by system (2.2.1) on $[0, \beta]$.

Consequently, $[0, \infty)$ is the maximal interval of existence of $(\bar{S}_H^*(t), \dots, N_H^*(t))$ [38, Section 2.4, Theorem 3, Corollary 1, and Problem 3, Problem Set 4]. Therefore, R_+^7 is positively invariant. \square

We will now follow the method outlined by Esteva and Vargas [11] to introduce proportions to system (2.2.1).

Let

$$\begin{aligned} \frac{\bar{S}_H}{N_H} &= S_H, \quad \frac{\bar{I}_H}{N_H} = I_H \\ \frac{\bar{R}_H}{N_H} &= R_H, \quad \frac{\bar{I}_M}{N_M} = I_M \\ \frac{\bar{I}_P}{N_M} &= I_P, \quad \frac{\bar{I}_E}{N_M} = I_E. \end{aligned} \tag{2.3.4}$$

We assume $N_H > 0$, $N_M > 0$. We may do so since by Theorem 2.1, if $N_H(0) > 0$, $N_H(\cdot)$ remains positive for all $t \geq 0$.

Then system (2.2.1) can be written as

$$\begin{aligned} S_H' &= v_H - v_H S_H - \lambda_H S_H I_M + \alpha_H S_H I_H \\ I_H' &= \lambda_H S_H I_M - (y_H + \alpha_H + v_H) I_H + \alpha_H I_H^2 \\ I_M' &= p_1 I_P (1 - I_M) - u_m I_M + \lambda_V (1 - I_M) I_H \\ I_P' &= \tau_1 I_E (1 - I_P) - p_1 I_P (1 - I_M) - u_q I_P \\ I_E' &= g r_m I_M (1 - I_E) - \tau_1 I_E (1 - I_P) - u_e I_E \end{aligned} \tag{2.3.5}$$

with $1 \geq S_H(0) \geq 0$, $1 \geq I_H(0) \geq 0$, $1 \geq S_H(0) + I_H(0) \geq 0$, $1 \geq I_M(0) \geq 0$,
 $1 \geq I_P(0) \geq 0$, $1 \geq I_E(0) \geq 0$, $v_H > 0$.

Corollary 2.2. *Let $\Omega = \{(S_H, I_H, I_M, I_P, I_E) : 0 \leq S_H \leq 1, 0 \leq I_H \leq 1, 0 \leq S_H + I_H \leq 1, 0 \leq I_M \leq 1, 0 \leq I_P \leq 1, 0 \leq I_E \leq 1\}$. Then Ω is positively invariant with respect to the flow defined by system (2.3.5).*

Proof. Let $(S_H^*(t), \dots, I_E^*(t))$ with $(S_{H_0}^*, \dots, I_{E_0}^*) \in \Omega$ be a fixed solution of system (2.3.5) on $[0, \infty)$.

Suppose $(S_H^*(0), \dots, I_E^*(0))$ is on $Bde(\Omega)$. (*)

If $S_H^*(0) = 0$, then by equation 1 of (2.3.5), $S_H^{\prime*}(0) = v_H > 0$. If $S_H^*(0) = 1$, then since by (*), $S_H^*(0) + I_H^*(0) \leq 1$, $I_H^*(0) = 0$, so by equation 1 of (2.3.5) and (*), $S_H^{\prime*}(0) = -\lambda_H I_M^*(0) \leq 0$. Similarly, if $I_H^*(0) = 0$, then by equation 2 of (2.3.5) and (*), $I_H^{\prime*}(0) = \lambda_H S_H^*(0) I_M^*(0) \geq 0$. If $I_H^*(0) = 1$, then by (*), $S_H^*(0) = 0$, so by equation 2 of (2.3.5), $I_H^{\prime*}(0) = -y_H - v_H < 0$.

If $S_H^*(0) + I_H^*(0) = 0$, then by equations 1 and 2 of (2.3.5), $S_H^{\prime*}(0) + I_H^{\prime*}(0) = v_H > 0$.

Now if $I_H^*(0) + S_H^*(0) = 1$, then by (2.3.4) and (*), $\max(I_H^*(0), S_H^*(0)) \leq 1$ and by equations 1 and 2 of (2.3.5) and (*),

$$\begin{aligned}
S_H^{\prime*}(0) + I_H^{\prime*}(0) &= v_H(1 - S_H^*(0)) + \alpha_H S_H^*(0)(1 - S_H^*(0)) - (y_H + \alpha_H + v_H)(1 - S_H^*(0)) \\
&+ \alpha_H(1 - S_H^*(0))^2 \\
&= -y_H(1 - S_H^*(0)) + \alpha_H(1 - S_H^*(0))^2 + \alpha_H S_H^*(0)(1 - S_H^*(0)) \\
&- \alpha_H(1 - S_H^*(0)) \\
&= (1 - S_H^*(0))(-y_H) \\
&\leq 0
\end{aligned}$$

By equations 3, 4, and 5 and (*), if $I_M^*(0) = 0$, $I_M^{*\prime}(0) = p_1 I_P^*(0) + \lambda_V I_H^*(0) \geq 0$; if $I_P^*(0) = 0$, $I_P^{*\prime}(0) = \tau_1 I_E^*(0) \geq 0$; and if $I_E^*(0) = 0$, $I_E^{*\prime}(0) = gr_m I_M^*(0) \geq 0$.

Finally, by equations 3, 4, and 5 and (*), if $I_M^*(0) = 1$, $I_M^{*\prime}(0) = -u_m \leq 0$; if $I_P^*(0) = 1$, $I_P^{*\prime}(0) = -p_1(1 - I_M^*(0)) - u_q \leq -u_q \leq 0$; and if $I_E^*(0) = 1$, $I_E^{*\prime}(0) = -\tau_1(1 - I_P^*(0)) - u_e \leq 0$. (**)

Suppose $(S_{H_0}^*, \dots, I_{E_0}^*)$ is in $Interior(\Omega)$. (+)

Let $t_0 = \inf\{t \in (0, \infty) : (S_H^*(t), \dots, I_E^*(t)) \text{ on } Bde(\Omega)\}$. (++)

By the continuity of the solution on $[0, \infty)$, $(S_H^*(t), \dots, I_E^*(t)) \in Interior(\Omega)$ on $[0, t_0)$. So $\lim_{t \rightarrow t_0^-} (S_H^*(t), \dots, I_E^*(t)) \in \bar{\Omega}$. So we may substitute t_0 for 0 in the arguments following (*), so that (**) holds at t_0 . (***)

If we substitute any $t' \in [0, \infty)$ for 0 in (+) and $t_{t'}$ for t_0 in (++) , (***) holds. (++++)

By (**), (***), (++++) and [26, Proposition 3.3], we have our result. \square

Observe that system (2.3.5) does not depend on N_H . In fact, we have,

$$N_H' = (v_H - u_H - \alpha_H I_H) N_H. \quad (2.3.6)$$

Note that the first two equations of system (2.3.5) and equation (2.3.6) are exactly those obtained by Esteva and Vargas [11, system (2.2)].

2.3.1 \mathcal{R}_0 for an Autonomous ODE System

If we set system (2.3.5) and the infective components to 0, we obtain a disease-free equilibrium (DFE), $E_0 = (1, 0, 0, 0, 0)^T$. We seek to derive \mathcal{R}_0 , the basic reproductive number and threshold parameter for the persistence of disease. We follow the method

described by van den Driessche and Watmough [52], who establish \mathcal{R}_0 as a threshold parameter by defining it as the spectral radius of the “next generation matrix,” a positive linear operator. If $\mathcal{R}_0 < 1$, then the (DFE) is locally asymptotically stable. If $\mathcal{R}_0 > 1$, then the DFE is unstable and an epidemic can develop.

2.3.2 Compartmentalized Modeling and Threshold Analysis

Consider the mosquito and human populations compartmentalized in the 5 classes of system (2.3.5). An epidemic model based on this system is developed in this section. Let $x = (x_1, \dots, x_5)^T$, with $x \in \Omega$, be the number of individuals in each compartment. Because we introduced proportions with system (2.3.5), here one whole individual represents the entire human or vector phase population ^(*). In other words, each dependent variable denotes a fraction of the total human or mosquito phase component ^(*). The first 4 compartments correspond to the infected components.

(*) when at carrying capacity

More specifically, we have that $I_H = x_1$, $I_M = x_2$, $I_P = x_3$, $I_E = x_4$, and $S_H = x_5$. Then $\Omega = \{(x_1, x_2, x_3, x_4, x_5) : 0 \leq x_i \leq 1 \text{ for } 1 \leq i \leq 5; 0 \leq x_1 + x_5 \leq 1\}$.

So by system (2.3.5),

$$\begin{aligned}
 \dot{x}_1 &= \lambda_H x_5 x_2 - (y_H + \alpha_H + v_H)x_1 + \alpha_H x_1^2 \\
 \dot{x}_2 &= p_1 x_3 (1 - x_2) - u_m x_2 + \lambda_V (1 - x_2)x_1 \\
 \dot{x}_3 &= \tau_1 x_4 (1 - x_3) - u_q x_3 - p_1 x_3 (1 - x_2) \\
 \dot{x}_4 &= gr_m x_2 (1 - x_4) - \tau_1 x_4 (1 - x_3) - u_e x_4 \\
 \dot{x}_5 &= v_H - v_H x_5 - \lambda_H x_5 x_2 + \alpha_H x_1 x_5
 \end{aligned} \tag{2.3.7}$$

where $(x_1, \dots, x_5) \in \Omega$, and $v_H > 0$.

Define X_S to be the set of all disease-free states. That is,

$$X_S = \{x \in \Omega : x_i = 0, i = 1, \dots, 4\}. \quad (2.3.8)$$

Let $\mathcal{F}_i(x)$ be the rate of appearance of new infections in compartment i , $\mathcal{V}_i^+(x)$ be the rate of transfer of individuals into compartment i by all other means, and $\mathcal{V}_i^-(x)$ be the rate of transfer of individuals out of compartment i . Let $\mathcal{V}_i = \mathcal{V}_i^- - \mathcal{V}_i^+$ for each i with $1 \leq i \leq 5$ (see [52, Section 2, (1)]).

The following assumptions can be made:

Assumption(A0): For each i with $1 \leq i \leq 5$, \mathcal{F}_i , \mathcal{V}_i^+ , \mathcal{V}_i^- are continuously differentiable at least twice in each x .

Observe that system (2.3.7) may be written as $\dot{x}_i = f_i(x) = \mathcal{F}_i(x) - \mathcal{V}_i(x)$ where $\mathcal{V}_i(x) = \mathcal{V}_i^-(x) - \mathcal{V}_i^+(x)$. Each \mathcal{F}_i , \mathcal{V}_i^+ , \mathcal{V}_i^- is a polynomial function in 5 variables and therefore continuous. It follows that for each i, j, k with $1 \leq i, j, k \leq 5$, $\frac{\partial f_i}{\partial x_j}$ and $\frac{\partial^2 f_i}{\partial x_j \partial x_k}$ are polynomials in 5 variables. So for each i with $1 \leq i \leq 5$, \mathcal{F}_i , \mathcal{V}_i^+ , \mathcal{V}_i^- are continuous and twice-differentiable in each x .

Assumption(A1): If $x \in \Omega$, then \mathcal{F}_i , \mathcal{V}_i^+ , $\mathcal{V}_i^- \geq 0$ for $i = 1, \dots, 5$.

All parameters are nonnegative. So we have, $\mathcal{F}_1(x) = \lambda_H x_5 x_2 \geq 0$, $\mathcal{V}_1^+(x) = \alpha_H x_1^2 \geq 0$, $\mathcal{V}_1^-(x) = (y_H + \alpha_H + v_H)x_1 \geq 0$, $\mathcal{F}_2(x) = \lambda_V(1 - x_2)x_1 \geq 0$, $\mathcal{V}_2^+(x) = +p_1 x_3(1 - x_2) \geq 0$, $\mathcal{V}_2^-(x) = u_m x_2 \geq 0$, $\mathcal{F}_3(x) = 0$, $\mathcal{V}_3^+(x) = \tau_1 x_4(1 - x_3) \geq 0$, $\mathcal{V}_3^-(x) = p_1 x_3(1 - x_2) + u_q x_3 \geq 0$, $\mathcal{F}_4(x) = 0$, $\mathcal{V}_4^+(x) = gr_m x_2(1 - x_4) \geq 0$, $\mathcal{V}_4^-(x) = \tau_1 x_4(1 - x_3) + u_e x_4 \geq 0$, $\mathcal{F}_5(x) = 0$, $\mathcal{V}_5^+(x) = v_H + \alpha_H x_5 x_1 \geq 0$, $\mathcal{V}_5^-(x) = v_H x_5 + \lambda_H x_5 x_2 \geq 0$.

Assumption(A2): If $x_i = 0$, then $\mathcal{V}_i^- = 0$. In particular, if $x \in X_S$, then $\mathcal{V}_i^- = 0$ for $i = 1, \dots, 4$.

The first claim follows from the paragraph following **(A1)**. Now if $x \in X_S$, $x_i = 0$ for $i = 1, \dots, 4$. So the second claim follows from the first.

Assumption(A3): $\mathcal{F}_i = 0$ if $i = 5$.

Follows from the paragraph following **(A1)**.

Assumption(A4): If $x \in X_S$, $\mathcal{F}_i(x) = 0$ and $\mathcal{V}_i^+(x) = 0$ for $i = 1, \dots, 4$.

If $x \in X_S$, $x_i = 0$ for $i = 1, \dots, 4$. So result follows from the paragraph following **(A1)**.

Assumption(A5): Suppose $u_m, (u_q + p_1), (\tau_1 + u_e), v_H$ all > 0 , $\frac{gr_m p_1 \tau_1}{(\tau_1 + u_e)(p_1 + u_q)u_m} < 1$. If $\mathcal{F}(x)$ is set to zero, then all eigenvalues of $Df(x_0)$ have negative real part, where x_0 is a disease-free equilibrium (DFE) of system (2.3.7).

A DFE of system (2.3.7) is defined to be a (locally asymptotically stable) equilibrium of the disease-free model, i.e., system (2.3.7) restricted to X_S . So the single equilibrium solution with $x_i = 0$ for $1, \dots, 4$ is $x_0 = (0, 0, 0, 0, 1)^T$ (Recall from (2.3.5) the DFE $(1, 0, 0, 0, 0)^T$).

Recall that system (2.3.7) may be written as $\dot{x}_i = f_i(x) = \mathcal{F}_i(x) - \mathcal{V}_i(x)$ where $\mathcal{V}_i(x) = \mathcal{V}_i^-(x) - \mathcal{V}_i^+(x)$. So if $\mathcal{F}(x)$ is set to zero, then $F_i(x) = 0$ for each i . So $\dot{x}_i = f_i(x) = 0 - \mathcal{V}_i(x)$. So system (2.3.7) becomes

$$\begin{aligned}
 \dot{x}_1 &= -(y_H + \alpha_H + v_H)x_1 + \alpha_H x_1^2 \\
 \dot{x}_2 &= -u_m x_2 + p_1 x_3(1 - x_2) \\
 \dot{x}_3 &= \tau_1 x_4(1 - x_3) - u_q x_3 - p_1 x_3(1 - x_2) \\
 \dot{x}_4 &= gr_m x_2(1 - x_4) - \tau_1 x_4(1 - x_3) - u_e x_4 \\
 \dot{x}_5 &= v_H - v_H x_5 - \lambda_H x_5 x_2 + \alpha_H x_1 x_5
 \end{aligned} \tag{2.3.9}$$

So,

$$Df_x(x) = \begin{pmatrix} -(y_H + \alpha_H + v_H) + 2\alpha_H x_1 & 0 & 0 & 0 & 0 \\ 0 & -p_1 x_3 - u_m & p_1 - p_1 x_2 & 0 & 0 \\ 0 & +p_1 x_3 & -u_q - p_1 + p_1 x_2 - \tau_1 x_4 & \tau_1 - \tau_1 x_3 & 0 \\ 0 & gr_m - gr_m x_4 & +\tau_1 x_4 & -gr_m x_2 - \tau_1 - u_e + \tau_1 x_3 & 0 \\ \alpha_H x_5 & -\lambda_H x_5 & 0 & 0 & a_{55} \end{pmatrix} \quad (2.3.10)$$

where $a_{55} = -v_H + \alpha_H x_1 - \lambda_H x_2$.

Thus,

$$Df_x(x_0) = \begin{pmatrix} (-y_H - \alpha_H - v_H) & 0 & 0 & 0 & 0 \\ 0 & -u_m & p_1 & 0 & 0 \\ 0 & 0 & -(u_q + p_1) & \tau_1 & 0 \\ 0 & gr_m & 0 & -(\tau_1 + u_e) & 0 \\ \alpha_H & -\lambda_H & 0 & 0 & -v_H \end{pmatrix} \quad (2.3.11)$$

The eigenvalues of $Df_x(x_0)$ are $-v_H$ and the eigenvalues of the submatrix of $Df_x(x_0)$ obtained by deleting the fifth row and the fifth column of $Df_x(x_0)$. We will denote this submatrix by $J_0 = [b_{ij}]$, $1 \leq i, j \leq 4$. Now $-J_0$ has the *Z-pattern*, that is, $-b_{ij} \leq 0$ for all $i \neq j$. A *non-singular M-matrix* is a matrix B with the *Z-pattern* such that all principal leading minors are positive [16, 28]. Observe that the principal leading minors of $-J_0$ are given by $(y_H + \alpha_H + v_H) > 0$, $(y_H + \alpha_H + v_H)u_m > 0$, $(y_H + \alpha_H + v_H)u_m(u_q + p_1) > 0$, and $\det(-J_0) = (y_H + \alpha_H + v_H)((u_m)(\tau_1 + u_e)(p_1 + u_q) - gr_m p_1 \tau_1) > 0$, since by assumption, $u_m, (u_q + p_1), (\tau_1 + u_e)$ all > 0 and $\frac{gr_m p_1 \tau_1}{(\tau_1 + u_e)(p_1 + u_q)(u_m)} < 1$. Therefore, $-J_0$ is a non-singular M-matrix and its eigenvalues all have positive real part [16, 18, 28]. So the eigenvalues of J_0 , and, consequently, $Df_x(x_0)$, all have negative real part.

Given the above assumptions, we have the following result [52, Section 2, Lemma 1]:

If x_0 is a DFE of (2.3.7) and $f_i(x)$ satisfies **(A0)**-**(A5)**, then $D\mathcal{F}(x_0)$ and $D\mathcal{V}(x_0)$ are partitioned as

$$D\mathcal{F}(x_0) = \begin{bmatrix} F & 0 \\ 0 & 0 \end{bmatrix}, \quad D\mathcal{V}(x_0) = \begin{bmatrix} V & 0 \\ J_3 & J_4 \end{bmatrix},$$

where F and V are the $m \times m$ matrices defined by

$$F = \left[\frac{\partial \mathcal{F}_i}{\partial x_j}(x_0) \right] \quad \text{and} \quad V = \left[\frac{\partial \mathcal{V}_i}{\partial x_j}(x_0) \right] \quad \text{with} \quad 1 \leq i, j \leq m.$$

Furthermore, F is non-negative, V is a non-singular M-matrix and all eigenvalues of J_4 have positive real part.

We will now establish \mathcal{R}_0 . The matrix FV^{-1} is called the next generation matrix for the model and the basic reproduction number is defined as

$$\mathcal{R}_0 = \rho(FV^{-1}), \tag{2.3.12}$$

where $\rho(A)$ denotes the spectral radius of the matrix A .

We therefore have the following important proposition:

Proposition 2.3. *Assume $u_m, (u_q + p_1), (\tau_1 + u_e), v_H$ all > 0 , $\frac{gr_m p_1 \tau_1}{(\tau_1 + u_e)(p_1 + u_q)(u_m)} < 1$, all other parameters nonnegative. Then we may define \mathcal{R}_0 for system (2.3.7) by*

$$\mathcal{R}_0 = \sqrt{\frac{\lambda_V \lambda_H (p_1 + u_q)(\tau_1 + u_e)}{(y_H + \alpha_H + v_H)((\tau_1 + u_e)(p_1 + u_q)u_m - gr_m p_1 \tau_1)}}. \tag{2.3.13}$$

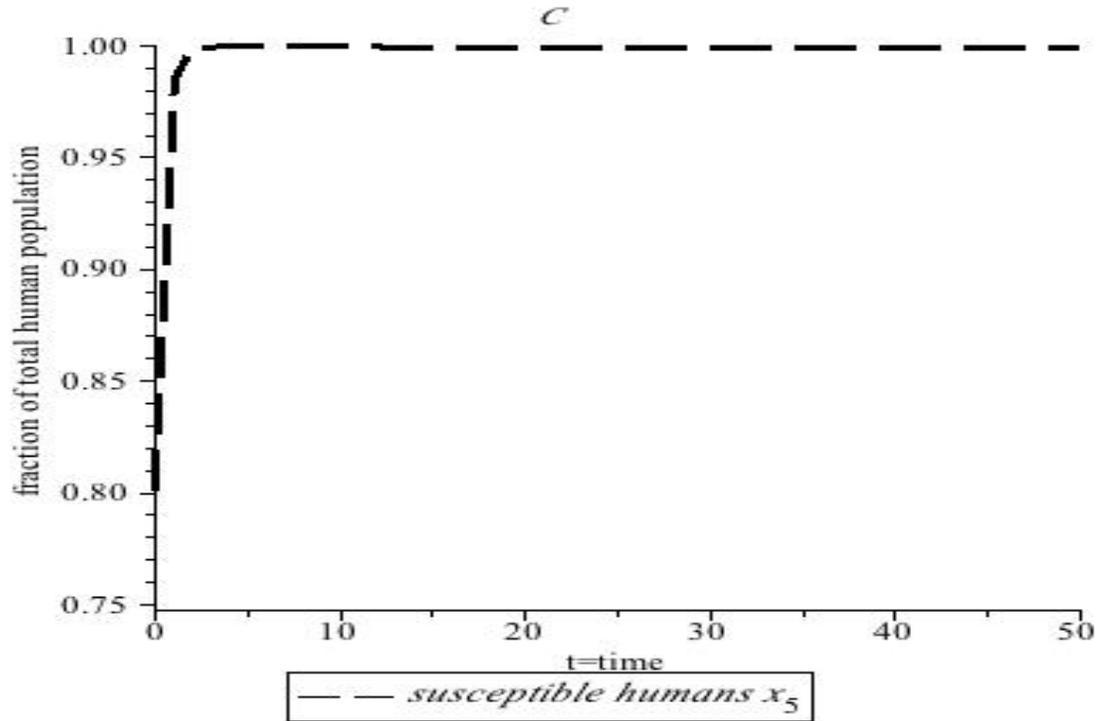


Figure 2.2: Solutions of system (2.3.7) converge to the steady-state values when $\mathcal{R}_0 = 1.21$, all other parameters are given in Table 2.2.

Proof. Recall that system (2.3.7) may be written as $\dot{x}_i = f_i(x) = \mathcal{F}_i(x) - \mathcal{V}_i(x)$ where $\mathcal{V}_i(x) = \mathcal{V}_i^-(x) - \mathcal{V}_i^+(x)$ and where

$$\mathcal{F} = \begin{pmatrix} \lambda_H x_5 x_2 \\ \lambda_V (1 - x_2) x_1 \\ 0 \\ 0 \\ 0 \end{pmatrix} \quad (2.3.14)$$

$$\mathcal{V} = \begin{pmatrix} (y_H + \alpha_H + v_H)x_1 - \alpha_H x_1^2 \\ u_m x_2 - p_1 x_3(1 - x_2) \\ p_1 x_3(1 - x_2) + u_q x_3 - \tau_1 x_4(1 - x_3) \\ \tau_1 x_4(1 - x_3) + u_e x_4 - gr_m x_2(1 - x_4) \\ v_H x_5 + \lambda_H x_5 x_2 - v_H - \alpha_H x_5 x_1 \end{pmatrix} \quad (2.3.15)$$

By the lemma stated above, we then have,

$$F = \begin{pmatrix} 0 & \lambda_H & 0 & 0 \\ \lambda_V & 0 & 0 & 0 \\ 0 & 0 & 0 & 0 \\ 0 & 0 & 0 & 0 \end{pmatrix} \quad (2.3.16)$$

$$V = \begin{pmatrix} y_H + \alpha_H + v_H & 0 & 0 & 0 \\ 0 & u_m & -p_1 & 0 \\ 0 & 0 & u_q + p_1 & -\tau_1 \\ 0 & -gr_m & 0 & \tau_1 + u_e \end{pmatrix} \quad (2.3.17)$$

$$J_3 = \begin{pmatrix} -\alpha_H & \lambda_H & 0 & 0 \end{pmatrix} \quad (2.3.18)$$

and

$$J_4 = \begin{pmatrix} v_H \end{pmatrix} \quad (2.3.19)$$

where F is non-negative, V is a non-singular M-matrix and all eigenvalues of J_4 have positive real part.

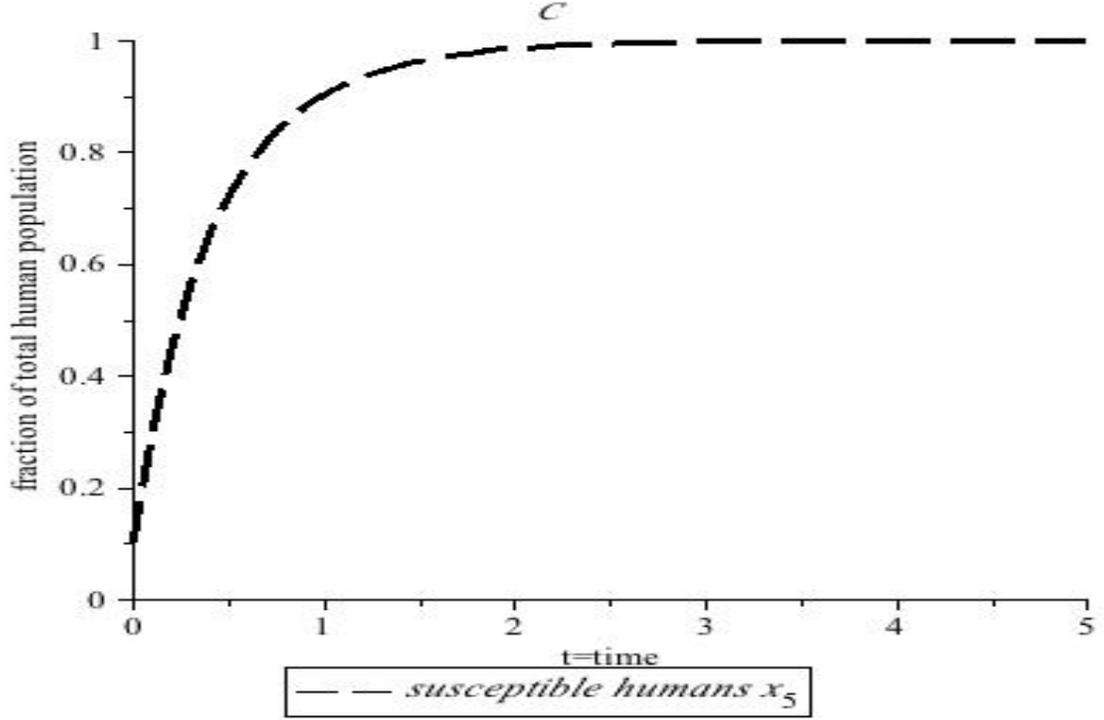


Figure 2.3: Solutions of system (2.3.7) converge to the DFE when $\mathcal{R}_0 = .24$, all other parameters are given in Table 2.2.

Now by (2.3.16) and (2.3.17) we have that $FV^{-1} =$

$$\begin{pmatrix} 0 & \frac{\lambda_H(\tau_1+u_e)(p_1+u_q)}{(u_m(\tau_1+u_e)(p_1+u_q)-gr_m p_1 \tau_1)} & \frac{\lambda_H p_1(\tau_1+u_e)}{(u_m(\tau_1+u_e)(p_1+u_q)-gr_m p_1 \tau_1)} & \frac{\lambda_H p_1(\tau_1)}{(u_m(\tau_1+u_e)(p_1+u_q)-gr_m p_1 \tau_1)} \\ \frac{\lambda_V}{y_H+\alpha_H+v_H} & 0 & 0 & 0 \\ 0 & 0 & 0 & 0 \\ 0 & 0 & 0 & 0 \end{pmatrix} \quad (2.3.20)$$

So the eigenvalues of FV^{-1} are given by the solutions to the characteristic equation of FV^{-1} :

$$\lambda^4 - \frac{\lambda_V \lambda_H (\tau_1+u_e)(p_1+u_q)}{(y_H+\alpha_H+v_H)((\tau_1+u_e)(p_1+u_q)u_m-gr_m p_1 \tau_1)} \lambda^2 = 0. \quad (2.3.21)$$

Clearly, 0 is a solution of this equation. The others are:

$$\lambda_{1,2} = \pm \sqrt{\frac{\lambda_V \lambda_H (p_1 + u_q)(\tau_1 + u_e)}{(y_H + \alpha_H + v_H)((\tau_1 + u_e)(p_1 + u_q)u_m - gr_m p_1 \tau_1)}}. \quad (2.3.22)$$

So by (2.3.12), we have our desired result. \square

Proposition 2.4. *Let \mathcal{R}_0 , parameters be as in Proposition 2.3. The following conditions characterize the stability of $(0, 0, 0, 0, 1)^T$.*

- 1) *If $\mathcal{R}_0 < 1$, then $(0, 0, 0, 0, 1)^T$ is locally asymptotically stable.*
- 2) *If $\mathcal{R}_0 > 1$, then $(0, 0, 0, 0, 1)^T$ is unstable.*

Proof. The result follows from [52, Section 3, Theorem 2]. \square

Proposition 2.5. *Assume conditions in Proposition 2.3 are satisfied and $\mathcal{R}_0 < 1$. Assume further that $\alpha_H = 0$ and $(y_H + v_H)(u_m u_q u_e - gr_m p_1 \tau_1) > \lambda_V \lambda_H u_q u_e$. Then the DFE is globally asymptotically stable.*

Proof. Let $u(t)$ be a solution of system (2.3.7) with $u(0) = u_0 \in \Omega$. Consider system (2.3.7). If we omit f_5 and assume that $\alpha_H = 0$, we have, by the invariance of Ω , that

$$\begin{aligned} f_1(u) &= \lambda_H u_5 u_2 - (y_H + v_H) u_1 \leq \lambda_H u_2 - (y_H + v_H) u_1 \\ f_2(u) &= p_1 u_3 (1 - u_2) - u_m u_2 + \lambda_V (1 - u_2) u_1 \leq p_1 u_3 - u_m u_2 + \lambda_V u_1 \\ f_3(u) &= \tau_1 u_4 (1 - u_3) - u_q u_3 - p_1 u_3 (1 - u_2) \leq \tau_1 u_4 - u_q u_3 \\ f_4(u) &= gr_m u_2 (1 - u_4) - \tau_1 u_4 (1 - u_3) - u_e u_4 \leq gr_m u_2 - u_e u_4 \end{aligned} \quad (2.3.23)$$

Let

$$A = \begin{pmatrix} -(y_H + v_H) & \lambda_H & 0 & 0 \\ \lambda_V & -u_m & p_1 & 0 \\ 0 & 0 & -u_q & \tau_1 \\ 0 & gr_m & 0 & -u_e \end{pmatrix} \quad (2.3.24)$$

Then we may rewrite (2.3.23) as

$$\begin{bmatrix} f_1(u) \\ f_2(u) \\ f_3(u) \\ f_4(u) \end{bmatrix} \leq A \begin{bmatrix} u_1 \\ u_2 \\ u_3 \\ u_4 \end{bmatrix}, \quad (2.3.25)$$

where the inequality holds pointwise.

Now $-A$ has the Z-pattern (see **(A5)**). First observe that $\mathcal{R}_0 < 1 \Rightarrow (\lambda_V \lambda_H)(p_1 + u_q)(\tau_1 + u_e) < (y_H + v_H)((\tau_1 + u_e)(p_1 + u_q)u_m - gr_m p_1 \tau_1) < (y_H + v_H)(\tau_1 + u_e)(p_1 + u_q)u_m$ (*).

Now the principal leading minors of $-A$ are given by $(y_H + v_H)u_m > 0$, $(y_H + v_H)u_m - \lambda_V \lambda_H > 0$ (by (*)), $u_q((y_H + v_H)u_m - \lambda_V \lambda_H) > 0$, and $\det(-A) = ((y_H + v_H)(u_m u_q u_e - gr_m p_1 \tau_1) - \lambda_V \lambda_H u_q u_e) > 0$ (by assumption).

So $-A$ is a nonsingular M-matrix [16, 28], which implies that the eigenvalues of A all have negative real part.

Solving for the differential inequality expressed in (2.3.23), we obtain that

$$\begin{bmatrix} u_1(t) \\ u_2(t) \\ u_3(t) \\ u_4(t) \end{bmatrix} \leq e^{At} \begin{bmatrix} u_1(0) \\ u_2(0) \\ u_3(0) \\ u_4(0) \end{bmatrix} \quad (2.3.26)$$

Now since the eigenvalues of A all have negative real part,

$$\lim_{t \rightarrow \infty} \left(e^{At} \begin{bmatrix} u_1(0) \\ u_2(0) \\ u_3(0) \\ u_4(0) \end{bmatrix} \right) = 0 \quad [38, \text{Section 1.9, Theorem 2}].$$

So $(u_1(t), u_2(t), u_3(t), u_4(t)) \rightarrow 0$ as $t \rightarrow \infty$.

Now by (2.3.4), $\frac{dR_H}{dt} = -\left(\frac{dS_H}{dt} + \frac{dI_H}{dt}\right) = -\left(\frac{u_1}{dt} + \frac{u_5}{dt}\right) = -(-y_H u_1(t) + v_H(1 - u_5(t) - u_1(t))) = y_H u_1(t) - v_H(1 - u_5(t) - u_1(t)) \leq 0$ for all but finitely many t , since $u_1(t) \rightarrow 0$ as $t \rightarrow \infty$, and $u_1(t) + u_5(t) \leq 1 \forall t \geq 0$. So $R_H(t) = 1 - S_H(t) - I_H(t) = 1 - u_1(t) - u_5(t) \rightarrow 0$ as $t \rightarrow \infty$. So $u_5(t) \rightarrow 1$ as $t \rightarrow \infty$ and we have our desired result. \square

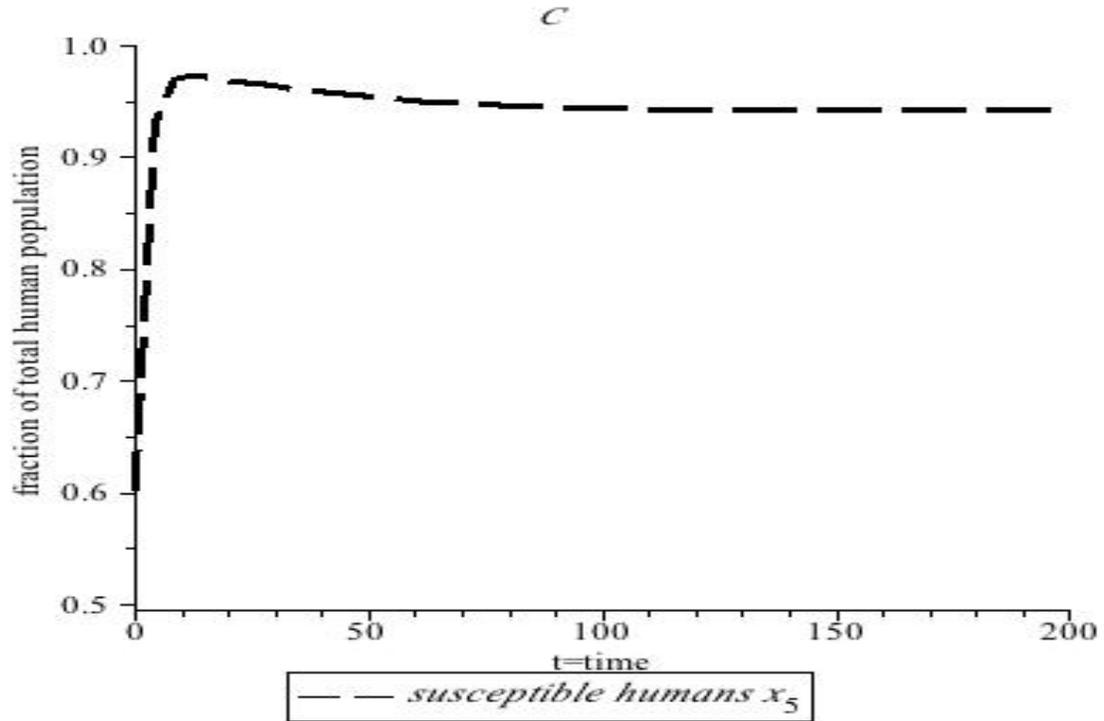


Figure 2.4: Solutions of system (2.3.7) converge to the endemic equilibrium when $\mathcal{R}_0 = 1.05$, all other parameters are given in Table 2.2.

2.3.3 Analysis of the Endemic Equilibria

We are now ready to investigate the existence of endemic equilibria.

First, we set system (2.3.7) to 0. So

$$\begin{aligned}
 \lambda_H x_5 x_2 - (y_H + \alpha_H + v_H) x_1 + \alpha_H x_1^2 &= 0 \\
 p_1 x_3 (1 - x_2) - u_m x_2 + \lambda_V (1 - x_2) x_1 &= 0 \\
 \tau_1 x_4 (1 - x_3) - u_q x_3 - p_1 x_3 (1 - x_2) &= 0 \\
 gr_m x_2 (1 - x_4) - \tau_1 x_4 (1 - x_3) - u_e x_4 &= 0 \\
 v_H - v_H x_5 - \lambda_H x_5 x_2 + \alpha_H x_1 x_5 &= 0
 \end{aligned} \tag{2.3.27}$$

We seek to derive conditions under which $\mathcal{R}_0 > 1 \Leftrightarrow$ system (2.3.7) has an endemic equilibrium. Let $(\bar{x}_1, \bar{x}_2, \bar{x}_3, \bar{x}_4, \bar{x}_5)$ be a solution of system (2.3.27). Then it is given by

$$\begin{aligned}\bar{x}_5 &= \frac{v_H}{v_H + \lambda_H \bar{x}_2 - \alpha_H \bar{x}_1} \\ \bar{x}_4 &= \frac{gr_m \bar{x}_2}{gr_m \bar{x}_2 + \tau_1 - \tau_1 \bar{x}_3 + u_e} \\ \bar{x}_3 &= \frac{\tau_1 \bar{x}_4 + u_q + p_1 - p_1 \bar{x}_2}{\tau_1 \bar{x}_4 + u_q + p_1 - p_1 \bar{x}_2} \\ \bar{x}_2 &= \frac{p_1 \bar{x}_3 + \lambda_V \bar{x}_1}{p_1 \bar{x}_3 + \lambda_V \bar{x}_1 + u_m}\end{aligned}\tag{2.3.28}$$

and

$$-(y_H + \alpha_H + v_H)\bar{x}_1 + \alpha_H \bar{x}_1^2 = -\lambda_H \bar{x}_2 \bar{x}_5.\tag{2.3.29}$$

We will consider the special case $\alpha_H = 0$, $u_q = 0$, $u_e = 0$. We want $(\bar{x}_1, \bar{x}_2, \bar{x}_3, \bar{x}_4, \bar{x}_5)$ to be in Ω . With this in mind, we have the following proposition:

Proposition 2.6. *Let $\alpha_H = 0$, $u_q = 0$, $u_e = 0$, all other parameters positive. Also assume $gr_m < u_m$. Then $\mathcal{R}_0 > 1 \Leftrightarrow$ system (2.3.7) has an endemic equilibrium, E_1 in Ω .*

Proof. \Rightarrow Suppose $\mathcal{R}_0 > 1$. Let $R' = (\mathcal{R}_0)^2 = \frac{\lambda_H \lambda_V}{(y_H + v_H)(u_m - gr_m)}$. Then, $R' > 1$ (*).

If we solve for x_4 in system (2.3.27), we see that it can take on five possible values: 0 and the roots of a degree-four polynomial function f , where $f(x_4)$ has real coefficients (see Appendix I).

By (*), $f(0) > 0$. Now $f(1) = -p_1 \tau_1 \lambda_H u_m (y_H + v_H) (\lambda_H + v_H) (u_m (y_H + v_H) + \lambda_V v_H) < 0$. So by the intermediate value theorem, f has a real root between 0 and 1. If we substitute this value, say b^* , for x_4 in system (2.3.27), and solve for the other components in terms of b^* , we see that system (2.3.27) is consistent. So a solution of system (2.3.27), with $x_4 = b^*$, exists. Additionally, the other solution components are

uniquely determined by b^* . Let E_1 be this solution, so that $\bar{x}_4 = b^*$. Then $0 < \bar{x}_4 < 1$. So E_1 is not the DFE. By (2.3.28) and (2.3.29), $\bar{x}_i \neq 0$ for each i with $1 \leq i \leq 5$. Now $\alpha_H = 0$, $u_q = 0$, $u_e = 0$. So if we add (LHS) of equations 2-4 of (2.3.27), then E_1 is given by

$$\begin{aligned}\bar{x}_1 &= v_H \frac{1-\bar{x}_5}{v_H+y_H} \\ \bar{x}_2 &= v_H \frac{1-\bar{x}_5}{\lambda_H \bar{x}_5} \\ \bar{x}_3 &= \frac{\tau_1 \bar{x}_4}{\tau_1 \bar{x}_4 + p_1 - p_1 \bar{x}_2} \\ \bar{x}_4 &= \frac{\bar{x}_5 - \frac{\lambda_H + v_H R'}{R'(\lambda_H + v_H)}}{gr_m(y_H + v_H)} \\ \bar{x}_5 &= \frac{v_H}{v_H + \lambda_H \bar{x}_2}\end{aligned}\tag{2.3.30}$$

Since $0 < \bar{x}_4 < 1$, by equation 4 of (2.3.30), $\bar{x}_5 > \frac{\lambda_H + v_H R'}{R'(\lambda_H + v_H)}$. So by (*), $\bar{x}_5 > 0$. So by equation 2 of (2.3.30) and (*), $\bar{x}_2 < \frac{v_H \lambda_H (R' - 1)}{\lambda_H (\lambda_H + R' v_H)} < 1$. So by equation 3 of (2.3.30), $0 < \bar{x}_3 < 1$, since $0 < \bar{x}_4 < 1$ and $\bar{x}_2 < 1$. Now since $\alpha_H = 0$, $u_q = 0$, $u_e = 0$, if we evaluate system (2.3.27) at E_1 , we have that $\tau_1 \bar{x}_4 (1 - \bar{x}_3) = gr_m \bar{x}_2 (1 - \bar{x}_4)$. So since $0 < \bar{x}_4 < 1$ and $0 < \bar{x}_3 < 1$, $\bar{x}_2 > 0$. So by equation 5 of (2.3.30), $\bar{x}_5 < 1$. So by equation 1 of (2.3.30) and the fact that $0 < \bar{x}_5 < 1$, $0 < \bar{x}_1 < 1$. Finally, $\bar{x}_1 + \bar{x}_5 = \frac{v_H + \bar{x}_5 y_H}{v_H + y_H} \in [0, 1]$.

\Leftarrow Suppose $\mathcal{R}_0 < 1$. Then $R' < 1$. Consider the equation for \bar{x}_4 , (2.3.30). If $\bar{x}_4 > 0$, then, since $\frac{\lambda_H + v_H R'}{R'(\lambda_H + v_H)} = \frac{\lambda_H}{R'} + v_H > 1$, $\bar{x}_5 > 1$. This implies that $\bar{x}_1 < 0$, a contradiction. \square

We will now study the local stability of the endemic equilibrium, E_1 .

Proposition 2.7. *Assume conditions are as in Proposition 2.6 and $\mathcal{R}_0 > 1$. Then E_1 is locally asymptotically stable.*

Proof. Consider the linearized system of (2.3.7) at E_1 . The Jacobian matrix at E_1 is given by:

$$A = \begin{pmatrix} -(y_H + v_H) & \lambda_H \bar{x}_5 & 0 & 0 & \bar{x}_2 \lambda_H \\ \lambda_V (1 - \bar{x}_2) & -p_1 \bar{x}_3 - u_m - \lambda_V \bar{x}_1 & p_1 - p_1 \bar{x}_2 & 0 & 0 \\ 0 & +p_1 \bar{x}_3 & -p_1 + p_1 \bar{x}_2 - \tau_1 \bar{x}_4 & \tau_1 - \tau_1 \bar{x}_3 & 0 \\ 0 & gr_m - gr_m \bar{x}_4 & +\tau_1 \bar{x}_4 & -gr_m \bar{x}_2 - \tau_1 + \tau_1 \bar{x}_3 & 0 \\ 0 & -\lambda_H \bar{x}_5 & 0 & 0 & a_{55} \end{pmatrix} \quad (2.3.31)$$

where $a_{55} = -v_H - \lambda_H \bar{x}_2$.

Now, given a square, complex-valued $n \times n$ matrix $P = [p_{ij}]$ with $1 \leq i, j \leq n$, we define its *companion matrix* $M(P) = [m_{ij}]$ with $1 \leq i, j \leq n$ by

$$m_{ij} = \begin{cases} |p_{ij}| & \text{if } j = i \\ -|p_{ij}| & \text{if } j \neq i \end{cases} \quad ([28, \text{Definition 2.5.10}], \text{ see also [60]}) \quad (2.3.32)$$

P is called an H -matrix if its companion matrix $M(P)$ is a (non-singular) M -matrix ([28, pp. 124], see also [60]). Now $M(-A)$ has the Z -pattern (see (A5)). Also, by equations 1 and 2 of (2.3.27), the principal leading minors of $M(-A)$ are given by $(y_H + v_H) > 0$, $\frac{1}{\bar{x}_2}(y_H + v_H)(p_1 \bar{x}_3 + \lambda_V \bar{x}_1 \bar{x}_2) > 0$, $\frac{1}{\bar{x}_2}(y_H + v_H)(p_1 \bar{x}_3(1 - \bar{x}_2) + \lambda_V \bar{x}_1 \bar{x}_2)(p_1(1 - \bar{x}_2) + \tau_1 \bar{x}_4) + (y_H + v_H)(p_1 \bar{x}_3)(\tau_1 \bar{x}_4) > 0$, $(y_H + v_H)(\lambda_V \bar{x}_1)p_1(1 - \bar{x}_2)\tau_1(1 - \bar{x}_3) + (y_H + v_H)p_1(1 - \bar{x}_2)gr_m(p_1 \bar{x}_3(1 - \bar{x}_2) + \lambda_V \bar{x}_1 \bar{x}_2) + (y_H + v_H)\tau_1 \bar{x}_4 gr_m(p_1 \bar{x}_3 + \lambda_V \bar{x}_1 \bar{x}_2) > 0$, and $\det(M(-A)) = (v_H + \lambda_H \bar{x}_2)(y_H + v_H)(\lambda_V \bar{x}_1)p_1(1 - \bar{x}_2)\tau_1(1 - \bar{x}_3) + (v_H)(y_H + v_H)p_1(1 - \bar{x}_2)gr_m(p_1 \bar{x}_3(1 - \bar{x}_2) + \lambda_V \bar{x}_1 \bar{x}_2) + (v_H)(y_H + v_H)\tau_1 \bar{x}_4 gr_m(p_1 \bar{x}_3 + \lambda_V \bar{x}_1 \bar{x}_2) + (\lambda_H \bar{x}_2)(y_H + v_H)p_1(1 - \bar{x}_2)gr_m(u_m \bar{x}_2 + \lambda_V \bar{x}_1 \bar{x}_2) + (\lambda_H \bar{x}_2)(y_H + v_H)\tau_1 \bar{x}_4 gr_m(\frac{u_m \bar{x}_2}{1 - \bar{x}_2} + 2\lambda_V \bar{x}_1 \bar{x}_2) > 0$.

So $M(-A)$ is a non-singular M-matrix [16, 28] and $-A$ is an H-Matrix. Now an $n \times n$ complex-valued square matrix is said to be *positive stable* if its eigenvalues all have positive real part [5, pp. 134]. An H-matrix with real entries is positive stable iff it has positive diagonal entries [28, Exercise, pp. 124; 60, Lemma 2]. Now $-A$ clearly has positive diagonal entries. So it is positive stable. It follows that the eigenvalues of A all have negative real part.

So E_1 is locally asymptotically stable. □

2.4 Numerical Simulations

We now conduct numerical simulations to illustrate our analytical results.

Values for $v_H, \lambda_H, y_H, u_m, r_m$ and g are comparable to those presented by Coutinho *et al.* [8] on the basis of estimates known from the dengue infection process and human and mosquito vital statistics. We assume that the entire egg and larval populations are at carrying capacity.

We first take $\alpha_H = u_q = u_e = 0, gr_m = 5 > 1 = u_m$. For parameter values given in column 2 of Table 2.2, an endemic equilibrium exists and is given by $E_1 = (\bar{x}_1, \bar{x}_2, \bar{x}_3, \bar{x}_4, \bar{x}_5) = (.01, .27, .52, .8, .99)$. The simulations show that the DFE is unstable and trajectories of system (2.3.7) converge to E_1 (see Figure 2.5). We see that more than half of the larval and adult mosquito populations will eventually be infected. Additionally, Figure 2.5 A indicates that one percent of the human population will contract the virus, a number that, in the short run, is comparable to the 2009 worldwide estimate of 50 million cases, or 2 percent of the 2.5 billion people at risk [4]. When we take into account that we have assumed in the simulations for

Description	Values for Figure				
	2.5	2.6	2.7, 2.2	2.8, 2.3	2.9, 2.4
Initial Condition					
x_1	.005	.005	.0001	.8	.02
x_2	.1	.1	.001	.33	.03
x_3	.6	.6	.01	.5	.00035
x_4	.5	.5	.005	.33	.002
x_5	.95	.95	.8	.1	.6
Parameter					
v_H	2.5	2.5	2.5	2.5	0.5
λ_H	0.1	0.1	0.75	0.75	0.95
y_H	0.067	0.067	0.067	0.067	0.05
α_H	0	0	0	0.002	0.001
u_q	0	0	0	2.6	10
u_m	1	1	2.6	2.6	1.5
λ_V	0.1	0.1	0.5	0.5	0.95
r_m	20	3	10	10	5
g	0.25	0.25	0.25	0.25	0.25
u_e	0	0	0	2.6	10
τ_1	0.7	0.7	0.7	0.7	0.9
p_1	0.7	0.7	0.7	0.7	0.9

Table 2.2: Values for parameters and variables of Model (2.3.7)

Figure 2.5 that the number of juvenile mosquito deaths is 0, our numbers seem to reasonably approximate the epidemiological picture.

We next reduce the oviposition rate and therefore assume that $gr_m = 3/4 < 1 = u_m$. For parameter values given in column 3 of Table 2.2, $\mathcal{R}_0 = .13$. Accordingly, the simulations show that the DFE is asymptotically stable (see Figure 2.6). We then take λ_H, λ_V large and modify other parameters so that $\mathcal{R}_0 = 1.21$ (see column 4 of Table 2.2). Following Proposition 2.6, there exists an endemic equilibrium of system (2.3.7), given by $E_1 = (.0015, .005, .018, .018, .998)$. The trajectories of system (2.3.7) converge to E_1 , as predicted by Proposition 2.7 (see Figures 2.7 and 2.2).

Because $u_m = 2.6 > 2.5 = gr_m$, however, values for this endemic equilibrium are close to the values for the DFE.

We then take $\alpha_H, u_q, u_e > 0$ and other parameter values such that $\mathcal{R}_0 = .24$ (see column 5 of Table 2.2). The DFE is accordingly asymptotically stable (see Figures 2.8 and 2.3). Finally, we take contact and maturation rates high and human birth and recovery rates low so that $\mathcal{R}_0 = 1.05$. There then exists an endemic equilibrium $E_1 = (.05, .03, .0003, .0038, .94)$. Because by assumption **(A5)** we require that $u_m > gr_m$, the larval, mosquito, and egg populations will remain largely uninfected (see Figure 2.9). But because human-mosquito contact rates are high, eventually 5 percent of the human population will be infected (see Figure 2.9). Assuming that the human population remains constant, this represents, based on 2009 estimates [4], more than an additional 200 million cases of dengue worldwide. An epidemic may therefore ensue even if a low proportion of the vector population is infected. Since high-risk regions often observe high human growth rates, it is reasonable to expect this to be a conservative estimate.

2.5 Discussion

In this chapter, we first explored the temporal dynamics of dengue viral transmission by presenting a model that combines an SIR human host- with a multi-stage SI mosquito vector transmission system. Our model modulates the maturation of the vector from the egg into the larval phase by a climatic factor. In this chapter, we set this factor to 1, in effect assuming that this maturation is not affected by climatic/seasonal variation. We then analyzed this simplified version of the model.

We first proved that if initial conditions are positive, the size of the total human population may vary but will never subside to 0. We then made variable substitutions to obtain a simplified, proportion-based system. Next we assumed that the natural adult mosquito death rate, the natural human birth rate, and the rates at which eggs and juveniles transfer out of their compartments are positive. Under these assumptions, we proved the existence of a threshold parameter, the reproductive number, denoting the expected number of secondary cases produced by a typically infective individual.

In the case where the juvenile populations are at carrying capacity, juvenile mosquito mortality rates are sufficiently small to be absorbed by juvenile maturation rates, and no humans die from dengue, both the analysis and numerical simulations demonstrate that an epidemic will persist if the oviposition rate is greater than the adult mosquito death rate. If the oviposition rate is smaller than the natural adult mosquito death rate, then the stability of the disease-free equilibrium and the ensuing existence of an epidemic will be heavily influenced by human-mosquito contact rates. If these are high, an epidemic may then occur. These results indicate that while intervention at the reproductive phase of the mosquito life-cycle remains necessary, it is more important at the juvenile stages than previously considered. Additionally, if dengue mortality becomes more substantial, restricting human-mosquito contact is crucial (see Section (2.4)).

Since most humans who contract dengue do not die of the virus, the traditional view of dengue has been of a rather benign disease. The sheer scale of the epidemic and the subsequent possibility of the emergence of new, more lethal serotypes, however, are a cause for alarm. As a whole, our conclusions indicate a need for intervention at all levels of the mosquito life-cycle if an epidemic is to be prevented.

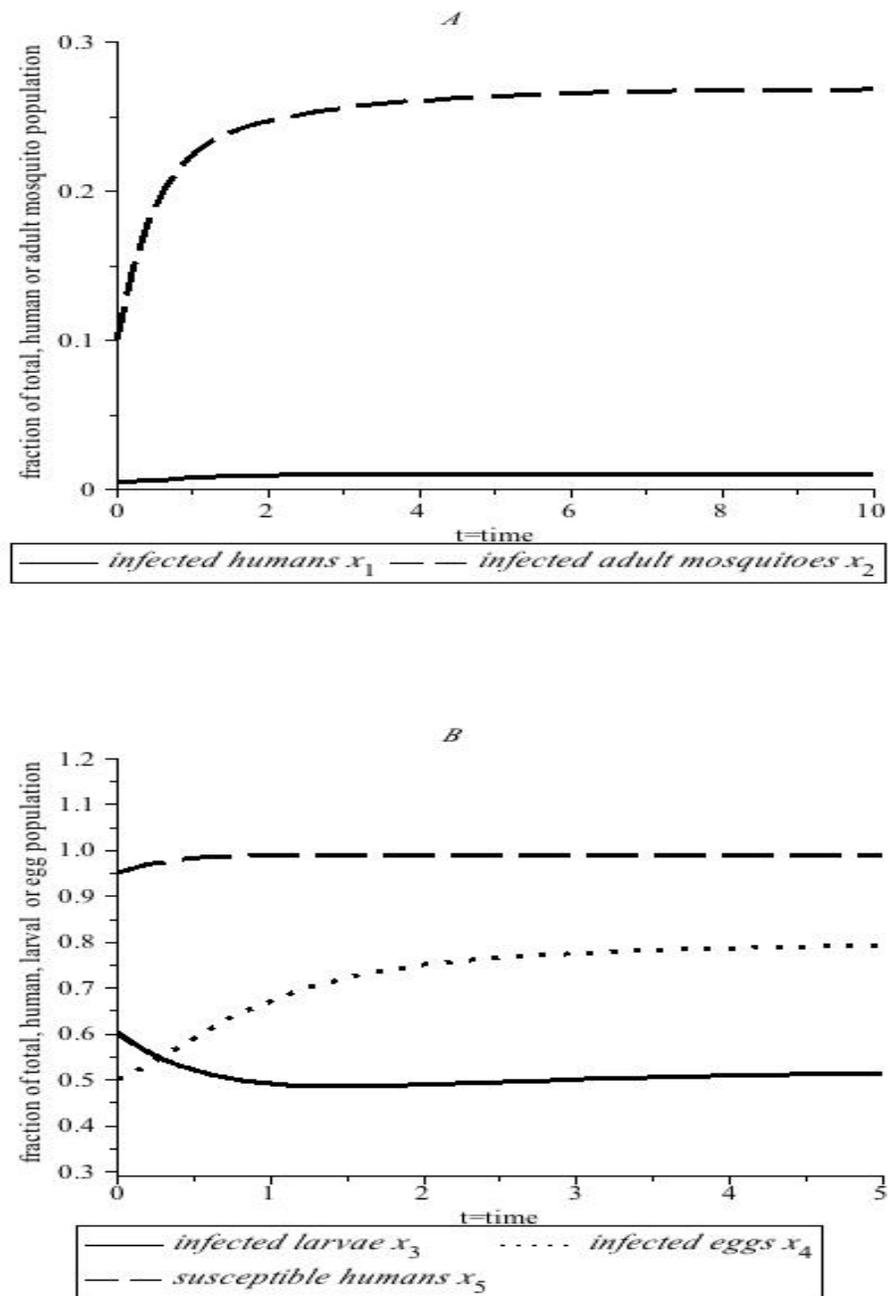


Figure 2.5: Solutions of system (2.3.7) converge to the steady-state values when $gr_m = 5 > 1 = u_m$, all other parameters are given in Table 2.2.

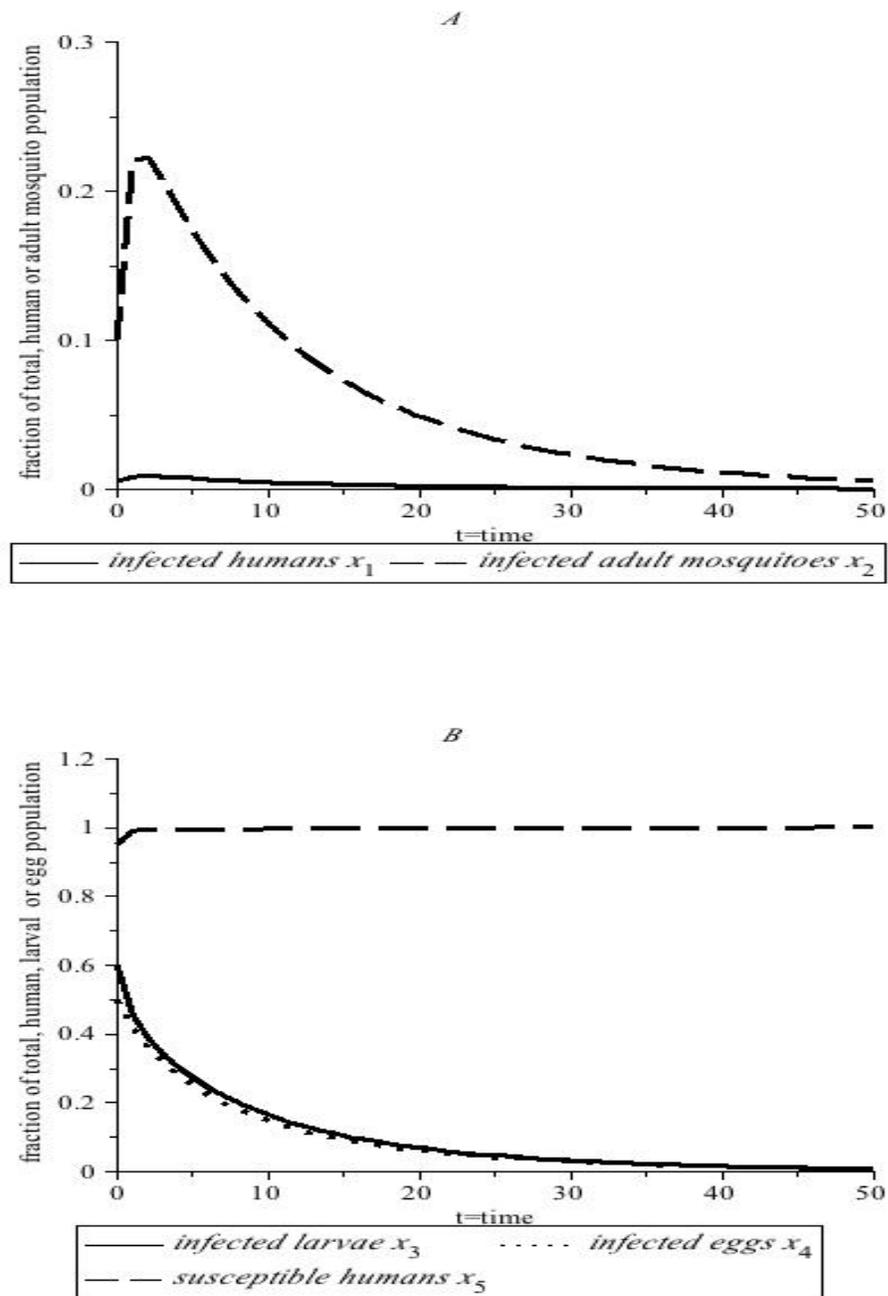


Figure 2.6: Solutions of system (2.3.7) converge to the DFE when $\mathcal{R}_0 = .13$, all other parameters are given in Table 2.2.

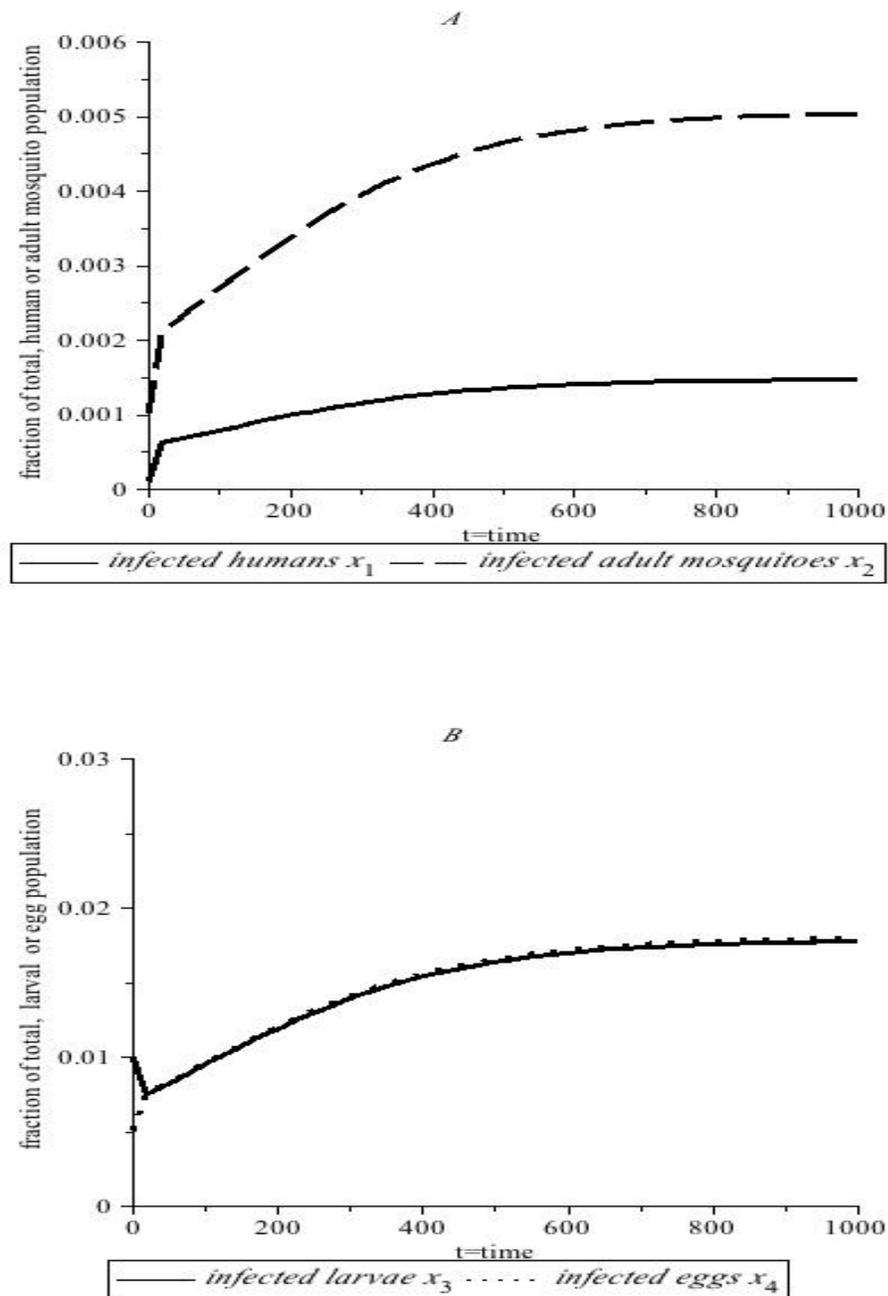


Figure 2.7: Solutions of system (2.3.7) converge to the steady-state values when $\mathcal{R}_0 = 1.21$, all other parameters are given in Table 2.2.

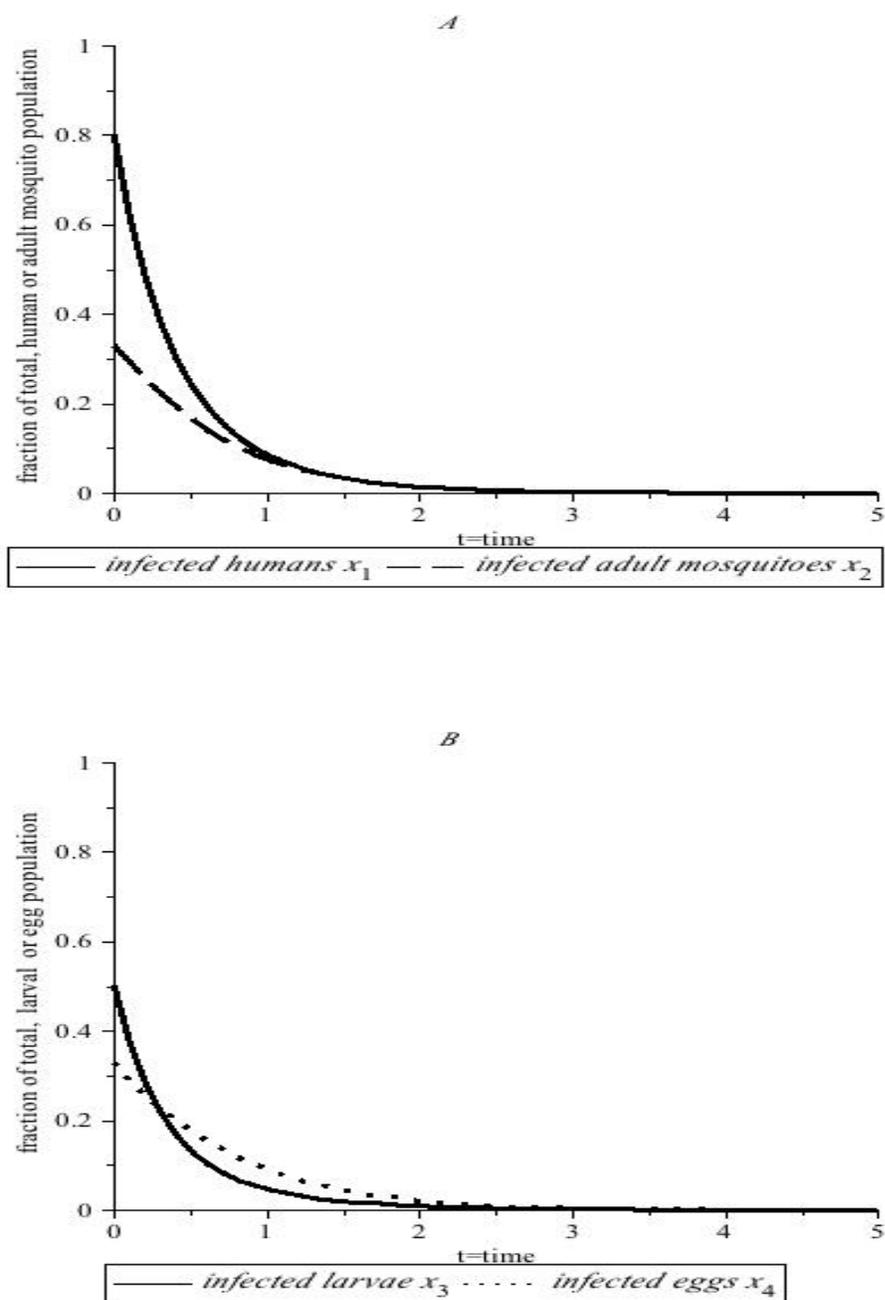


Figure 2.8: Solutions of system (2.3.7) converge to the DFE when $\mathcal{R}_0 = .24$, all other parameters are given in Table 2.2.

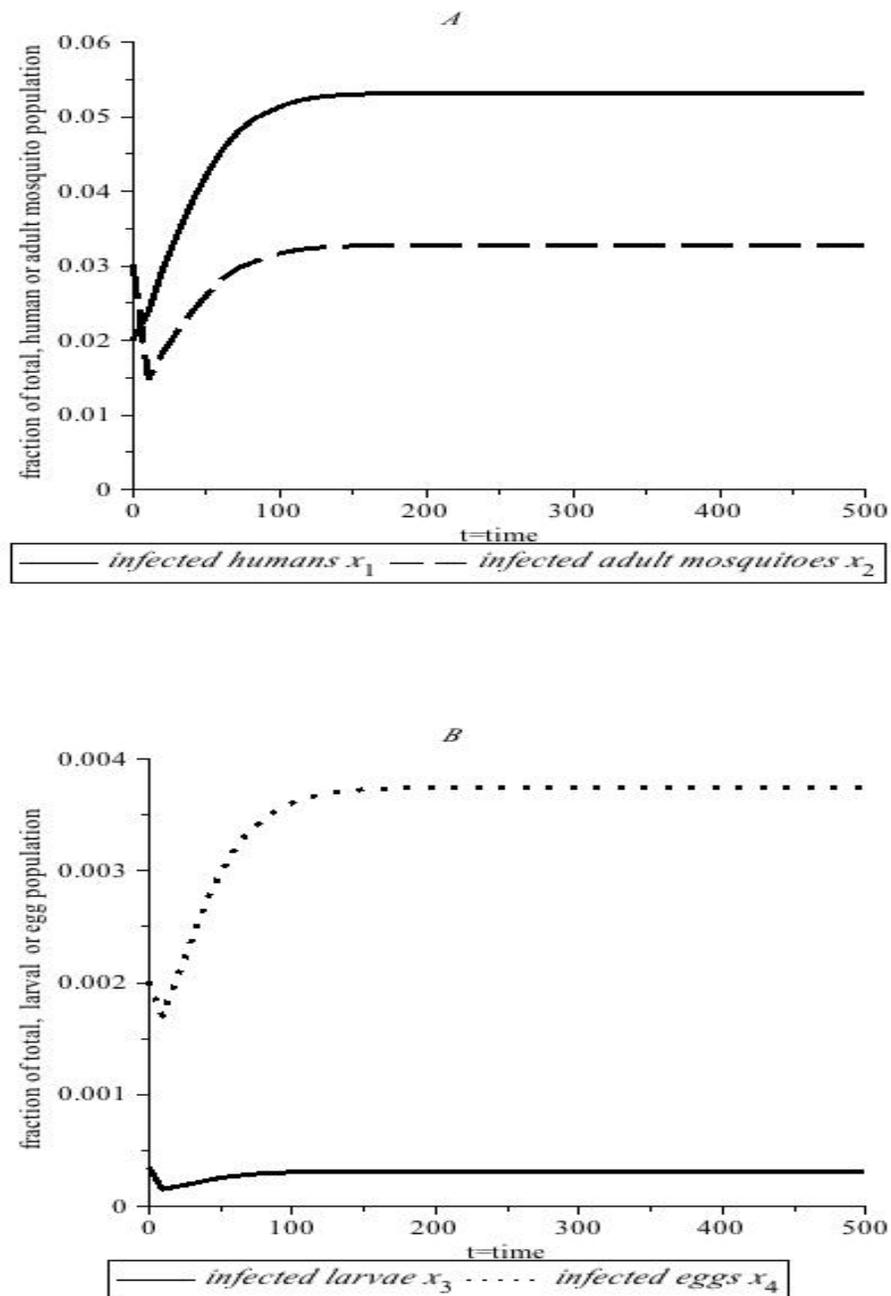


Figure 2.9: Solutions of system (2.3.7) converge to the endemic equilibrium when $\mathcal{R}_0 = 1.05$, all other parameters are given in Table 2.2.

Chapter 3

THE SEASONAL ODE MODEL

3.1 Introduction and Assumptions

In this chapter, we analyze the seasonal ODE model for the transmission of the dengue virus between mosquitoes and humans. Before doing so, we extend the arguments of the previous chapter to motivate the incorporation of seasonality into the modeling of dengue transmission dynamics.

The consideration of seasonality as a factor in the development of a dengue epidemic stems from several observations. First, in certain tropical, subtropical and temperate regions, epidemics recur on a yearly basis and exhibit a fixed seasonal pattern. Secondly, the disease and rain cycles are correlated: the epidemic starts at the beginning of the rainy, spring-summer season, peaks 3-4 months afterward and ends in the beginning of the dry autumn-winter season [8]. During this time, the adult *Aedes aegypti* population virtually disappears. After the dry winter season, the epidemic starts again, a phenomenon defined as disease “over-wintering” [8]. This phenomenon indicates that the mosquito population survives in the wild. Because mosquito eggs are laid in the beginning of autumn, the egg population “hibernates” until the beginning of the winter. Eggs must be laid and hibernate in warm water,

so cold winters and/or dry summers reduce oviposition and affect egg maturation adversely [8]. The degree to which the egg population successfully hibernates is thus correlated with the length and severity of winter. If the winter period is dramatically shortened, the larval population may rise dramatically, contributing to an eventual rise in the adult, infectious mosquito population. Ultimately, the exhibition of a fixed epidemic seasonal pattern and the possible containment of an epidemic are functions of a fixed climatic pattern. If climate is sufficiently disrupted, epidemic patterns may be shifted and containment becomes difficult.

The extent to which the latter may have taken place is extrinsically suggested by the fact that the resurgence of dengue transmission has coincided with evidence of global warming. In Brazil, for example, the first report of a dengue epidemic with viral isolation took place in 1981; the first nation-wide outbreak occurred in 1986, when the epidemic appeared in Rio de Janeiro and other major urban centers [49]. Between 1986-1998, the epidemic exhibited bi-yearly over-wintering, appearing every other year, peaking in the summer and disappearing in the winter. During this period, epidemics were contained. In 1998, however, an exponential increase in the number of cases was reported, marking the first dengue pandemic in Brazil [49]. This increase was attributed to an increase in urban density; a rise in the yearly average temperature, however, may also have influenced the outbreak. Such climatic changes have been recently investigated: according to the Intergovernmental Panel on Climate Change report on global warming, released in Paris in 2007, average temperatures in Brazil's impoverished, semi-arid northeast might rise by between $2^{\circ}C$ and $5^{\circ}C$ by the end of the 21st century [37].

More specifically, climate-based studies and epidemiological models which incorporate climatic factors and successfully predict epidemic outbreaks indicate a correlation

between climatic change and an epidemic resurgence. Using data from meteorological stations, for example, climate-based studies have revealed a relationship between dengue fever/dengue hemorrhagic fever (DF/DHF) outbreaks and climatic variation. Recently, Fuller *et. al* presented a model based on weekly El Niño Southern Oscillation sea-surface temperature observations to predict weekly DF/DHF outbreaks in Costa-Rica from 2003-2007 [19]. Another study investigated the causes of the seasonal outbreak pattern on Samui Island, Thailand [50]. The global nature of the epidemic resurgence further indicates its relationship with climate, the local change of which is affected by changes in disparate geographical areas. A strong El Niño event, for example, took place in 1998. Its climatic effects can be felt in regions that do not share a Pacific coast; regions susceptible to dengue, such as Brazil, are consequently susceptible to El Niño effects, which may have influenced the 1998-99 pandemic. In light of this evidence, we have modulated egg hibernation by a periodic factor, the mechanics upon which are elaborated by Coutinho *et al.* [8].

In this chapter, we reintroduce the main ODE model and take the climatic factor to be periodic. We then conduct the mathematical analysis of the seasonal, non-autonomous ODE model. Following the method devised by Wang and Zhao [54], we establish the numerical computation of the basic reproductive ratio, \mathcal{R}_0 , which, as in the autonomous case, is the expected number of secondary cases produced, in a completely susceptible population, by a typically infective individual. We also derive an analytic expression for \mathcal{R}_1 , the basic reproduction number of the “time-averaged” autonomous system of a periodic epidemic model over a particular time period. The existence of periodic solutions when the disease-free state is unstable is proven. Finally, we conduct numerical simulations to illustrate our analytic results.

3.2 The Seasonal ODE Model

In this and the following section, we present and analyze the seasonal ODE model.

Recall, then, the main ODE model:

$$\begin{aligned}
\frac{d\bar{S}_H}{dt} &= v_H N_H - u_H \bar{S}_H - \lambda_H \bar{S}_H \frac{\bar{I}_M}{N_M} \\
\frac{d\bar{I}_H}{dt} &= \lambda_H \bar{S}_H \frac{\bar{I}_M}{N_M} - (y_H + \alpha_H + u_H) \bar{I}_H \\
\frac{d\bar{R}_H}{dt} &= y_H \bar{I}_H - u_H \bar{R}_H \\
\frac{d\bar{I}_M}{dt} &= p_1 \left(\frac{N_M - \bar{I}_M}{N_M} \right) \bar{I}_P - u_m \bar{I}_M + \lambda_V (N_M - \bar{I}_M) \frac{\bar{I}_H}{N_H} \\
\frac{d\bar{I}_P}{dt} &= \tau_1 S(t) \left(\frac{N_M - \bar{I}_P}{N_M} \right) \bar{I}_E - p_1 \left(\frac{N_M - \bar{I}_M}{N_M} \right) \bar{I}_P - u_q \bar{I}_P \\
\frac{d\bar{I}_E}{dt} &= gr_m \left(\frac{N_M - \bar{I}_E}{N_M} \right) \bar{I}_M - \tau_1 S(t) \left(\frac{N_M - \bar{I}_P}{N_M} \right) \bar{I}_E - u_e \bar{I}_E
\end{aligned} \tag{3.2.1}$$

with $N_M \geq \bar{I}_M(0)$, $N_M \geq \bar{I}_P(0)$, $N_M \geq \bar{I}_E(0)$, $N_M > 0$, $N_H(0) > 0$, $v_H \geq u_H > 0$.

The parameters in Model (3.2.1) can be understood by referring to Table 2.1. In this chapter, we henceforth assume that all constant parameters are nonnegative.

Observe that the fifth and sixth equations incorporate the concept of seasonality, the modeling of which we borrow from Coutinho *et al.* [8].

The infected larval population density may vary in size with a t -dependent rate,

$$\tau_1 S(t) \left(\frac{N_M - \bar{I}_P}{N_M} \right), \quad (3.2.2)$$

determining the number of infected eggs hatching per unit time and surviving to the larval stage, that is, through winter. In this chapter, S , a time- dependent climatic index depicting seasonal variation, is allowed to be non-constant. In fact, it is set to the ω -periodic seasonality function,

$$t \rightarrow (c - d(\sin(2\pi wt + \sigma)))\theta(c - d(\sin(2\pi wt + \sigma))) \quad (3.2.3)$$

which simulates climatic influence on the larval maturation rate. By setting $w=1/365$, one reproductive cycle, taking place over the course of one year, is fixed, with $\omega=365$. The terms c and d refer to winter mildness and length, respectively. The Heaviside θ -function ensures the term is nonnegative. So if $c < d$, with c small and d large, summer and winter are long and winter is severe. If $c > d$, with c large and d small, summer and winter are short and winter is mild. Maturation into the larval stage is therefore influenced accordingly and progression into it becomes a function of seasonality. Note that the element of vertical transmission is present in the sixth equation, represented by the parameter g , which also absorbs the fraction of male eggs, inconsequential with respect to the transmission of the dengue virus. For further discussion of the seasonality effect, see Coutinho *et al.* [8].

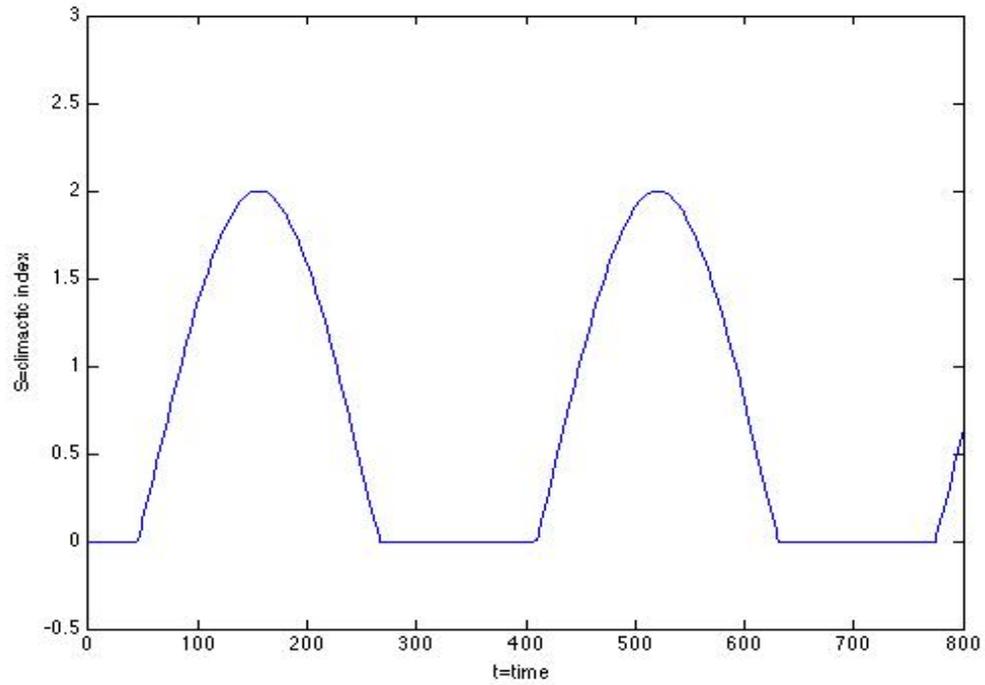


Figure 3.1: Climatic index as function of time, $c = .5$, $d = 1.5$, $\sigma = 90$, $w = 1/365$, units are given in Table 2.1. See Remark at end of Section 3.4.

Note that $\frac{dN_H}{dt} = \frac{d\bar{S}_H}{dt} + \frac{d\bar{I}_H}{dt} + \frac{d\bar{R}_H}{dt}$. So if we add the RHS (right-hand side) of equations 1 - 3 of Model (3.2.1) we obtain the following equation:

$$\frac{dN_H}{dt} = (v_H - u_H)N_H - \alpha_H \bar{I}_H \quad (3.2.4)$$

We now add this equation to Model (3.2.1).

3.3 Analysis of the Seasonal Model

Define $f : [0, \infty)^8 \rightarrow R^7$ by $f(t, y) = (f_1(t, y), \dots, f_7(t, y))$, where $f_i : [0, \infty)^8 \rightarrow R$ is defined by $f_i(t, y) = \frac{dy_i}{dt}$ for each i with $1 \leq i \leq 7$.

System (3.2.1) then allows us to define an initial value problem

$$\begin{aligned} \dot{y} &= f(t, y) \\ y(0) &= y_0 \end{aligned} \tag{3.3.1}$$

where $y = (\bar{S}_H, \dots, N_H)$.

Observe that if $y_0 \in [0, \infty)^7$, then $f(t, y)$ is continuous in t on some small interval $[0, \beta]$, where $f(t, y) \in R_+^7$ for each $t \in [0, \beta]$. Also, $f(t, y)$ is continuously differentiable in y for all $y \in R_+^7$. So if $y_0 \in R_+^7$, by the Picard-Lindelof theorem, IVP (3.3.1) has a unique solution.

Theorem 3.1. *Let $y_0 \in R_+^7$. Any solution $\Phi(t, 0, y_0)$ of IVP (3.3.1) through $(0, y_0)$ is defined for all $t \geq 0$, and R_+^7 is positively invariant.*

Proof. On a fixed interval $[0, \beta)$, with β real, let $\Phi(t, 0, y_0^*) = (y_1^*(t), \dots, y_7^*(t))$ be a fixed solution of IVP (3.3.1) through $(0, y_0^*)$ with $y_0^* \in R_+^7$. Observe that $0 \leq S(t) \leq c+d$ for all $t \geq 0$. By the continuity of the solution on $[0, \beta)$, there exists a δ with $0 < \delta < \beta$ such that $y_1^*(t') > 0, \dots, y_7^*(t') > 0$ for any $t' \in [0, \delta]$.

Now $y_4^*(0) = \bar{I}_M^*(0) \leq N_M$. Further, if $N_M = \bar{I}_M^*(t')$ for some t' in $[0, \delta]$, $\frac{d\bar{I}_M^*(t')}{dt} \leq 0$. The previous two statements also hold for $y_5^*(t) = \bar{I}_P^*(t)$, $y_6^*(t) = \bar{I}_E^*(t)$. By Theorem 4.2 in ([26]) and the continuity of each solution component on $[0, \delta]$, $\frac{y_4^*(t)}{N_M} \leq 1$ on $[0, \delta]$. The latter also holds for $y_5^*(t)$, $y_6^*(t)$.

By reasoning similar as in the proof of Theorem 2.1 , we have that, on $[0, \delta]$,

$$\frac{dy_1^*}{dt} \geq y_1^*(-u_H - \lambda_H).$$

We may obtain similar inequalities for the other components.

So on $[0, \delta]$, by the comparison principle [44, Chapter 3, Proposition 1.1 and Remark 1.2],

$$y_1^*(t) \geq e^{(-u_H - \lambda_H)t} y_{10}^* > 0. \quad (3.3.2)$$

The positivity of the other components on $[0, \delta]$ can be shown similarly. By the continuity of $y_1^*(t)$ on $[0, \beta)$, equation (3.3.2) holds on $[0, \beta)$. So $y_1^*(t)$ is bounded below by a positive number on $[0, \beta)$. The same holds for the other components on $[0, \beta)$. So $\lim_{t \rightarrow \beta^-} y^*(t) > 0$ and $y^*(t)$ can be continuously extended to $[0, \beta]$.

Consequently, on $[0, \beta]$, R_+^7 is invariant under system (3.2.1) [26, Theorem 4.2]. So $[0, \infty)$ is the maximal interval of existence of $\Phi(t, 0, y_0^*)$ [38, Section 2.4, Theorems 3 and 4 and Problem 3, Problem Set 4]. At each $t \geq 0$, each solution component is therefore positive. Therefore, R_+^7 is positively invariant. \square

We will now follow the method outlined by Esteva and Vargas [11] to introduce proportions to system (3.2.1). This is possible by either treating (3.2.1) as an autonomous system in 8 variables, strictly for the purpose of variable substitution, or by differentiating each new variable point-wise. The equivalence of systems (3.2.1) and (3.3.4) holds at each $t' \geq 0$, and therefore, at every $t' \geq 0$.

For each $t \in R_{\geq 0}$, then, let

$$\begin{aligned}\frac{\bar{S}_H(t)}{N_H(t)} &= S_H(t), \quad \frac{\bar{I}_H(t)}{N_H(t)} = I_H(t) \\ \frac{\bar{R}_H(t)}{N_H(t)} &= R_H(t), \quad \frac{\bar{I}_M(t)}{N_M} = I_M(t) \\ \frac{\bar{I}_P(t)}{N_M} &= I_P(t), \quad \frac{\bar{I}_E(t)}{N_M} = I_E(t).\end{aligned}\tag{3.3.3}$$

We assume $N_H(t) > 0$ for each $t \in R_{\geq 0}$, and $N_M > 0$. We may do so since by Theorem 3.1, if $N_H(0) > 0$, $N_H(\cdot)$ remains positive for all $t \geq 0$.

System (3.2.1) can therefore be written as

$$\begin{aligned}\frac{dS_H}{dt} &= v_H - v_H S_H - \lambda_H S_H I_M + \alpha_H S_H I_H \\ \frac{dI_H}{dt} &= \lambda_H S_H I_M - (y_H + \alpha_H + v_H) I_H + \alpha_H I_H^2 \\ \frac{dI_M}{dt} &= p_1 I_P (1 - I_M) - u_m I_M + \lambda_V (1 - I_M) (I_H) \\ \frac{dI_P}{dt} &= \tau_1 S(t) I_E (1 - I_P) - p_1 I_P (1 - I_M) - u_q I_P \\ \frac{dI_E}{dt} &= gr_m I_M (1 - I_E) - \tau_1 S(t) I_E (1 - I_P) - u_e I_E\end{aligned}\tag{3.3.4}$$

with $1 \geq S_H(0) \geq 0$, $1 \geq I_H(0) \geq 0$, $1 \geq S_H(0) + I_H(0) \geq 0$, $1 \geq I_M(0) \geq 0$, $1 \geq I_P(0) \geq 0$, $1 \geq I_E(0) \geq 0$, $v_H > 0$.

Corollary 3.2. *Let $\Omega' = \{(S_H, I_H, I_M, I_P, I_E) : 0 \leq S_H \leq 1, 0 \leq I_H \leq 1, 0 \leq S_H + I_H \leq 1, 0 \leq I_M \leq 1, 0 \leq I_P \leq 1, 0 \leq I_E \leq 1\}$. Then Ω' is positively invariant for system (3.3.4).*

Proof. Let $(S_H^*(t), \dots, I_E^*(t))$ be a fixed solution of system (3.3.4) through $(0, (S_{H_0}^*, \dots, I_{E_0}^*))$ with $(S_{H_0}^*, \dots, I_{E_0}^*) \in \Omega'$.

Suppose $(S_H^*(0), \dots, I_E^*(0))$ is on $Bde(\Omega')$. (*)

By reasoning similar as in the proof of Corollary 2.2 in Chapter 2 and (*), we have that $\frac{dS_H^*(0)}{dt} \geq 0$ if $S_H^*(0) = 0$ and $\frac{dS_H^*(0)}{dt} \leq 0$ if $S_H^*(0) = 1$. We may obtain similar results for $I_H^*(t), S_H^*(t) + I_H^*(t), I_M^*(t)$.

By equations 4 and 5 of (3.3.4) and (*), if $I_P^*(0) = 0$, $\frac{dI_P^*(0)}{dt} = \tau_1 S(0) I_E^*(0) \geq 0$, since $0 \leq S(t) \leq c + d$; and if $I_E^*(0) = 0$, $\frac{dI_E^*(0)}{dt} = gr_m I_E^*(0) \geq 0$.

Finally, by equations 4 and 5 of (3.3.4) and (*), if $I_P^*(0) = 1$, $\frac{dI_P^*(0)}{dt} = -p_1(1 - I_M^*(0)) - u_q \leq -u_q \leq 0$; and if $I_E^*(0) = 1$, $\frac{dI_E^*(0)}{dt} = -\tau_1 S(0)(1 - I_P^*(0)) - u_e \leq 0$, since $0 \leq S(t) \leq c + d$. (**)

Suppose $(S_{H_0}^*, \dots, I_{E_0}^*)$ is in $Interior(\Omega')$. (+)

Let $t_0 = inf\{t \in (0, \infty) : (S_H^*(t), \dots, I_E^*(t)) \text{ on } Bde(\Omega')\}$. (++)

By the continuity of the solution on $[0, \infty)$, $(S_H^*(t), \dots, I_E^*(t)) \in Interior(\Omega')$ on $[0, t_0)$. So $\lim_{t \rightarrow t_0^-} (S_H^*(t), \dots, I_E^*(t)) \in \overline{\Omega'}$. So we may substitute t_0 for 0 in the arguments following (*), so that (**) holds at t_0 . (***)

If we substitute any $t' \in [0, \infty)$ for 0 in (+) and t_ν for t_0 in (++), (***) holds. (+++)

By (**), (***), (+++) and [26, Proposition 3.3], we have our result. \square

Observe that system (3.3.4) does not depend on N_H . In fact, we have,

$$\frac{dN_H}{dt} = (v_H - u_H - a_H I_H)N_H. \quad (3.3.5)$$

Note that the first two equations of system (3.3.4) and equation (3.3.5) are exactly those obtained by Esteva and Vargas [11, system (2.2)].

3.3.1 The Basic Reproductive Ratio for a Non-Autonomous ODE System

If we set system (3.3.4) and the infective states to 0, we obtain a disease-free steady state (DFS) $= (1, 0, 0, 0, 0)^T$. Since the entire human population is susceptible in the absence of disease, the DFS is the only disease-free steady state. We seek to derive \mathcal{R}_0 , the basic reproductive ratio and threshold parameter for the local stability of the DFS [54]. We follow the method described by Wang and Zhao [54], who devise a way to define and compute the basic reproduction ratio associated with periodic epidemic models. Wang and Zhao define \mathcal{R}_0 as the spectral radius of the “next infection operator,” which gives the cumulative distribution of new infections at some fixed time t , given an initial distribution of infective individuals at some previous time [54]. \mathcal{R}_0 is shown to be a threshold parameter: if $\mathcal{R}_0 < 1$, then the DFS is asymptotically stable. If $\mathcal{R}_0 > 1$, then the DFS is unstable and an epidemic may develop.

3.3.2 The Compartmentalized Seasonal Model and Analysis of Threshold Parameters

Consider the mosquito and human populations compartmentalized in the 5 classes of system (3.3.4). Let $x = (x_1, \dots, x_5)^T$, with $x \in \Omega'$, be the state of individuals in each compartment (see Subsection 2.3.2 for an explanation of the compartmentalized model for a proportion-based system). The first 4 compartments correspond to the infected components.

More specifically, we have that $I_H = x_1$, $I_M = x_2$, $I_P = x_3$, $I_E = x_4$, and $S_H = x_5$. Then $\Omega' = \{(x_1, x_2, x_3, x_4, x_5) : 0 \leq x_i \leq 1 \text{ for } 1 \leq i \leq 5; 0 \leq x_1 + x_5 \leq 1\}$.

So by system (3.3.4),

$$\begin{aligned} \frac{dx_1}{dt} &= \lambda_H x_5 x_2 - (y_H + \alpha_H + v_H)x_1 + \alpha_H x_1^2 \\ \frac{dx_2}{dt} &= p_1 x_3 (1 - x_2) - u_m x_2 + \lambda_V (1 - x_2)x_1 \\ \frac{dx_3}{dt} &= \tau_1 S(t)x_4(1 - x_3) - u_q x_3 - p_1 x_3(1 - x_2) \\ \frac{dx_4}{dt} &= gr_m x_2(1 - x_4) - \tau_1 S(t)x_4(1 - x_3) - u_e x_4 \\ \frac{dx_5}{dt} &= v_H - v_H x_5 - \lambda_H x_5 x_2 + \alpha_H x_1 x_5 \end{aligned} \tag{3.3.6}$$

where $v_H > 0$, $(x_{1_0}, \dots, x_{5_0}) \in \Omega'$.

Define X_S to be the set of all disease-free states. That is,

$$X_S = \{x \in \Omega' : x_i = 0, i = 1, \dots, 4\}. \tag{3.3.7}$$

Let $\mathcal{F}_i(t, x)$ be the input rate of newly infected individuals in the i th compartment, $\mathcal{V}_i^+(t, x)$ be the input rate by all other means, and $\mathcal{V}_i^-(t, x)$ be the rate of transfer of individuals out of compartment i . Observe that system (3.3.6) may be written as

$$\frac{dx_i}{dt} = f_i(t, x) = \mathcal{F}_i(t, x) - \mathcal{V}_i(t, x), \quad i = 1, \dots, 5 \quad (3.3.8)$$

where $\mathcal{V}_i = \mathcal{V}_i^- - \mathcal{V}_i^+$ for each i with $1 \leq i \leq 5$.

The following assumptions can be made (see [54]):

Assumption(A1N): For each i with $1 \leq i \leq 5$, $\mathcal{F}_i(t, x)$, $\mathcal{V}_i^+(t, x)$, $\mathcal{V}_i^-(t, x)$ are nonnegative and continuous on $[0, \infty) \times \Omega'$ and continuously differentiable in x .

All parameters are nonnegative and $0 \leq S(t) \leq c + d$, where c, d are as in (3.2.3). So we have, $\mathcal{F}_1(t, x) = \lambda_H x_5 x_2 \geq 0$, $\mathcal{V}_1^+(t, x) = \alpha_H x_1^2 \geq 0$, $\mathcal{V}_1^-(t, x) = (y_H + \alpha_H + v_H)x_1 \geq 0$, $\mathcal{F}_2(t, x) = \lambda_V(1 - x_2)x_1 \geq 0$, $\mathcal{V}_2^+(t, x) = +p_1 x_3(1 - x_2) \geq 0$, $\mathcal{V}_2^-(t, x) = u_m x_2 \geq 0$, $\mathcal{F}_3(t, x) = 0$, $\mathcal{V}_3^+(t, x) = \tau_1 S(t)x_4(1 - x_3) \geq 0$, $\mathcal{V}_3^-(t, x) = p_1 x_3(1 - x_2) + u_q x_3 \geq 0$, $\mathcal{F}_4(t, x) = 0$, $\mathcal{V}_4^+(t, x) = gr_m x_2(1 - x_4) \geq 0$, $\mathcal{V}_4^-(t, x) = \tau_1 S(t)x_4(1 - x_3) + u_e x_4 \geq 0$, $\mathcal{F}_5(t, x) = 0$, $\mathcal{V}_5^+(t, x) = v_H + \alpha_H x_5 x_1 \geq 0$, $\mathcal{V}_5^-(t, x) = v_H x_5 + \lambda_H x_5 x_2 \geq 0$.

For each i , $\mathcal{F}_i(t, \cdot)$, $\mathcal{V}_i^+(t, \cdot)$, $\mathcal{V}_i^-(t, \cdot)$ are polynomial functions. Now S is well-defined and continuous, and $0 \leq S(t) \leq c + d$, where c, d are as in (3.2.3). So for each i , $\mathcal{F}_i(t, \cdot)$, $\mathcal{V}_i^+(t, \cdot)$, $\mathcal{V}_i^-(t, \cdot)$ are continuously differentiable on Ω' . Also, by the continuity of S , for each i , $\mathcal{F}_i(\cdot, x)$, $\mathcal{V}_i^+(\cdot, x)$, $\mathcal{V}_i^-(\cdot, x)$ are continuous on $[0, \infty)$. So we have our result.

Assumption(A2N): There is a real number $\omega > 0$ such that for each $1 \leq i \leq 5$, the functions $\mathcal{F}_i(t, x)$, $\mathcal{V}_i^+(t, x)$, $\mathcal{V}_i^-(t, x)$ are ω -periodic in t .

As mentioned we set $w = 1/365$ (see Table 2.1). Then $S(t) = (c - d(\sin(2\pi wt + \sigma)))\theta(c - d(\sin(2\pi wt + \sigma)))$ has period $\omega = 365$.

This implies that for each i , $\mathcal{F}_i(\cdot, x)$ is ω -periodic. The same holds for $\mathcal{V}_i^+(\cdot, x)$, $\mathcal{V}_i^-(\cdot, x)$.

Assumption (A3N): If $x_i = 0$, then $\mathcal{V}_i^- = 0$. In particular, if $x \in X_S$, then $\mathcal{V}_i^- = 0$ for $i = 1, \dots, 4$.

The first claim follows from the paragraph following **(A1N)**. Now if $x \in X_S$, $x_i = 0$ for $i = 1, \dots, 4$. So the second claim follows from the first.

Assumption(A4N): $\mathcal{F}_i = 0$ if $i = 5$.

Follows from paragraph following **(A1N)**.

Assumption(A5N): If $x \in X_S$, $\mathcal{F}_i(t, x) = 0$, and $\mathcal{V}_i^+(t, x) = 0$ for $i = 1, \dots, 4$.

If $x \in X_S$, $x_i = 0$ for $i = 1, \dots, 4$. So result follows from paragraph following **(A1N)**.

Let $f = (f_1, \dots, f_n)^T$, the DFS = $x^0(t) = (0, 0, 0, 0, 1)^T$, and define an 1×1 matrix

$$M(t) := \left(\frac{\partial f_i(t, x^0(t))}{\partial x_j} \right)_{i=5}. \quad (3.3.9)$$

Let $\Phi_M(t)$ be the fundamental matrix solution of the linear ω -periodic system $\frac{dz}{dt} = M(t)z$. We have,

Assumption(A6N): $\rho(\Phi_M(\omega)) < 1$, where $\rho(\Phi_M(\omega))$ is the spectral radius of $\Phi_M(\omega)$.

Now $M(t) = (-v_H)$. Since by assumption $v_H > 0$, the result is immediate.

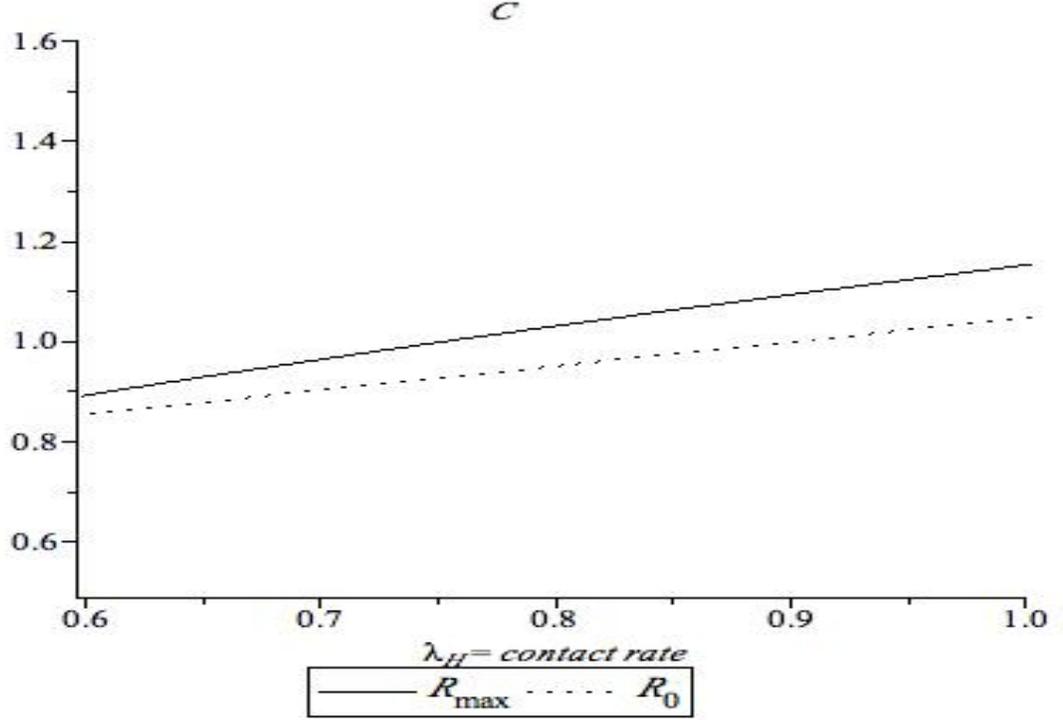


Figure 3.2: The graph of the basic reproduction ratio \mathcal{R}_0 and $\mathcal{R}_{0_{\max}}$ when λ_H varies.

Assumptions (A1N)-(A6N) imply that

$$D_x \mathcal{F}(t, x^0(t)) = \begin{pmatrix} F(t) & 0 \\ 0 & 0 \end{pmatrix}, \quad D_x \mathcal{V}(x^0(t)) = \begin{pmatrix} V(t) & 0 \\ J(t) & -M(t) \end{pmatrix},$$

where $F(t)$ and $V(t)$ are the 4×4 matrices defined by

$$F(t) = \left(\frac{\partial \mathcal{F}_i(t, x^0(t))}{\partial x_j} \right)_{1 \leq i, j \leq 4} \quad \text{and} \quad V(t) = \left(\frac{\partial \mathcal{V}_i(t, x^0(t))}{\partial x_j} \right)_{1 \leq i, j \leq 4},$$

respectively, and $J(t)$ is a 1×5 matrix. $F(t)$ is non-negative, and $-V(t)$ is cooperative [54, (2.2)].

Following [54], let $Y(t, s)$, $t \geq s$, be the evolution operator of the linear ω -periodic system

$$\frac{dy}{dt} = -V(t)y. \quad (3.3.10)$$

So for each $s \in R$, the 4×4 matrix $Y(t, s)$ satisfies

$$\frac{d}{dt}Y(t, s) = -V(t)Y(t, s), \quad \forall t \geq s, \quad Y(s, s) = I \quad (3.3.11)$$

where I is the identity matrix. The fundamental matrix solution $\Phi_{-V}(t)$ of (3.3.10) $= Y(t, 0)$, $\forall t \geq 0$. We have

Assumption(A7N): $\rho(\Phi_{-V}(\omega)) < 1$.

Observe that

$$V(t) = \begin{pmatrix} y_H + \alpha_H + v_H & 0 & 0 & 0 \\ 0 & u_m & -p_1 & 0 \\ 0 & 0 & u_q + p_1 & -\tau_1 S(t) \\ 0 & -gr_m & 0 & \tau_1 S(t) + u_e \end{pmatrix} \quad (3.3.12)$$

By (3.3.11), the identity matrix is a fundamental matrix solution for (3.3.10), that is, $\Phi_{-V}(0) = I$. If we equip R_4 with a matrix norm, by (A1N) and (A2N), the matrix-valued function $V(t)$ is continuous, competitive, and ω -periodic. By Floquet's theorem [38], for any $t \in R$, any fundamental matrix solution $\Phi_{-V}(t)$ for (3.3.10) can be written as $\Phi_{-V}(t) = Q(t)e^{Bt}$ where $Q(t)$ is a non-singular, differentiable, ω -periodic matrix and B is a constant matrix. Floquet's theorem implies that since $\Phi_{-V}(0) = I$, $Q(0) = Q(\omega) = I$. So $\Phi_{-V}(\omega) = e^{B\omega}$. Now by Liouville's Theorem [38],

$\det(e^{B\omega}) = \exp\left(\int_0^\omega \text{tr}(-V(t)) dt\right) \leq \exp(-(\omega(y_H + \alpha_H + v_H + u_m + u_q + p_1 + u_e)))$.
 So $\det(e^{-B\omega}) \geq \exp((\omega(y_H + \alpha_H + v_H + u_m + u_q + p_1 + u_e))) > 1$, which implies that
 $\rho(\Phi_V(\omega)) > 1$. Now $1/z$ is analytic on the punctured plane. So by [42, Theorem
 6.17], $\rho(\Phi_V(\omega)) = \frac{1}{\rho(\Phi_{-V}(\omega))}$. So $\rho(\Phi_V(\omega)) * \rho(\Phi_{-V}(\omega)) = 1$. So $\rho(\Phi_{-V}(\omega)) < 1$.

We also have that

$$F(t) = \begin{pmatrix} 0 & \lambda_H & 0 & 0 \\ \lambda_V & 0 & 0 & 0 \\ 0 & 0 & 0 & 0 \\ 0 & 0 & 0 & 0 \end{pmatrix} \quad (3.3.13)$$

If we omit f_5 , we obtain the linearization of system (3.3.6) at the DFS:

$$\frac{dx}{dt} = (F(t) - V(t))x. \quad (3.3.14)$$

where $x = (x_1, \dots, x_4)^\omega$. We shall return to this system later.

We now establish \mathcal{R}_0 .

Following both [33] and [54, (2.6)], let C_ω be the Banach space of all ω -periodic functions from R to R^4 , equipped with the *sup* norm. We define $L : C_\omega \rightarrow C_\omega$ by

$$(L\psi)(t) = \int_0^\infty Y(t, t-a)F(t-a)\psi(t-a) da, \quad \forall t \in R, \psi \in C_\omega. \quad (3.3.15)$$

L is the next infection operator, since $(L\psi)(t)$ is the distribution of new infections at time t produced by infective individuals who were infected at time $t-a$. The basic reproduction ratio is therefore $\mathcal{R}_0 := \rho(L)$, the spectral radius of L [52, 54].

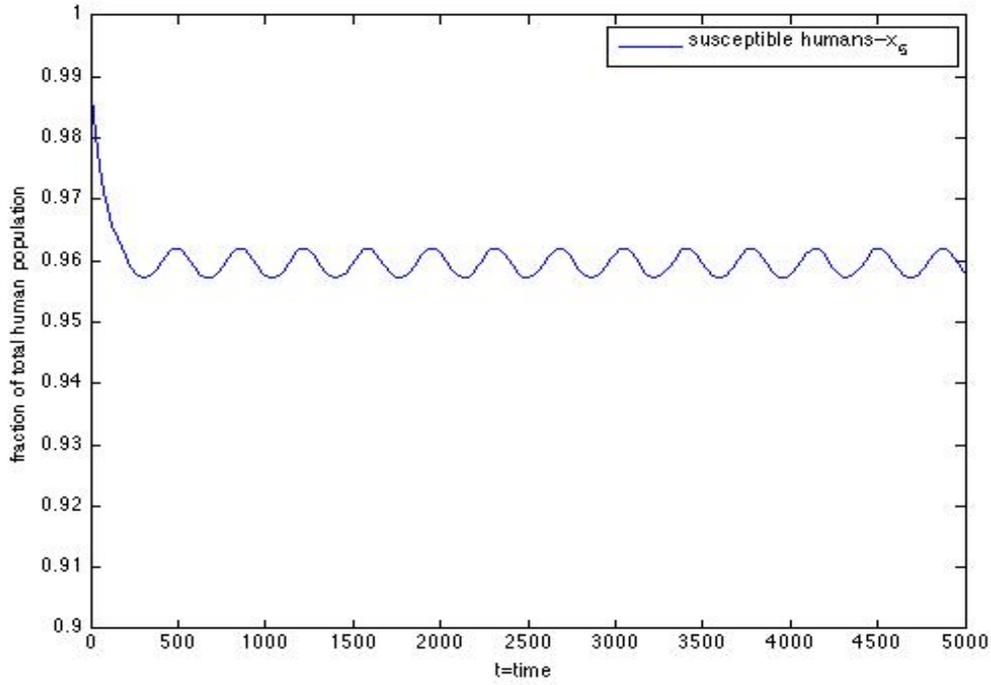


Figure 3.3: Positive periodic solutions of system (3.3.6) when $\mathcal{R}_0 = 1.03$, $d = 1 < 1.5 = c$, $\sigma = 0$, all other parameters are given in Table 3.1.

Following [54], let $W(t, s, \lambda)$, $t \geq s$, $s \in R$, be the fundamental matrix solution of the following ω -periodic system

$$\frac{dq(t)}{dt} = \left(-V(t) + \frac{1}{\lambda} F(t) \right) q(t), \quad t \in R, \quad (3.3.16)$$

with parameter $\lambda \in (0, \infty)$.

Given (A1N) – (A7N), we have the following results:

(i) If $\rho(W(\omega, 0, \lambda)) = 1$ has a positive solution λ_0 , then λ_0 is an eigenvalue of L , and hence $\mathcal{R}_0 > 0$ [54, Theorem 2.1 (i)].

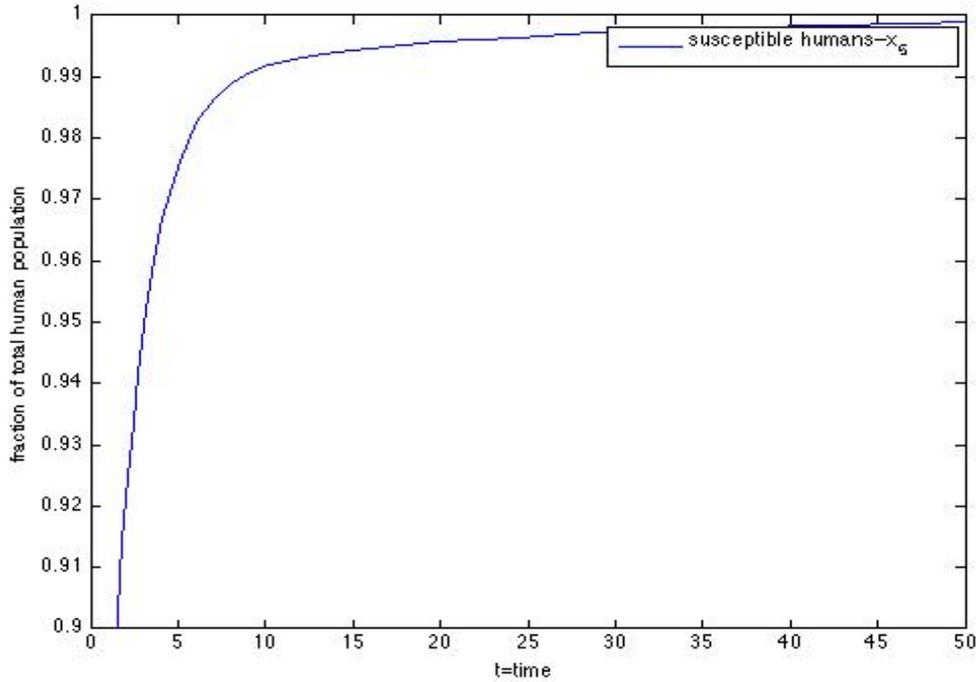


Figure 3.4: Solutions of system (3.3.6) converge to the DFS when $\mathcal{R}_0 = .958$, $d = 1 < 1.5 = c$, $\sigma = 0$, all other parameters are given in Table 3.1.

(ii) If $\mathcal{R}_0 > 0$, then $\lambda = \mathcal{R}_0$ is the unique solution of $\rho(W(\omega, 0, \lambda)) = 1$ [54, Theorem 2.1 (ii)].

(iii) $\mathcal{R}_0 = 0$ if and only if $\rho(W(\omega, 0, \lambda)) < 1$ for all $\lambda > 0$ [54, Theorem 2.1 (iii)].

(iv) The DFS is asymptotically stable if $\mathcal{R}_0 < 1$ and unstable if $\mathcal{R}_0 > 1$ [54, Theorem 2.2].

Results (i)-(iii) imply that, in the case where $V(t)$ and $F(t)$ are not constant or diagonal matrices, obtaining an explicit analytic expression for \mathcal{R}_0 would require deriving analytic expressions for the characteristic multipliers of $W(\omega, 0, \lambda)$. In the case of Mathieu's equation, for example, such a problem remains open (see [23, Section 8.6]). With this in mind, we obtain an analytic expression for the basic reproductive

number of the time-averaged autonomous system based on Model (3.3.6) over the time interval $[0, \omega]$, which we denote as \mathcal{R}_1 . By applying results (i) - (iii) to the numerical calculation of \mathcal{R}_0 , we will show that under certain conditions, \mathcal{R}_1 over- or under- estimates the risk of transmission and serves as an upper or lower bound for \mathcal{R}_0 .

In Proposition 2.3, Chapter 2 we determine that \mathcal{R}_0 for the aseasonal Model (2.3.7) is given by

$$\sqrt{\frac{\lambda_V \lambda_H (p_1 + u_q)(\tau_1 S + u_e)}{(y_H + \alpha_H + v_H)((\tau_1 S + u_e)(p_1 + u_q)u_m - gr_m p_1 \tau_1 S)}} \quad (3.3.17)$$

where $S = S(t) = 1$.

To obtain an analytic expression for the basic reproductive number of the time-averaged autonomous system of Model (3.3.6) over the time interval $[0, \omega]$, we proceed as follows:

For a continuous periodic function $g(t)$ with the period w , we define its average (see [54]) as

$$[g] := \frac{1}{w} \int_0^w g(t) dt \quad (3.3.18)$$

Therefore,

$$\mathcal{R}_1 := \sqrt{\frac{\lambda_V \lambda_H (p_1 + u_q)(\tau_1 [S(t)] + u_e)}{(y_H + \alpha_H + v_H)((\tau_1 [S(t)] + u_e)(p_1 + u_q)u_m - gr_m p_1 \tau_1 [S(t)])}}, \quad (3.3.19)$$

with S as in (3.2.3).

Denote $\int_0^w S(t) dt$ by M . We have the following proposition:

Proposition 3.3. *Assume that u_m , $(u_q + p_1)$, $([S(t)]\tau_1 + u_e)$, v_H all > 0 ,*

$$\frac{gr_m p_1 \tau_1 [S(t)]}{(\tau_1 [S(t)] + u_e)(p_1 + u_q)u_m} < 1, \quad (y_H + \alpha_H + v_H)((u_e)(p_1 + u_q)u_m - gr_m p_1 \tau_1 (c + d)) > 0.$$

$$(i) \quad \mathcal{R}_1 = \sqrt{\frac{\lambda_V \lambda_H (p_1 + u_q)(\tau_1 \frac{M}{w} + u_e)}{(y_H + \alpha_H + v_H)((\tau_1 \frac{M}{w} + u_e)(p_1 + u_q)u_m - gr_m p_1 \tau_1 \frac{M}{w})}}.$$

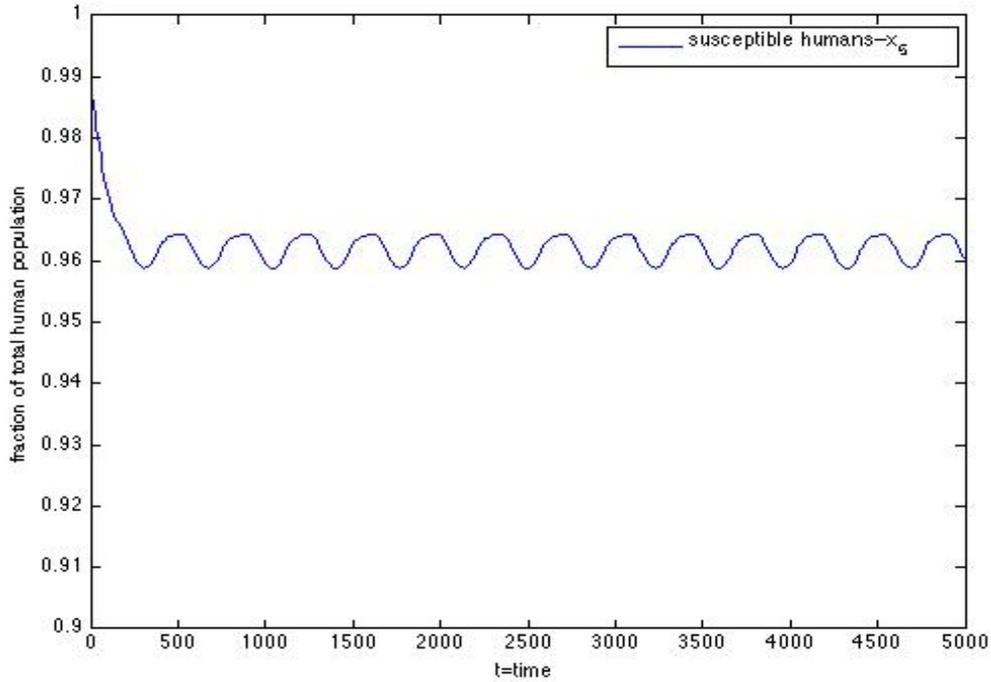


Figure 3.5: Positive periodic solutions of system (3.3.6) when $\mathcal{R}_0 = 1.025$, $d = 1.5 > .5 = c$, $\sigma = 0$, all other parameters are given in Table 3.1.

(ii) If \mathcal{R}_1 is a lower bound for \mathcal{R}_0 , then $\mathcal{R}_{0_{min}} = \sqrt{\frac{\lambda_V \lambda_H (p_1 + u_q)(u_e)}{(y_H + \alpha_H + v_H)((\tau_1(c+d) + u_e)(p_1 + u_q)u_m)}}$.

(iii) If \mathcal{R}_1 is an upper bound for \mathcal{R}_0 , then $\mathcal{R}_{0_{max}} = \sqrt{\frac{\lambda_V \lambda_H (p_1 + u_q)(\tau_1(c+d) + u_e)}{(y_H + \alpha_H + v_H)((u_e)(p_1 + u_q)u_m - gr_m p_1 \tau_1(c+d))}}$.

Proof. This is immediate from (3.3.19) and the fact that $0 \leq S(t) \leq c + d$, so $0 \leq M \leq (c + d)\omega$. \square

Following earlier notation, denote the DFS by $x^0(t)$. For any solution $u(t, 0, \psi_0)$ of system (3.3.6) through $(0, \psi_0)$ where $\psi_0 \in \Omega'$, denote ψ_0 as ψ and $u(t, 0, \psi_0) = u(t, 0, \psi)$ as $u(t, \psi)$.

In part (2) of Theorem 3.5, we will make use of the following lemma:

Lemma 3.4. *Suppose all parameters are positive. Let $X = \Omega'$, $X_0 = \{(x_1, \dots, x_5) \in X : 0 < x_i \leq 1, i = 1, \dots, 4\}$. Then X_0 is positively invariant for system (3.3.6).*

Proof. First observe that if $x \in X_0$, then $0 \leq x_5 < 1$ and $0 < x_1 + x_5 \leq 1$. So $X_0 = \{(x_1, x_2, x_3, x_4, x_5) : 0 < x_i \leq 1, 1 \leq i \leq 4; 0 < x_1 + x_5 \leq 1, 0 \leq x_5 < 1\}$ is open in the subspace topology of X . So $X \setminus X_0 = \partial X_0 = \{x \in X : x_i = 0 \text{ for some } i \text{ with } i = 1, \dots, 4 \text{ or } x_5 = 1\}$ is closed in the subspace topology of X .

Let $u(t, \psi)$ be a fixed, unique solution of system (3.3.6) with $u_0(\psi) = \psi \in X_0$. Suppose $\psi \in X_0$. If $\psi_5 = 0$, then by equation 5 of (3.3.6), $\frac{du_5(0, \psi)}{dt} = v_H > 0$. So by the continuity of the functions on the RHS of (3.3.6), there exists a small $t' > 0$ such that on $(0, t']$, $0 < u_5(t, \psi) < 1$ and $u(t, \psi) \in X_0$. So if $u(t, \psi_5) + u(t, \psi_1) = 1$ for some t'' in $(0, t']$, then, $\frac{du_5(t'', \psi)}{dt} + \frac{du_1(t'', \psi)}{dt} = (1 - u_5(t'', \psi))(-y_H) < 0$ (see proof of Corollary 2.2 in Chapter 2). By reasoning similar as that in Theorem 3.1, $0 < u_5(t, \psi) + u_1(t, \psi) < 1$, $0 < u_i(t, \psi)$ on (t'', ∞) . So $u(t, \psi) \in X_0$ for all $t > t''$, and consequently, all $t \geq 0$. So we have our desired result. \square

We now closely follow the arguments in [33] and [59] to obtain the following \mathcal{R}_0 -based results:

Theorem 3.5. *The following hold:*

(1) *Suppose conditions are as in Proposition 3.3. Assume further that $\mathcal{R}_1 < 1$, $\alpha_H = 0$, and $(y_H + v_H)(u_m u_q u_e - gr_m p_1(c + d)\tau_1) > \lambda_V \lambda_H u_q u_e$. If $\mathcal{R}_0 < 1$, then $x^0(t)$ is globally asymptotically stable.*

(2) *Assume all parameters are positive, and that $S(\omega) > 0$. If $\mathcal{R}_0 > 1$, then system (3.3.6) admits at least one periodic solution in Ω' .*

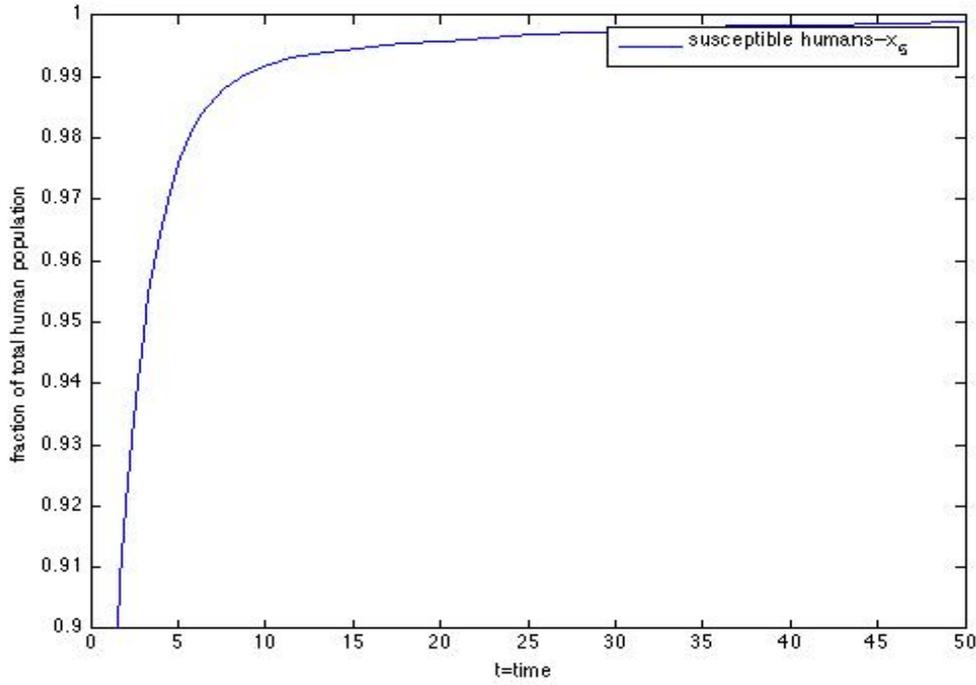


Figure 3.6: Solutions of system (3.3.6) converge to the DFS when $\mathcal{R}_0 = .956$, $d = 1.5 > .5 = c$, $\sigma = 0$, all other parameters are given in Table 3.1.

Proof. (1) First observe that as stated in result (iv), $\mathcal{R}_0 < 1 \Rightarrow x^0(t)$ is stable.

Let $u(t, \psi)$ be a solution of system (3.3.6) with $u_0(\psi) = \psi \in \Omega'$. Consider system (3.3.6). If we omit f_5 and assume that $\alpha_H = 0$, we have, by the invariance of Ω' , that

$$\begin{aligned}
 f_1(t, u) &= \lambda_H u_5 u_2 - (y_H + v_H) u_1 \leq \lambda_H u_2 - (y_H + v_H) u_1 \\
 f_2(t, u) &= p_1 u_3 (1 - u_2) - u_m u_2 + \lambda_V (1 - u_2) u_1 \leq p_1 u_3 - u_m u_2 + \lambda_V u_1 \\
 f_3(t, u) &= \tau_1 S(t) u_4 (1 - u_3) - u_q u_3 - p_1 u_3 (1 - u_2) \leq (c + d) \tau_1 u_4 - u_q u_3 \\
 f_4(t, u) &= gr_m u_2 (1 - u_4) - S(t) \tau_1 u_4 (1 - u_3) - u_e u_4 \leq gr_m u_2 - u_e u_4
 \end{aligned} \tag{3.3.20}$$

Let

$$A = \begin{pmatrix} -(y_H + v_H) & \lambda_H & 0 & 0 \\ \lambda_V & -u_m & p_1 & 0 \\ 0 & 0 & -u_q & (c + d)\tau_1 \\ 0 & gr_m & 0 & -u_e \end{pmatrix} \quad (3.3.21)$$

Then we may rewrite (3.3.20) as

$$\begin{bmatrix} f_1(t, u) \\ f_2(t, u) \\ f_3(t, u) \\ f_4(t, u) \end{bmatrix} \leq A \begin{bmatrix} u_1 \\ u_2 \\ u_3 \\ u_4 \end{bmatrix}, \quad (3.3.22)$$

where the inequality holds pointwise.

Now $-A$ has the Z-pattern (see **(A5)**, Chapter 2). First observe that $\mathcal{R}_1 < 1 \Rightarrow (\lambda_V \lambda_H)(p_1 + u_q)([S(t)]\tau_1 + u_e) < (y_H + v_H)(([S(t)]\tau_1 + u_e)(p_1 + u_q)u_m - gr_m p_1 [S(t)]\tau_1) < (y_H + v_H)([S(t)]\tau_1 + u_e)(p_1 + u_q)u_m$ (*).

Now the principal leading minors of $-A$ are given by $(y_H + v_H)u_m > 0$, $(y_H + v_H)u_m - \lambda_V \lambda_H > 0$ (by (*)), $u_q((y_H + v_H)u_m - \lambda_V \lambda_H) > 0$, and $\det(-A) = ((y_H + v_H)(u_m u_q u_e - gr_m p_1 (c + d)\tau_1) - \lambda_V \lambda_H u_q u_e) > 0$ (by assumption).

So $-A$ is a nonsingular M-matrix [16, 28], which implies that the eigenvalues of A all have negative real part.

Now by the comparison principle [44, Chapter 3, Proposition 1.1 and Remark 1.2],

$$\begin{bmatrix} u_1(t, \psi) \\ u_2(t, \psi) \\ u_3(t, \psi) \\ u_4(t, \psi) \end{bmatrix} \leq e^{At} \begin{bmatrix} \psi_1 \\ \psi_2 \\ \psi_3 \\ \psi_4 \end{bmatrix} \quad \forall t \in [0, \infty) \quad (3.3.23)$$

So since the eigenvalues of A all have negative real part,

$$\lim_{t \rightarrow \infty} \left(e^{At} \begin{bmatrix} \psi_1 \\ \psi_2 \\ \psi_3 \\ \psi_4 \end{bmatrix} \right) = 0 \quad [38, \text{Section 1.9, Theorem 2}].$$

So $(u_1(t, \psi), u_2(t, \psi), u_3(t, \psi), u_4(t, \psi)) \rightarrow 0$ as $t \rightarrow \infty$, where the convergence is component-wise.

Now by (3.3.3), $\frac{dR_H(t', \psi)}{dt} = -\left(\frac{dS_H(t', \psi)}{dt} + \frac{dI_H(t', \psi)}{dt}\right) = -\left(\frac{du_1(t', \psi)}{dt} + \frac{du_5(t', \psi)}{dt}\right) = -(-y_H u_1(t', \psi) + v_H(1 - u_5(t', \psi) - u_1(t', \psi))) = y_H u_1(t', \psi) - v_H(1 - u_5(t', \psi) - u_1(t', \psi)) \leq 0$ for all but finitely many $t' \in [0, \infty)$, since $u_1(t', \psi) \rightarrow 0$ as $t' \rightarrow \infty$, and $u_1(t', \psi) + u_5(t', \psi) \leq 1$. So $R_H(t', \psi) = 1 - S_H(t', \psi) - I_H(t', \psi) = 1 - u_1(t', \psi) - u_5(t', \psi) \rightarrow 0$ as $t' \rightarrow \infty$. So $u_5(t', \psi) \rightarrow 1$ as $t' \rightarrow \infty$ and we have our desired result.

(2) Let X, X_0 be as in Lemma 3.4. Equip Ω' with the *sup* norm.

We have that X_0 is an open set in the subspace topology on X (see Lemma 3.4). Let $u(t, \psi)$ be a fixed, unique solution of system (3.3.6) with $u_0(\psi) = \psi$ where $\psi \in X$. Let $\Phi(t)(\psi) = u_t(\psi)$ and $P : X \rightarrow X$ be the Poincaré map associated with system (3.3.6), that is, $P(\psi) = u_\omega(\psi)$. By Lemma 3.4, $\Phi(t)(X_0) \subset X_0$.

Consider the discrete-time system $P : X \rightarrow X$. By the positive invariance of X , the closure of the forward orbit $\{P^n(\psi) : n \geq 1\}$ is a bounded subset of X and, by

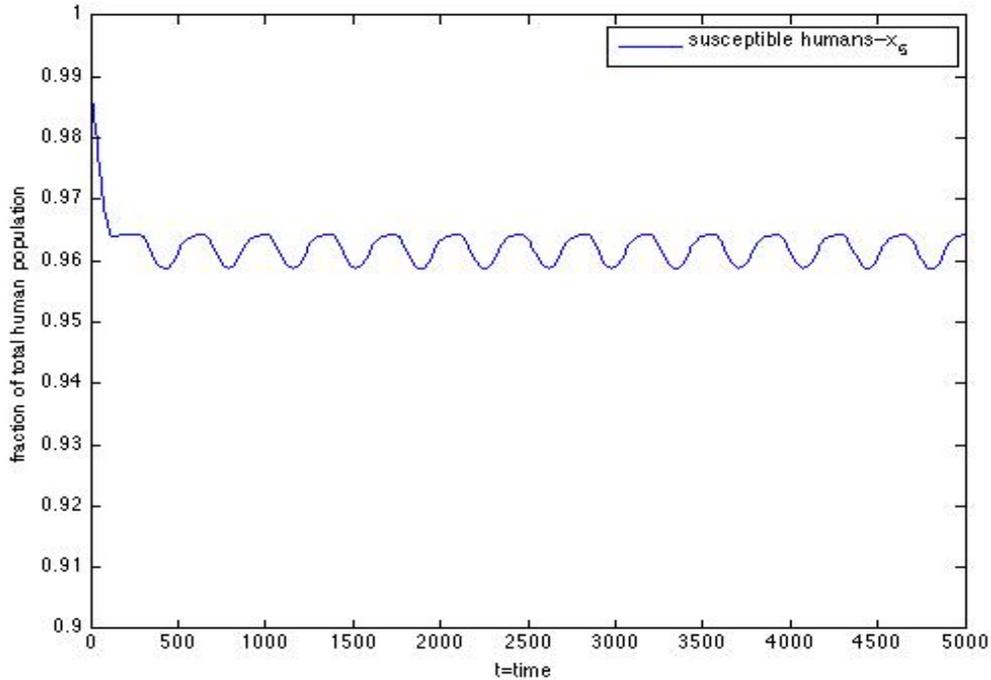


Figure 3.7: Positive periodic solutions of system (3.3.6) when $\mathcal{R}_0 = 1.028$, $d = 1.5 > .5 = c$, $\sigma = -90$, all other parameters are given in Table 3.1.

the Bolzano-Weierstrass theorem, compact. Similarly, the image under P^n of every bounded set in X is relatively compact, so P^n is compact for each $n \geq 0$. The discrete-time system is therefore point dissipative and P^n is compact for all $n \geq 0$. By [34, Theorem 2.6; 35, Theorem 2.9], P admits a global attractor B in X . We prove that P is uniformly persistent with respect to $(X_0, \partial X_0 \setminus D_1)$, where D_1 is as in (3.3.27).

Let $M_1 := \{(0, 0, 0, 0, 1)\}$. For any $t \in [0, \omega]$, $\lim_{\psi \rightarrow M_1} \Phi(t)(\psi) - M_1 = 0$, where the convergence is uniform [38, Section 2.4, Theorem 4]. So we may choose $\delta_1 < 1$ such that for some $\delta_0 > 0$, $\|(\Phi(t)(\psi) - M_1)\| < \delta_1$ when $\|(\psi - M_1)\| < \delta_0$, $\forall t \in [0, \omega]$.

We have the following claim: If $\psi \in X_0$, $\limsup_{n \rightarrow \infty} \|(\Phi(n\omega)\psi - M_1)\| \geq \delta_0$. (*)

Suppose not. Then $\limsup_{n \rightarrow \infty} \|(\Phi(n\omega)\psi - M_1)\| < \delta_0$. Then there exists an integer $N_1 \geq 1$ such that for any $t \geq N_1\omega$, $\|(\Phi(t)\psi - M_1)\| \leq \delta_1$ [33, Theorem 3.2, Claim 1; 59, Theorem 2.3] and, consequently, $\|u_i(t, \psi)\| < \delta_1$. So for any $t \geq N_1\omega$, we have

$$\begin{aligned}
\frac{du_1(t, \psi)}{dt} &\geq \lambda_H(1 - \delta_1)u_2(t, \psi) - (y_H + \alpha_H + v_H)u_1(t, \psi) \\
\frac{du_2(t, \psi)}{dt} &\geq p_1u_3(t, \psi)(1 - \delta_1) - u_mu_2(t, \psi) + \lambda_V(1 - \delta_1)u_1(t, \psi) \\
\frac{du_3(t, \psi)}{dt} &\geq \tau_1S(t)u_4(t, \psi)(1 - \delta_1) - u_qu_3(t, \psi) - p_1u_3(t, \psi) \\
\frac{du_4(t, \psi)}{dt} &\geq gr_mu_2(t, \psi)(1 - \delta_1) - u_eu_4(t, \psi) - \tau_1S(t)u_4(t, \psi)
\end{aligned} \tag{3.3.24}$$

Let

$$\overline{M}_{\delta_1}(t) = \begin{pmatrix} -(y_H + \alpha_H + v_H) & \lambda_H(1 - \delta_1) & 0 & 0 \\ \lambda_V(1 - \delta_1) & -u_m & +p_1(1 - \delta_1) & 0 \\ 0 & 0 & -(p_1 + u_q) & +\tau_1S(t)(1 - \delta_1) \\ 0 & gr_m(1 - \delta_1) & 0 & -(\tau_1S(t) + u_e) \end{pmatrix} \tag{3.3.25}$$

Consider the system

$$\begin{aligned}
\frac{dz}{dt} &= \overline{M}_{\delta_1}(t)z. \\
z(0) &= z_0
\end{aligned} \tag{3.3.26}$$

Now, $\mathcal{R}_0 > 1$ implies that, for a sufficiently small choice of δ_1 , $z(t) \rightarrow \infty$ as $t \rightarrow \infty$, where $z(t) = e^{\frac{1}{\omega} \ln \rho(\Phi_{\overline{M}_{\delta_1}(\cdot)}(\omega))t} v(t)$ with $v(t)$ positive and ω -periodic, is a solution of (3.3.26) [59, Theorem 2.2]. Now $\psi \in X_0$. By Lemma 3.4, $\Phi(t)\psi \in X_0$, $\forall t \geq 0$. So there exists $\eta > 0$ such that $\|u(N_1\omega, \psi)\| \geq \eta\|z_0\|$. By the comparison principle,

$\|u_i(N_1\omega + t, \psi)\| \geq \eta \|z_i(t)\|$, for all $t \geq 0$, $1 \leq i \leq 4$ [33, Theorem 3.2, Claim 2]. So $\lim_{t \rightarrow \infty} \|(u_1(t, \psi), \dots, u_4(t, \psi))\| = \infty$, a contradiction.

Define

$$\begin{aligned} D_1 &:= \{\phi \in X : \phi_i = 0, \forall i \text{ with } 1 \leq i \leq 4\} \\ M_\partial &:= \{\phi \in \partial X_0 : P^n(\phi) \in \partial X_0, \forall n \geq 0\} \end{aligned} \quad (3.3.27)$$

Claim: $D_1 = M_\partial$.

One inclusion, $D_1 \subset M_\partial$, is clear. For the other: Let $x(t, \phi)$ be a solution of system (3.3.6) with $x_0(\phi) = \phi \in X$. Let $\phi \in M_\partial$. Now suppose that $\phi \notin D_1$. Then $x_j(0, \phi) = \phi_j > 0$ for some fixed j with $1 \leq i \leq 4$. Observe that $S(0) > 0$, so by continuity of S , there is a small $t_0 > 0$ such that $S(t) > 0$ on $[0, t_0]$. By the continuity of $x_j(t, \phi)$ in t on X , we may assume, without loss of generality, that $x_j(t, \phi) > 0$ on $[0, t_0]$. (')

Now observe that for any i with $1 \leq i \leq 5$, $x_i(t_0, \phi) = 0 \Rightarrow \frac{dx_i(t_0, \phi)}{dt} = 0$:

Let $i = 4$. Then if $x_4(t_0, \phi) = 0$, by equation 4 of (3.3.6), $\frac{dx_4(t_0, \phi)}{dt} = gr_m x_2(t_0, \phi) \geq 0$. Now suppose $gr_m x_2(t_0, \phi) > 0$. Then $x_4(t_0, \phi)$ is increasing in t at t_0 . So $x_4(t', \phi) < 0$ for some $t' < t_0$. But by assumption, $x_0(\phi) = \phi \in X$, which is positively invariant. So $0 \leq x_4(t', \phi) \leq 1$, a contradiction. By similar reasoning, we have that $x_i(t_0, \phi) = 0 \Rightarrow \frac{dx_i(t_0, \phi)}{dt} = 0$ for $i = 1, 2, 3, 5$. (+).

Now we show that $x_i(t_0, \phi) = 0$ for some i with $1 \leq i \leq 4 \Rightarrow x_i(t_0, \phi) = 0$ for all i with $1 \leq i \leq 4$: (")

All parameters are positive, so $x_4(t_0, \phi) = 0$ and $\frac{dx_4(t_0, \phi)}{dt} = 0 \Rightarrow x_2(t_0, \phi) = 0$ and $\frac{dx_2(t_0, \phi)}{dt} = 0$ (by (+) and equation 4, (3.3.6)) $\Rightarrow x_1(t_0, \phi) = 0$ and $\frac{dx_1(t_0, \phi)}{dt} = 0$, $x_3(t_0, \phi) = 0$ and $\frac{dx_3(t_0, \phi)}{dt} = 0$ (by (+) and equations 1,2, (3.3.6)). Note that if $x_5(t_0, \phi) = 0$, $\frac{dx_5(t_0, \phi)}{dt} = v_H > 0$, a contradiction. So $x_1(t_0, \phi) = 0$ and $\frac{dx_1(t_0, \phi)}{dt} = 0 \Rightarrow x_2(t_0, \phi) = 0$ and $\frac{dx_2(t_0, \phi)}{dt} = 0$ (by (+) and equation 1, (3.3.6)). Finally, $x_3(t_0, \phi) = 0$

and $\frac{dx_3(t_0, \phi)}{dt} = 0 \Rightarrow x_4(t_0, \phi) = 0$ and $\frac{dx_4(t_0, \phi)}{dt} = 0$ (by equation 3, (3.3.6), (+), and the fact that $S(t_0) > 0$).

So by (') and (''), $x_i(t_0, \phi) \neq 0$ for all i with $1 \leq i \leq 4$. But by Lemma 3.4, X_0 is positively invariant. So $x_i(t_0, \phi) \neq 0$ for all i with $1 \leq i \leq 4$, all $t \geq t_0$. By definition of M_∂ , this is a contradiction. So $D_1 = M_\partial$. (++)

Now since ϕ is in D_1 , M_1 is the ω -limit set of any positive half-trajectory Γ_ϕ^+ through ϕ . So by (++), $\tilde{M}_\partial := \bigcup_{\phi \in M_\partial} w(\Gamma_\phi^+) = M_1$ has an isolated and acyclic covering in ∂X_0 , namely, M_1 . In view of (*), $W^s(M_1) \cap X_0 = \emptyset$, where $W^s(M_1)$ is the stable set of M_1 for P . (+++)

Now $M_\partial \equiv D_1$ and an application of the above arguments to any subset of $M_\partial \Rightarrow \{\phi \in \partial X_0 : P^n(\phi) \in \partial X_0 \text{ for infinitely many } n\} \subset D_1 \Rightarrow P^n(\partial X_0 \setminus D_1) \not\subset \partial X_0$ for sufficiently large $n \Rightarrow P^n(\partial X_0 \setminus D_1) \subset X_0$ for sufficiently large n . (**)

By the acyclicity theorem on uniform persistence of maps, (+++) and (**), P is uniformly persistent with respect to $(X_0, \partial X_0 \setminus D_1)$ [61, Theorem B]. The periodic semiflow $\Phi(t)$ is also uniformly persistent with respect to $(X_0, \partial X_0 \setminus D_1)$ ([61, Remark 3.1], see also [59, Theorem 3.1.1] and [7, Section 3, Theorem]). System (3.3.6) therefore admits an ω -periodic solution $\Phi(t)\psi$ with $\psi \in X_0 \cup \partial X_0 \setminus D_1$ [61, Remark 3.1].

□

Initial Condition	<i>Value</i>
\bar{x}_1	.01
\bar{x}_2	.01
\bar{x}_3	.0001
\bar{x}_4	.0015
\bar{x}_5	.8
Parameter	<i>Value</i>
v_H	.5
λ_H	varies
y_H	0.067
α_H	0.002
u_q	10
u_m	1.5
λ_V	.95
r_m	5
g	0.25
u_e	10
τ_1	0.9
p_1	0.9
σ	varies
c	varies
d	varies

Table 3.1: Values for parameters and variables of Model (3.3.6) with units explained in Table (2.1).

3.4 Numerical Simulations

We now conduct numerical simulations to illustrate our analytical results (see *Remark* at the end of this section).

As in Chapter 2, values for $v_H, \lambda_H, y_H, u_m, r_m$ and g are comparable to those presented by Coutinho *et al.* [8] on the basis of estimates known from the dengue infection process and human and mosquito vital statistics. We assume that the entire egg and larval populations are at carrying capacity.

Recall the basic reproductive number of the time-averaged autonomous system based on Model (3.3.6), denoted as \mathcal{R}_1 and established by Proposition 3.3. We show, by numerical example, that $\mathcal{R}_{0_{max}}$ (Proposition 3.3, (iii)), an upper bound for \mathcal{R}_1 , serves also as an upper bound for \mathcal{R}_0 as λ_H , the contact rate between susceptible humans and mosquitoes, varies. This is a stronger result than that implied by Proposition 3.3. Other parameters are as in Table 3.1. We use [54, Theorem 2.1 (ii)] to compute \mathcal{R}_0 when $\lambda_H = 0$ and 2 (though the latter is a theoretical, and not necessarily biologically feasible, value), and obtain a linear approximation for \mathcal{R}_0 in the given range for λ_H (see Figures 3.9 and 3.2). In the case when $d = 1 < 1.5 = c$, $\sigma = 0$, we see that $\mathcal{R}_{0_{max}} = 1$ when $\lambda_H = .72$ while computations show that $\mathcal{R}_0 = 1$ when $\lambda_H = .9$, showing that $\mathcal{R}_{0_{max}}$ overestimates the disease transmission risk. In the case when $d = 1.5 > .5 = c$, $\sigma = 0$, $\mathcal{R}_{0_{max}} = 1$ when $\lambda_H = .75$ and $\mathcal{R}_0 = 1$ when $\lambda_H = .91$, showing that, when the winter is relatively long and severe, a higher contact rate is necessary to destabilize the DFS. In the case when $d = 1.5 > .5 = c$, $\sigma = -90$ (relaxing the condition that all parameters be nonnegative since $-\sigma$ does not imply $S(t) < 0$), $\mathcal{R}_{0_{max}} = 1$ when $\lambda_H = .75$ and $\mathcal{R}_0 = 1$ when $\lambda_H = .9$, demonstrating that a late winter onset can mitigate the effect of the cold weather by facilitating disease transmission as the reproductive cycle progresses.

Next, we look for the existence of periodic solutions. We first take $\lambda_H = .95$, $d = 1 < 1.5 = c$, $\sigma = 0$. For parameter values given in column 2 of Table 3.1, $\mathcal{R}_0 = 1.03$. The simulations show that the DFS is unstable and trajectories of system (3.3.6) remain positive and are eventually periodic. When the winter is relatively short and mild, we see that the proportions of infected humans and adult mosquitoes will eventually oscillate between 3 and 4 and 2 and 2.5 percent, respectively. The former number exceeds the 2009 worldwide estimate of 50 million cases, or 2 percent

of the 2.5 billion people at risk [4]. Our numbers seem to indicate that, given the worldwide nature of the epidemic and relatively large number of infected individuals, global warming stands to significantly exacerbate the risk of transmission (see Figures 3.10 and 3.3).

We next reduce λ_H by setting it to .8. For $d = 1 < 1.5 = c$, $\sigma = 0$ all other parameters are given in Table 3.1, $\mathcal{R}_0 = .958$. Accordingly, the simulations show that the DFS is asymptotically stable (see Figures 3.11 and 3.4). We then again take $\lambda_H = .95$ and $d = 1.5 > .5 = c$, $\sigma = 0$ so that $\mathcal{R}_0 = 1.025$. The trajectories of system (3.3.6) eventually oscillate periodically. Because $d < c$, however, the winter is relatively long and severe, so the oscillations are not as seemingly “smooth” as in the previous case, factoring in the perturbations introduced by the Heaviside function (see Figures 3.12 and 3.5). When again we reduce λ_H to .8 ($d = 1.5 > .5 = c$, $\sigma = 0$, all other parameters are given in Table 3.1), $\mathcal{R}_0 = .956$. The DFS is shown to be asymptotically stable (Figures 3.13 and 3.6).

Finally, we take $\lambda_H = .95$, $d = 1.5 > .5 = c$, $\sigma = -90$. We obtain $\mathcal{R}_0 = 1.028$. A late winter onset does not seem to alter the simulations presented in Figures 3.13 and 3.6 qualitatively. Again, the solution is eventually periodic (Figures 3.14 and 3.7). When $\lambda_H = .8$, the DFS is asymptotically stable (Figures 3.15 and 3.8). As a whole, the numerical simulations indicate that seasonality does not diminish the importance of controlling human-mosquito contact; rather, the possibility that global warming may increase the number of human infectives by millions, if not hundreds of millions, highlights the importance of intervention at this level.

Remark: Numerical simulations of solution curves were done on MATLAB, which defines the Heaviside function as $1/2$, and not 0, at 0.

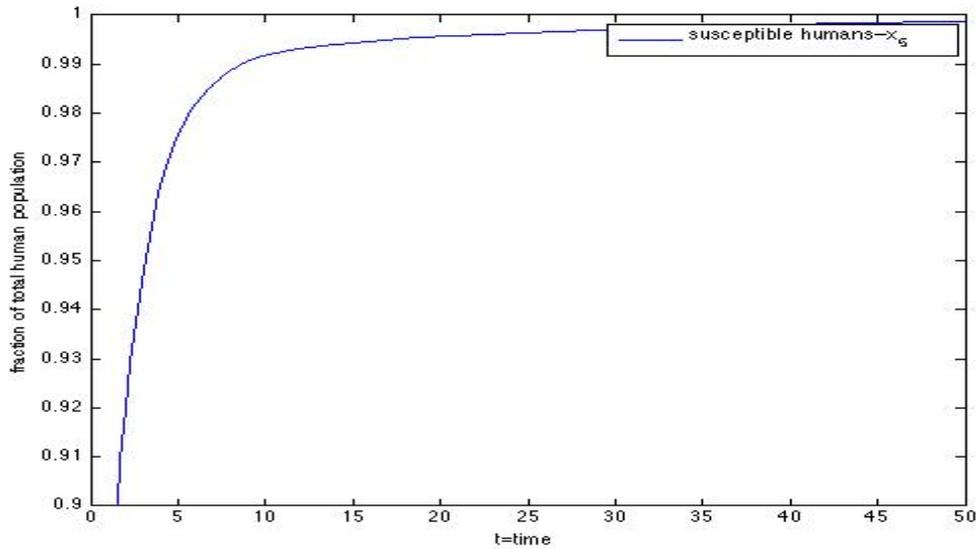


Figure 3.8: *Solutions of system (3.3.6) converge to the DFS when $\mathcal{R}_0 = .959$, $d = 1.5 > .5 = c$, $\sigma = -90$, all other parameters are given in Table 3.1.*

3.5 Discussion

In this chapter, we first presented a non-autonomous, non-linear ODE system that incorporates seasonality into the modeling of the transmission of the dengue virus. As previously stated, our model simulates seasonality by modulating the maturation of the vector from the egg into the larval phase by an ω -periodic factor. We then analyzed this model, a simplified version of which we presented in Chapter 2. We therefore explored the biological consequences of combining an SIR system for dengue viral transmission in the human host with a corresponding non-autonomous, multi-stage SI model for the mosquito vector, which is divided into adult, larval and egg populations.

As in the previous chapter, we first proved that if initial conditions are positive, the size of the total human population may vary but will never subside to 0. We then made

variable substitutions to obtain a simplified, proportion-based system. Next we set the reproductive cycle unit w to $1/365$ days and showed the existence of a real number $\omega > 0$, namely $\omega = 365$, such that the input and output rates of individuals into respective compartments are ω -periodic. Under this and other assumptions, we were able to derive conditions for the existence of a threshold parameter, the basic reproductive ratio, \mathcal{R}_0 , denoting the expected number of secondary cases produced by a typically infective individual. We then used the basic reproductive number of the time-averaged autonomous system based on Model (3.3.6), \mathcal{R}_1 , to establish possible analytic upper and lower bounds for \mathcal{R}_0 . Using the fact that \mathcal{R}_0 is a threshold parameter, we were able to derive conditions under which the DFS is globally asymptotically stable and prove the existence of positive periodic solutions when it is unstable.

In the case where the juvenile populations are at carrying capacity, both the analysis and numerical simulations demonstrate that the persistence of an epidemic is affected by climatic factors. If the winter is short and mild, then the stability of the disease-free equilibrium and the ensuing existence of an epidemic will be heavily influenced by human-mosquito contact rates. If these are high, warm weather further exacerbates the intensity of the epidemic, as the proportions of infected humans and adult mosquitoes oscillate between positive values. If the winter is long and severe, a high human-mosquito contact can destabilize the DFS. On a positive note, however, the late onset of the winter phase did not seem to perturb oscillations so as to increase the proportions of infected individuals. On the whole, the results indicate that intervention at the reproductive phase of the mosquito life-cycle is crucial, particularly if average global temperatures continue to increase.

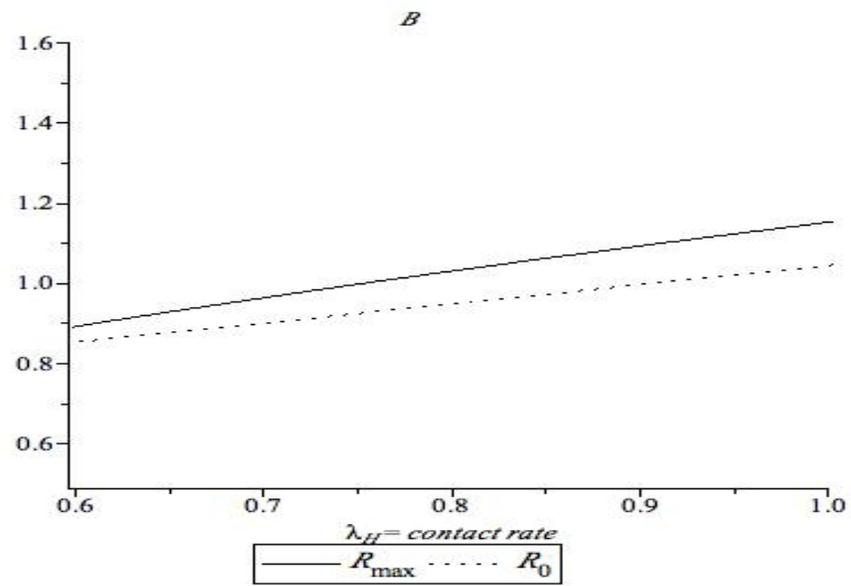
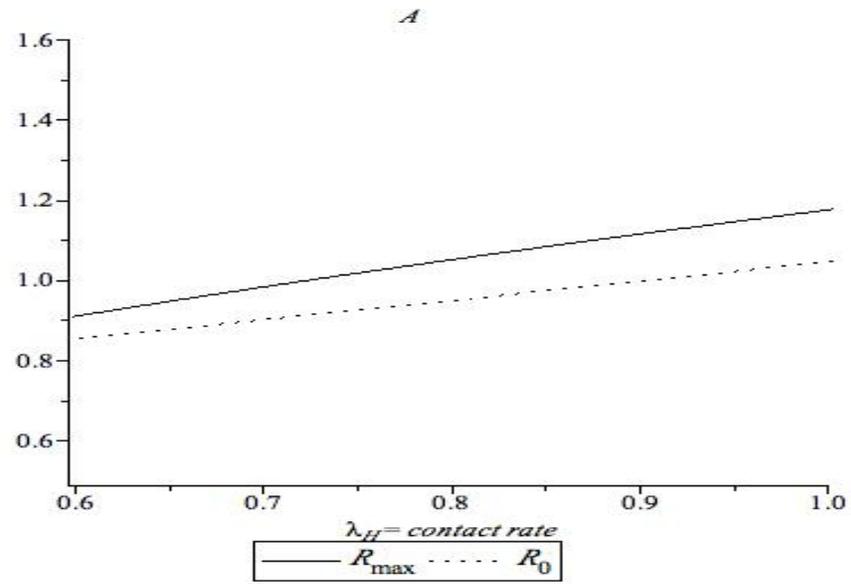


Figure 3.9: The graph of the basic reproduction ratio \mathcal{R}_0 and $\mathcal{R}_{0_{\max}}$ when λ_H varies.

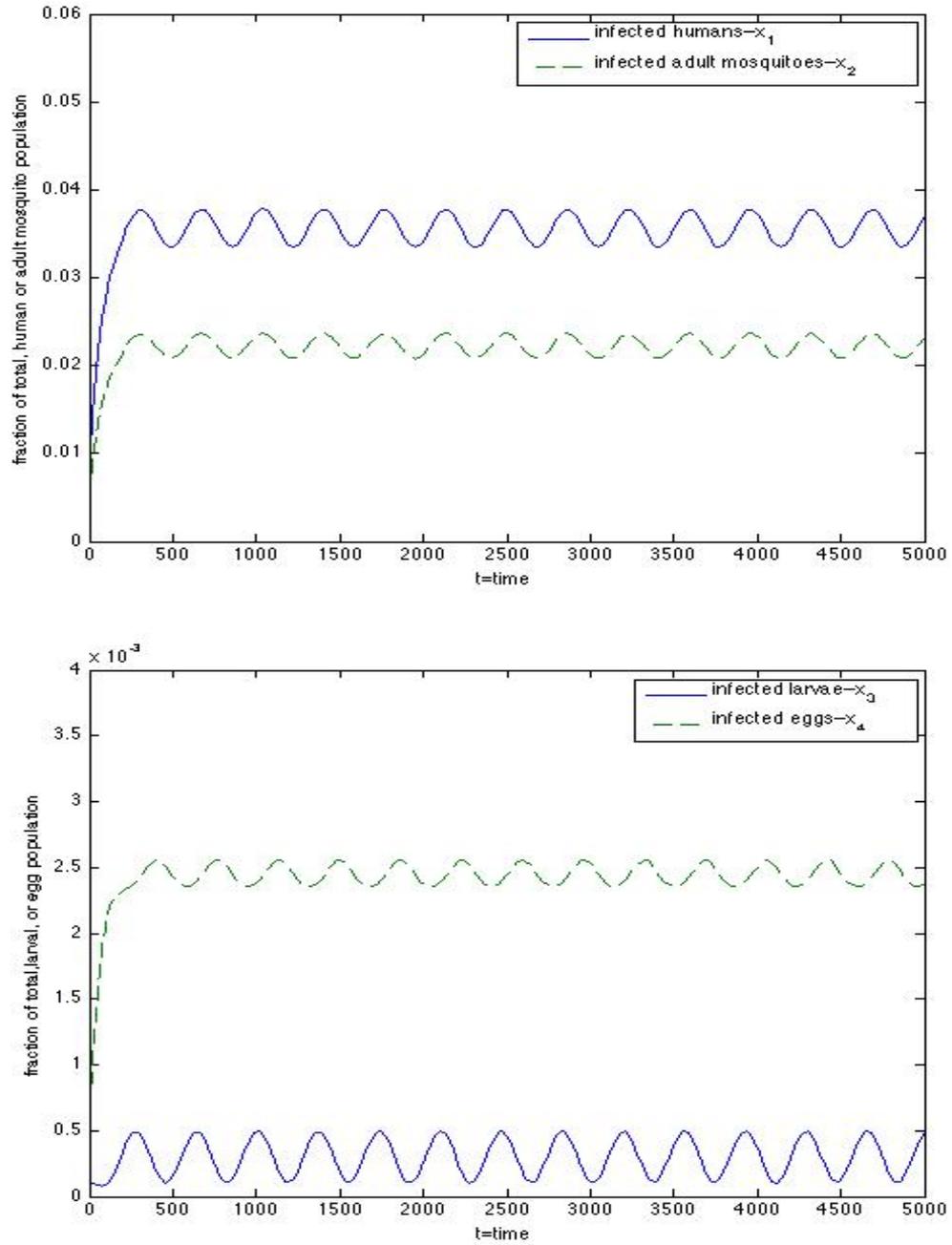


Figure 3.10: Positive periodic solutions of system (3.3.6) when $\mathcal{R}_0 = 1.03$, $d = 1 < 1.5 = c$, $\sigma = 0$, all other parameters are given in Table 3.1.

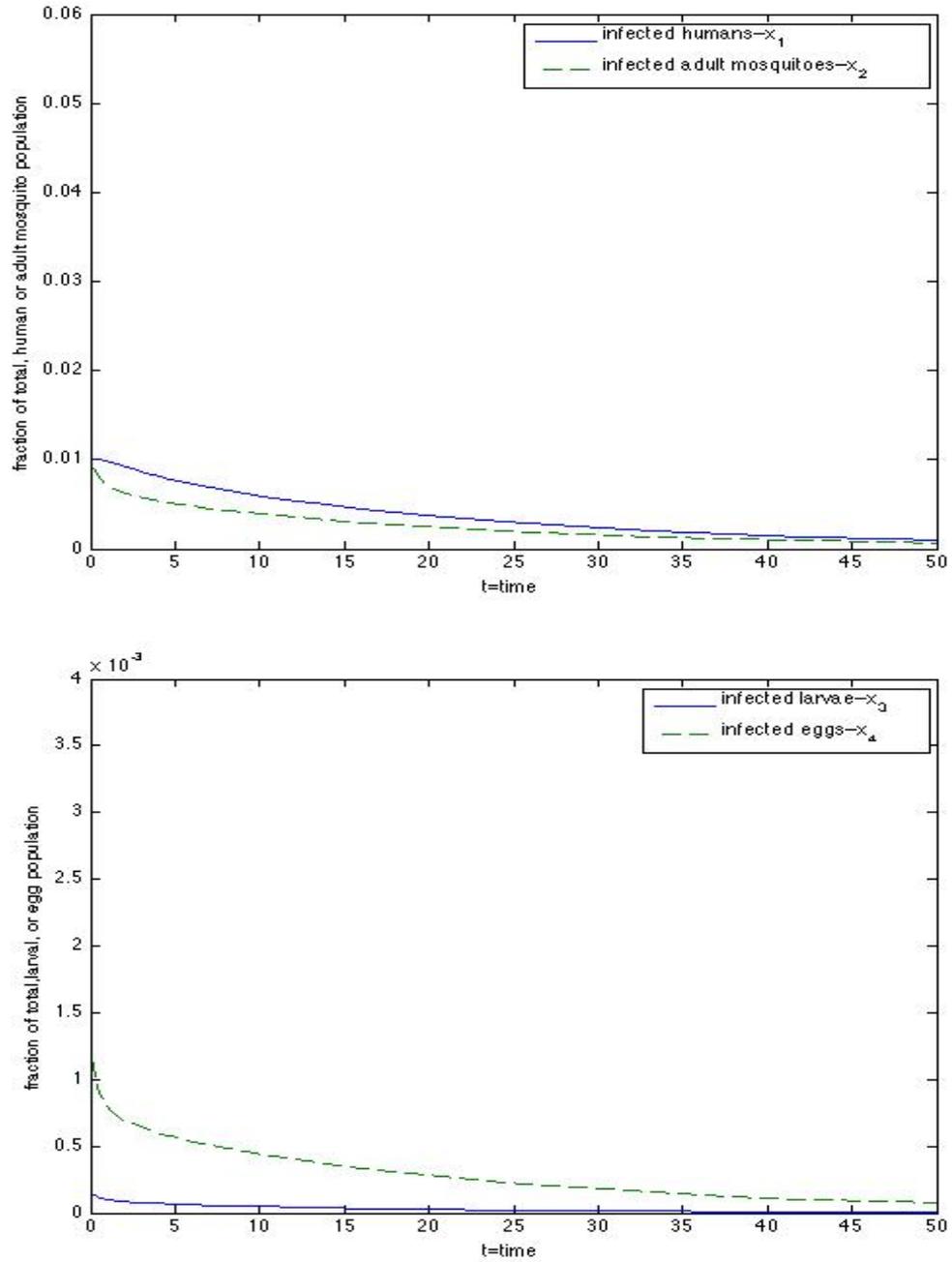


Figure 3.11: Solutions of system (3.3.6) converge to the DFS when $\mathcal{R}_0 = .958$, $d = 1 < 1.5 = c$, $\sigma = 0$, all other parameters are given in Table 3.1.

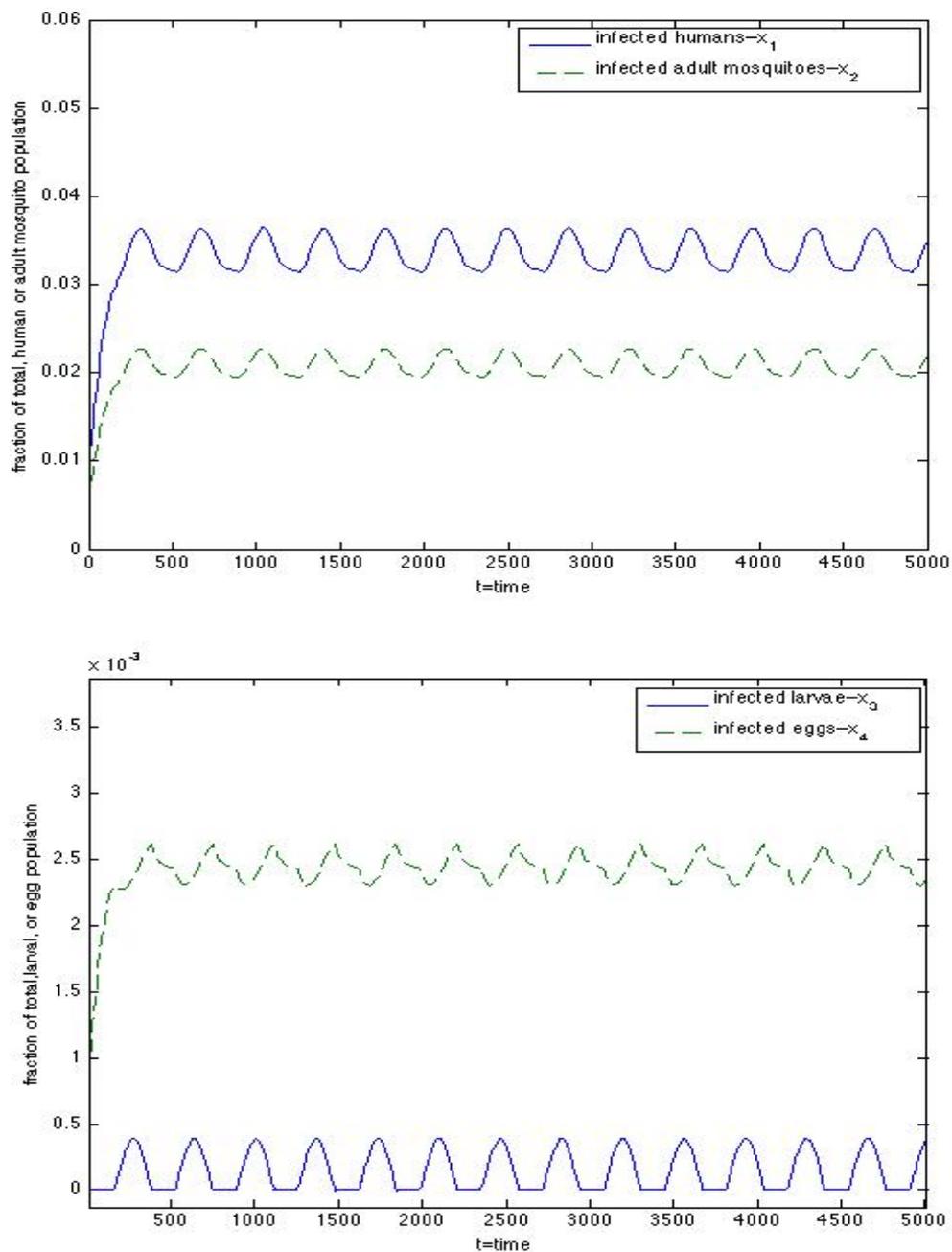


Figure 3.12: Positive periodic solutions of system (3.3.6) when $\mathcal{R}_0 = 1.025$, $d = 1.5 > .5 = c$, $\sigma = 0$, all other parameters are given in Table 3.1.

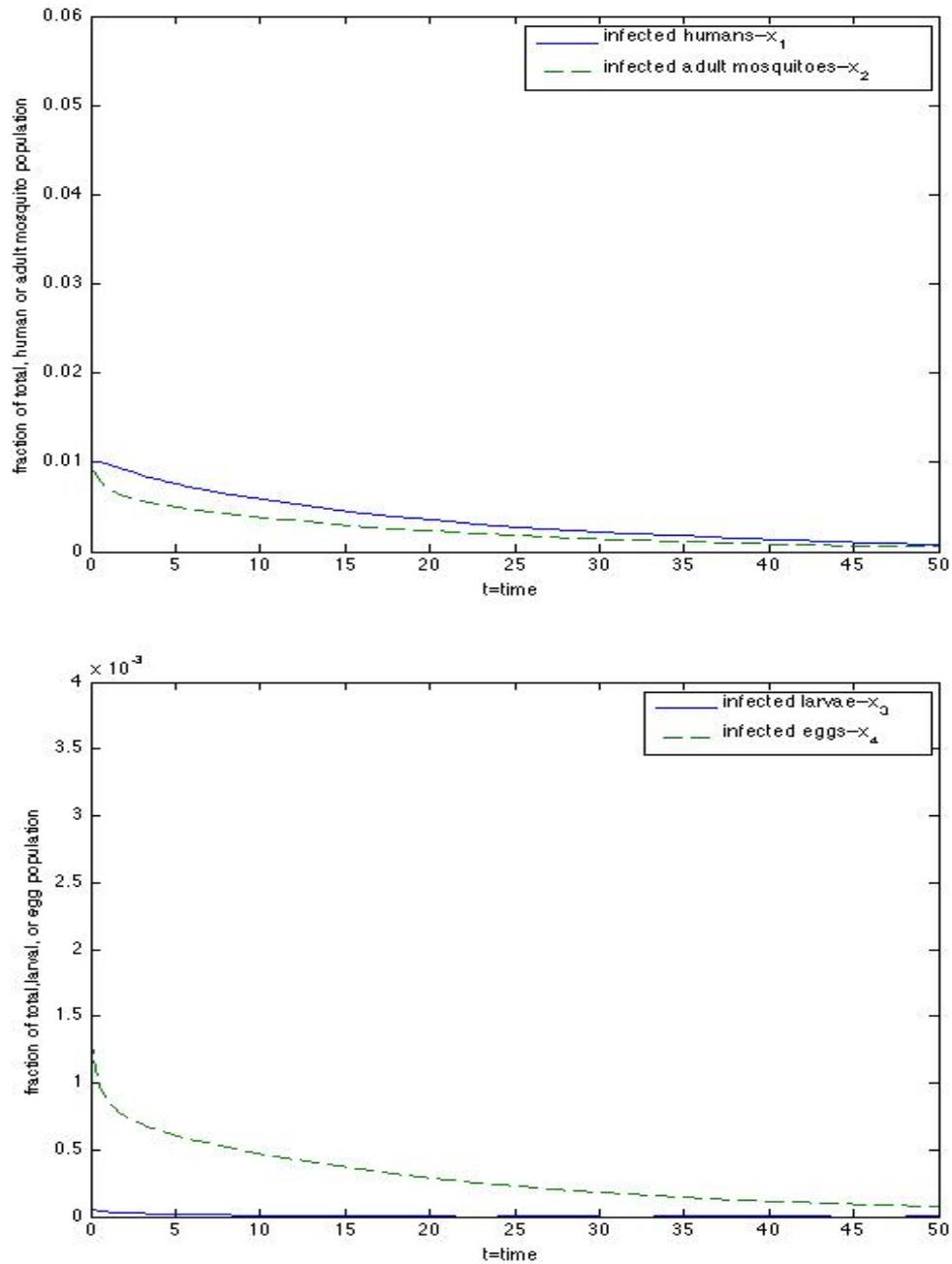


Figure 3.13: Solutions of system (3.3.6) converge to the DFS when $\mathcal{R}_0 = .956$, $d = 1.5 > .5 = c$, $\sigma = 0$, all other parameters are given in Table 3.1.

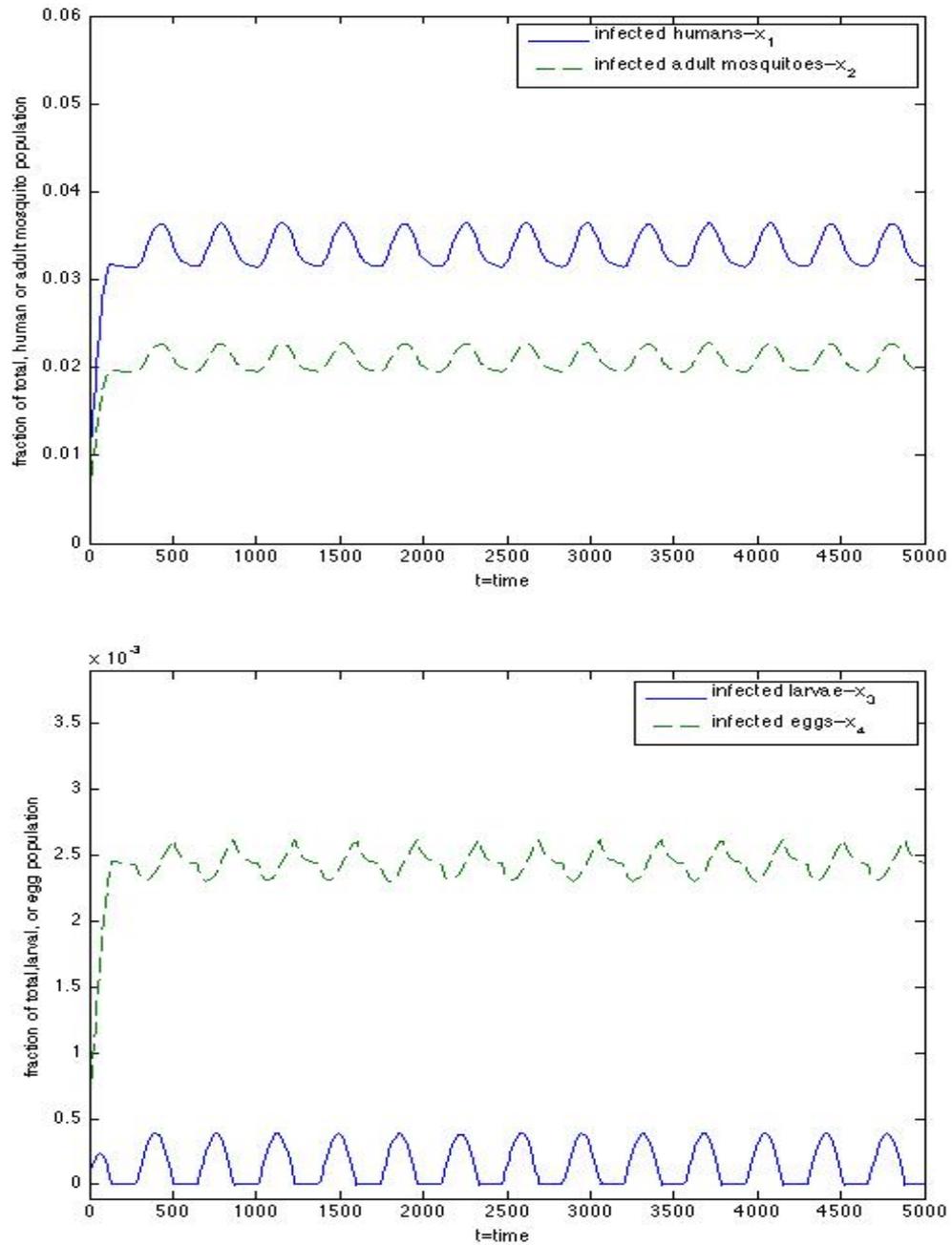


Figure 3.14: Positive periodic solutions of system (3.3.6) when $\mathcal{R}_0 = 1.028$, $d = 1.5 > .5 = c$, $\sigma = -90$, all other parameters are given in Table 3.1.

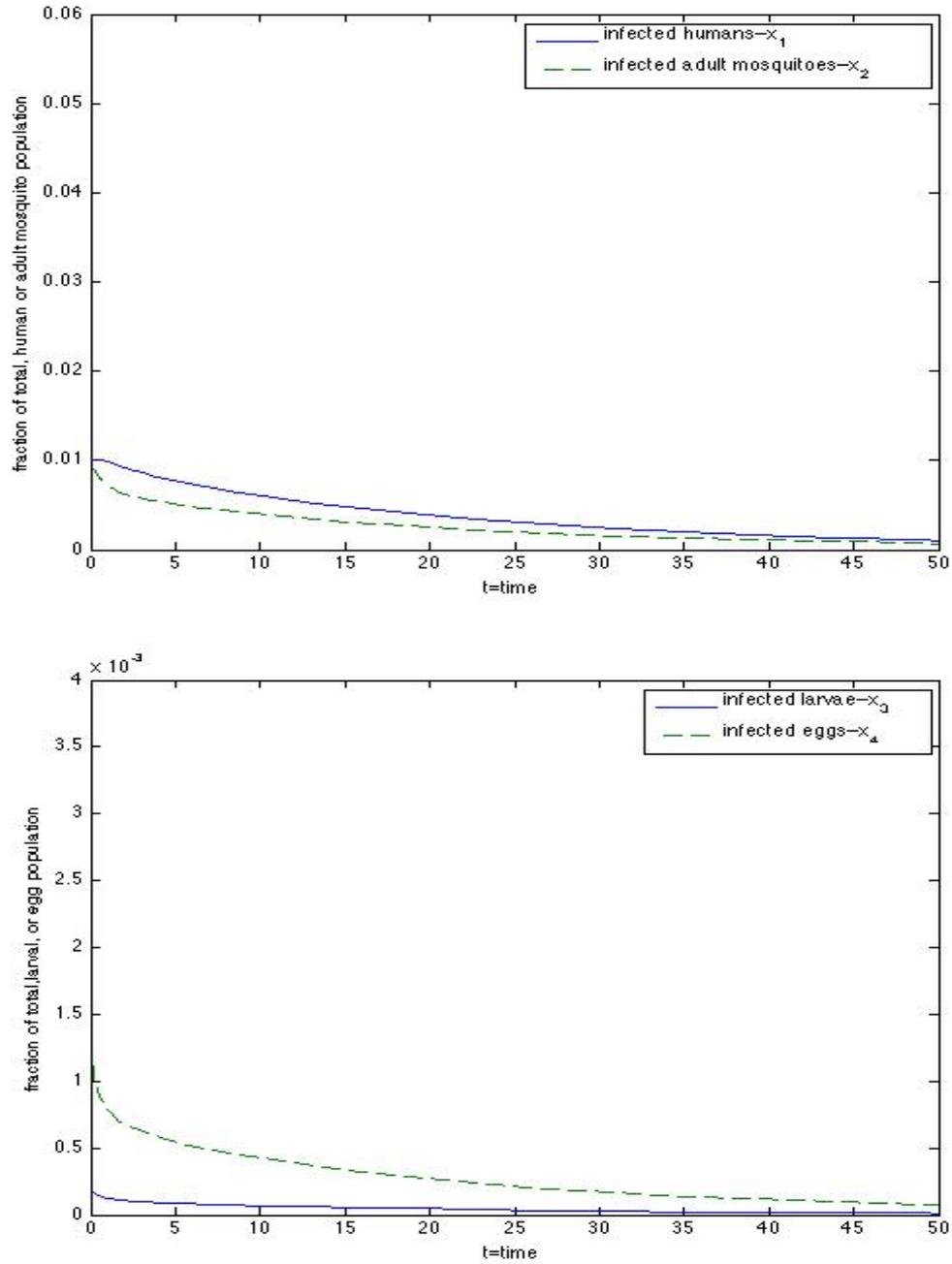


Figure 3.15: Solutions of system (3.3.6) converge to the DFS when $\mathcal{R}_0 = .959$, $d = 1.5 > .5 = c$, $\sigma = -90$, all other parameters are given in Table 3.1.

Chapter 4

TRAVELING WAVES AND SPREAD RATES FOR THE PDE MODEL

4.1 Introduction and Assumptions

Despite the abundance of both dengue-specific time-based models for disease transmission dynamics and theoretical work on reaction-diffusion epidemic models, few PDE-based studies of the spatial spread of dengue and other specific diseases exist [40]. In this chapter, we study the spatial dissemination of dengue by proposing a model of partial differential reaction-diffusion equations. Before doing so, we discuss the theory and importance of finding traveling wave solutions for the containment of dengue epidemics, review the biology of the disease's spatial spread, and outline the analytical foundation of our model.

One theoretical method of introducing spatial heterogeneity into epidemic models involves assuming random types of individual movements, leading to a system of reaction diffusion equations

$$\partial_t q = \underline{D} \nabla^2 q + R(q) \tag{4.1.1}$$

where \underline{D} is a diagonal matrix of diffusion coefficients, each component of the vector $q(x, t)$ represents population density or proportion, ∇^2 is the Laplace operator, and R describes the infection dynamics [30, Part II, Section D]. This approach is based on the work of Fisher (1937), who incorporated a diffusive element into a logistic equation simulating the propagation of a gene in a homogeneous population [17, 40]. Epidemic models based on Fisher's studies predict the development of a disease invasion front which moves progressively from invaded to uninvaded regions with a constant velocity [40]. Solutions of such systems that link (stable) disease-endemic and (unstable) disease-free stationary states are known as *traveling wave solutions*. A traveling front moving with speed c to the right is a solution of an epidemic system of type (4.1.1) such that ahead of the wave, a local segment of the population is disease-free and after the wave, a stable number of infectives and/or reduced number of susceptibles remains [30]. As the epidemic wave moves in time and space, the epidemic moves from initially infested regions to newly infested regions. Determining the existence of traveling wave solutions for models based on Fisher's approach is therefore of immense utility in disease prevention: such solutions can predict when and whether an epidemic will reach a specific location, move from an initial outbreak location, and whether and at what level an infected component will coexist with the disease-free population after the wave.

With regard to the study of dengue, the incorporation of a spatial element stems from the observation that the development of an epidemic is directly attributed to both human and adult mosquito movements. In search of human blood, winged female adult *Aedes aegypti* move in space and are therefore responsible for the spatial spread of the disease. Additionally, wind currents cause an advection movement of mosquitoes and resulting infestation [40, Section 1.3]. In its juvenile form, the

mosquito is not winged and does not bite; consequently, juveniles are not a factor in disease transmission. Human movement, caused by and resulting in complex social, economic, and environmental phenomena, leads to increased geographic exposure to the mosquito and disease incidence. In fact, human diffusive movement is the main reason for the fast spread of the disease ([36], see also [9]). Based on these biological factors, several studies on the spatial spread of dengue have been published [9, 14, 36, 47, 48].

In formulating our model, we pay close attention to these factors and follow closely the methodology established by Lewis *et al.* in establishing the existence of traveling wave solutions and calculating spread rates for a non-linear system of coupled reaction-diffusion equations modeling the spread of West Nile Virus [31]. As such, we make use of our \mathcal{R}_0 -based study conducted in Chapter 2. In this chapter, we interpret seasonality in broad terms, so that a climatic factor is given by a nonnegative parameter. First, we make parameter assumptions that imply the existence of a disease-endemic equilibrium for the non-spatial, main ODE model (see Section 2.2, Chapter 2). Next, we consider the non-diffusive juvenile mosquito and the recovered human components at their respective endemic equilibrium levels, assuming that their contribution to the evolution of an epidemic is a function of the parameters for the main ODE model and is constant. We use this assumption to construct a two-dimensional, spatially homogeneous ODE model consisting of infected adult mosquito and human components. We derive the basic reproductive number and establish conditions for the existence of an endemic equilibrium for the new model. We then incorporate the spatial element into this model to obtain a non-linear system of coupled reaction-diffusion equations. In so doing, we make use of the fact that human diffusive movement is the main contributing cause of the fast spread of the disease.

As such, we emphasize human and mosquito wing diffusion but consider mosquito movement by wind advection as causes of disease dissemination.

Assuming the wind advection coefficient is zero, we prove the existence of traveling wave solutions for the PDE system by using the \mathcal{R}_0 -based theory of Li *et al.* ([32]) for linear systems, following which we use the theory of Lewis *et al.* and others to calculate disease spread rates. We then lay a foundation for deriving the minimum wave speed in the case where the wind advection coefficient is not zero, which is considered separately. Numerical simulations in the case $\bar{v} = 0$ follow.

Remark: In [31], the method by which the main ODE model is simplified is somewhat different from ours. In [31], diffusion is incorporated into the unsimplified, main ODE model. Assumptions are put on parameters so that non-diffusive components vanish. Certain diffusive components are then frozen in time and are assumed to be initially constant in space. By using rigorous analysis, the authors state, it can be shown that these components remain constant in space. Comparison theory is then used to show that the traveling wave solutions of the resulting simplified spatial model can be used to conduct spatial analysis of the original unsimplified spatial model. In this chapter, we use Model (2.2.1) to construct a new 2-compartment system and then incorporate the spatial element into this model. The analysis for the spatial model presented in this chapter has no direct bearing on the analysis for a PDE model that directly incorporates a spatial element into Model (2.2.1). But for the purposes of establishing traveling wave solutions for the spatial model presented here, it is not necessary to establish this link.

4.2 The New ODE Model

In this section, we use the main ODE model, presented in Section 2.2, Chapter 2 to construct a new, 2-compartment ODE model for dengue transmission.

Consider, then, Model (2.2.1), with parameters explained in Table 2.1, all nonnegative. Set $S(t) = c$, the winter mildness index, which ranges between 0 (severe) and 2 (mild), where “mildness” is quantified by comparing a particular winter’s average temperature with that of previous winters (see Table 2.1). Consequently, the milder (more severe) the winter, the greater (smaller) the maturation rate. We will refer to c as γ , since c will be used in another context.

Let $x_1 = I_H, x_2 = I_M, x_3 = I_P, x_4 = I_E, x_5 = S_H$. We may simplify Model (2.2.1) (see Section 2.3, Chapter 2) to obtain

$$\begin{aligned}
 \dot{x}_1 &= \lambda_H x_5 x_2 - (y_H + \alpha_H + v_H)x_1 + \alpha_H x_1^2 \\
 \dot{x}_2 &= p_1 x_3 (1 - x_2) - u_m x_2 + \lambda_V (1 - x_2)x_1 \\
 \dot{x}_3 &= \tau_1 \gamma x_4 (1 - x_3) - u_q x_3 - p_1 x_3 (1 - x_2) \\
 \dot{x}_4 &= g r_m x_2 (1 - x_4) - \tau_1 \gamma x_4 (1 - x_3) - u_e x_4 \\
 \dot{x}_5 &= v_H - v_H x_5 - \lambda_H x_5 x_2 + \alpha_H x_1 x_5
 \end{aligned} \tag{4.2.1}$$

where $(x_1, \dots, x_5) \in \Omega = \{(x_1, x_2, x_3, x_4, x_5) : 0 \leq x_1 \leq 1, 0 \leq x_5 \leq 1, 0 \leq x_1 + x_5 \leq 1, 0 \leq x_2 \leq 1, 0 \leq x_3 \leq 1, 0 \leq x_4 \leq 1\}$.

We have that Ω is positively invariant (see Corollary 2.2 in Chapter 2), and that the DFE for this system is $(0, 0, 0, 0, 1)^T$.

The following proposition establishes a threshold parameter, \mathcal{R}_0 , for system (4.2.1):

Proposition 4.1. *Assume $u_m, (u_q+p_1), (\tau_1\gamma+u_e), v_H$ all > 0 , $\frac{gr_m p_1 \tau_1 \gamma}{(\tau_1\gamma+u_e)(p_1+u_q)(u_m)} < 1$, all other parameters nonnegative.*

Then we may define \mathcal{R}_0 for system (4.2.1) by

$$\mathcal{R}_0 = \sqrt{\frac{\lambda_V \lambda_H (p_1+u_q)(\tau_1\gamma+u_e)}{(y_H+\alpha_H+v_H)((\tau_1\gamma+u_e)(p_1+u_q)u_m-gr_m p_1 \tau_1 \gamma)}}. \quad (4.2.2)$$

The following conditions characterize the stability of the DFE of system (4.2.1):

- i) If $\mathcal{R}_0 < 1$, then the DFE is locally asymptotically stable.*
- ii) If $\mathcal{R}_0 > 1$, then the DFE is unstable.*

For proof see Propositions 2.3-2.4, Chapter 2.

In view of Proposition 4.1, we will make the following assumptions:

(A1) $\frac{gr_m p_1 \tau_1 \gamma}{(\tau_1\gamma+u_e)(p_1+u_q)(u_m)} < 1$.

(A2) $\mathcal{R}_0 > 1$.

Additionally, we will assume that

(A3) $\alpha_H = 0$, that is, there is no death due to dengue. This is not unreasonable, given the low immediate mortality rate of the disease.

(A4) u_q, u_e are 0, p_1, τ_1 large. This assumption is also not unreasonable, since the instability of the DFE implies that the diseased juvenile classes are not dying out. Consequently, u_q, u_e are sufficiently small to be absorbed by p_1, τ_1 . By **(A1)**, $gr_m < u_m$.

(A5) All other parameters are positive.

We have the following proposition:

Proposition 4.2. (A1) - (A5) \Rightarrow system (4.2.1) has a strongly endemic equilibrium, $E_1 = (\bar{x}_1, \bar{x}_2, \bar{x}_3, \bar{x}_4, \bar{x}_5)^T \in \Omega$, given by

$$\begin{aligned}\bar{x}_1 &= v_H \frac{1-\bar{x}_5}{v_H+y_H} \\ \bar{x}_2 &= v_H \frac{1-\bar{x}_5}{\lambda_H \bar{x}_5} \\ \bar{x}_3 &= \frac{\tau_1 \gamma \bar{x}_4}{\tau_1 \gamma \bar{x}_4 + p_1 - p_1 \bar{x}_2} \\ \bar{x}_4 &= \frac{gr_m \bar{x}_2}{gr_m \bar{x}_2 + \tau_1 \gamma - \tau_1 \gamma \bar{x}_3} \\ \bar{x}_5 &= \frac{v_H}{v_H + \lambda_H \bar{x}_2}\end{aligned}\tag{4.2.3}$$

E_1 is locally asymptotically stable.

Proof. See Propositions 2.6-2.7, Chapter 2. □

We now construct the new model.

Let $z^* = \bar{x}_5 + \bar{x}_1 = 1 - \frac{y_H}{v_H} \bar{x}_1 = v_H(1 - \bar{x}_5)$. Note that $z^* < 1$. Let \bar{x}_4 be as in (4.2.3).

Our new system is given by:

$$\begin{aligned}\dot{x}_1 &= \lambda_H(z^* - x_1)x_2 - (y_H + v_H)x_1 \\ \dot{x}_2 &= gr_m x_2(1 - \bar{x}_4) - u_m x_2 + \lambda_V(1 - x_2)x_1\end{aligned}\tag{4.2.4}$$

where $(x_{1_0}, x_{2_0}) \in [0, z^*] \times [0, 1]$, which is positively invariant.

Recall that $x_1 = I_H$, $x_2 = I_M$ (see Subsection 2.3.2, Chapter 2).

Then system (4.2.4) can be written as

$$\begin{bmatrix} I_M \\ I_H \end{bmatrix}_t = f \left(\begin{bmatrix} I_M \\ I_H \end{bmatrix} \right)$$

with $f = (f_1, f_2)^T$ given as

$$\begin{aligned} f_1(I_M, I_H) &= gr_m I_M(1 - \bar{x}_4) - u_m I_M + \lambda_V(1 - I_M)I_H \\ f_2(I_M, I_H) &= \lambda_H(z^* - I_H)I_M - (y_H + v_H)I_H \end{aligned} \quad (4.2.5)$$

where $(I_{M_0}, I_{H_0}) \in [0, 1] \times [0, z^*]$.

Note that **(A4)** and $\bar{x}_4 \in \Omega$ guarantee that $gr_m(1 - \bar{x}_4) - u_m < 0$.

4.2.1 Analysis of System (4.2.5)

The Jacobian matrix at the trivial stationary solution $(I_M, I_H) = (0, 0)^T$ is given by

$$\mathcal{T} = Df(0) = \begin{pmatrix} gr_m(1 - \bar{x}_4) - u_m & \lambda_V \\ \lambda_H z^* & -(y_H + v_H) \end{pmatrix} \quad (4.2.6)$$

Denoting the eigenvalues of \mathcal{T} by λ_1, λ_2 , it follows that $\lambda_1 + \lambda_2 = \text{tr}\mathcal{T} = gr_m(1 - \bar{x}_4) - u_m - (y_H + v_H) < 0$, and $\lambda_1\lambda_2 = \det\mathcal{T} = (gr_m(1 - \bar{x}_4) - u_m)(-y_H - v_H) - \lambda_H z^* \lambda_V = 1 - (\mathcal{R}'_0)^2$, where $\mathcal{R}'_0 = \sqrt{\frac{\lambda_H z^* \lambda_V}{(gr_m(1 - \bar{x}_4) - u_m)(-y_H - v_H)}}$ is the basic reproductive number for system (4.2.5) (see [52] for a definition and calculation of \mathcal{R}'_0). It follows that $(0, 0)^T$ is locally asymptotically stable (a node) iff $\det\mathcal{T} > 0 \Leftrightarrow \mathcal{R}'_0 < 1$ and unstable (a saddle point) iff $\det\mathcal{T} < 0 \Leftrightarrow \mathcal{R}'_0 > 1$. In the latter case, there exists a positive eigenvalue with positive components of the corresponding eigenvector. We therefore make the following assumption:

(B1) $(gr_m(1 - \bar{x}_4) - u_m)(-y_H - v_H) < \lambda_H z^* \lambda_V$, giving $\det\mathcal{T} < 0$ and $\mathcal{R}'_0 > 1$.

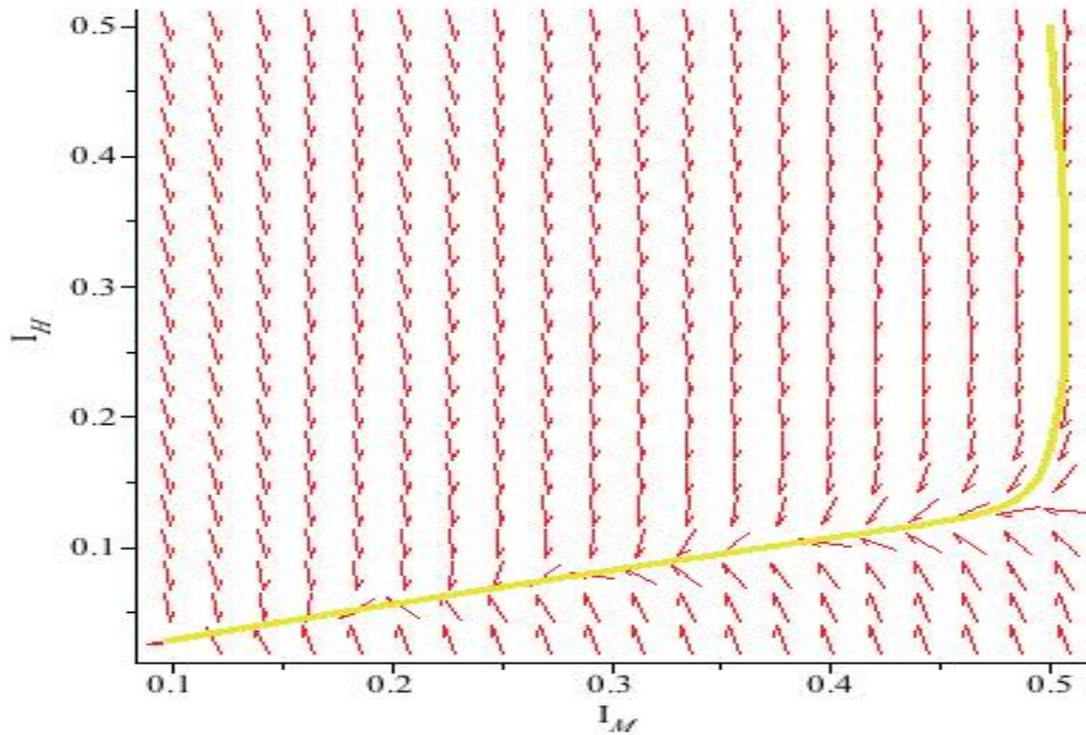


Figure 4.1: Phase portrait for system (4.2.5), $\gamma = 1$, all other parameters and values are given in Table 4.1.

We also consider the positive equilibrium of system (4.2.5) given by $(I_M^*, I_H^*)^T \in [0, 1] \times [0, z^*]$, where

$$\begin{aligned} I_M^* &= \frac{(y_H + v_H)(gr_m(1 - \bar{x}_4) - u_m) + z^* \lambda_H \lambda_V}{\lambda_H(\lambda_V z^* - gr_m(1 - \bar{x}_4) + u_m)} \\ I_H^* &= \frac{(y_H + v_H)(gr_m(1 - \bar{x}_4) - u_m) + z^* \lambda_H \lambda_V}{\lambda_V(y_H + v_H + \lambda_H)}. \end{aligned} \quad (4.2.7)$$

Proposition 4.3. *If $(I_{M_0}, I_{H_0}) \in [0, 1] \times [0, z^*]$, then the endemic equilibrium $(I_M^*, I_H^*)^T$ is globally asymptotically stable in $[0, 1] \times [0, z^*]$.*

Proof. Consider the linearized system of (4.2.5) at $(I_M^*, I_H^*)^T$. The Jacobian matrix at $(I_M^*, I_H^*)^T$ is given by

$$\mathcal{T}^* = Df((I_M^*, I_H^*)^T) = \begin{pmatrix} gr_m(1 - \bar{x}_4) - u_m - \lambda_V I_H^* & \lambda_V(1 - I_M^*) \\ \lambda_H(z^* - I_H^*) & -(y_H + v_H) - \lambda_H I_M^* \end{pmatrix} \quad (4.2.8)$$

Consequently, we have that $tr\mathcal{T}^* = gr_m(1 - \bar{x}_4) - u_m - (y_H + v_H) - \lambda_V I_H^* - \lambda_H I_M^* = tr\mathcal{T} - \lambda_V I_H^* - \lambda_H I_M^* < 0$, and $\det\mathcal{T}^* = (y_H + v_H)(gr_m(1 - \bar{x}_4) - u_m) + z^* \lambda_H \lambda_V = -\det\mathcal{T} > 0$, showing that $(I_M^*, I_H^*)^T$ is locally asymptotically stable.

From (4.2.5) we have that $\nabla f = \frac{\partial f_1}{\partial I_M} + \frac{\partial f_2}{\partial I_H} = gr_m(1 - \bar{x}_4) - u_m - \lambda_V I_H - (y_H + v_H) - \lambda_H I_M < 0$. So by Bendixson's criterion, we have our desired result. \square

4.3 Spread Rates and Traveling Waves

Here I consider spatial extensions of the system (4.2.5). The general form for the model in the case where the wind advection coefficient is 0 will be

$$u_t = \mathcal{D}u_{xx} + f(u), \quad (4.3.1)$$

where u denotes the mosquito and human components, $f(u)$ describes the infection dynamics (where f is as in (4.2.5)), and \mathcal{D} is a non-negative diagonal diffusion matrix. The dynamics are assumed to have a disease-free (i.e., all infected components equal to zero) equilibrium u_0 satisfying $f(u_0) = 0$, and an endemic equilibrium $u^* > 0$ satisfying $f(u^*) = 0$.

Two alternative approaches for analyzing the spread of infection involve analyzing traveling wave solutions and calculating spread rates. To analyze traveling wave solutions, we proceed as follows:

Let $u(x, t) = U(z)$ with $z = x - ct$, so that system (4.3.1) can be rewritten in terms of a coordinate frame moving with speed c to the right. System (4.3.1) becomes $c\dot{U} + f(U) + D\ddot{U} = 0$. Boundary conditions that join the disease-free and endemic equilibrium are assumed, namely

$$\begin{aligned} \lim_{z \rightarrow -\infty} U(z) &= u_0 \\ \lim_{z \rightarrow +\infty} U(z) &= u^*. \end{aligned} \tag{4.3.2}$$

Alternatively, to calculate spread rates, we first establish the following definitions ([31])*Definitions 1.1, 1.2):

Definition 4.4. *The spread rate for the non-linear system (4.3.1) with initial conditions not equal to u_0 on a compact set, is a number c_G^* such that for $u_0 \neq u^*$ and small $\epsilon > 0$,*

$$\begin{aligned} \lim_{t \rightarrow \infty} \left\{ \sup_{|x| \geq (c_G^* + \epsilon)t} \|u(x, t) - u_0\| \right\} &= 0 \\ \lim_{t \rightarrow \infty} \left\{ \sup_{|x| \leq (c_G^* - \epsilon)t} \|u(x, t) - u^*\| \right\} &> 0. \end{aligned} \tag{4.3.3}$$

We also define the spread rate for the linearized system corresponding to system (4.3.1):

Definition 4.5. *The spread rate \bar{c} for the simplified linear system corresponding to system (4.3.1),*

$$u_t = \mathcal{D}u_{xx} + \mathcal{A}u, \tag{4.3.4}$$

where $f(0) = 0$ and $\mathcal{A} = Df(0)$ is the Jacobian matrix, is defined as a number

satisfying

$$\begin{aligned} \lim_{t \rightarrow \infty} \left\{ \sup_{|x| \geq (\bar{c} + \epsilon)t} ||u(x, t)|| \right\} &= 0 \\ \lim_{t \rightarrow \infty} \left\{ \sup_{|x| \leq (\bar{c} - \epsilon)t} ||u(x, t)|| \right\} &> 0. \end{aligned} \quad (4.3.5)$$

When the spread rates for the non-linear and linear systems are identical, then the spread rate for the non-linear system is said to be linearly determinate [31, Subsection 1.2]. Following [31], we use the methods of Li *et al.* [32] to show the existence of a class of traveling wave solutions for system (4.3.1) and use the methods of Weinberger *et al.* [55] to relate the speed c to c_G^* and \bar{c} .

4.4 Spatially-Dependent Model

To account for the possible impact of spatial movement of humans and mosquitoes, diffusion and wind advection terms are incorporated to system (4.2.5), giving the following spatially-dependent model in which variables are functions of space x , with $-\infty < x < \infty$, and time t , and assumptions are as in system (4.2.5). So we have,

$$\begin{aligned} \frac{\partial I_M}{\partial t} &= gr_m I_M (1 - \bar{x}_4) - u_m I_M + \lambda_V (1 - I_M) I_H + \epsilon \frac{\partial^2 I_M}{\partial x^2} + \bar{v} \frac{\partial I_M}{\partial x} \\ \frac{\partial I_H}{\partial t} &= \lambda_H (z^* - I_H) I_M - (y_H + v_H) I_H + D \frac{\partial^2 I_H}{\partial x^2}, \end{aligned} \quad (4.4.1)$$

where the diffusion coefficients D, ϵ , are positive, $I_H(x, 0), I_M(x, 0) \in [0, 1] \times [0, z^*]$. Until further notice, we set the advection coefficient $\bar{v} = 0$.

System (4.4.1) can then be written as a system of reaction-diffusion equations:

$$\begin{bmatrix} I_M \\ I_H \end{bmatrix}_t = \mathcal{D} \begin{bmatrix} I_M \\ I_H \end{bmatrix}_{xx} + f \left(\begin{bmatrix} I_M \\ I_H \end{bmatrix} \right), \quad (4.4.2)$$

with $f = (f_1, f_2)^T$ given as in (4.2.5) and

$$\mathcal{D} = \begin{bmatrix} \epsilon & 0 \\ 0 & D \end{bmatrix}. \quad (4.4.3)$$

There is a positive stationary solution of system (4.4.1), namely (I_M^*, I_H^*) , given by (4.2.7). System (4.2.5) is the spatially-independent version of system (4.4.1), so the results of the analysis of system (4.2.5) are applicable.

4.5 Traveling Wave Solutions

We start by defining traveling waves for system (4.4.1) ([31, Definition 4.1]):

Definition 4.6. *A traveling wave solution with speed c for (4.4.1) is a solution that has the form $(I_M(x-ct), I_H(x-ct))$ and connects the disease-free and disease-endemic stationary points of the system so that*

$$\begin{aligned} \lim_{z \rightarrow -\infty} (I_M, I_H) &= (I_M^*, I_H^*) \\ \lim_{z \rightarrow +\infty} (I_M, I_H) &= (0, 0). \end{aligned} \quad (4.5.1)$$

The traveling front solution with speed c satisfies the ODE system,

$$\begin{aligned} -c\dot{I}_M &= \epsilon\ddot{I}_M + gr_m I_M(1 - \bar{x}_4) - u_m I_M + \lambda_V(1 - I_M)I_H \\ -c\dot{I}_H &= D\ddot{I}_H + \lambda_H(z^* - I_H)I_M - (y_H + v_H)I_H \end{aligned} \quad (4.5.2)$$

with boundary conditions at $\pm\infty$ determined by stationary solutions of this system.

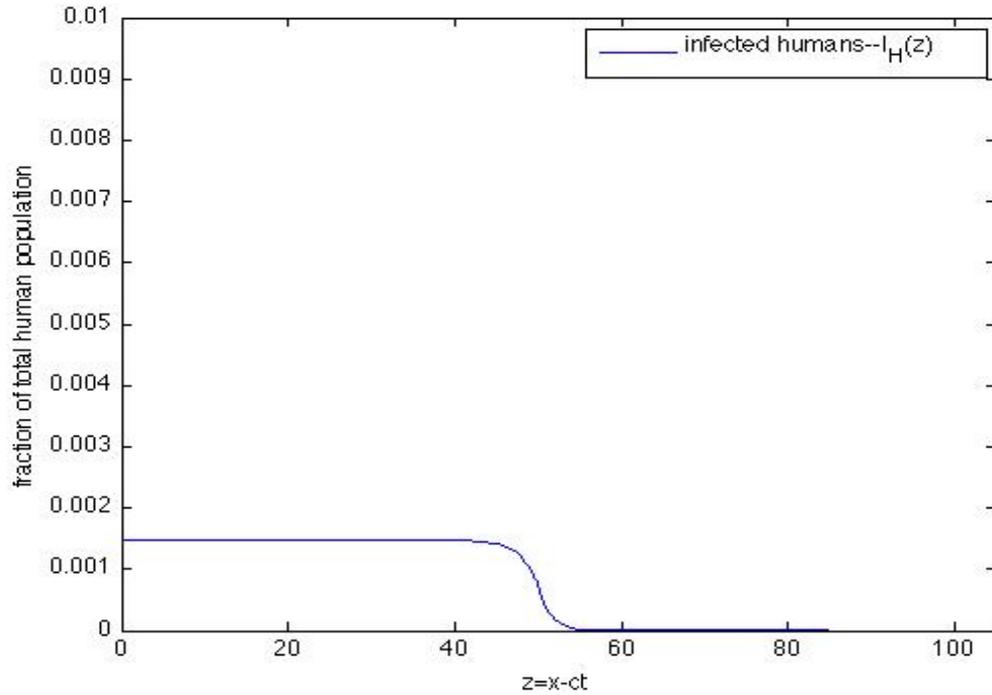


Figure 4.2: *Traveling waves for the system (4.5.2) when $\epsilon = 1/10$, $D = 10$, $\gamma = 1$, $c = 1$, all other parameters and values are given in Table 4.1.*

Following [31, Section 4], we use the theorem on the existence of traveling waves proved in [32] (see also [53, Theorem 4.2]). To this end, we examine and list the properties of the nonlinear system (4.4.1), as written in (4.4.2), that are necessary to apply the result:

1. f has two stationary solutions: $(0, 0)$ and (I_M^*, I_H^*) .
2. f is cooperative, i.e., f_1, f_2 are non-decreasing in off-diagonal components.

We have that $\frac{\partial f_1}{\partial I_H} = \lambda_V(1 - I_M) \geq 0$, $\frac{\partial f_2}{\partial I_M} = \lambda_H(z^* - I_H) \geq 0$, by the positive invariance of $[0, 1] \times [0, z^*]$.

3. f does not depend explicitly on either x or t .

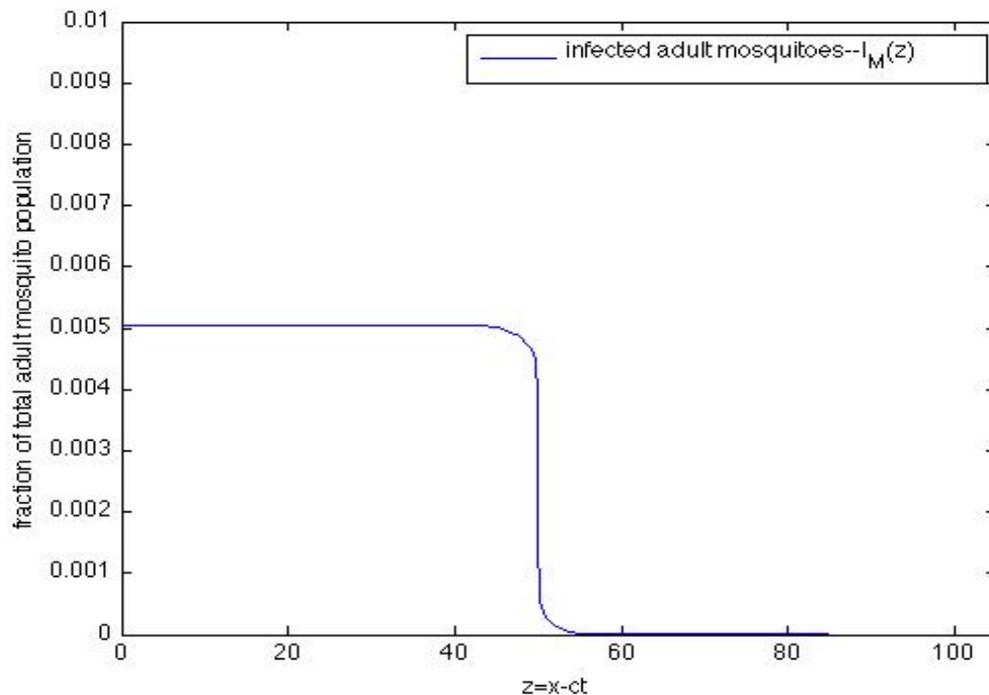


Figure 4.3: *Traveling waves for the system (4.5.2) when $\epsilon = 1/10$, $D = 10$, $\gamma = 1$, $c = 1$, all other parameters and values are given in Table 4.1.*

4. f is continuous, has uniformly bounded continuous first partial derivatives for $0 \leq (I_M, I_H) \leq (I_M^*, I_H^*)$ and is differentiable at zero.

Each f_i is a polynomial function, so f is uniformly continuous and differentiable. Further, $|\frac{\partial f_1}{\partial I_M}| = |gr_m(1-\bar{x}_4) - u_m - \lambda_V I_H| \leq gr_m + u_m + \lambda_V$, $|\frac{\partial f_1}{\partial I_H}| = |\lambda_V(1 - I_M)| \leq \lambda_V$, $|\frac{\partial f_2}{\partial I_M}| = |\lambda_H(z^* - I_H)| \leq \lambda_H z^*$, and $|\frac{\partial f_2}{\partial I_H}| = |-(y_H + v_H) - \lambda_H I_M| < (y_H + v_H) + \lambda_H$.

4b. The Jacobian matrix $\mathcal{T} = Df(0)$, given by (4.2.6), has nonnegative off-diagonal entries and has a positive eigenvalue whose eigenvector has positive components.

5. Matrix \mathcal{D} is diagonal with constant strictly positive diagonal entries.

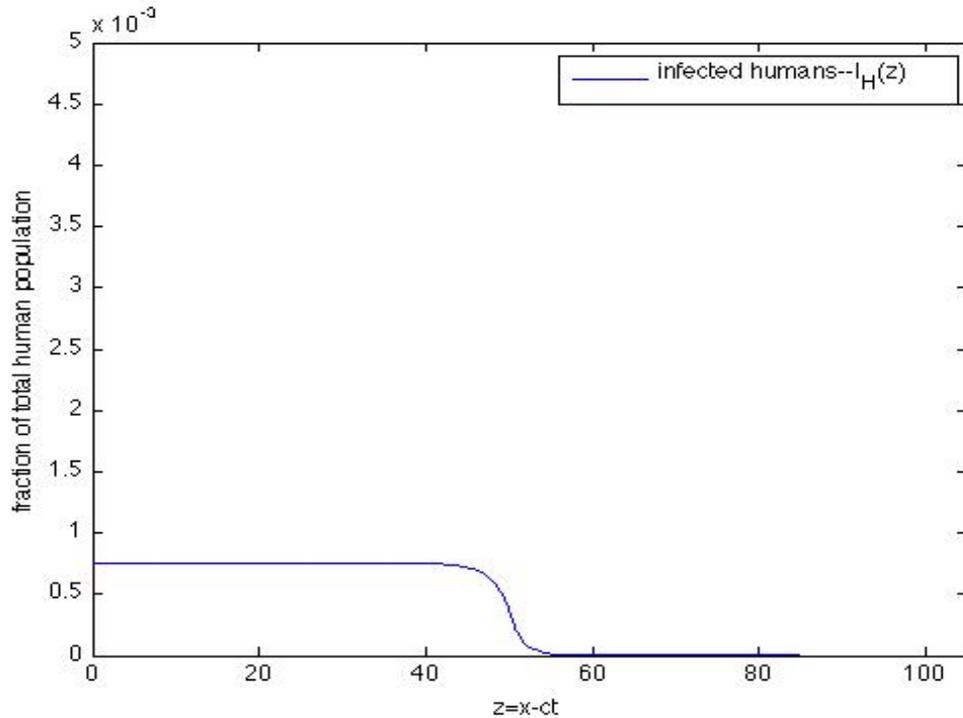


Figure 4.4: *Traveling waves for the system (4.5.2) when $\epsilon = 1/10, D = 10, \gamma = .5, c = 1$, all other parameters and values are given in Table 4.1.*

We have the following traveling wave result:

Theorem 4.7. ([31, Theorem 4.1], see also [32, Theorem 4.2]) *There exists a minimal speed of traveling fronts c_0 such that for $c \geq c_0$, the non-linear system (4.4.1) has a non-increasing traveling wave solution with speed c so that (4.5.1) holds. If $c < c_0$, there is no traveling wave solution of this form.*

Alternatively, we can investigate the spatial spread of the infection by calculating the spread rate of system (4.4.1), given by Definition 4.4. Properties 1-5 imply that the spread rate c_G^* can be described in terms of c_0 .

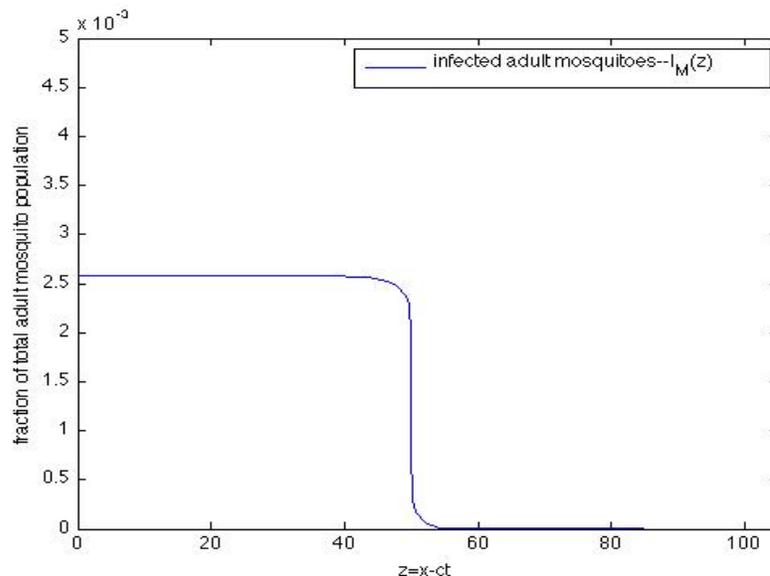


Figure 4.5: *Traveling waves for the system (4.5.2) when $\epsilon = 1/10, D = 10, \gamma = .5, c = 1$, all other parameters and values are given in Table 4.1.*

In fact, we have the following result [31, Theorem 4.2]:

The minimal wave speed c_0 for the non-linear system (4.4.1) is equal to c_G^* , the spread rate for this system.

4.6 Spread-Rate Analysis

We seek to calculate c_G^* . To that end, we have the following theorem:

Theorem 4.8. *The spread rate c_G^* of the non-linear system (4.4.1) and the spread rate \bar{c} (see Definition 4.5) of the linearized system*

$$\begin{bmatrix} I_M \\ I_H \end{bmatrix}_t = \mathcal{D} \begin{bmatrix} I_M \\ I_H \end{bmatrix}_{xx} + \mathcal{T} \begin{bmatrix} I_M \\ I_H \end{bmatrix}, \quad (4.6.1)$$

both exist and $c_G^* = \bar{c}$.

Proof. Observe that the Jacobian matrix $\mathcal{T} = Df(0)$, given by (4.2.6), is irreducible. Additionally, the subtangential condition

$$f \left(\rho \begin{bmatrix} I_M \\ I_H \end{bmatrix} \right) \leq \rho \mathcal{T} \begin{bmatrix} I_M \\ I_H \end{bmatrix} \quad (4.6.2)$$

where ρ is a positive number, is satisfied, since

$$\begin{aligned} f \left(\rho \begin{bmatrix} I_M \\ I_H \end{bmatrix} \right) &= (f_1(\rho I_M, \rho I_H), f_2(\rho I_M, \rho I_H)) \\ &= (gr_m \rho I_M (1 - \bar{x}_4) - u_m \rho I_M + \lambda_V (1 - \rho I_M) \rho I_H, \\ &\quad \lambda_H (z^* - \rho I_H) \rho I_M - (y_H + v_H) \rho I_H) \\ &\leq (\rho ((gr_m (1 - \bar{x}_4) - u_m) I_M + \lambda_V I_H), \\ &\quad \rho ((\lambda_H z^*) I_M - (y_H + v_H) I_H)) \\ &= \rho \mathcal{T} \begin{bmatrix} I_M \\ I_H \end{bmatrix}. \end{aligned} \quad (4.6.3)$$

By [55, Theorem 4.2] (see also Theorem 5.1(i) of [31]), we have the desired result. \square

We then have the following result [31, Theorem 5.1(ii)]:

The spread rate \bar{c} of (4.6.1) is given by

$$\bar{c} = \inf_{\lambda > 0} \sigma_1(\lambda) \quad (4.6.4)$$

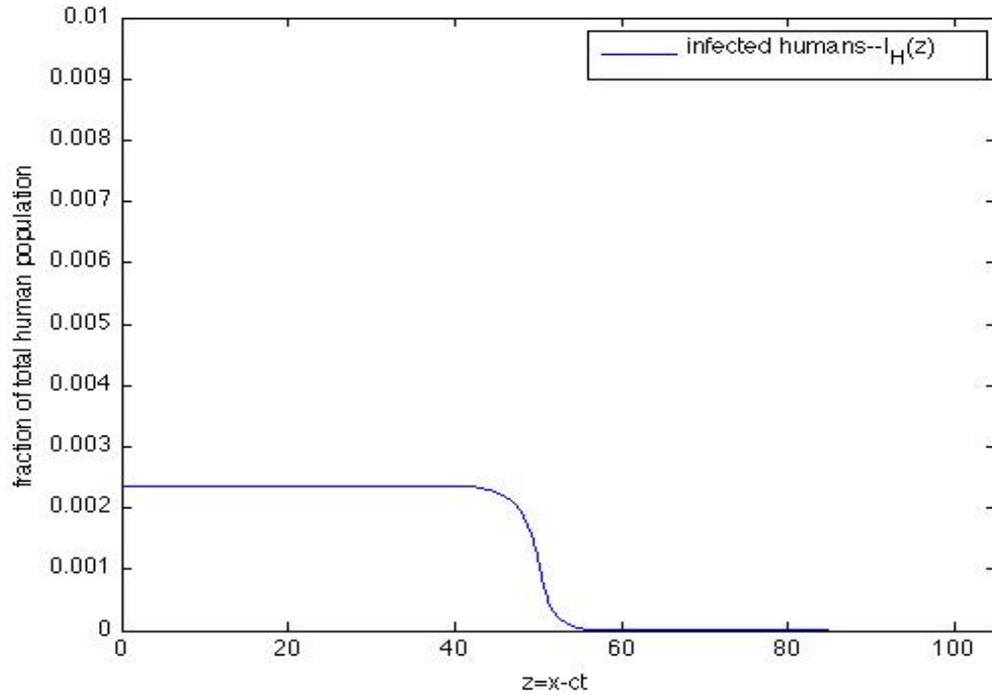


Figure 4.6: *Traveling waves for the system (4.5.2) when $\epsilon = 1/10$, $D = 10$, $\gamma = 2$, $c = 1$, all other parameters and values are given in Table 4.1.*

where $\sigma_1(\lambda)$ is the largest eigenvalue, i.e. the spectral bound, of the matrix

$$B_\lambda = \frac{\mathcal{T} + \lambda^2 \mathcal{D}}{\lambda} \quad (4.6.5)$$

This result and Theorem 4.8 do not rely upon the positivity of the diagonal elements of \mathcal{D} and thus remain true in the limiting case $\epsilon = 0$ [31, Theorem 5.1].

Now

$$B_\lambda = \begin{pmatrix} \frac{gr_m(1-\bar{x}_4) - u_m}{\lambda} + \epsilon\lambda & \frac{\lambda_V}{\lambda} \\ \frac{\lambda_H z^*}{\lambda} & \frac{-(y_H + v_H)}{\lambda} + D\lambda \end{pmatrix} \quad (4.6.6)$$

Denoting $tr\mathcal{T} = gr_m(1 - \bar{x}_4) - u_m - (y_H + v_H) \equiv \theta < 0$ and $\det \mathcal{T} = (gr_m(1 - \bar{x}_4) - u_m)(-y_H - v_H) - \lambda_H z^* \lambda_V \equiv j < 0$, the characteristic polynomial of B_λ is

$$\begin{aligned} p(\sigma; \lambda, \epsilon) &= \sigma^2 - \sigma \left(\frac{\theta + (D + \epsilon)\lambda^2}{\lambda} \right) + \frac{j}{\lambda^2} + (gr_m(1 - \bar{x}_4) - u_m)D \\ &\quad - \epsilon(y_H + v_H) + \epsilon D \lambda^2 = 0. \end{aligned} \quad (4.6.7)$$

We have the following result [31, Lemma 5.1]:

For any finite λ , the roots $\sigma_i(\lambda, \epsilon)$, $i = 1, 2$ of the characteristic polynomial $p(\sigma; \lambda, \epsilon)$ of the matrix B_λ depend continuously on ϵ at zero, that is, $\lim_{\epsilon \rightarrow 0} \sigma_i(\lambda, \epsilon) = \sigma_i(\lambda, 0)$. In the general case $\epsilon > 0$, the larger root $\sigma_1(\lambda, \epsilon)$ can have more than one extremum: if $\epsilon \neq \epsilon'$, we can have that $\inf_{\lambda > 0} \sigma_1(\lambda, \epsilon) \neq \inf_{\lambda > 0} \sigma_1(\lambda, \epsilon')$. To determine \bar{c} , we therefore study the limiting case $\epsilon = 0$.

We have the following result, based on [31, Theorem 5.2] (see also [22, Section 6]):

Let $\det \mathcal{T} \equiv j < 0$ and $\epsilon = 0$. Consider

$$\begin{aligned} P(\sigma; \lambda) &= \lambda^2 p(\sigma; \lambda, 0) = -D\sigma\lambda^3 + (\sigma^2 + D(gr_m(1 - \bar{x}_4) - u_m))\lambda^2 \\ &\quad - \theta\sigma\lambda + j. \end{aligned} \quad (4.6.8)$$

The spread rate of the linear system (4.6.1) can be obtained as the largest value σ such that the polynomial $P(\sigma; \lambda)$ has a real-positive double root. The double-root condition implies that \bar{c} is the largest number Γ such that $P(\Gamma; \lambda) = \frac{\partial P}{\partial \lambda} = 0$ [31, Theorem 5.2], that is, \bar{c} is the largest number Γ such that $Q(\Gamma) = 0$, where Q is

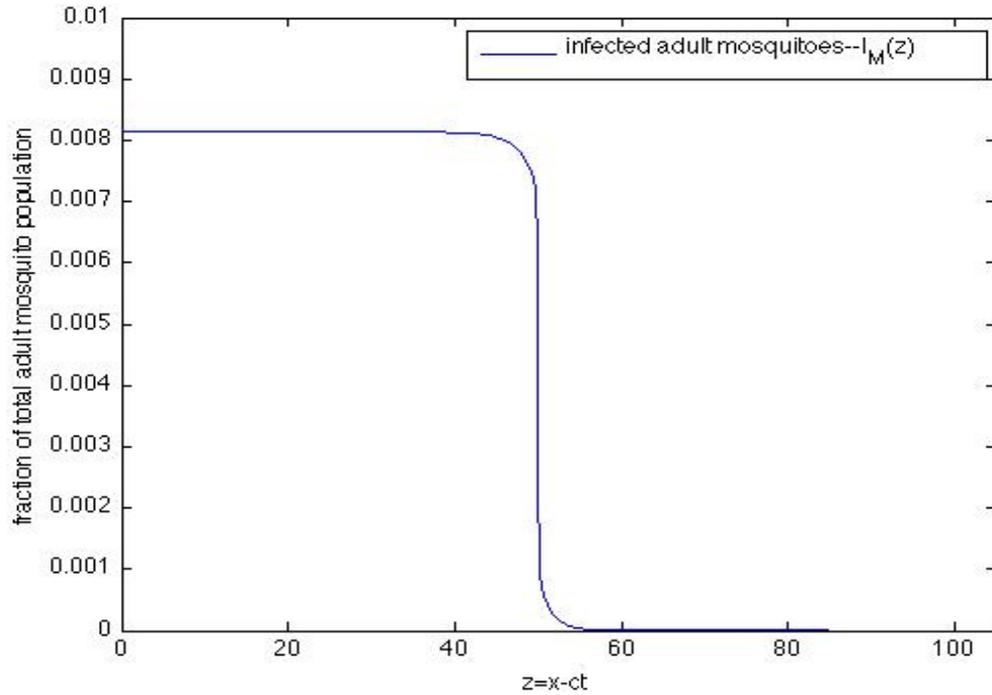


Figure 4.7: *Traveling waves for the system (4.5.2) when $\epsilon = 1/10, D = 10, \gamma = 2, c = 1$, all other parameters and values are given in Table 4.1.*

the resultant of the polynomial P and its derivative [56]. Now,

$$\begin{aligned}
 Q(\Gamma) = & \Gamma^6(D\Gamma\theta^2 - 4D\Gamma j) + \Gamma^4[-4\theta^3 D^2\Gamma - 12(gr_m(1 - \bar{x}_4) - u_m)jD^2\Gamma \\
 & + 2(gr_m(1 - \bar{x}_4) - u_m)\theta^2 D^2\Gamma + 18\theta jD^2\Gamma] \\
 & + \Gamma^2[18\theta(gr_m(1 - \bar{x}_4) - u_m)jD^3\Gamma - 12(gr_m(1 - \bar{x}_4) - u_m)^2 jD^3\Gamma + \\
 & (gr_m(1 - \bar{x}_4) - u_m)^2\theta^2 D^3\Gamma - 27j^2 D^3\Gamma] - 4D^4(gr_m(1 - \bar{x}_4) - u_m)^3 j\Gamma.
 \end{aligned} \tag{4.6.9}$$

So the roots of Q are 0 and the roots of the polynomial $C_3(\Gamma^2)^3 + C_2(\Gamma^2)^2 + C_1(\Gamma^2) + C_0$, where $C_3 = (\theta^2 - 4j)$ and $C_2 = [-4\theta^3 D - 12(gr_m(1 - \bar{x}_4) - u_m)jD + 2(gr_m(1 - \bar{x}_4) - u_m)\theta^2 D + 18\theta jD]$, $C_1 = [18\theta(gr_m(1 - \bar{x}_4) - u_m)jD^2 - 12(gr_m(1 - \bar{x}_4) - u_m)^2 jD^2 + (gr_m(1 - \bar{x}_4) - u_m)^2\theta^2 D^2 - 27j^2 D^2]$ and $C_0 = -4D^3(gr_m(1 - \bar{x}_4) - u_m)^3 j$. Let $x = \Gamma^2$.

Then $C_3(\Gamma^2)^3 + C_2(\Gamma^2)^2 + C_1(\Gamma^2) + C_0$ is clearly cubic in x . Let $f(x) = C_3x^3 + C_2x^2 + C_1x + C_0$. Then f is concave up for $x > 0$, since $j < 0, \theta < gr_m(1 - \bar{x}_4) - u_m < 0$ imply that $f''(x) = 6C_3x + 2C_2 = 6(\theta^2 - 4j)x + 2[-4\theta^3D - 12(gr_m(1 - \bar{x}_4) - u_m)jD + 2(gr_m(1 - \bar{x}_4) - u_m)\theta^2D + 18\theta jD] > 0$. Now $f(0) = C_0 < 0$. This implies that f and, consequently, Q , has one positive root. So \bar{c} is the positive square root of the largest zero of Q [31, (25)].

By [31, Theorem 5.3], we may summarize our results in the following manner:

Assume that $\det \mathcal{T} < 0$ and $\epsilon > 0$. Then the spread rate c_G^ of the non-linear system (4.4.1) is the lower bound for the speed of a class of traveling wave solutions, and the spread rate is linearly determinate. As $\epsilon \rightarrow 0$, the spread rate for the non-linear system approaches the positive square root of the largest zero of the resultant of the polynomial P and its derivative.*

4.7 Case: Advection $\bar{v} \neq 0$

We now relax the condition that $\bar{v} = 0$. If we take $\bar{v} > 0$, we may define a traveling wave as a solution with speed c of the ODE system

$$\begin{aligned} -(c + \bar{v})\dot{I}_M &= \epsilon\ddot{I}_M + gr_m I_M(1 - \bar{x}_4) - u_m I_M + \lambda_V(1 - I_M)I_H \\ -c\dot{I}_H &= D\ddot{I}_H + \lambda_H(z^* - I_H)I_M - (y_H + v_H)I_H \end{aligned} \quad (4.7.1)$$

with boundary conditions at $\pm\infty$ determined as in system (4.5.2).

We may reduce (4.7.1) to a first-order system in 4 dimensions. To determine the existence of traveling waves, we look for a heteroclinic orbit from $(I_M^*, 0, I_H^*, 0)$ to $(0, 0, 0, 0)$ such that the orbit components I_M, I_H remain in $[0, 1] \times [0, z^*]$. The

existence of such an orbit follows from properties 1-5 above, which hold for (4.7.1) if the advection coefficient is nonnegative [32, Theorem 4.2]. The minimal wave speed c_{min} for the non-linear system (4.7.1) is equal to the spread rate for this system [32, Theorem 4.2]. We establish an informal analytic framework for finding c_{min} .

Consider now the linearization of the first order system at $(0, 0, 0, 0)$. The Jacobian at $(0, 0, 0, 0)$ is given by:

$$\begin{pmatrix} -\frac{c+\bar{v}}{\epsilon} & 0 & -\frac{gr_m(1-\bar{x}_4)-u_m}{\epsilon} & -\frac{\lambda_V}{\epsilon} \\ 0 & -\frac{c}{D} & -\frac{\lambda_H z^*}{D} & \frac{(y_H+v_H)}{D} \\ 1 & 0 & 0 & 0 \\ 0 & 1 & 0 & 0 \end{pmatrix} \quad (4.7.2)$$

The characteristic polynomial of (4.7.2) is

$$\begin{aligned} \bar{P}(x) = & x^4 + \frac{c\epsilon+Dc+D\bar{v}}{D\epsilon}x^3 - \frac{c y_H + c v_H - D gr_m + D gr_m \bar{x}_4 + D u_m - c^2 - c \bar{v}}{D\epsilon}x^2 \\ & - \frac{y_H c + y_H \bar{v} + c v_H + v_H \bar{v} - c gr_m + c gr_m \bar{x}_4 + c u_m}{D\epsilon}x \\ & - \frac{\lambda_H z^* \lambda_V + y_H gr_m - y_H gr_m \bar{x}_4 - y_H u_m + v_H gr_m - v_H gr_m \bar{x}_4 - v_H u_m}{D\epsilon} \end{aligned} \quad (4.7.3)$$

If all the eigenvalues of (4.7.2) are real, oscillations about $(0, 0, 0, 0)$ will be avoided and the heteroclinic orbit will be nonnegative (see [36, Section 4 and Appendix B.] and [30, Chapter 18]). Let $\bar{P}(x) = P(c, x)$. The minimum speed c_{min} of the traveling wave solution is therefore the minimum positive number c such that the roots of $P(c, \cdot)$ are all real. Now $P(c, 0) = -\frac{\lambda_H z^* \lambda_V + y_H gr_m - y_H gr_m \bar{x}_4 - y_H u_m + v_H gr_m - v_H gr_m \bar{x}_4 - v_H u_m}{D\epsilon} = \det \mathcal{T} < 0$. Also, $\lim_{x \rightarrow \pm\infty} P(c, \cdot) = \infty$ (*). So $P(c, \cdot)$ has at least one positive and one negative root. By Descartes' rule of signs, $P(c, \cdot)$ has exactly 1 positive real root. Also, $\frac{\partial P}{\partial x}|_{x=0} = -\frac{y_H c + y_H \bar{v} + c v_H + v_H \bar{v} - c gr_m + c gr_m \bar{x}_4 + c u_m}{D\epsilon} < 0$, since $gr_m < u_m$, and $\lim_{x \rightarrow \infty} \frac{\partial P}{\partial x} = \infty$

and $\lim_{x \rightarrow -\infty} \frac{\partial P}{\partial x} = -\infty$. So $\frac{\partial P}{\partial x}$ has at least one positive real root. Descartes' rule of signs implies that $\frac{\partial P}{\partial x}$ has exactly 1 positive real root. Let $x_0 = \sup\{x : x < 0, \frac{\partial P}{\partial x} = P(c, x) = 0\}$, where x_0 is a triple-root of $P(c, \cdot)$ and a double-root of $\frac{\partial P}{\partial x}$ (**). Now if $x^* < 0$, with $|x^*|$ is small, $\frac{\partial P}{\partial x}|_{x=x^*}$ is nonnegative and increasing in c and if $|x^*|$ is large, $\frac{\partial P}{\partial x}|_{x=x^*}$ is nonpositive and decreasing in c (***). So if $|x_0|$ is small, $\frac{\partial P}{\partial x}|_{x=x_0}$ and $P(c, x_0)$ are increasing in c . Let c_0 be the minimum $c > 0$ corresponding to x_0 . Then for $c > c_0$, $\frac{\partial P}{\partial x}$ has 1 positive root and 2 negative roots, say $x_{1,2}$, with x_1 a local minimizer of $P(c, \cdot)$, x_2 a local maximizer, and $x_1 < x_2$. It can be shown that as $c \rightarrow \infty$, $x_1 \rightarrow -\infty$ and $x_2 \rightarrow 0$. By (***), $P(c, x_1)$ decreases in c and $P(c, x_2)$ increases in c as c increases. So for $c > c_0$, $P(c, x_1) \leq 0$ and $P(c, x_2) \geq 0$. By this and (*), if $c > c_0$, $P(c, \cdot) = \bar{P}$ has 4 real roots, 1 positive and three negative, and $c_0 = c_{min}$.

To find c_0 , it is therefore necessary to find the resultant of $P(c, \cdot)$ and its derivative in x . This, is not, however, sufficient, since, for one, it does not ensure that the heteroclinic orbit remains in $[0, 1] \times [0, z^*]$. We leave this for future work.

4.8 Numerical Simulations

As in Chapters 2 and 3, values for $v_H, \lambda_H, y_H, u_m, r_m$ and g are comparable to those presented by Coutinho *et al.* [8] on the basis of estimates known from the dengue infection process and human and mosquito vital statistics. We assume that the entire egg and larval populations are at carrying capacity.

Figures 4.8 - 4.10 show plots of the numerical estimates for the spread rate $c_G^* = \bar{c}$ of system (4.4.1) with $\epsilon = 0$, calculated using (4.6.9) and other parameters as in

\bar{x}_4 in	Value
Figures 4.2-4.3, 4.8, 4.1	0.01805790889
Figures 4.4-4.5, 4.9	0.01824582550
Figures 4.6-4.7, 4.10	0.01770341177
Parameter	Value
v_H	2.5
λ_H	0.75
y_H	0.067
α_H	0
u_q	0
u_m	2.6
λ_V	0.5
r_m	10
g	0.25
u_e	0
τ_1	0.7
\bar{v}	0
p_1	0.7
γ	varies
ϵ	varies
D	varies

Table 4.1: Values for parameters and variables of Model (4.4.1), ϵ and D are given in $\frac{km^2}{day}$, other units explained in Table (2.1).

Table 4.1. Recall that the minimal wave speed c_0 for the non-linear system (4.4.1) is equal to c_G^* . Here, the spread rate is treated as a function of human diffusion, the coefficient of which is given by D . We take the range of D to be between 0 and 10 $\frac{km^2}{day}$. Interestingly, Maidana and Yang [36] express the theoretical front wave speed of dengue dissemination in the state of São Paulo, Brazil as a function of the average annual temperature. Mosquito diffusion by wind, or advection, is disregarded. As with our simulations, the spread rate increases as temperature increases, indicating the importance of warm weather for the spread of the disease. Our values for \bar{c} are

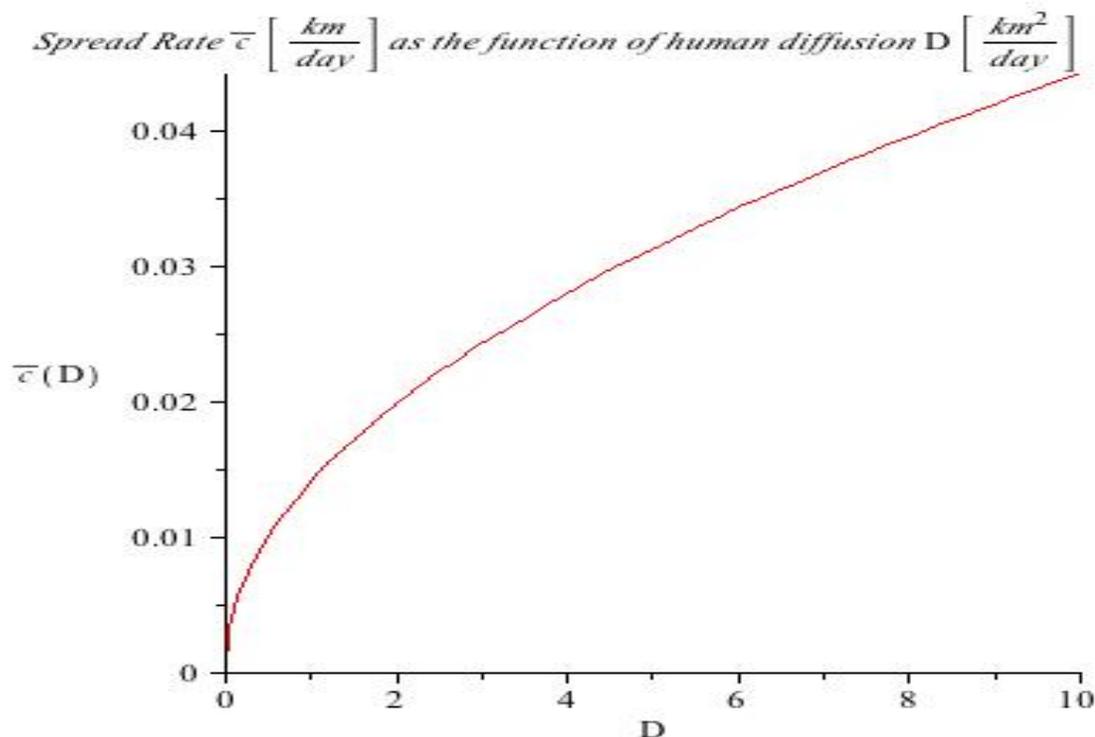


Figure 4.8: Spread rate for the system (4.5.2) when $\epsilon = 0, \gamma = 1$, all other parameters and values are given in Table 4.1.

comparable to those obtained by Maidana and Yang, who determine that the wave speed of the disease ranges between 0 and $21.53 \frac{km}{year}$, or between 0 and $.06 \frac{km}{day}$ [36, Table 5]. As stated, this figure seems consistent with our range for \bar{c} , $0 - .11 \frac{km}{day}$ (see Figures 4.8-4.10). When the annual average temperature ranges between $20^{\circ}C$ and $25^{\circ}C$, the median interval, Maidana and Yang find that the front wave speed varies between 13.43 and $18.24 \frac{km}{year}$, or between $.04$ and $.05 \frac{km}{day}$ [36, Table 5]. Comparably, when we take $\gamma = 1$, which corresponds to an average winter temperature that coincides with the mean for previous years' winters, we obtain wave speeds of $.03 \frac{km}{day}$ when $D = 5 \frac{km^2}{day}$ and $.045 \frac{km}{day}$ when $D = 10 \frac{km^2}{day}$ (see Figure 4.8).

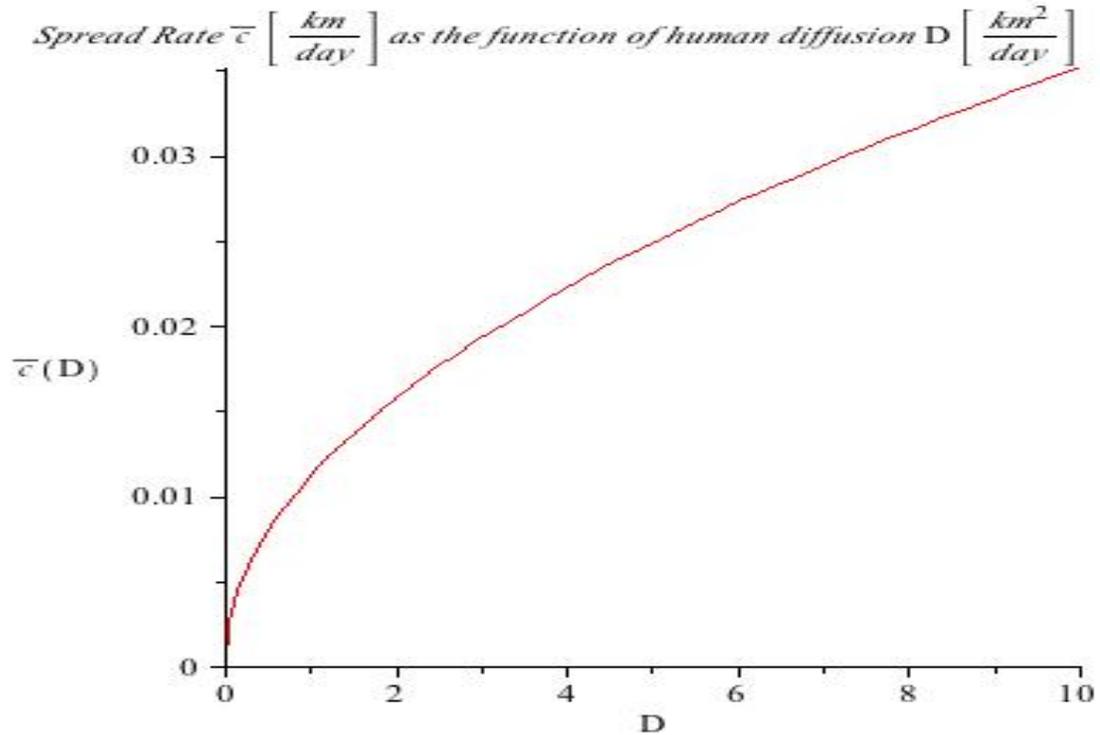


Figure 4.9: Spread rate for the system (4.5.2) when $\epsilon = 0, \gamma = .5$, all other parameters and values are given in Table 4.1.

When the average winter temperature falls below the mean, at $\gamma = .5$, we obtain spread rates of $.024 \frac{km}{day}$ when $D = 5 \frac{km^2}{day}$ and $.035 \frac{km}{day}$ when $D = 10 \frac{km^2}{day}$ (see Figure 4.9). When the annual average temperature ranges between $15^\circ C$ and $20^\circ C$, the lowest interval, Maidana and Yang determine a front wave speed range of $0 - 13.43 \frac{km}{year}$, or between 0 and $.04 \frac{km}{day}$ [36, Table 5]. Finally, when the average winter temperature rises above the mean, at $\gamma = 2$, we obtain minimum wave speeds of $.07 \frac{km}{day}$ when $D = 5 \frac{km^2}{day}$ and $.11 \frac{km}{day}$ when $D = 10 \frac{km^2}{day}$ (see Figure 4.10). When the annual average temperature ranges between $25^\circ C$ and $30^\circ C$, the highest interval, Maidana and Yang find a range of $18.24 - 21.53 \frac{km}{year}$, or between $.05$ and $.06 \frac{km}{day}$ [36, Table 5].

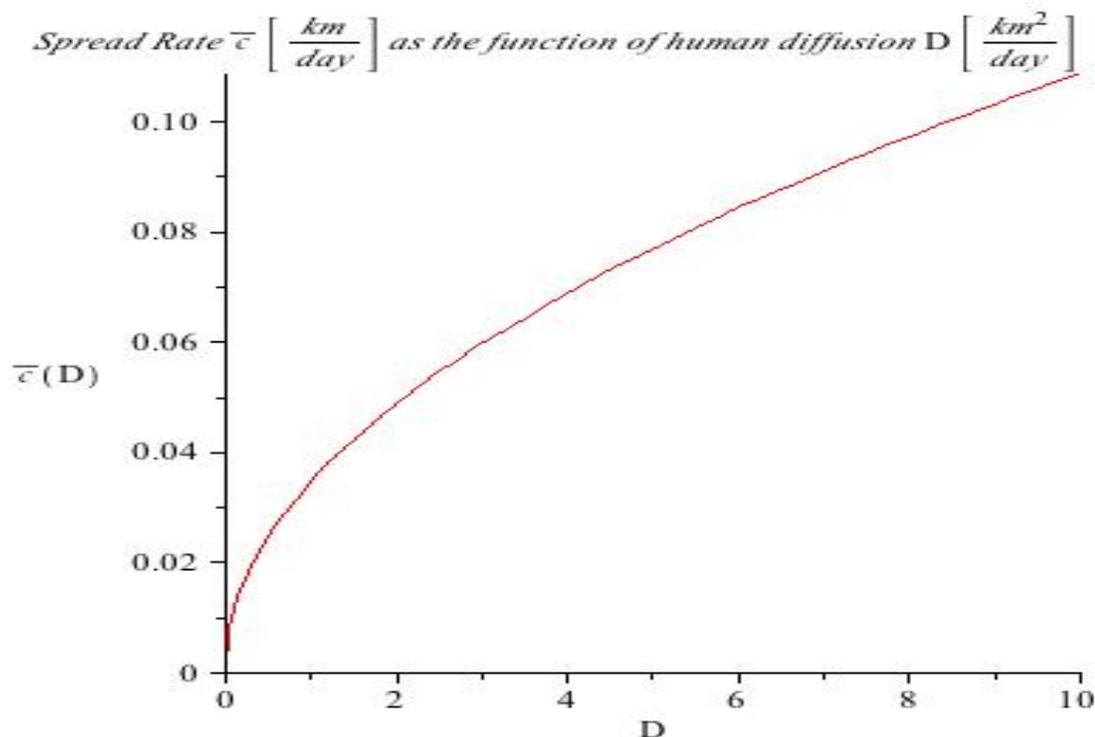


Figure 4.10: Spread rate for the system (4.5.2) when $\epsilon = 0, \gamma = 2$, all other parameters and values are given in Table 4.1.

Recall that the spread rate of system (4.4.1) approaches the estimates presented by Figures 4.8-4.10 as ϵ approaches 0. Since Maidana and Yang take ϵ small, .0125 $\frac{km^2}{day}$ [36, Table 1], our figures shed light on the effect of incorporating human diffusion into a system of partial differential equations for dengue dissemination.

Figures 4.2 to 4.7 show traveling wave solutions for system (4.4.1) with $\epsilon = 1/10, D = 10$ and other parameters as in Table 4.1. To simulate traveling waves, we refer to [29] to look for a solution of the ODE system (4.5.2), which rewrites system (4.4.2) in terms of a coordinate frame moving with speed c to the right. We take $c = 1$ and boundary conditions at $\pm\infty$ determined by stationary solutions of (4.5.2). For $\gamma = 1$, a positive stationary solution of system (4.5.2) exists at (I_M^*, I_H^*)

$= (.0051, .0015)$. Figures 4.2 and 4.3 therefore show that after the wave, we may expect the proportions of infectives in the human and adult mosquito populations to be given by $(I_M^*, I_H^*) = (.0051, .0015)$. When the average winter temperature falls below the mean, at $\gamma = .5$, the positive stationary solution is given by $(I_M^*, I_H^*) = (.0026, .00075)$. Accordingly, the epidemic wave is comparably less intense: after the wave, the proportions of infective individuals in both human and adult mosquito populations exist at lower thresholds. On the other hand, when the average winter temperature rises above the mean, at $\gamma = 2$, the positive stationary solution is given by $(I_M^*, I_H^*) = (.0081, .0024)$. The epidemic wave is comparably more intense: the proportions of infectives individuals in both human and adult mosquito populations achieve higher thresholds.

4.9 Discussion

In this chapter, we presented a non-linear system of coupled reaction-diffusion equations modeling the spatial spread of the dengue virus. In formulating our model, we sought to establish the existence of traveling wave solutions and to calculate spread rates for the spatial dissemination of the disease. In so doing, we made use results presented in Chapter 2. In this chapter, climate was modeled by a nonnegative parameter, γ . First, we made parameter assumptions that imply the existence of a disease-free equilibrium for Model (2.2.1) with $S(t) = \gamma$. Next, we considered the non-diffusive juvenile mosquito and the recovered human components at their respective endemic equilibrium levels, in effect assuming that their contribution to the evolution of the epidemic when the infected adult mosquito and human popula-

tions are stationary is a function of the parameters for the non-spatial system and is constant, simulating biological conditions before the wave hits. Using these assumptions, we constructed a new, two-dimensional ODE model consisting of infected adult mosquito and human components. We derived a reproductive number and established conditions for the existence of an endemic equilibrium for this model. We then incorporated the spatial element into the new ODE model to obtain a non-linear system of coupled reaction-diffusion equations. In so doing, we assumed that human diffusive movement is the main contributing cause of the fast spread of the disease. In the case where the wind advection coefficient $\bar{v} = 0$, we used results presented in [31], [32], [22], and [55] to show that the spread rate c_G^* of the non-linear system is the lower bound for the speed of a class of traveling wave solutions, and that this spread rate is linearly determinate. For small values of ϵ , the adult mosquito diffusion coefficient, we derived an analytic expression for the spread rate for the non-linear system. In the case where the wind advection coefficient $\bar{v} \neq 0$, a different analytic framework was used to determine the spread rate for the non-linear system.

Numerical simulations in the case $\bar{v} = 0$ were presented to illustrate our results. We treated the spread rate, shown to be the minimal wave speed for the non-linear system, as a function of human diffusion, and compared our results to those of Maidana and Yang [36], who expressed the theoretical front wave speed of dengue dissemination in the state of São Paulo, Brazil as a function of the average annual temperature. As Maidana and Yang, we determined that the epidemic wave speed increases as average annual, and in our case, winter, temperatures increase. Warmer weather therefore intensifies the spatial spread of the disease.

We simulated traveling wave solutions for varying annual winter temperatures. Predictably, the proportions of infected humans and mosquitoes reached higher

thresholds in warmer weather. After the wave, then, we expect that, with increasingly higher annual winter temperatures, higher proportions of infected individuals will coexist with local human populations.

As has been previously noted, we emphasized human and mosquito wing diffusion as causes of disease dissemination. More realistic models should look at wind advection more closely. Because obtaining analytic expressions for spread rates for such models requires a different analytic framework than that for cases when advection is not a factor, more work needs to be done on that front. Also, the use of comparison theory, as done in [31] for dengue models in more than two dimensions, provides a further venue for analysis and research.

Chapter 5

A MULTI-SEROTYPE ODE MODEL FOR DENGUE VIRAL TRANSMISSION

5.1 Introductory Remarks

We now consider one of the possible implications of global climatic changes for the spread of dengue: the emergence of new, and epidemics featuring multiple serotypes of the virus. As shown in Chapters 3 and 4, global warming exacerbates the epidemic both temporally and spatially, increasing the likelihood of mutations that create new strains of the virus. In this chapter, we modify the main ODE model presented in Chapter 2 to incorporate 2 distinct serotypes of the dengue virus. Before doing so, we discuss its existing serotypes, elaborate on the medical importance of taking them into account in the development of new mathematical models for the transmission of dengue, and outline the chapter.

Dengue fever is caused by the Dengue virus (DENV), a species belonging to a mosquito-borne viral genus, *Flavivirus*, that includes West Nile and Yellow Fever [1, 43,51]. Four serotypes (antigen-based viral groups) of DENV are presently recognized, each of which, as was mentioned in Chapter 1, presents permanent immunity to itself

but not to any other serotype [6, 41, 51]. While all four serotypes are endemic in the Asian tropics, only recently has this trend been observed in the Americas, where serotypes I, II and IV have been circulating for more than 10 years [12]. All serotypes are associated with both DF and DHF/DSS.

The dissemination of various serotypes has had significant medical implications. In 1953, in the Philippines, and in 1955, in Thailand, the first cases of Dengue Hemorrhagic Fever and the associated Dengue Shock Syndrome, (DHF/DSS), were recognized [12]. Unlike DF, DHF patients present more severe symptoms and can develop DSS, which has a high mortality rate [1, 3, 12]. Additionally, DHF is implicated in a relatively rapid progression to liver cancer in cirrhotic patients [57]. While the risk factors for DHF/DSS have not strictly been identified, studies suggest that susceptibility to the stronger form of the disease is present in those who experience secondary dengue infections and in infants who are conferred neo-natal immunity to a primary strain [12]. A well-known argument based on these findings, known as the “secondary infection” or “immune enhancement” hypothesis, states that DHF/DSS can only occur in patients secondarily infected with a different serotype [12, 20]. Under this hypothesis, a DHF epidemic implies a multi-strain pandemic. Esteva and Vargas state, however, that there is “no reliable information about the geographic spread of DHF/DSS due to the introduction of a serotype to areas currently affected by a different serotype” [12, Introduction]. Consequently, there is no reliable information that verifies the “secondary infection” hypothesis.

Based on these factors, we present a model that incorporates two serotypes of the virus and allows for the possibility of both primary and secondary infections with each serotype. Several studies featuring models for multiple serotypes of the dengue virus have been published (see [12, 15, 46]). We follow the presentation and analysis

of the multi-serotype model for dengue viral transmission introduced by Esteva and Vargas in [12] closely. Our model replicates the transmission dynamics of the human subsystem presented in [12, Model (2.1)] while modifying the vector subsystem by allowing for the vertical transmission of the virus from contaminated mosquito adults to eggs, and by modulating juvenile maturation by a climatic factor. We are therefore able to extend the analysis in [12] by observing changes in the infected proportions of the juvenile subpopulation and by determining how these changes contribute to the possible existence of an epidemic. We derive our model's basic reproduction number, and, additionally, derive the basic reproductive number for each serotype/strain. We look for conditions under which serotype 2 (1) can destabilize the coexistence between the disease-free population and the serotype 1 (2)-endemic population. We leave the study of the existence and analysis of a serotype 1 and 2 coexistence equilibrium for a future paper, though this is investigated in numerical simulations, which follow.

5.2 Presentation of the Model and Assumptions

In this section, we formulate and discuss the model, which depicts dengue transmission in 3 components: human hosts, adult mosquitoes, and juvenile mosquitoes. One time t unit denotes a day. For the sake of mathematical simplicity, we assume the existence of two strains/serotypes. The human population is broken down into the following compartments: susceptible (\bar{S}_H); primarily infected with serotype i , $i = 1, 2$ (\bar{I}_{H_i}); recovered from serotype i , susceptible to serotype j , $i, j = 1, 2$, $i \neq j$, (\bar{Z}_{H_i}); secondarily infected with serotype i , $i = 1, 2$ (\bar{Y}_{H_i}); and recovered from and immune to both serotypes (\bar{Z}_H). The total human population, assumed to be constant, is

therefore given by $N_H = \bar{S}_H + \bar{I}_{H_1} + \bar{I}_{H_2} + \bar{Z}_{H_1} + \bar{Z}_{H_2} + \bar{Z}_H + \bar{Y}_{H_1} + \bar{Y}_{H_2}$. We assume that in a human, infection with a particular serotype results in immunity to that serotype but not necessarily to the other. Further, a human may only experience a secondary infection after recovery from a primary infection. While infected with a particular strain, that is, a human cannot be infected by another strain. For humans, the primary infection rate with serotype i is given by $\lambda_{H_i} \bar{S}_H \frac{\bar{I}_{M_i}}{N_M}$, where λ_{H_i} is the effective contact rate between mosquitoes infected with serotype i and susceptible humans. The secondary infection rate with serotype i is given by $\beta_i \lambda_{H_i} \frac{\bar{I}_{M_i}}{N_M} \bar{Z}_{H_j}$. If $0 \leq \beta_i \leq 1$, primary infection with serotype j confers partial or total immunity to serotype i ; if $\beta_i > 1$, primary infection with serotype j increases susceptibility to serotype i . If $\beta_i = 1$, primary infection with serotype j neither increases nor decreases susceptibility to serotype i . Though the case $\beta_i = 1$ is biologically unlikely, it is included for the sake of mathematical completeness [12]. We assume that the human mortality rate from dengue is 0 and that the recovery rate y_{H_i} from a primary or secondary infection with serotype i is the same.

The total adult mosquito population, denoted by N_M , is constant. We assume that adult mosquitoes infected with one serotype never recover from that serotype but cannot be infected with the other serotype: there are no secondary infections in mosquitoes. The total adult mosquito population is broken down into the following compartments: susceptible (\bar{S}_M) and infected with serotype i , $i = 1, 2$ (\bar{I}_{M_i}). We have that $\bar{I}_{M_1} + \bar{I}_{M_2} + \bar{S}_M = N_M$. Infected adult mosquitoes with either serotype may lay infected eggs; that is, there is an element of vertical transmission, represented by g , in both serotypes. The juvenile population is therefore broken down into susceptible (\bar{S}_E) and infected with serotype i , $i = 1, 2$ (\bar{I}_{E_i}).

We assume that total number of juveniles does not exceed N_M , an upper bound for both \bar{I}_{M_i} and \bar{I}_{E_i} , $i = 1, 2$ (see Section 2.2, Chapter 2). At carrying capacity, then, $\bar{I}_{E_1} + \bar{I}_{E_2} + \bar{S}_E = N_M$.

For adult mosquitoes, the infection rate with serotype i is given by $\lambda_{V_i} \left(\frac{\bar{I}_{H_i}}{N_H} + \frac{\bar{Y}_{H_i}}{N_H} \right) (N_M - \bar{I}_{M_1} - \bar{I}_{M_2})$, where λ_{V_i} is the effective contact rate between humans infected with serotype i , primarily or secondarily, and uninfected mosquitoes (see [12, Section 2]). Further, we assume that the fraction of mosquito eggs laid by an infected female that is infected and female, g ; the natural egg mortality rate, u_e ; the fraction of infected eggs that proceeds to the adult stage, τ ; and the daily oviposition rate, r_m ; are the same for both each infected subpopulation.

We observe that, as in Chapter 2, the fact that $u_e \neq 1 - \tau$ implies that at any given time t , not all surviving juveniles progress to the next phase; they may remain in their present state. As already discussed, total mosquito and juvenile populations, respectively, remain constant in the absence of seasonality and disease. The last four equations incorporate saturation terms, $\left(\frac{N_M - \bar{I}_{E_1} - \bar{I}_{E_2}}{N_M} \right)$, $\left(\frac{N_M - \bar{I}_{M_1} - \bar{I}_{M_2}}{N_M} \right)$, that take into account the fact that the maturation rate into the next phase of mosquito development is stifled if the population in the next phase is reaching N_M . This ensures that infected populations remain below a threshold, N_M , for the adult and juvenile population densities.

Finally, the climatic factor is given by the parameter c , denoting the winter mildness index, which quantifies the average winter temperature, as compared to previous years' mean, $c = 1$.

The model is as follows ($i, j = 1, 2; i \neq j$):

$$\begin{aligned}
\frac{d\bar{S}_H}{dt} &= u_H N_H - u_H \bar{S}_H - \left(\lambda_{H_1} \frac{\bar{I}_{M_1}}{N_M} + \lambda_{H_2} \frac{\bar{I}_{M_2}}{N_M} \right) \bar{S}_H \\
\frac{d\bar{I}_{H_i}}{dt} &= \lambda_{H_i} \frac{\bar{I}_{M_i}}{N_M} \bar{S}_H - (y_{H_i} + u_H) \bar{I}_{H_i} \\
\frac{d\bar{Z}_{H_i}}{dt} &= y_{H_i} \bar{I}_{H_i} - \beta_j \lambda_{H_j} \frac{\bar{I}_{M_j}}{N_M} \bar{Z}_{H_i} - u_H \bar{Z}_{H_i} \\
\frac{d\bar{Y}_{H_i}}{dt} &= \beta_i \lambda_{H_i} \frac{\bar{I}_{M_i}}{N_M} \bar{Z}_{H_j} - (y_{H_i} + u_H) \bar{Y}_{H_i} \\
\frac{d\bar{Z}_H}{dt} &= y_{H_1} \bar{Y}_{H_1} + y_{H_2} \bar{Y}_{H_2} - u_H \bar{Z}_H \\
\frac{d\bar{I}_{M_i}}{dt} &= c\tau \left(\frac{N_M - \bar{I}_{M_1} - \bar{I}_{M_2}}{N_M} \right) \bar{I}_{E_i} - u_m \bar{I}_{M_i} + \lambda_{V_i} \left(\frac{\bar{I}_{H_i}}{N_H} + \frac{\bar{Y}_{H_i}}{N_H} \right) (N_M - \bar{I}_{M_1} - \bar{I}_{M_2}) \\
\frac{d\bar{I}_{E_i}}{dt} &= gr_m \left(\frac{N_M - \bar{I}_{E_1} - \bar{I}_{E_2}}{N_M} \right) \bar{I}_{M_i} - c\tau \left(\frac{N_M - \bar{I}_{M_1} - \bar{I}_{M_2}}{N_M} \right) \bar{I}_{E_i} - u_e \bar{I}_{E_i}
\end{aligned} \tag{5.2.1}$$

with $N_M \geq \bar{I}_{M_i}(0)$, $N_M \geq \bar{I}_{E_i}(0)$, $N_M > 0$, $\bar{S}_H + \bar{I}_{H_1} + \bar{I}_{H_2} + \bar{Z}_{H_1} + \bar{Z}_{H_2} + \bar{Z}_H + \bar{Y}_{H_1} + \bar{Y}_{H_2} = N_H > 0$, $u_H > 0$.

Remark: As mentioned, our model replicates the transmission dynamics of the human subsystem presented in Model (2.1) of [12]. Our vector subsystem is different, however, in that it allows for the vertical transmission of the virus from contaminated adult mosquitoes to eggs, and, consequently, for the incorporation of juvenile compartments, $\bar{I}_{E_1}, \bar{I}_{E_2}$, to our model (equations 11 and 12 of (5.2.1)). Additionally, we

modify the vector subsystem of [12, Model (2.1)] by incorporating a climatic factor, c , which modulates juvenile maturation. As such, the juvenile contributions to the adult infected classes, seen in equations 9 and 10 of (5.2.1), reflect a climatic influence. These equations therefore differ from the corresponding ones in [12, (2.1)], equations 10 and 11, by incorporating the terms

$$c\tau \left(\frac{N_M - \bar{I}_{M_1} - \bar{I}_{M_2}}{N_M} \right) \bar{I}_{E_i}. \quad (5.2.2)$$

Finally, we omit the equations describing change in the susceptible adult mosquito and juvenile population densities because these subpopulations are assumed to be constant. In the next section, we will show how these changes extend the analysis of Esteva and Vargas in [12].

Note that $\frac{dN_H}{dt} = 0$, since N_H is constant.

The parameters in Model (5.2.1) can be understood by referring to Table 5.1. In this chapter, we will henceforth assume all parameters are nonnegative.

5.3 Analysis of Model (5.2.1)

Let $y_{t_0} = (\bar{S}_H(t_0), \dots, I_{E_i}(t_0))$ be in R_+^{12} . As all functions on the RHS of Model (5.2.1) are continuously differentiable, there exists a real number $\beta > 0$ such that on some interval $[t_0, t_0 + \beta)$, there exists a unique solution $\phi(t, y) = y(t) = (\bar{S}_H(t), \dots, I_{E_i}(t))$ through y_{t_0} to system (5.2.1).

Additionally, we have the following theorem:

Theorem 5.1. *Let $y_0 \in R_+^{12}$. Any solution $y(t)$ of system (5.2.1) through y_0 is defined for all $t \geq 0$, and R_+^{12} is positively invariant.*

<i>Parameter</i>	<i>Definition</i>	<i>Unit and/or Range</i>
u_H	natural human mortality rate	(births/ 10^3 humans) day^{-1}
λ_{H_i}	effective contact rate between susceptible humans and mosquitoes infected with serotype i , $i = 1, 2$	$\frac{\text{infected bites}}{\text{susceptible human}}$
β_i	susceptibility of a host to serotype i after recovering from infection with serotype j , estimate based on proportion of secondarily infected humans	humans
γ_{H_i}	recovery rate from infection with serotype i	$\frac{\text{recovered humans}}{10^3 \text{serotype } i\text{-infectives}}$ day^{-1}
u_m	natural adult mosquito mortality rate	$\frac{\text{deaths}}{10^3 \text{larvae}}$ day^{-1}
λ_{V_i}	effective contact rate between humans infected with serotype i , primarily or secondarily, and uninfected mosquitoes	$\frac{\text{infective bites}}{\text{uninfected mosquito}}$
c	winter mildness index: average winter temperature, as compared to previous years' mean of $c = 1$	between 0 and 2
r_m	daily oviposition rate	$\frac{\text{eggs}}{10^3 \text{mosquitoes}}$ day^{-1}
g	proportion of mosquito eggs laid by an infected female that is infected and female	eggs
u_e	natural juvenile mosquito mortality rate	$\frac{\text{deaths}}{10^3 \text{juveniles}}$ day^{-1}
τ	proportion of infected juveniles that proceeds to the adult stage	infected juveniles

Table 5.1: *Parameters for Model (5.2.1)*

Proof. The reasoning is similar to that of the proof of Theorem 2.1 in Chapter 2. \square

Consider the following variable changes (see [12, (2.2)-(2.3)]):

$$\begin{aligned}\frac{\bar{S}_H}{N_H} &= S_H, \frac{\bar{I}_{H_i}}{N_H} = I_{H_i}, \frac{\bar{Y}_{H_i}}{N_H} = Y_{H_i} \\ \frac{\bar{Z}_{H_i}}{N_H} &= Z_{H_i}, \frac{\bar{Z}_H}{N_H} = Z_H \\ \frac{\bar{I}_{M_i}}{N_M} &= I_{M_i}, \frac{\bar{I}_{E_i}}{N_M} = I_{E_i}.\end{aligned}\tag{5.3.1}$$

Let $x_1 = I_{H_1}, x_2 = I_{H_2}, x_3 = Z_{H_1}, x_4 = Z_{H_2}, x_5 = Y_{H_1}, x_6 = Y_{H_2}, x_7 = I_{M_1}, x_8 = I_{M_2}, x_9 = I_{E_1}, x_{10} = I_{E_2}, x_{11} = S_H$. The resulting system is

$$\begin{aligned}\dot{x}_1 &= \lambda_{H_1} x_7 x_{11} - (y_{H_1} + u_H) x_1 \\ \dot{x}_2 &= \lambda_{H_2} x_8 x_{11} - (y_{H_2} + u_H) x_2 \\ \dot{x}_3 &= y_{H_1} x_1 - \beta_2 \lambda_{H_2} x_8 x_3 - u_H x_3 \\ \dot{x}_4 &= y_{H_2} x_2 - \beta_1 \lambda_{H_1} x_7 x_4 - u_H x_4 \\ \dot{x}_5 &= \beta_1 \lambda_{H_1} x_7 x_4 - (y_{H_1} + u_H) x_5 \\ \dot{x}_6 &= \beta_2 \lambda_{H_2} x_8 x_3 - (y_{H_2} + u_H) x_6 \\ \dot{x}_7 &= c\tau(1 - x_7 - x_8) x_9 - u_m x_7 + \lambda_{V_1} (x_1 + x_5) (1 - x_7 - x_8) \\ \dot{x}_8 &= c\tau(1 - x_7 - x_8) x_{10} - u_m x_8 + \lambda_{V_2} (x_2 + x_6) (1 - x_7 - x_8) \\ \dot{x}_9 &= gr_m (1 - x_9 - x_{10}) x_7 - c\tau(1 - x_7 - x_8) x_9 - u_e x_9 \\ \dot{x}_{10} &= gr_m (1 - x_9 - x_{10}) x_8 - c\tau(1 - x_7 - x_8) x_{10} - u_e x_{10} \\ \dot{x}_{11} &= u_H (1 - x_{11}) - (\lambda_{H_1} x_7 + \lambda_{H_2} x_8) x_{11}\end{aligned}\tag{5.3.2}$$

where $(x_{10}, \dots, x_{11_0}) \in \Omega = \{(x_1, \dots, x_{11}) : 0 \leq x_i \leq 1 \text{ for } i \text{ with } 1 \leq i \leq 11, 0 \leq x_7 + x_8 \leq 1, 0 \leq x_9 + x_{10} \leq 1, 0 \leq x_1 + x_2 + x_3 + x_4 + x_5 + x_6 + x_{11} \leq 1\}$, $u_H > 0$.

The first six equations and the last, corresponding to the human subsystem, are exactly those obtained by Esteva and Vargas in [12, Model (2.4)]. Differences between equations seven to ten of (5.3.2) and equations eight to nine of Model (2.4) correspond to the differences between the vector subsystems of (5.2.1) and Model (2.1) in [12] (see *Remark*, Section 5.2). Having introduced proportions to our system, we are now able to extend the analysis in [12] by observing how the parameters c , τ , and g affect the calculation of the basic reproduction number, \mathcal{R}_0 . Additionally, the incorporation of compartments x_9 and x_{10} allows us to observe change in the infected proportions of the juvenile subpopulation, as demonstrated by the numerical simulations.

Corollary 5.2. *The region Ω is positively invariant for system (5.3.2).*

Proof. Let $(x_1^*(t), \dots, x_{11}^*(t))$ with $(x_{1_0}^*, \dots, x_{11_0}^*) \in \Omega$ be a fixed solution of system (5.3.2) on $[0, \infty)$.

Suppose $(x_{1_0}^*, \dots, x_{11_0}^*)$ is on $Bde(\Omega)$. (*)

If $x_{11}^*(0) = 0$, then by equation 11 of (5.3.2), $x_{11}^{\prime*}(0) = u_H > 0$. If $x_{11}^*(0) = 1$, then by (*), $x_{11}^{\prime*}(0) = -(\lambda_{H_1}x_7(0) + \lambda_{H_2}x_8(0)) \leq 0$. We may obtain similar results for $x_i^*(t)$ for i with $i = 1, 2, 3, 4, 5, 6$.

If $x_1^*(0) + x_2^*(0) + x_3^*(0) + x_4^*(0) + x_5^*(0) + x_6^*(0) + x_{11}^*(0) = 0$, then by equations 1, 2, 3, 4, 5, 6, 11 of (5.3.2), $x_1^{\prime*}(0) + x_2^{\prime*}(0) + x_3^{\prime*}(0) + x_4^{\prime*}(0) + x_5^{\prime*}(0) + x_6^{\prime*}(0) + x_{11}^{\prime*}(0) = u_H > 0$.

Now if $x_1^*(0) + x_2^*(0) + x_3^*(0) + x_4^*(0) + x_5^*(0) + x_6^*(0) + x_{11}^*(0) = 1$, then by (5.3.1) and (*), $\max(x_1^*(0), x_2^*(0), x_3^*(0), x_4^*(0), x_5^*(0), x_6^*(0), x_{11}^*(0)) \leq 1$ and by equations 1, 2, 3, 4, 5, 6, 11 of (5.3.2) and (*), $x_1^{\prime*}(0) + x_2^{\prime*}(0) + x_3^{\prime*}(0) + x_4^{\prime*}(0) + x_5^{\prime*}(0) + x_6^{\prime*}(0) + x_{11}^{\prime*}(0) = u_H(1 - (x_1^*(0) + x_2^*(0) + x_3^*(0) + x_4^*(0) + x_5^*(0) + x_6^*(0) + x_{11}^*(0))) - y_{H_1}x_5^*(0) - y_{H_2}x_6^*(0) =$

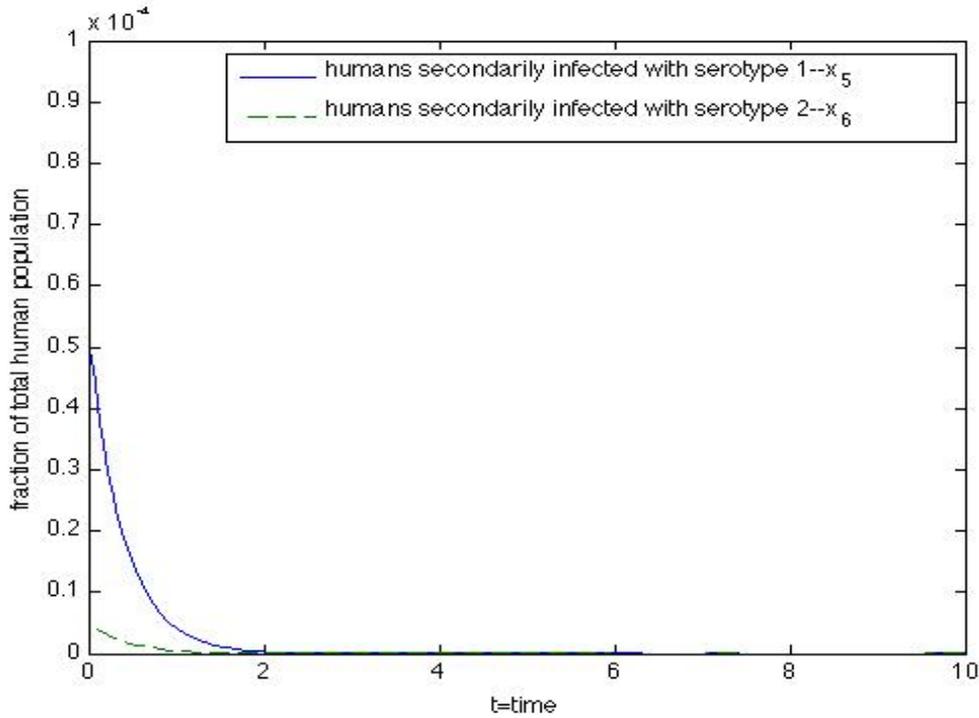


Figure 5.1: Solutions of system (5.3.2) converge to the DFE when $\mathcal{R}_0 = .25$; parameter values given in Table 5.2.

$$-y_{H_1}x_5^*(0) - y_{H_2}x_6^*(0) \leq 0.$$

By equations 7, 8, 9, 10 and (*), if $x_7^*(0) = 0$, $x_7'^*(0) = c\tau(1 - x_8^*(0))x_9^*(0) + \lambda_{V_1}(x_1^*(0) + x_5^*(0))(1 - x_8^*(0)) \geq 0$; if $x_8^*(0) = 0$, $x_8'^*(0) = c\tau(1 - x_7^*(0))x_{10}^*(0) + \lambda_{V_2}(x_2^*(0) + x_6^*(0))(1 - x_7^*(0)) \geq 0$; if $x_9^*(0) = 0$, $x_9'^*(0) = gr_m(1 - x_{10}^*(0))x_7^*(0) \geq 0$; if $x_{10}^*(0) = 0$, $x_{10}'^*(0) = gr_m(1 - x_9^*(0))x_8^*(0) \geq 0$.

By equations 7, 8, 9, 10 and (*), if $x_7^*(0) = 1$, $x_7'^*(0) = -u_m \leq 0$; if $x_8^*(0) = 1$, $x_8'^*(0) = -u_m \leq 0$; if $x_9^*(0) = 1$, $x_9'^*(0) = -c\tau(1 - x_7^*(0) - x_8^*(0)) - u_e \leq 0$; if $x_{10}^*(0) = 1$, $x_{10}'^*(0) = -c\tau(1 - x_7^*(0) - x_8^*(0)) - u_e \leq 0$. If $x_7^*(0) + x_8^*(0) = 1$, $x_7'^*(0) + x_8'^*(0) = -u_m \leq 0$, If $x_9^*(0) + x_{10}^*(0) = 1$, $x_9'^*(0) + x_{10}'^*(0) = -c\tau(1 - x_7^*(0) - x_8^*(0)) - u_e \leq 0$.

So $x_i^*(0) \geq 0$ if $x_i'(0) = 0$ for i with $1 \leq i \leq 11$ and $x_i^*(0) \leq 0$ if $x_i(0) = 1$ for i with $1 \leq i \leq 11$, $x_7(0) + x_8(0) = 1$, $x_9(0) + x_{10}(0) = 1$, $x_1(0) + x_2(0) + x_3(0) + x_4(0) + x_5(0) + x_6(0) + x_{11}(0) = 1$. (**)

Suppose $(x_{1_0}^*, \dots, x_{11_0}^*)$ is in $Interior(\Omega)$. (+)

Let $t_0 = \inf\{t \in (0, \infty) : (x_1^*(t), \dots, x_{11}^*(t)) \text{ on } Bde(\Omega)\}$. (++)

By the continuity of the solution on $[0, \infty)$, $(x_1^*(t), \dots, x_{11}^*(t)) \in Interior(\Omega)$ on $[0, t_0)$. So $\lim_{t \rightarrow t_0^-} (x_1^*(t), \dots, x_{11}^*(t)) \in \bar{\Omega}$. So we may substitute t_0 for 0 in the arguments following (*), so that (**) holds at t_0 . (***)

If we substitute any $t' \in [0, \infty)$ for 0 in (+) and $t_{t'}$ for t_0 in (++) , (***) holds. (+++)

By (**), (***), (+++), and [26, Proposition 3.3], we have our result. \square

Define X_S to be the set of all disease-free states. That is,

$$X_S = \{x \in \Omega : x_i = 0, i = 1, \dots, 10\}. \quad (5.3.3)$$

Let $\mathcal{F}_i(x)$ be the rate of appearance of new infections in compartment i , $\mathcal{V}_i^+(x)$ be the rate of transfer of individuals into compartment i by all other means, and $\mathcal{V}_i^-(x)$ be the rate of transfer of individuals out of compartment i . Let $\mathcal{V}_i = \mathcal{V}_i^- - \mathcal{V}_i^+$ for each i with $1 \leq i \leq 11$ (see [52, Section 2, (1)]).

The following assumptions can be made:

Assumption(B0): For each i with $1 \leq i \leq 11$, \mathcal{F}_i , \mathcal{V}_i^+ , \mathcal{V}_i^- are continuously differentiable at least twice in each x .

Observe that system (5.3.2) may be written as $\dot{x}_i = f_i(x) = \mathcal{F}_i(x) - \mathcal{V}_i(x)$ where $\mathcal{V}_i(x) = \mathcal{V}_i^-(x) - \mathcal{V}_i^+(x)$. Each \mathcal{F}_i , \mathcal{V}_i^+ , \mathcal{V}_i^- is a polynomial function in 11 variables and therefore continuous. It follows that for each i, j, k with $1 \leq i, j, k \leq 11$, $\frac{\partial f_i}{\partial x_j}$ and

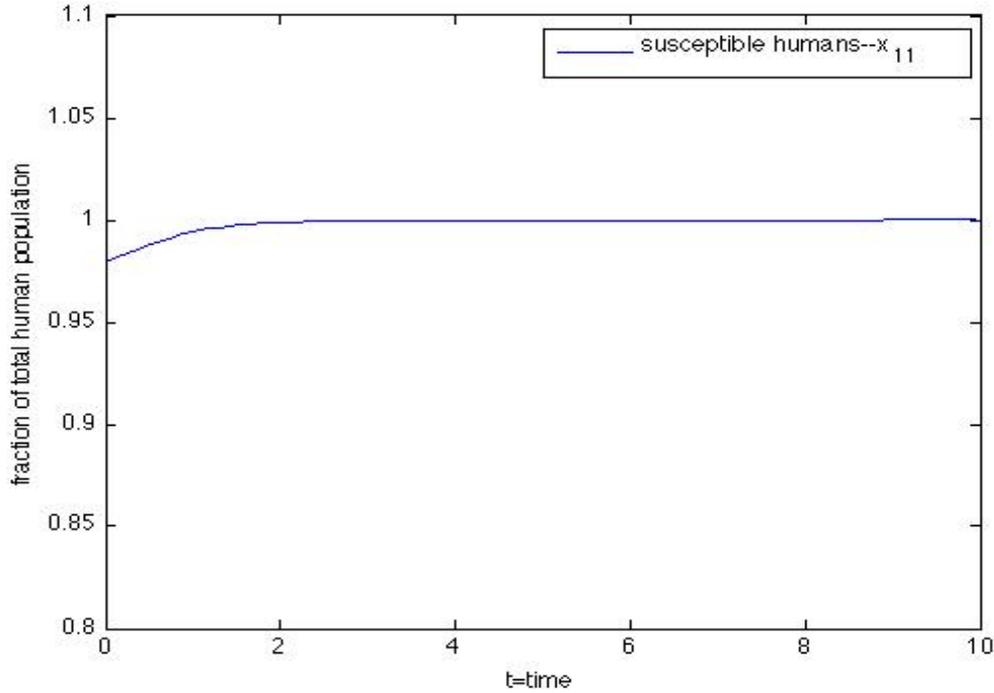


Figure 5.2: Solutions of system (5.3.2) converge to the DFE when $\mathcal{R}_0 = .25$; parameter values given in Table 5.2.

$\frac{\partial^2 f_i}{\partial x_j \partial x_k}$ are polynomials in 11 variables. So for each i with $1 \leq i \leq 11$, \mathcal{F}_i , \mathcal{V}_i^+ , \mathcal{V}_i^- are continuous and twice-differentiable in each x .

Assumption(B1): If $x \in \Omega$, then \mathcal{F}_i , \mathcal{V}_i^+ , $\mathcal{V}_i^- \geq 0$ for $i = 1, \dots, 11$.

All parameters are nonnegative. So we have, $\mathcal{F}_1(x) = \lambda_{H_1} x_7 x_{11} \geq 0$, $\mathcal{V}_1^+(x) = 0$, $\mathcal{V}_1^-(x) = (y_{H_1} + u_H) x_1 \geq 0$, $\mathcal{F}_2(x) = \lambda_{H_2} x_8 x_{11} \geq 0$, $\mathcal{V}_2^+(x) = 0$, $\mathcal{V}_2^-(x) = (y_{H_2} + u_H) x_2 \geq 0$, $\mathcal{F}_3(x) = 0$, $\mathcal{V}_3^+(x) = y_{H_1} x_1 \geq 0$, $\mathcal{V}_3^-(x) = \beta_2 \lambda_{H_2} x_8 x_3 + u_H x_3 \geq 0$, $\mathcal{F}_4(x) = 0$, $\mathcal{V}_4^+(x) = y_{H_2} x_2 \geq 0$, $\mathcal{V}_4^-(x) = \beta_1 \lambda_{H_1} x_7 x_4 + u_H x_4 \geq 0$, $\mathcal{F}_5(x) = \beta_1 \lambda_{H_1} x_7 x_4$, $\mathcal{V}_5^+(x) = 0$, $\mathcal{V}_5^-(x) = (y_{H_1} + u_H) x_5 \geq 0$, $\mathcal{F}_6(x) = \beta_2 \lambda_{H_2} x_8 x_3$, $\mathcal{V}_6^+(x) = 0$, $\mathcal{V}_6^-(x) = (y_{H_2} + u_H) x_6 \geq 0$, $\mathcal{F}_7(x) = \lambda_{V_1} (x_1 + x_5) (1 - x_7 - x_8) \geq 0$, $\mathcal{V}_7^+(x) = c\tau (1 - x_7 - x_8) x_9 \geq 0$, $\mathcal{V}_7^-(x) = u_m x_7 \geq 0$, $\mathcal{F}_8(x) = \lambda_{V_2} (x_2 + x_6) (1 - x_7 - x_8) \geq 0$, $\mathcal{V}_8^+(x) = c\tau (1 - x_7 -$

$$\begin{aligned}
& x_8)x_{10} \geq 0, \mathcal{V}_8^-(x) = u_m x_8 \geq 0, \mathcal{F}_9(x) = 0, \mathcal{V}_9^+(x) = gr_m(1 - x_9 - x_{10})x_7 \geq 0, \\
& \mathcal{V}_9^-(x) = c\tau(1 - x_7 - x_8)x_9 + u_e x_9 \geq 0, \mathcal{F}_{10}(x) = 0, \mathcal{V}_{10}^+(x) = gr_m(1 - x_9 - x_{10})x_8 \geq 0, \\
& \mathcal{V}_{10}^-(x) = c\tau(1 - x_7 - x_8)x_{10} + u_e x_{10} \geq 0, \mathcal{F}_{11}(x) = 0, \mathcal{V}_{11}^+(x) = u_H \geq 0, \mathcal{V}_{11}^-(x) = \\
& u_H x_{11} + (\lambda_{H_1} x_7 + \lambda_{H_2} x_8)x_{11} \geq 0.
\end{aligned}$$

Assumption(B2): If $x_i = 0$, then $\mathcal{V}_i^- = 0$. In particular, if $x \in X_S$, then $\mathcal{V}_i^- = 0$ for $i = 1, \dots, 10$.

The first claim follows from the paragraph following **(B1)**. Now if $x \in X_S$, $x_i = 0$ for $i = 1, \dots, 10$. So the second claim follows from the first.

Assumption(B3): $\mathcal{F}_i = 0$ if $i = 11$.

Follows from the paragraph following **(B1)**.

Assumption(B4): If $x \in X_S$, $\mathcal{F}_i(x) = 0$ and $\mathcal{V}_i^+(x) = 0$ for $i = 1, \dots, 10$.

If $x \in X_S$, $x_i = 0$ for $i = 1, \dots, 10$. So result follows from the paragraph following **(B1)**.

Assumption(B5): Assume $y_{H_1} > 0$, $y_{H_2} > 0$, $u_H > 0$, $c\tau > 0$, $gr_m > 0$, $u_m > 0$, $(u_m c\tau + u_e u_m - gr_m c\tau) > 0$, all other parameters nonnegative. If $\mathcal{F}(x)$ is set to zero, then all eigenvalues of $Df(x_0)$ have negative real part, where x_0 is a disease-free equilibrium (DFE) of system (5.3.2).

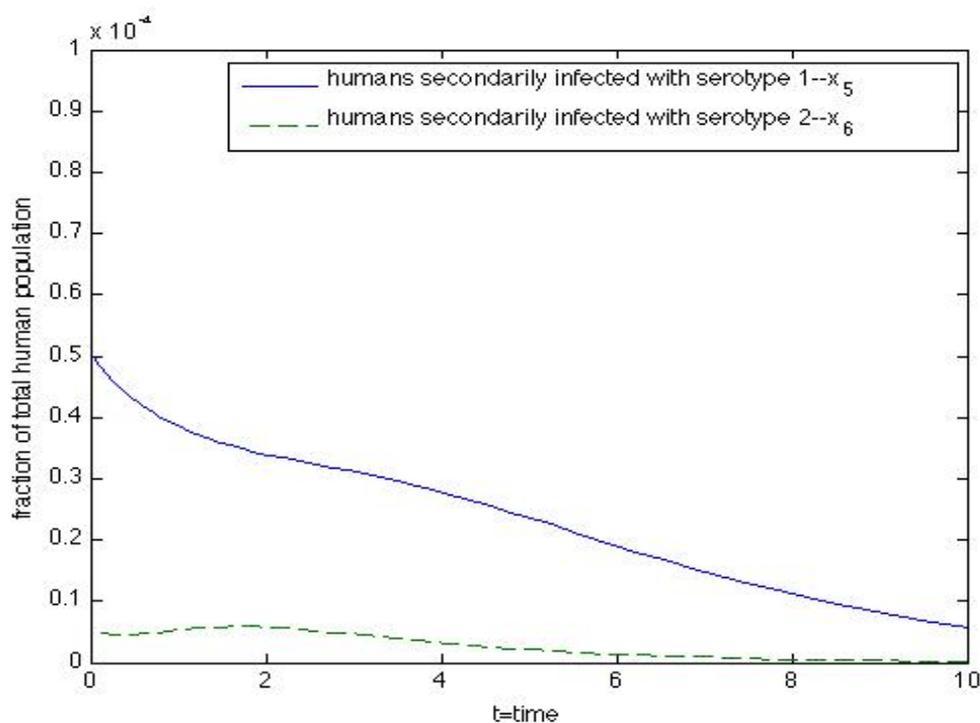


Figure 5.3: Solutions of system (5.3.2) converge to E_1 when $\mathcal{R}_1 = 1.08$, $\mathcal{R}_2 = .25$, $\beta_1 = \beta_2 = .5$; parameter values given in Table 5.2.

A DFE of system (5.3.2) is defined to be a (locally asymptotically stable) equilibrium of the disease-free model, i.e., system (5.3.2) restricted to X_S . So the single equilibrium solution with $x_i = 0$ for $1, \dots, 10$ is $x_0 = (0, 0, 0, 0, 0, 0, 0, 0, 0, 0, 1)^T$.

Recall that system (5.3.2) may be written as $\dot{x}_i = f_i(x) = \mathcal{F}_i(x) - \mathcal{V}_i(x)$ where $\mathcal{V}_i(x) = \mathcal{V}_i^-(x) - \mathcal{V}_i^+(x)$. So if $\mathcal{F}(x)$ is set to zero, then $F_i(x) = 0$ for each i . So $\dot{x}_i = f_i(x) = 0 - \mathcal{V}_i(x)$.

So system (5.3.2) becomes

$$\begin{aligned}
\dot{x}_1 &= -(y_{H_1} + u_H)x_1 \\
\dot{x}_2 &= -(y_{H_2} + u_H)x_2 \\
\dot{x}_3 &= y_{H_1}x_1 - \beta_2\lambda_{H_2}x_8x_3 - u_Hx_3 \\
\dot{x}_4 &= y_{H_2}x_2 - \beta_1\lambda_{H_1}x_7x_4 - u_Hx_4 \\
\dot{x}_5 &= -(y_{H_1} + u_H)x_5 \\
\dot{x}_6 &= -(y_{H_2} + u_H)x_6 \\
\dot{x}_7 &= c\tau(1 - x_7 - x_8)x_9 - u_mx_7 \\
\dot{x}_8 &= c\tau(1 - x_7 - x_8)x_{10} - u_mx_8 \\
\dot{x}_9 &= gr_m(1 - x_9 - x_{10})x_7 - c\tau(1 - x_7 - x_8)x_9 - u_ex_9 \\
\dot{x}_{10} &= gr_m(1 - x_9 - x_{10})x_8 - c\tau(1 - x_7 - x_8)x_{10} - u_ex_{10} \\
\dot{x}_{11} &= u_H(1 - x_{11}) - (\lambda_{H_1}x_7 + \lambda_{H_2}x_8)x_{11}
\end{aligned} \tag{5.3.4}$$

So,

$$Df_x(x) =$$

$$\begin{pmatrix}
a_{11} & 0 & 0 & 0 & 0 & 0 & 0 & 0 & 0 & 0 & 0 \\
0 & a_{22} & 0 & 0 & 0 & 0 & 0 & 0 & 0 & 0 & 0 \\
y_{H_1} & 0 & a_{33} & 0 & 0 & 0 & 0 & a_{38} & 0 & 0 & 0 \\
0 & y_{H_2} & 0 & a_{44} & 0 & 0 & a_{47} & 0 & 0 & 0 & 0 \\
0 & 0 & 0 & 0 & a_{55} & 0 & 0 & 0 & 0 & 0 & 0 \\
0 & 0 & 0 & 0 & 0 & a_{66} & 0 & 0 & 0 & 0 & 0 \\
0 & 0 & 0 & 0 & 0 & 0 & a_{77} & -c\tau x_9 & a_{79} & 0 & 0 \\
0 & 0 & 0 & 0 & 0 & 0 & -c\tau x_{10} & a_{88} & 0 & a_{8 \ 10} & 0 \\
0 & 0 & 0 & 0 & 0 & 0 & a_{97} & c\tau x_9 & a_{99} & -gr_mx_7 & 0 \\
0 & 0 & 0 & 0 & 0 & 0 & c\tau x_{10} & a_{10 \ 8} & -gr_mx_8 & a_{10 \ 10} & 0 \\
0 & 0 & 0 & 0 & 0 & 0 & -(\lambda_{H_1}x_{11}) & -(\lambda_{H_2}x_{11}) & 0 & 0 & a_{11 \ 11}
\end{pmatrix} \tag{5.3.5}$$

where

$$a_{11} = -(y_{H_1} + u_H),$$

$$\begin{aligned}
a_{22} &= -(y_{H_2} + u_H), \\
a_{33} &= -\beta_2 \lambda_{H_2} x_8 - u_H, \\
a_{38} &= -\beta_2 \lambda_{H_2} x_3, \\
a_{44} &= -\beta_1 \lambda_{H_1} x_7 - u_H, \\
a_{47} &= -\beta_1 \lambda_{H_1} x_4, \\
a_{55} &= -(y_{H_1} + u_H), \\
a_{66} &= -(y_{H_2} + u_H), \\
a_{77} &= -c\tau x_9 - u_m, \\
a_{79} &= c\tau(1 - x_7 - x_8), \\
a_{88} &= -c\tau x_{10} - u_m, \\
a_{8\ 10} &= c\tau(1 - x_7 - x_8), \\
a_{97} &= gr_m(1 - x_9 - x_{10}) + c\tau x_9, \\
a_{99} &= -c\tau(1 - x_7 - x_8) - u_e - gr_mx_7, \\
a_{10\ 8} &= gr_m(1 - x_9 - x_{10}) + c\tau x_{10}, \\
a_{10\ 10} &= -c\tau(1 - x_7 - x_8) - u_e - gr_mx_8, \\
a_{11\ 11} &= -u_H - (\lambda_{H_1} x_7 + \lambda_{H_2} x_8).
\end{aligned}$$

and,

$$Df_x(x_0) =$$

$$\begin{pmatrix}
b_{11} & 0 & 0 & 0 & 0 & 0 & 0 & 0 & 0 & 0 & 0 \\
0 & b_{22} & 0 & 0 & 0 & 0 & 0 & 0 & 0 & 0 & 0 \\
y_{H_1} & 0 & -u_H & 0 & 0 & 0 & 0 & 0 & 0 & 0 & 0 \\
0 & y_{H_2} & 0 & -u_H & 0 & 0 & 0 & 0 & 0 & 0 & 0 \\
0 & 0 & 0 & 0 & b_{55} & 0 & 0 & 0 & 0 & 0 & 0 \\
0 & 0 & 0 & 0 & 0 & b_{66} & 0 & 0 & 0 & 0 & 0 \\
0 & 0 & 0 & 0 & 0 & 0 & -u_m & 0 & c\tau & 0 & 0 \\
0 & 0 & 0 & 0 & 0 & 0 & 0 & -u_m & 0 & c\tau & 0 \\
0 & 0 & 0 & 0 & 0 & 0 & gr_m & 0 & -c\tau - u_e & 0 & 0 \\
0 & 0 & 0 & 0 & 0 & 0 & 0 & gr_m & 0 & -c\tau - u_e & 0 \\
0 & 0 & 0 & 0 & 0 & 0 & -(\lambda_{H_1}) & -(\lambda_{H_2}) & 0 & 0 & -u_H
\end{pmatrix} \quad (5.3.6)$$

where

$$\begin{aligned}
b_{11} &= -(y_{H_1} + u_H), \\
b_{22} &= -(y_{H_2} + u_H), \\
b_{55} &= -(y_{H_1} + u_H), \\
b_{66} &= -(y_{H_2} + u_H).
\end{aligned}$$

The eigenvalues of $Df_x(x_0)$ are $-u_H$ and the eigenvalues of the submatrix of $Df_x(x_0)$ obtained by deleting the eleventh row and the eleventh column of $Df_x(x_0)$. We will denote this submatrix by $J_0 = [b_{ij}], 1 \leq i, j \leq 10$. Now $-J_0$ has the *Z-pattern*, that is, $-b_{ij} \leq 0$ for all $i \neq j$. A *non-singular M-matrix* is a matrix B with the *Z-pattern* such that B is non-singular and the inverse of B is non-negative [16, 28].

Now $\det(-J_0) = (y_{H_1} + u_H)^2(y_{H_2} + u_H)^2(u_H)^2(u_m c\tau + u_e u_m - gr_m c\tau)^2 > 0$, by assumption. Also, the inverse of $-J_0$ is given by

$$\begin{pmatrix} c_{11} & 0 & 0 & 0 & 0 & 0 & 0 & 0 & 0 & 0 \\ 0 & c_{22} & 0 & 0 & 0 & 0 & 0 & 0 & 0 & 0 \\ c_{31} & 0 & (u_H)^{-1} & 0 & 0 & 0 & 0 & 0 & 0 & 0 \\ 0 & c_{42} & 0 & (u_H)^{-1} & 0 & 0 & 0 & 0 & 0 & 0 \\ 0 & 0 & 0 & 0 & c_{55} & 0 & 0 & 0 & 0 & 0 \\ 0 & 0 & 0 & 0 & 0 & c_{66} & 0 & 0 & 0 & 0 \\ 0 & 0 & 0 & 0 & 0 & 0 & c_{77} & 0 & c_{79} & 0 \\ 0 & 0 & 0 & 0 & 0 & 0 & 0 & c_{88} & 0 & c_{8\ 10} \\ 0 & 0 & 0 & 0 & 0 & 0 & c_{97} & 0 & c_{99} & 0 \\ 0 & 0 & 0 & 0 & 0 & 0 & 0 & c_{10\ 8} & 0 & c_{10\ 10} \end{pmatrix} \quad (5.3.7)$$

where

$$\begin{aligned} c_{11} &= \frac{1}{(y_{H_1} + u_H)}, \\ c_{31} &= \frac{y_{H_1}}{(y_{H_1} + u_H)u_H}, \\ c_{42} &= \frac{y_{H_2}}{(y_{H_2} + u_H)u_H}, \\ c_{22} &= \frac{1}{(y_{H_2} + u_H)}, \\ c_{55} &= \frac{1}{(y_{H_1} + u_H)}, \end{aligned}$$

$$\begin{aligned}
C_{66} &= \frac{1}{(y_{H_2} + u_H)}, \\
C_{77} &= \frac{c\tau + u_e}{u_m c\tau + u_e u_m - g r_m c\tau}, \\
C_{79} &= \frac{c\tau}{u_m c\tau + u_e u_m - g r_m c\tau}, \\
C_{88} &= \frac{c\tau + u_e}{u_m c\tau + u_e u_m - g r_m c\tau}, \\
C_{8\ 10} &= \frac{c\tau}{u_m c\tau + u_e u_m - g r_m c\tau}, \\
C_{97} &= \frac{g r_m}{u_m c\tau + u_e u_m - g r_m c\tau}, \\
C_{99} &= \frac{u_m}{u_m c\tau + u_e u_m - g r_m c\tau}, \\
C_{10\ 8} &= \frac{g r_m}{u_m c\tau + u_e u_m - g r_m c\tau}, \\
C_{10\ 10} &= \frac{u_m}{u_m c\tau + u_e u_m - g r_m c\tau}.
\end{aligned}$$

So $-J_0$ is a non-singular M -matrix and its eigenvalues all have positive real part [16, 28]. So the eigenvalues of J_0 , and, consequently, $Df_x(x_0)$, all have negative real part.

Given the above assumptions, we have the following result [52, Section 2, Lemma 1]:

If x_0 is a DFE of (5.3.2) and $f_i(x)$ satisfies **(B0)**-**(B5)**, then the derivatives $D\mathcal{F}(x_0)$ and $D\mathcal{V}(x_0)$ are partitioned as

$$D\mathcal{F}(x_0) = \begin{bmatrix} F & 0 \\ 0 & 0 \end{bmatrix}, \quad D\mathcal{V}(x_0) = \begin{bmatrix} V & 0 \\ J_3 & J_4 \end{bmatrix},$$

where F and V are the 10×10 matrices defined by

$$F = \left[\frac{\partial \mathcal{F}_i}{\partial x_j}(x_0) \right] \quad \text{and} \quad V = \left[\frac{\partial \mathcal{V}_i}{\partial x_j}(x_0) \right] \quad \text{with} \quad 1 \leq i, j \leq 10.$$

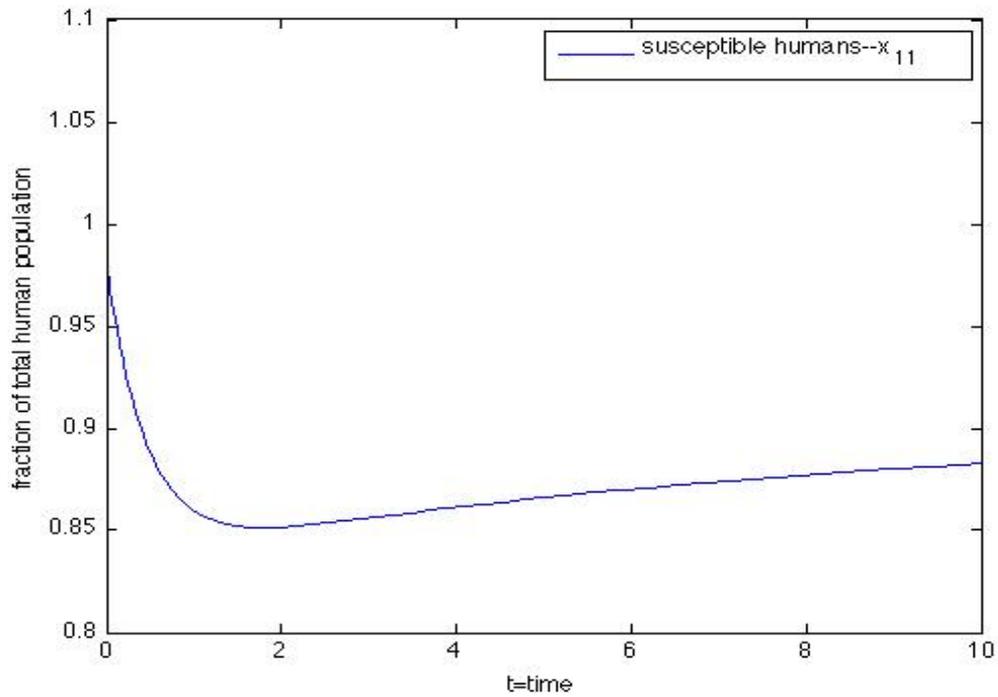


Figure 5.4: Solutions of system (5.3.2) converge to E_1 when $\mathcal{R}_1 = 1.08$, $\mathcal{R}_2 = .25$, $\beta_1 = \beta_2 = .5$; other parameter values given in Table 5.2.

Furthermore, F is non-negative, V is a non-singular M-matrix and all eigenvalues of J_4 have positive real part.

We will now establish \mathcal{R}_0 .

The matrix FV^{-1} is called the next generation matrix for the model and the basic reproduction number is defined as

$$\mathcal{R}_0 = \rho(FV^{-1}), \quad (5.3.8)$$

where $\rho(A)$ denotes the spectral radius of the matrix A .

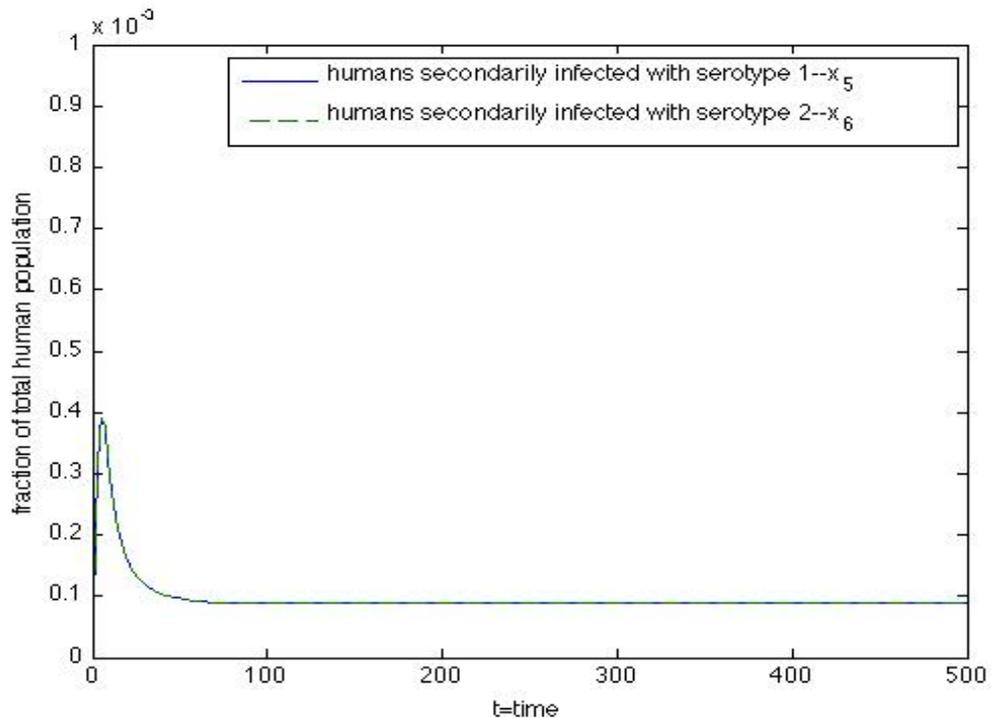


Figure 5.5: System (5.3.2) decouples when $\mathcal{R}_1 = 1.08$, $\mathcal{R}_2 = 1.08$, $\beta_1 = \beta_2 = .5$; other parameter values given in Table 5.2.

We therefore have the following proposition:

Proposition 5.3. Assume $(y_{H_1} + u_H) > 0$, $(y_{H_2} + u_H) > 0$, $u_H > 0$, $c\tau > 0$ and $u_m > 0$, $(u_m c\tau + u_e u_m - g r_m c\tau) > 0$, all other parameters nonnegative.

Then we may define \mathcal{R}_0 for system (5.3.2) by

$$\mathcal{R}_0 = \max_{i=1,2} \mathcal{R}_i,$$

where

$$\mathcal{R}_i = \sqrt{\frac{\lambda_{H_i} \lambda_{V_i} (c\tau + u_e)}{(u_m c\tau + u_e u_m - g r_m c\tau)(u_H + y_{H_i})}}$$
(5.3.9)

Proof. Recall that system (5.3.2) may be written as $\dot{x}_i = f_i(x) = \mathcal{F}_i(x) - \mathcal{V}_i(x)$ where

$\mathcal{V}_i(x) = \mathcal{V}_i^-(x) - \mathcal{V}_i^+(x)$ and where

$$\mathcal{F} = \begin{pmatrix} \lambda_{H_1} x_7 x_{11} \\ \lambda_{H_2} x_8 x_{11} \\ 0 \\ 0 \\ \beta_1 \lambda_{H_1} x_7 x_4 \\ \beta_2 \lambda_{H_2} x_8 x_3 \\ \lambda_{V_1} (x_1 + x_5) (1 - x_7 - x_8) \\ \lambda_{V_2} (x_2 + x_6) (1 - x_7 - x_8) \\ 0 \\ 0 \\ 0 \end{pmatrix} \quad (5.3.10)$$

$$\mathcal{V} = \begin{pmatrix} (y_{H_1} + u_H) x_1 \\ (y_{H_2} + u_H) x_2 \\ -y_{H_1} x_1 + \beta_2 \lambda_{H_2} x_8 x_3 + u_H x_3 \\ -y_{H_2} x_2 + \beta_1 \lambda_{H_1} x_7 x_4 + u_H x_4 \\ (y_{H_1} + u_H) x_5 \\ (y_{H_2} + u_H) x_6 \\ -c\tau(1 - x_7 - x_8) x_9 + u_m x_7 \\ -c\tau(1 - x_7 - x_8) x_{10} + u_m x_8 \\ -gr_m(1 - x_9 - x_{10}) x_7 + c\tau(1 - x_7 - x_8) x_9 + u_e x_9 \\ -gr_m(1 - x_9 - x_{10}) x_8 + c\tau(1 - x_7 - x_8) x_{10} + u_e x_{10} \\ -u_H(1 - x_{11}) + (\lambda_{H_1} x_7 + \lambda_{H_2} x_8) x_{11} \end{pmatrix} \quad (5.3.11)$$

By the lemma stated above, we then have,

$$F = \begin{pmatrix} 0 & 0 & 0 & 0 & 0 & 0 & \lambda_{H_1} & 0 & 0 & 0 \\ 0 & 0 & 0 & 0 & 0 & 0 & 0 & \lambda_{H_2} & 0 & 0 \\ 0 & 0 & 0 & 0 & 0 & 0 & 0 & 0 & 0 & 0 \\ 0 & 0 & 0 & 0 & 0 & 0 & 0 & 0 & 0 & 0 \\ 0 & 0 & 0 & 0 & 0 & 0 & 0 & 0 & 0 & 0 \\ 0 & 0 & 0 & 0 & 0 & 0 & 0 & 0 & 0 & 0 \\ \lambda_{V_1} & 0 & 0 & 0 & \lambda_{V_1} & 0 & 0 & 0 & 0 & 0 \\ 0 & \lambda_{V_2} & 0 & 0 & 0 & \lambda_{V_2} & 0 & 0 & 0 & 0 \\ 0 & 0 & 0 & 0 & 0 & 0 & 0 & 0 & 0 & 0 \\ 0 & 0 & 0 & 0 & 0 & 0 & 0 & 0 & 0 & 0 \end{pmatrix} \quad (5.3.12)$$

$$V = \begin{pmatrix} d_{11} & 0 & 0 & 0 & 0 & 0 & 0 & 0 & 0 & 0 \\ 0 & d_{22} & 0 & 0 & 0 & 0 & 0 & 0 & 0 & 0 \\ -y_{H_1} & 0 & u_H & 0 & 0 & 0 & 0 & 0 & 0 & 0 \\ 0 & -y_{H_2} & 0 & u_H & 0 & 0 & 0 & 0 & 0 & 0 \\ 0 & 0 & 0 & 0 & d_{55} & 0 & 0 & 0 & 0 & 0 \\ 0 & 0 & 0 & 0 & 0 & d_{66} & 0 & 0 & 0 & 0 \\ 0 & 0 & 0 & 0 & 0 & 0 & u_m & 0 & -c\tau & 0 \\ 0 & 0 & 0 & 0 & 0 & 0 & 0 & u_m & 0 & -c\tau \\ 0 & 0 & 0 & 0 & 0 & 0 & -gr_m & 0 & c\tau + u_e & 0 \\ 0 & 0 & 0 & 0 & 0 & 0 & 0 & -gr_m & 0 & c\tau + u_e \end{pmatrix} \quad (5.3.13)$$

where

$$d_{11} = (y_{H_1} + u_H),$$

$$d_{22} = (y_{H_2} + u_H),$$

$$d_{55} = (y_{H_1} + u_H),$$

$$d_{66} = (y_{H_2} + u_H).$$

$$J_3 = \begin{pmatrix} 0 & 0 & 0 & 0 & 0 & 0 & (\lambda_{H_1}) & (\lambda_{H_2}) & 0 & 0 \end{pmatrix} \quad (5.3.14)$$

and

$$J_4 = \begin{pmatrix} u_H \end{pmatrix} \quad (5.3.15)$$

where F is non-negative, V is a non-singular M-matrix and all eigenvalues of J_4 have positive real part.

Now by (5.3.12) and (5.3.13) we have that the characteristic equation of FV^{-1} is given by:

$$\begin{aligned} \lambda^{10} + \frac{(\lambda_{V_1} \lambda_{H_1} (u_H + y_{H_2}) + \lambda_{V_2} \lambda_{H_2} (u_H + y_{H_1})) (c\tau + u_e)}{(u_H + y_{H_1})(u_H + y_{H_2})(-u_m c\tau - u_e u_m + g r_m c\tau)} \lambda^8 \\ + \frac{\lambda_{V_1} \lambda_{H_1} \lambda_{V_2} \lambda_{H_2} (c\tau + u_e)^2}{(u_H + y_{H_1})(u_H + y_{H_2})(-u_m c\tau - u_e u_m + g r_m c\tau)^2} \lambda^6 = 0. \end{aligned} \quad (5.3.16)$$

Clearly, 0 is a solution of this equation.

The others are:

$$\begin{aligned} \lambda_{1,2} &= \pm \sqrt{\frac{\lambda_{H_1} \lambda_{V_1} (c\tau + u_e)}{(u_m c\tau + u_e u_m - g r_m c\tau)(u_H + y_{H_1})}} \\ \lambda_{3,4} &= \pm \sqrt{\frac{\lambda_{H_2} \lambda_{V_2} (c\tau + u_e)}{(u_m c\tau + u_e u_m - g r_m c\tau)(u_H + y_{H_2})}} \end{aligned} \quad (5.3.17)$$

So by (5.3.8), we have our desired result. \square

Proposition 5.4. *Let \mathcal{R}_0 , parameters be as in Proposition 5.3. The following conditions characterize the stability of $(0, 0, 0, 0, 0, 0, 0, 0, 0, 0, 1)^T$:*

- 1) *If $\mathcal{R}_0 < 1$, then $(0, 0, 0, 0, 0, 0, 0, 0, 0, 0, 1)^T$ is locally asymptotically stable.*
- 2) *If $\mathcal{R}_0 > 1$, then $(0, 0, 0, 0, 0, 0, 0, 0, 0, 0, 1)^T$ is unstable.*

Proof. The result follows from [52, Section 3, Theorem 2]. \square

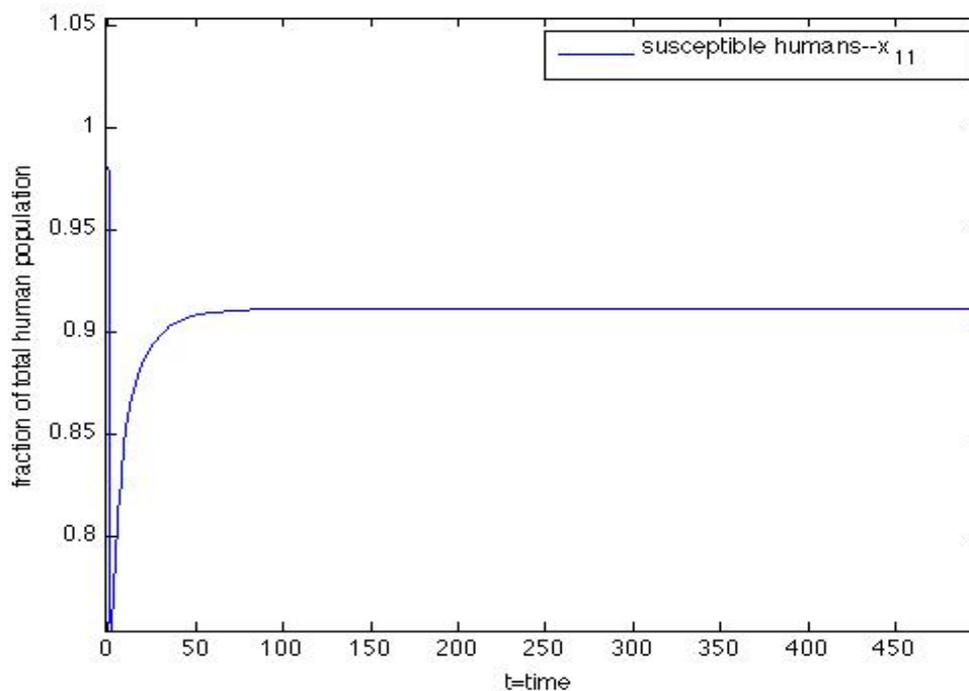


Figure 5.6: System (5.3.2) decouples when $\mathcal{R}_1 = 1.08$, $\mathcal{R}_2 = 1.08$, $\beta_1 = \beta_2 = .5$; other parameter values given in Table 5.2.

5.4 An Alternative Interpretation of Model (5.3.2)

By an alternative interpretation of Model (5.3.2), we have that x_1 , x_3 , x_7 , and x_9 are uninfected compartments and x_2 , x_4 , x_5 , x_6 , x_8 , x_{10} , infected compartments.

In this case, we look for conditions under which a boundary equilibrium of Model (5.3.2), $E_1 = (\bar{x}_1, 0, \bar{x}_3, 0, 0, 0, \bar{x}_7, 0, \bar{x}_9, 0, \bar{x}_{11})$, exists and is (un-)stable; that is, the strain for serotype 2 (can) cannot invade E_1 , the equilibrium for the strain for serotype 1.

First, we set system (5.3.2) and compartments $x_2, x_4, x_5, x_6, x_8, x_{10}$ to 0. The remaining equations are given by:

$$\begin{aligned}
\dot{x}_1 &= \lambda_{H_1} x_7 x_{11} - (y_{H_1} + u_H) x_1 = 0 \\
\dot{x}_3 &= y_{H_1} x_1 - u_H x_3 = 0 \\
\dot{x}_7 &= c\tau(1 - x_7)x_9 - u_m x_7 + \lambda_{V_1}(x_1)(1 - x_7) = 0 \\
\dot{x}_9 &= gr_m(1 - x_9)x_7 - c\tau(1 - x_7)x_9 - u_e x_9 = 0 \\
\dot{x}_{11} &= u_H(1 - x_{11}) - (\lambda_{H_1} x_7) x_{11} = 0
\end{aligned} \tag{5.4.1}$$

Let $(\bar{x}_1, 0, \bar{x}_3, 0, 0, 0, \bar{x}_7, 0, \bar{x}_9, 0, \bar{x}_{11})$ be a solution of system (5.4.1), where compartments $x_2, x_4, x_5, x_6, x_8, x_{10}$ are set to 0. Then the equations for the nonvanishing compartments are given by:

$$\begin{aligned}
\bar{x}_1 &= \frac{\lambda_{H_1} \bar{x}_7 \bar{x}_{11}}{(y_{H_1} + u_H)} \\
\bar{x}_3 &= \frac{y_{H_1} \bar{x}_1}{u_H} \\
\bar{x}_7 &= \frac{c\tau \bar{x}_9 + \lambda_{V_1} \bar{x}_1}{c\tau \bar{x}_9 + \lambda_{V_1} \bar{x}_1 + u_m} \\
\bar{x}_9 &= \frac{gr_m \bar{x}_7}{c\tau(1 - \bar{x}_7) + gr_m \bar{x}_7 + u_e} \\
\bar{x}_{11} &= \frac{u_H}{u_H + \lambda_{H_1} \bar{x}_7}
\end{aligned} \tag{5.4.2}$$

We want $(\bar{x}_1, \bar{x}_3, \bar{x}_7, \bar{x}_9, \bar{x}_{11})$ to be in Ω . With this in mind, we have the following proposition:

Proposition 5.5. *Assume $(u_m c\tau + u_e u_m - gr_m c\tau) > 0$, all other parameters positive. Assume also that $gr_m > c\tau$ and $\lambda_{H_1}(c\tau + u_e) + u_H(c\tau - gr_m) > 0$. Then $\mathcal{R}_1 > 1 \Leftrightarrow$ system (5.3.2) has a boundary equilibrium, E_1 .*

Proof. \Rightarrow

Suppose $\mathcal{R}_1 > 1$. Let $R' = (\mathcal{R}_1)^2 = \frac{\lambda_{H_1} \lambda_{V_1} (c\tau + u_e)}{(u_m c\tau + u_e u_m - gr_m c\tau)(u_H + y_{H_1})}$. Then, $R' > 1$ (*). If we solve for x_{11} in system (5.4.1), we see that it can take on three possible values: 0 and the roots of a degree-two polynomial function f , where $f(x_{11}) = [(\lambda_{H_1} + u_H)\lambda_{V_1}(\lambda_{H_1} u_e + c\tau\lambda_{H_1} + c\tau u_H - gr_m u_H)]x_{11}^2 + [c\tau(gr_m - u_m)(u_H + \lambda_{H_1})(u_H + y_{H_1}) - (u_e \lambda_{H_1} u_m + gr_m u_H u_m)(u_H + y_{H_1}) - \lambda_{H_1} \lambda_{V_1} u_H (c\tau + u_e) + u_H \lambda_{V_1} (gr_m - c\tau)(2u_H + \lambda_{H_1})]x_{11} + u_H((c\tau - gr_m)(u_H \lambda_{V_1} + u_m(u_H + y_{H_1})) - c\tau gr_m(u_H + y_{H_1}))$. Now by assumption, $f(0) < 0$ (**). By (*), $f(1) = (R' - 1)\lambda_{H_1}(u_m c\tau + u_e u_m - gr_m c\tau) > 0$. So by the intermediate value theorem, f has a real root between 0 and 1. If we substitute this value, say b^* , for x_{11} in system (5.4.1), and solve for the other components in terms of b^* , we see that system (5.4.1) is consistent. So a solution of system (5.4.1), with $x_{11} = b^*$, exists. Additionally, the other solution components are uniquely determined by b^* . Let E_1 be this solution, so that $\bar{x}_{11} = b^*$. Then $0 < \bar{x}_{11} < 1$. So E_1 is not the DFE. By (5.4.2), the other components of $E_1 \neq 0$. Now if we add (LHS) of equations 1 and 5 of (5.4.1), then $\bar{x}_1 = u_H \frac{1 - \bar{x}_{11}}{u_H + y_{H_1}}$. So $0 < \bar{x}_1 < 1$ and $\bar{x}_{11} + \bar{x}_1 = \frac{u_H + \bar{x}_{11} y_{H_1}}{u_H + y_{H_1}} < 1$. If we add equations 1,3 and 5 of (5.4.1), we obtain $\bar{x}_3 = 1 - (x_1 + x_{11})$. So $0 < \bar{x}_3 < 1$. By equation 5 of (5.4.2), $\bar{x}_7 > 0$. By assumption, $gr_m > c\tau$. So by equation 4 of (5.4.2), $0 < \bar{x}_9 < 1$. By equation 3 of (5.4.2), $\bar{x}_7 < 1$.

\Leftarrow

Suppose $\mathcal{R}_1 < 1$. Then, $R' < 1$, by (*). So $f(1) = (R' - 1)\lambda_{H_1}(u_m c\tau + u_e u_m - gr_m c\tau) < 0$. By (**), $f(0) < 0$. Now the coefficient of the square term of f is > 0 , by assumption. So f is concave up and cannot have a root between 0 and 1. \square

We will now study the local stability of the endemic equilibrium, E_1 .

Proposition 5.6. *Assume conditions are as in Proposition 5.5, $\mathcal{R}_1 > 1$, and $\lambda_{H_1} < 1$. Suppose, additionally, that $\beta_2 \leq 1$. Then if $\mathcal{R}_2 < 1$, where \mathcal{R}_2 is as in (5.3.9), E_1 is locally asymptotically stable.*

Proof. Since we take x_1, x_3, x_7 , and x_9 to be uninfected and $x_2, x_4, x_5, x_6, x_8, x_{10}$ to be infected compartments, we may rewrite system (5.3.2) as

$$\begin{aligned}
\dot{x}_2 &= \lambda_{H_2} x_8 x_{11} - (y_{H_2} + u_H) x_2 \\
\dot{x}_4 &= y_{H_2} x_2 - \beta_1 \lambda_{H_1} x_7 x_4 - u_H x_4 \\
\dot{x}_6 &= \beta_2 \lambda_{H_2} x_8 x_3 - (y_{H_2} + u_H) x_6 \\
\dot{x}_8 &= c\tau(1 - x_7 - x_8) x_{10} - u_m x_8 + \lambda_{V_2} (x_2 + x_6) (1 - x_7 - x_8) \\
\dot{x}_{10} &= gr_m(1 - x_9 - x_{10}) x_8 - c\tau(1 - x_7 - x_8) x_{10} - u_e x_{10} \\
\dot{x}_5 &= \beta_1 \lambda_{H_1} x_7 x_4 - (y_{H_1} + u_H) x_5 \\
\dot{x}_1 &= \lambda_{H_1} x_7 x_{11} - (y_{H_1} + u_H) x_1 \\
\dot{x}_3 &= y_{H_1} x_1 - \beta_2 \lambda_{H_2} x_8 x_3 - u_H x_3 \\
\dot{x}_7 &= c\tau(1 - x_7 - x_8) x_9 - u_m x_7 + \lambda_{V_1} (x_1 + x_5) (1 - x_7 - x_8) \\
\dot{x}_9 &= gr_m(1 - x_9 - x_{10}) x_7 - c\tau(1 - x_7 - x_8) x_9 - u_e x_9 \\
\dot{x}_{11} &= u_H(1 - x_{11}) - (\lambda_{H_1} x_7 + \lambda_{H_2} x_8) x_{11}
\end{aligned} \tag{5.4.3}$$

where $(x_{10}, \dots, x_{11_0}) \in \Omega$, $u_H > 0$.

Consider the linearized system of (5.4.3) at E_1 . The Jacobian matrix at E_1 is given by:

$$\begin{pmatrix} A_1 & A_2 \\ A_3 & A_4 \end{pmatrix} \tag{5.4.4}$$

where

$$A_1 = \begin{pmatrix} (-y_{H_2} + u_H) & 0 & 0 & \lambda_{H_2}\bar{x}_{11} & 0 & 0 \\ y_{H_2} & -\beta_1\lambda_{H_1}\bar{x}_7 - u_H & 0 & 0 & 0 & 0 \\ 0 & 0 & -(y_{H_2} + u_H) & \beta_2\lambda_{H_2}\bar{x}_3 & 0 & 0 \\ \lambda_{V_2}(1 - \bar{x}_7) & 0 & \lambda_{V_2}(1 - \bar{x}_7) & -u_m & c\tau(1 - \bar{x}_7) & 0 \\ 0 & 0 & 0 & gr_m(1 - \bar{x}_9) & -c\tau(1 - \bar{x}_7) - u_e & 0 \\ 0 & \beta_1\lambda_{H_1}\bar{x}_7 & 0 & 0 & 0 & -(y_{H_1} + u_H) \end{pmatrix} \quad (5.4.5)$$

$$A_2 = 0,$$

$$A_3 = \begin{pmatrix} 0 & 0 & 0 & 0 & 0 & 0 \\ 0 & 0 & 0 & -\beta_2\lambda_{H_2}\bar{x}_3 & 0 & 0 \\ 0 & 0 & 0 & -c\tau\bar{x}_9 - \lambda_{V_1}\bar{x}_1 & 0 & \lambda_{V_1}(1 - \bar{x}_7) \\ 0 & 0 & 0 & c\tau\bar{x}_9 & -gr_m\bar{x}_7 & 0 \\ 0 & 0 & 0 & -\lambda_{H_2}\bar{x}_{11} & 0 & 0 \end{pmatrix} \quad (5.4.6)$$

and

$$A_4 = \begin{pmatrix} -(y_{H_1} + u_H) & 0 & \lambda_{H_1}\bar{x}_{11} & 0 & \lambda_{H_1}\bar{x}_7 \\ y_{H_1} & -u_H & 0 & 0 & 0 \\ \lambda_{V_1}(1 - \bar{x}_7) & 0 & -c\tau\bar{x}_9 - u_m - \lambda_{V_1}\bar{x}_1 & c\tau(1 - \bar{x}_7) & 0 \\ 0 & 0 & gr_m(1 - \bar{x}_9) + c\tau\bar{x}_9 & -gr_m\bar{x}_7 - c\tau(1 - \bar{x}_7) - u_e & 0 \\ 0 & 0 & -\lambda_{H_1}\bar{x}_{11} & 0 & -u_H - \lambda_{H_1}\bar{x}_7 \end{pmatrix} \quad (5.4.7)$$

Observe that the Jacobian matrix at E_1 is block lower triangular, so its eigenvalues are determined by the eigenvalues of $A_1 = [b_{ij}], 1 \leq i, j \leq 6$, $A_4 = [a_{ij}], 1 \leq i, j \leq 5$, where *henceforth*, $[a_{ij}]$ refers exclusively to A_4 and $[b_{ij}]$ refers exclusively to A_1 .

Consider the submatrix of A_4 obtained by deleting the fifth row and the fifth column of A_4 . We will denote this submatrix by $A_0 = [a_{ij}], 1 \leq i, j \leq 4$. Now $-A_0$ has the Z -pattern (see **B5**). Also, $\det(-A_0) = (y_{H_1} + u_H)u_H\lambda_{V_1}\bar{x}_1(gr_m\bar{x}_7 + c\tau(1 - \bar{x}_7) + u_e) + (y_{H_1} + u_H)u_Hc\tau\bar{x}_9(u_e + gr_m) > 0$. The inverse of $-A_0$ is given by

$$\frac{u_H}{\det(-A_0)} \times \begin{pmatrix} (u_m + c\tau\bar{x}_9 + \lambda_{V_1})(gr_m\bar{x}_7 + c\tau(1 - \bar{x}_7) + u_e) - c\tau\bar{x}_9 gr_m\bar{x}_7 & 0 & -a_{13}a_{44} & a_{13}a_{34} \\ \frac{a_{21}((u_m + c\tau\bar{x}_9 + \lambda_{V_1})(gr_m\bar{x}_7 + c\tau(1 - \bar{x}_7) + u_e) - c\tau\bar{x}_9 gr_m\bar{x}_7)}{u_H} & u_H^{-1} & -\frac{a_{21}a_{13}a_{44}}{u_H} & \frac{a_{21}a_{13}a_{34}}{u_H} \\ -a_{44}a_{31} & 0 & a_{11}a_{44} & -a_{34}a_{11} \\ a_{43}a_{31} & 0 & -a_{43}a_{11} & (y_{H_1} + u_H)\left(\frac{c\tau\bar{x}_9}{\bar{x}_7} + \lambda_{V_1}\bar{x}_1\right) \end{pmatrix} \quad (5.4.8)$$

By inspection, this inverse has all positive entries, so $-A_0$ is a nonsingular M-matrix (see **B5**). So the principal leading minors of $-A_0$ are all positive [16, 28]. (*)

Recall that given a complex-valued $n \times n$ matrix $P = [p_{ij}]$ with $1 \leq i, j \leq n$, we define its *companion matrix* $M(P) = [m_{ij}]$ with $1 \leq i, j \leq n$ by $m_{ij} = |p_{ij}|$ if $j = i$ and $m_{ij} = -|p_{ij}|$ if $j \neq i$ ([28, Definition 2.5.10], see also [60]). P is called an *H-matrix* if its companion matrix $M(P)$ is a (non-singular) M-matrix ([28, pp. 124] see also [60]). Now $M(-A_4)$ has the *Z-pattern* (see **B5**). Also, $-A_0$ is the submatrix of $M(-A_4)$ obtained by deleting its last row and column, so the principal leading minors of $M(-A_4)$ are the principal leading minors of $-A_0$, which, by (*), are positive, and $\det(M(-A_4)) = (u_H + \lambda_{H_1}\bar{x}_7)[(y_{H_1} + u_H)u_H\lambda_{V_1}\bar{x}_1(1 - (1 - \bar{x}_7)\lambda_{H_1})(gr_m\bar{x}_7 + c\tau(1 - \bar{x}_7) + u_e) + (y_{H_1} + u_H)u_Hc\tau\bar{x}_9(u_e + gr_m)] > 0$.

So $M(-A_4)$ is a non-singular M-matrix [16, 28] and $-A_4$ is an H-Matrix. Now an $n \times n$ complex-valued square matrix is said to be *positive stable* if its eigenvalues all have positive real part [5, pp. 134]. An H-matrix with real entries is positive stable iff it has positive diagonal entries [28, Exercise, pp. 124; 60, Lemma 2]. Now $-A_4$ clearly has positive diagonal entries. So it is positive stable. It follows that the eigenvalues of A_4 all have negative real part.

The eigenvalues of A_1 are $-(y_{H_1} + u_H)$ and the eigenvalues of the submatrix of A_1 obtained by deleting the sixth row and the sixth column of A_1 . We will denote this

submatrix by $B_0 = [b_{ij}]$, $1 \leq i, j \leq 5$. Observe that $-B_0$ has the Z -pattern. Also, $\det(-B_0) = (u_H + \beta_1 \lambda_{H_1} \bar{x}_7)[(y_{H_2} + u_H)^2(u_m u_e \bar{x}_7 + c\tau(1 - \bar{x}_7)\bar{x}_9) + (y_{H_2} + u_H)(1 - \bar{x}_7)(\lambda_{V_2} \lambda_{H_2})((1 - (\beta_2 \bar{x}_3 + \bar{x}_{11}))(u_e + c\tau) + c\tau \bar{x}_7(\beta_2 \bar{x}_3 + \bar{x}_{11})) + (y_{H_2} + u_H)(1 - \bar{x}_7)(1 - \mathcal{R}_2^2)] > 0$, by the assumption that $\beta_2 \leq 2$ and the fact that $\bar{x}_3 + \bar{x}_{11} \leq 1$. The inverse of $-B_0$ is given by

$$\frac{u_H + \beta_1 \lambda_{H_1} \bar{x}_1}{\det(-B_0)} \times \begin{pmatrix} \frac{\det(-B_0)}{b_{11}b_{22}} + \frac{b_{55}b_{14}b_{41}b_{33}}{-b_{11}} & 0 & -b_{14}b_{55}b_{43} & b_{14}b_{55}b_{33} & -b_{14}b_{45}b_{33} \\ -\frac{b_{21}}{b_{22}} \left(\frac{\det(-B_0)}{b_{11}b_{22}} + \frac{b_{55}b_{14}b_{41}b_{33}}{-b_{11}} \right) & -b_{22}^{-1} & -\frac{b_{21}}{b_{22}}(-b_{14}b_{55}b_{43}) & -\frac{b_{21}}{b_{22}}(b_{14}b_{55}b_{33}) & -\frac{b_{21}}{b_{22}}(-b_{14}b_{45}b_{33}) \\ -b_{34}b_{55}b_{43} & 0 & \frac{\det(-B_0)}{b_{22}b_{33}} + \frac{b_{55}b_{43}b_{34}b_{11}}{-b_{33}} & b_{34}b_{55}b_{11} & -b_{34}b_{45}b_{11} \\ b_{55}b_{33}b_{41} & 0 & b_{11}b_{55}b_{43} & -b_{55}b_{33}b_{11} & b_{45}b_{33}b_{11} \\ -b_{54}b_{33}b_{41} & 0 & -b_{54}b_{11}b_{43} & b_{54}b_{33}b_{11} & \frac{\det(-B_0)}{b_{22}b_{55}} + \frac{b_{54}b_{45}b_{33}b_{11}}{-b_{55}} \end{pmatrix} \quad (5.4.9)$$

By inspection, this inverse has all nonnegative entries, $-B_0$ is a nonsingular M-matrix and the eigenvalues of B_0 , and, consequently, A_1 , all have negative real part (see **B5**).

So the eigenvalues of the Jacobian matrix at E_1 all have negative real part, and E_1 is locally asymptotically stable. \square

Since system (5.3.2) is symmetric with respect to serotypes 1 and 2, we have analogous results for conditions under which the strain for serotype 1 can invade E_2 , the equilibrium for the strain for serotype 2.

We leave the study of the existence and analysis of a virus coexistence equilibrium for a future project.

5.5 Numerical Simulations

We now conduct numerical simulations to illustrate our analytical results.

Values for $u_H, \lambda_{H_{1,2}}, y_{H_{1,2}}, u_m, r_m$ and g are comparable to those presented by Coutinho *et al.* [8] on the basis of estimates known from the dengue infection process and human and mosquito vital statistics. We assume that the entire juvenile mosquito population is at carrying capacity.

We first take $\lambda_{H_{1,2}}, \lambda_{V_{1,2}}$ small, $y_{H_{1,2}}$ large, with $\lambda_{H_1} = \lambda_{H_2} = .1$, $\lambda_{V_1} = \lambda_{V_2} = .5$, $y_{H_1} = y_{H_2} = .067$. For parameter values given in column 2 of Table 5.2, $\mathcal{R}_0 = \max_{i=1,2} \mathcal{R}_i = .25$. Accordingly, the simulations show that the DFE is asymptotically stable (see Figures 5.10, 5.1, 5.11, 5.2). Next, we take $\lambda_{H_1}, \lambda_{V_1}$ large, y_{H_1} small, while maintaining parameter values for $\lambda_{H_2}, \lambda_{V_2}$ and y_{H_2} that are used in the simulations presented in Figures 5.10, 5.1, 5.11, 5.2. We modify other parameters so that $\mathcal{R}_0 = \mathcal{R}_1 = 1.08$ and $\mathcal{R}_2 = .25$. As seen in Figures 5.12, 5.3, 5.13, 5.4, the DFE is destabilized. Alternatively, we may take $x_1 = I_{H_1}$, $x_3 = Z_{H_1}$, $x_7 = I_{M_1}$ and $x_9 = I_{E_1}$ to be uninfected compartments and $x_2 = I_{H_2}$, $x_4 = Z_{H_2}$, $x_5 = Y_{H_1}$, $x_6 = Y_{H_2}$, $x_8 = I_{M_2}$, $x_{10} = I_{E_2}$ to be infected compartments. In this case, as mentioned in the previous section, we look for conditions under which a boundary equilibrium of system (5.3.2), $E_1 = (\bar{x}_1, 0, \bar{x}_3, 0, 0, 0, \bar{x}_7, 0, \bar{x}_9, 0, \bar{x}_{11})$, exists and is (un-)stable; that is, the strain for serotype 2 (can) cannot invade E_1 , the equilibrium for the strain for serotype 1. Following our analytical results, we see that when the conditions for Proposition 5.5 are met, the boundary equilibrium E_1 exists and is given by $(.08, 0, .008, 0, 0, 0, .051, 0, .006, 0, .912)$ (see Figures 5.12, 5.3, 5.13, 5.4). Additionally, the simulations suggest that when $\beta_2 \leq 1$ and $\mathcal{R}_2 < 1$, the trajectories of system (5.3.2) converge to E_1 , as indicated by Proposition 5.6 (see column 3

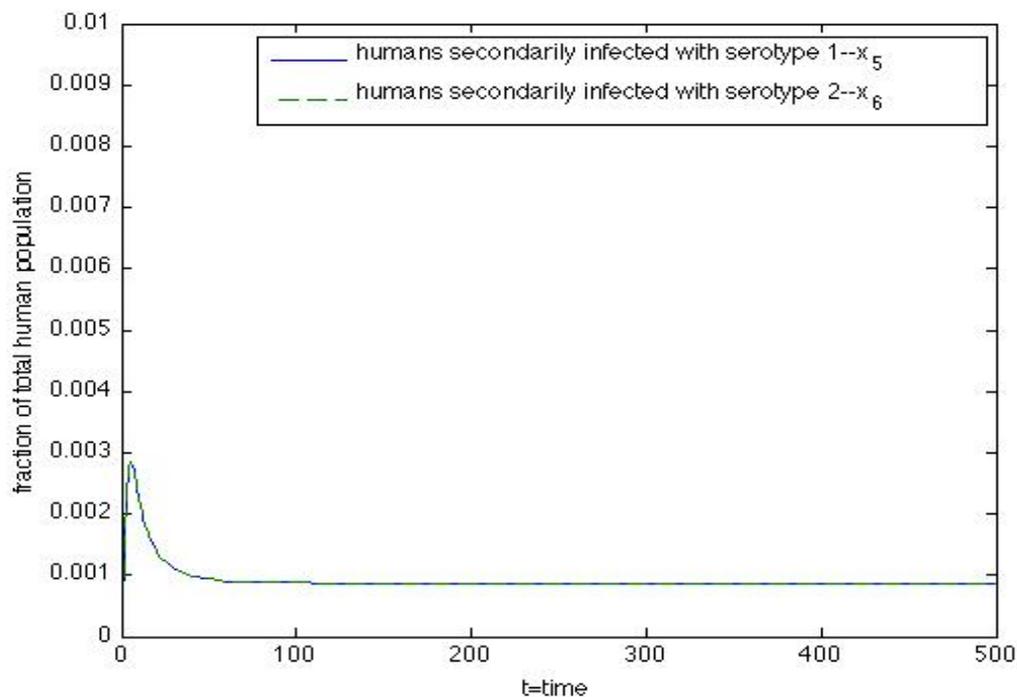


Figure 5.7: Solutions of system (5.3.2) converge to an endemic equilibrium when $\mathcal{R}_1 = 1.08$, $\mathcal{R}_2 = 1.08$, $\beta_1 = \beta_2 = 5$; other parameter values given in Table 5.2.

of Table 5.2). Figures 5.12, 5.3, 5.13, 5.4 suggest that E_1 is locally asymptotically stable and that the strain for serotype 2 cannot invade this boundary equilibrium. Under these conditions, then, a pandemic featuring both strains of the virus may be prevented. Under such a scenario, the prevalence of DHF cases would cast doubt on the “secondary infection” or “immune enhancement” hypothesis, since solutions for the secondarily infected classes converge to 0 (see Figure 5.3).

We then take $\lambda_{H_{1,2}}, \lambda_{V_{1,2}}$ large, $y_{H_{1,2}}$ small, with $\lambda_{H_1} = \lambda_{H_2} = .95$, $\lambda_{V_1} = \lambda_{V_2} = .95$, $y_{H_1} = y_{H_2} = .05$. We have $\mathcal{R}_0 = \mathcal{R}_1 = \mathcal{R}_2 = 1.08$, and conditions for the existence for the existence of both E_1 and E_2 , following Proposition 5.5 and the symmetry of system (5.3.2) with respect to serotypes 1 and 2, are met. When we take initial conditions

for the subsystems for serotypes 1 and 2, $\{x_1, x_3, x_7, x_9, x_{11}\}$ and $\{x_2, x_4, x_8, x_{10}, x_{11}\}$, respectively, to be the same and $\beta_1 = \beta_2 = .5 < 1$ (see column 4 of Table 5.2), system (5.3.2) decouples into these subsystems. Trajectories converge to endemic equilibria for these subsystems, $\tilde{E}_1 = \tilde{E}_2 = (.08, .008, .051, .006, .912)$, the restrictions of E_1 and E_2 to the subsystems for serotypes 1 and 2, respectively. Because $\beta_1 = \beta_2 = .5 < 1$, trajectories x_5 and x_6 converge to 0, so that we may observe two distinct epidemics for serotypes 1 and 2 (Figures 5.14, 5.5, 5.15, 5.6).

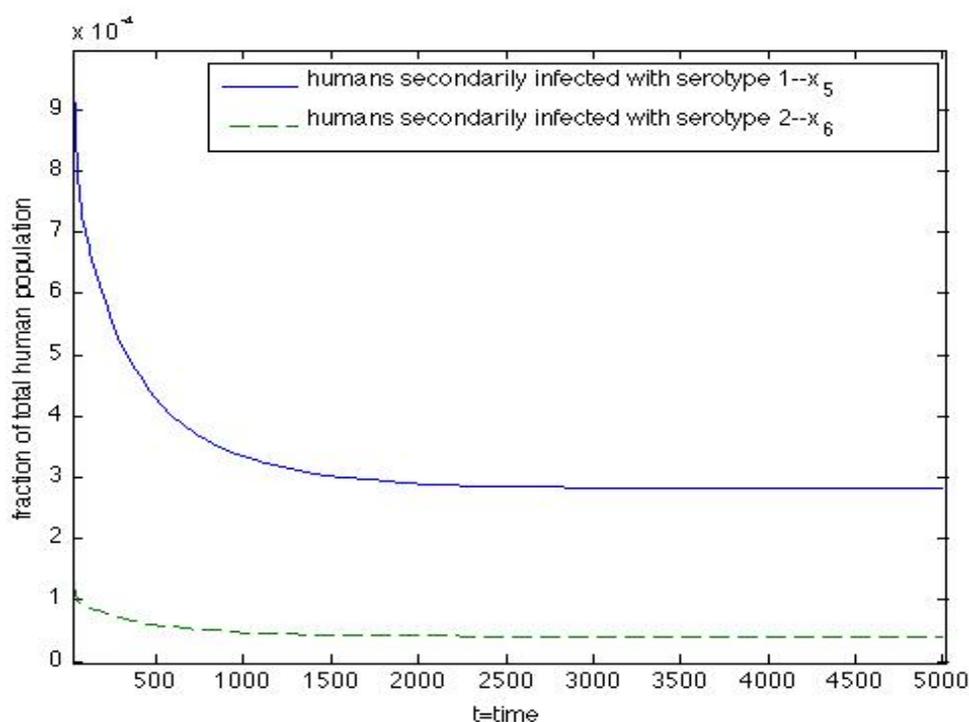


Figure 5.8: Solutions of system (5.3.2) converge to an endemic equilibrium when $\mathcal{R}_1 = 1.08$, $\mathcal{R}_2 = 1.08$, $\beta_1 = 5$, $\beta_2 = .5$; other parameter values given in Table 5.2.

We next take $\beta_1 = \beta_2 = 5 > 1$ while maintaining other parameter values used in the simulations presented in (Figures 5.14, 5.5, 5.15, 5.6) (see column 5 of Table 5.2). Trajectories x_5 and x_6 now converge to positive values (Figure 5.7).

We therefore obtain a virus coexistence equilibrium for system (5.3.2), whose values are given by (.08, .08, .008, .008, .0009, .0009, .051, .051, .006, .006, .912) (Figures 5.14, 5.5, 5.15, 5.6, 5.7). We conclude that when primary infections increase susceptibility to secondary infections, a pandemic featuring strains for both serotypes, where the prevalence of infection by one serotype contributes to that of the other, may ensue.

Finally, when we take $\beta_1 = 5 > .5 = \beta_2$, we obtain an endemic equilibrium whose values for those compartments corresponding to infection by serotype 1 ($\{x_1, x_3, x_5, x_7, x_9, x_{11}\}$) are greater than the values for their counterparts corresponding to infection by serotype 2 ($\{x_2, x_4, x_6, x_8, x_{10}, x_{11}\}$) (Figures 5.16, 5.8, 5.17, 5.9). We may observe, then, a pandemic featuring both serotypes where the sub-pandemic for serotype 1 is more intense than the one for serotype 2. Interestingly, even though $\beta_2 < 1$, we observe the persistence of the sub-pandemic for serotype 2, indicating that though infection with serotype 1 confers partial or total immunity to serotype 2, the prevalence of secondary infections of serotype 1 contributes to the prevalence of the sub-pandemic for serotype 2. This implies that increased susceptibility to serotype 2 due to primary infection with serotype 1 is not a necessary condition for a single pandemic featuring both serotypes.

5.6 Discussion

In this chapter, we presented an ODE model that incorporates two serotypes of the dengue virus and allows for the possibility of both primary and secondary infections with each serotype. Our model depicts dengue transmission in 3 components: human

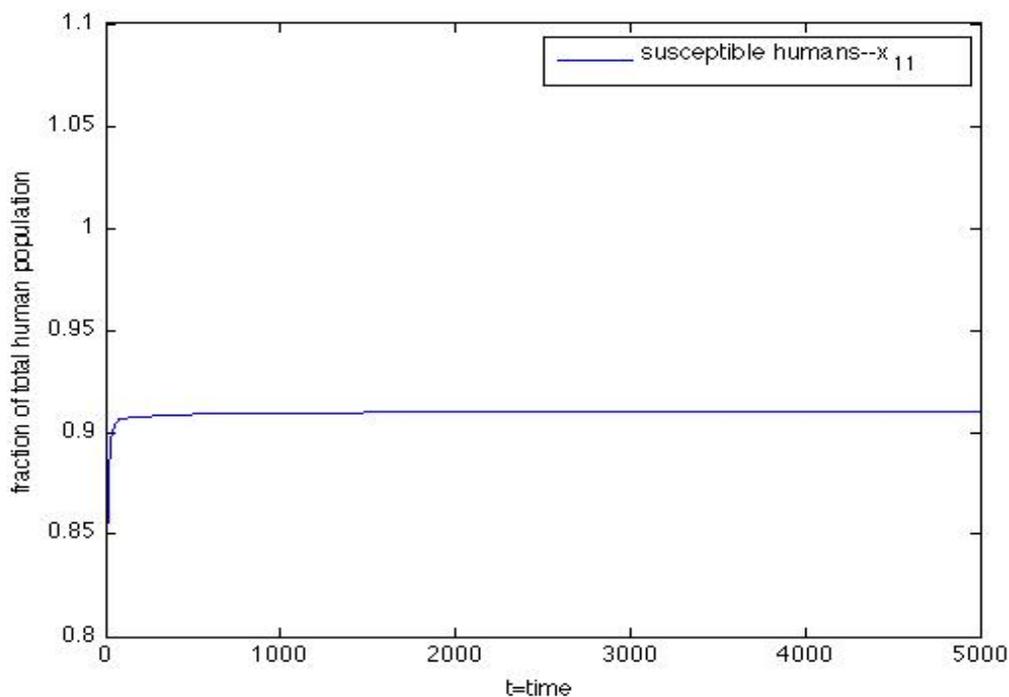


Figure 5.9: Solutions of system (5.3.2) converge to an endemic equilibrium when $\mathcal{R}_1 = 1.08$, $\mathcal{R}_2 = 1.08$, $\beta_1 = 5$, $\beta_2 = .5$; other parameter values given in Table 5.2.

hosts, adult mosquitoes, and juvenile mosquitoes, combining a coupled SIR system for disease transmission in the human host with a two-stage coupled SI model for disease transmission in the mosquito vector. We assumed that the entire human, adult, and juvenile mosquito populations remain constant.

We first proved that if initial conditions are positive, the positive cone will be positively invariant and solutions will exist for all time. We then made variable substitutions to obtain a simplified, proportion-based system. Next we assumed that the natural adult mosquito rate, the natural human death rate, and the rates at which juveniles transfer out of their compartments, among other conditions, are positive. Under these assumptions, we were able to derive conditions for the existence of a

threshold parameter, the reproductive number (\mathcal{R}_0), denoting the expected number of secondary cases produced by a typically infective individual. We obtained an analytical expression for \mathcal{R}_0 that defines it as the maximum of the reproduction numbers for each strain/serotype of the virus.

We next presented an alternative interpretation of Model (5.2.1) where compartments corresponding to primary infection by serotype 1 are uninfected compartments, and compartments corresponding to primary infection by serotype 2 are infected compartments. We looked for conditions under which the strain for serotype 2 can invade the equilibrium for the strain for serotype 1. Interestingly, Propositions 5.5 and 5.6 suggest that the existence of a boundary equilibrium for a particular strain destabilizes the boundary equilibrium for the other. Future work that explores this implication and proves and analyzes the existence of a virus coexistence equilibrium is indicated.

Simulations were conducted to illustrate analytical results and to numerically verify the existence of a virus coexistence equilibrium. The results suggest that in order to contain a two-strain pandemic, controlling β_i , the susceptibility of a host to serotype i due to infection with serotype j , is crucial. From a strategic, prevention-minded point of view, improving health and sanitation conditions in regions and among humans at high risk for contracting the dengue virus is therefore paramount. Despite the fact that contraction of the virus cannot take place between high-risk humans, the transmission dynamics indicate that the very existence of these high-risk groups and regions exacerbates the possibility of a pandemic.

Description	<i>Values for Figure</i>				
	5.10, 5.1, 5.11, 5.2	5.12, 5.3, 5.13, 5.4	5.14, 5.5, 5.15, 5.6	5.7	5.16, 5.8, 5.17, 5.9
Initial Condition					
x_1	.005	.005	.005	.005	.005
x_2	.0025	.0025	.005	.005	.0005
x_3	.0001	.0001	.0001	.0001	.0001
x_4	.00005	.00005	.0001	.0001	.0001
x_5	.00005	.00005	.00005	.00005	.00005
x_6	.000005	.000005	.00005	.00005	.00005
x_7	0.33	0.33	0.33	0.33	0.33
x_8	0.1	0.1	0.33	0.33	0.33
x_9	.075	.075	.075	.075	.075
x_{10}	.025	.025	.075	.075	.075
x_{11}	.98	.98	.98	.98	.98
Parameter					
u_H	2.5	0.5	0.5	0.5	0.5
λ_{H_1}	0.1	0.95	0.95	0.95	0.95
y_{H_1}	0.067	0.05	0.05	0.05	0.05
u_m	2.6	1.5	1.5	1.5	1.5
r_m	10	5	5	5	5
g	0.25	0.25	0.25	0.25	0.25
u_e	2.6	10	10	10	10
τ	0.7	0.9	0.9	0.9	0.9
λ_{H_2}	0.1	0.1	0.95	0.95	0.95
y_{H_2}	0.067	0.067	0.05	0.05	0.05
λ_{V_1}	0.5	0.95	0.95	0.95	0.95
λ_{V_2}	0.5	0.5	0.95	0.95	0.95
β_1	0.5	0.5	0.5	5	5
β_2	0.5	0.5	0.5	5	0.5
c	1	0.8	0.8	0.8	0.8

Table 5.2: *Values for parameters and variables of Model (5.3.2)*

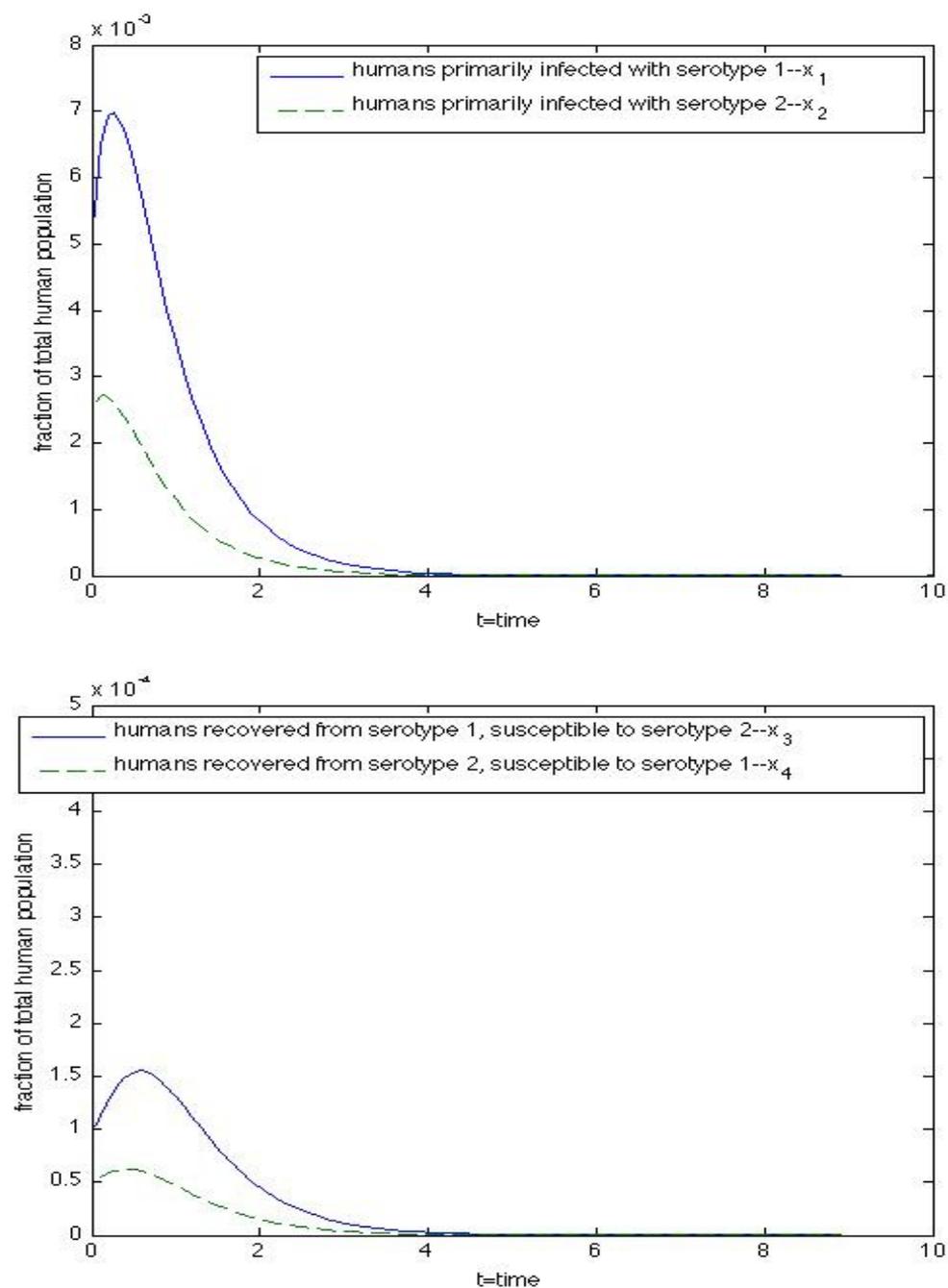


Figure 5.10: Solutions of system (5.3.2) converge to the DFE when $\mathcal{R}_0 = .25$; parameter values given in Table 5.2.

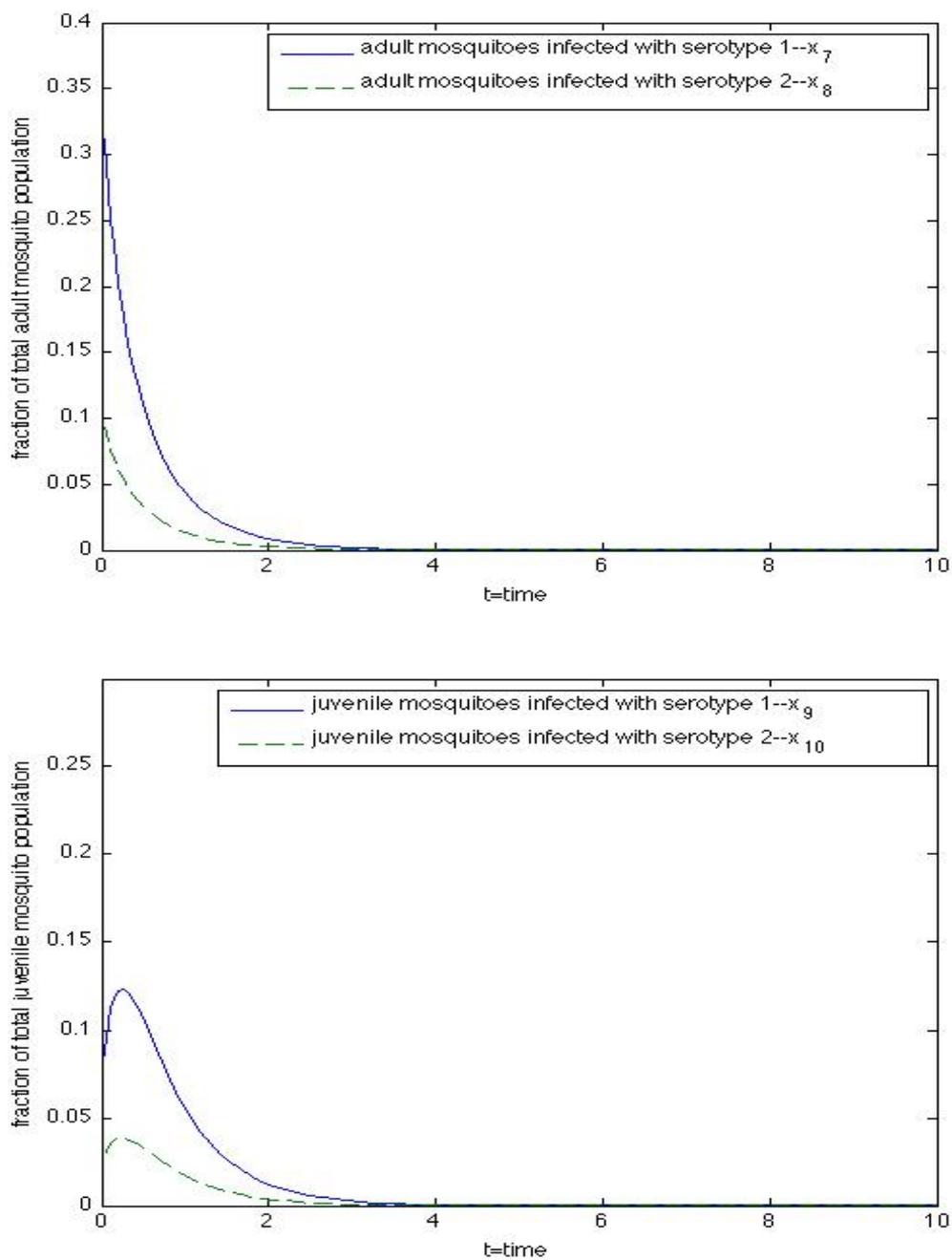


Figure 5.11: Solutions of system (5.3.2) converge to the DFE when $\mathcal{R}_0 = .25$; parameter values given in Table 5.2.

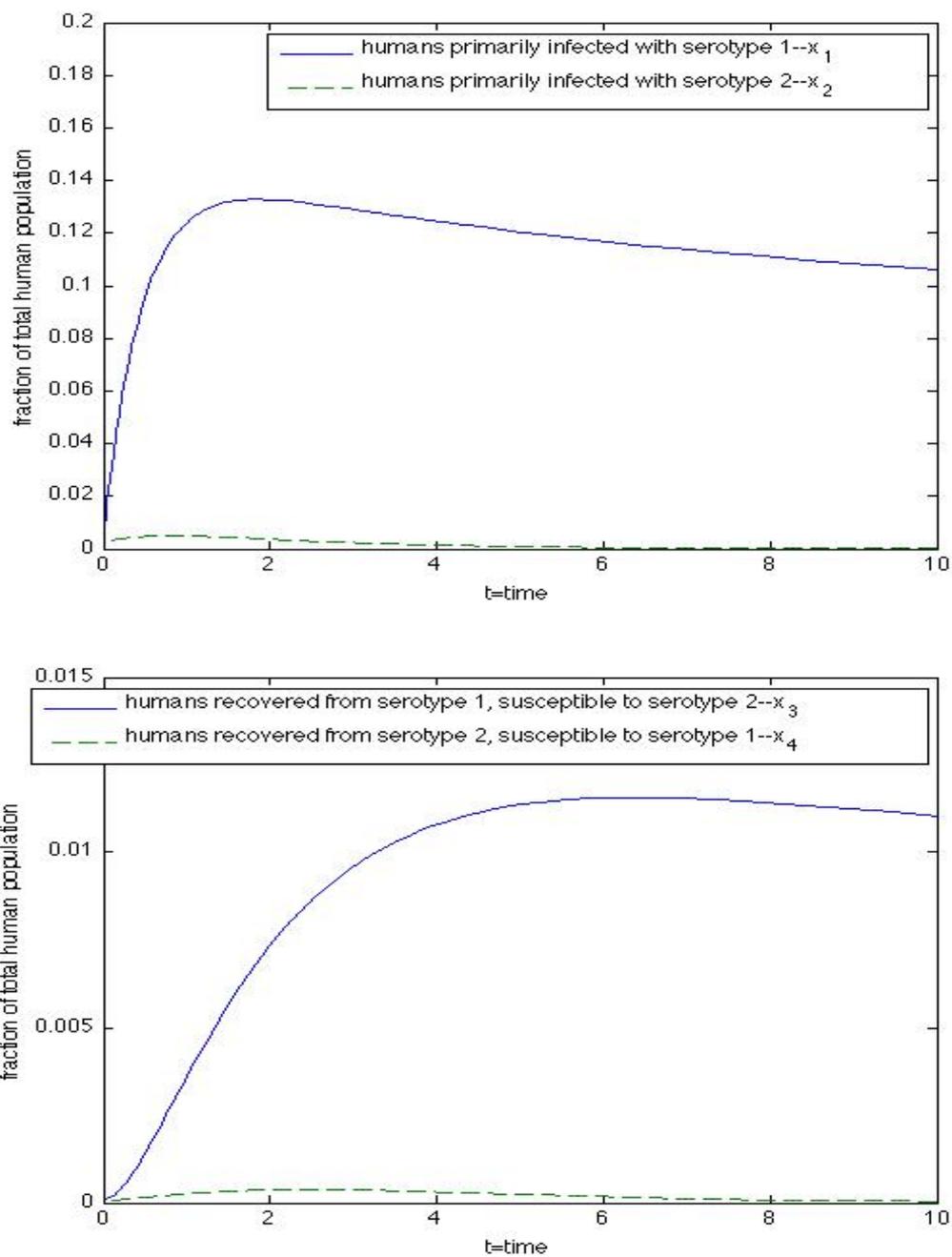


Figure 5.12: Solutions of system (5.3.2) converge to E_1 when $\mathcal{R}_1 = 1.08$, $\mathcal{R}_2 = .25$, $\beta_1 = \beta_2 = .5$; parameter values given in Table 5.2.

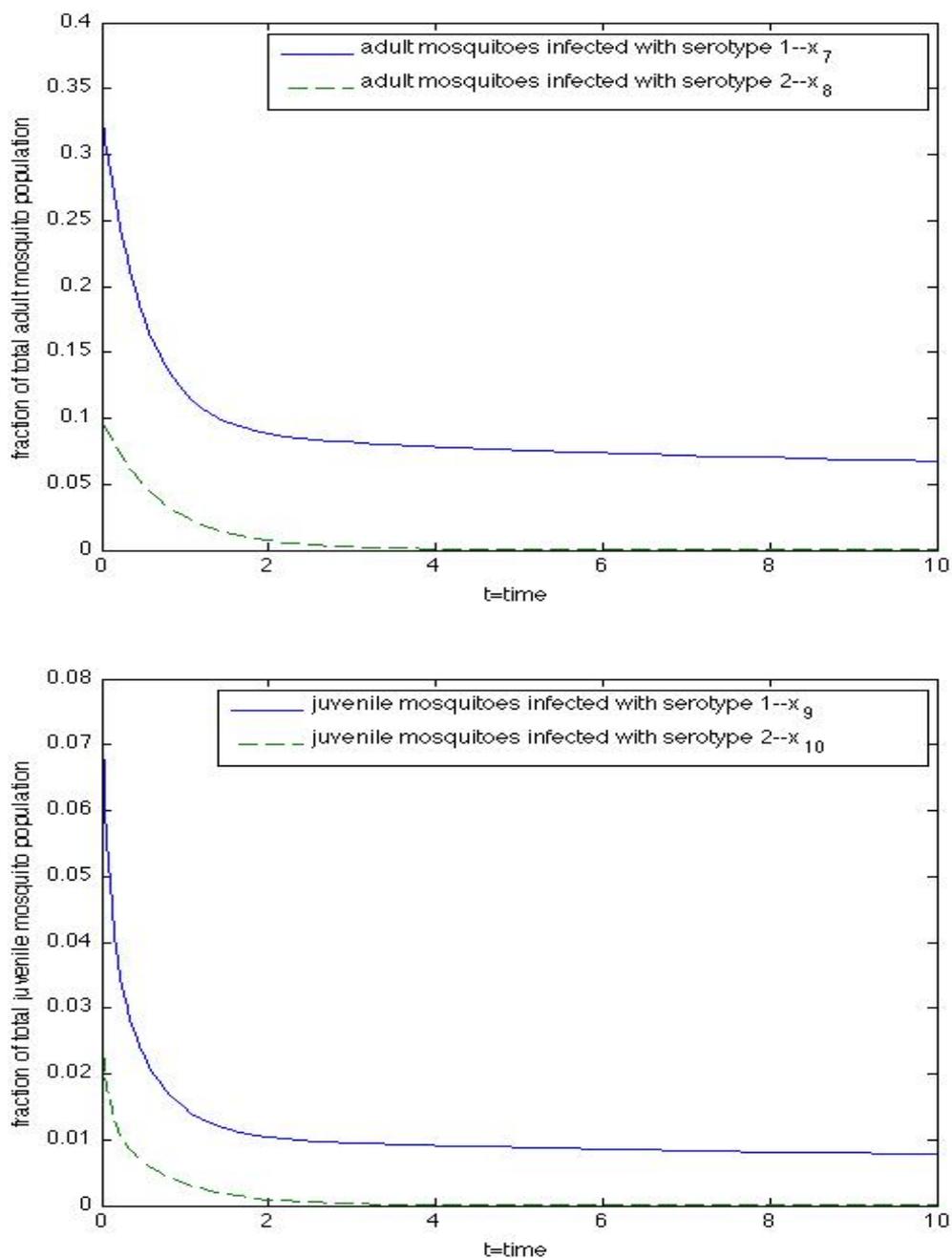


Figure 5.13: Solutions of system (5.3.2) converge to E_1 when $\mathcal{R}_1 = 1.08$, $\mathcal{R}_2 = .25$, $\beta_1 = \beta_2 = .5$; other parameter values given in Table 5.2.

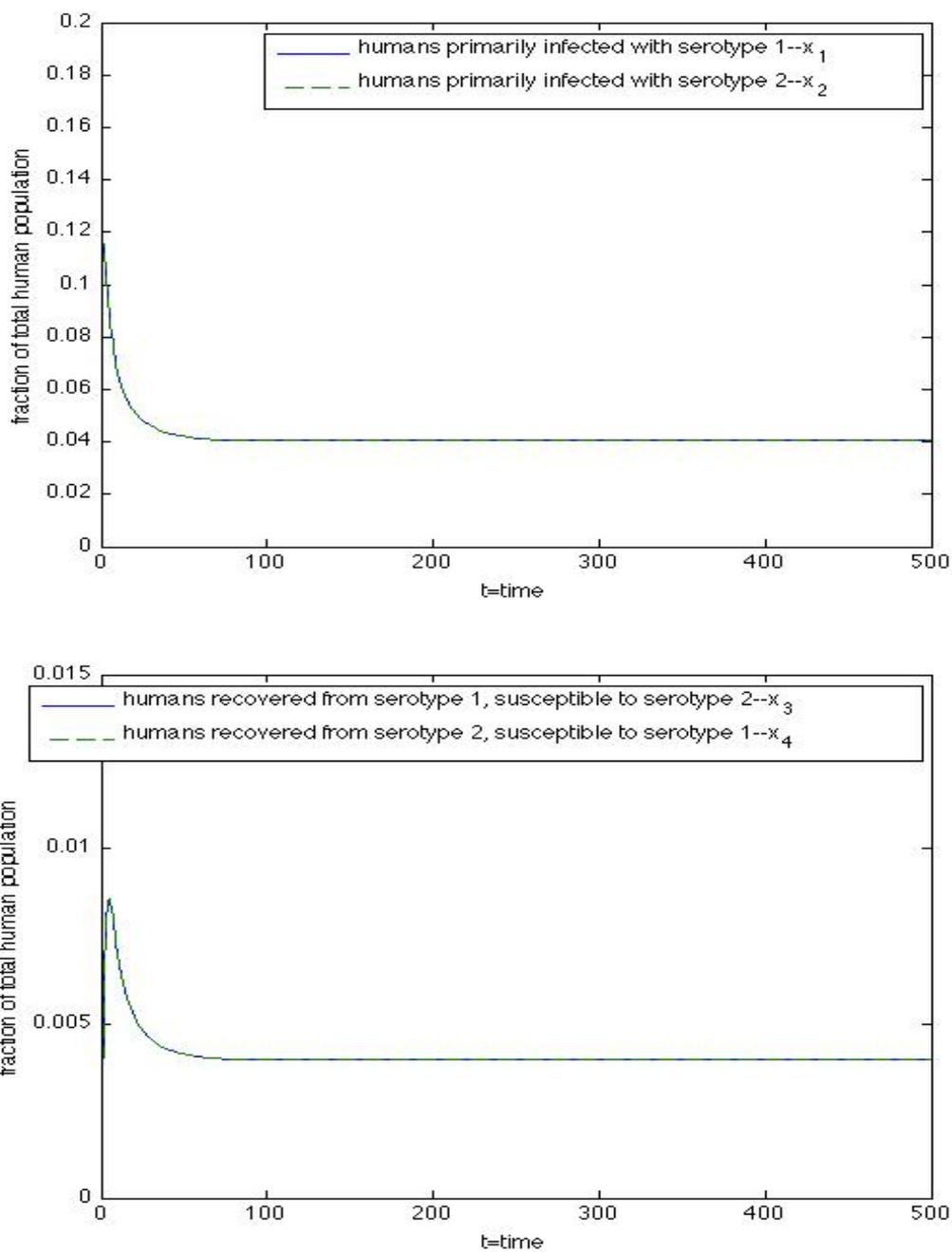


Figure 5.14: System (5.3.2) decouples when $\mathcal{R}_1 = 1.08$, $\mathcal{R}_2 = 1.08$, $\beta_1 = \beta_2 = .5$; other parameter values given in Table 5.2.

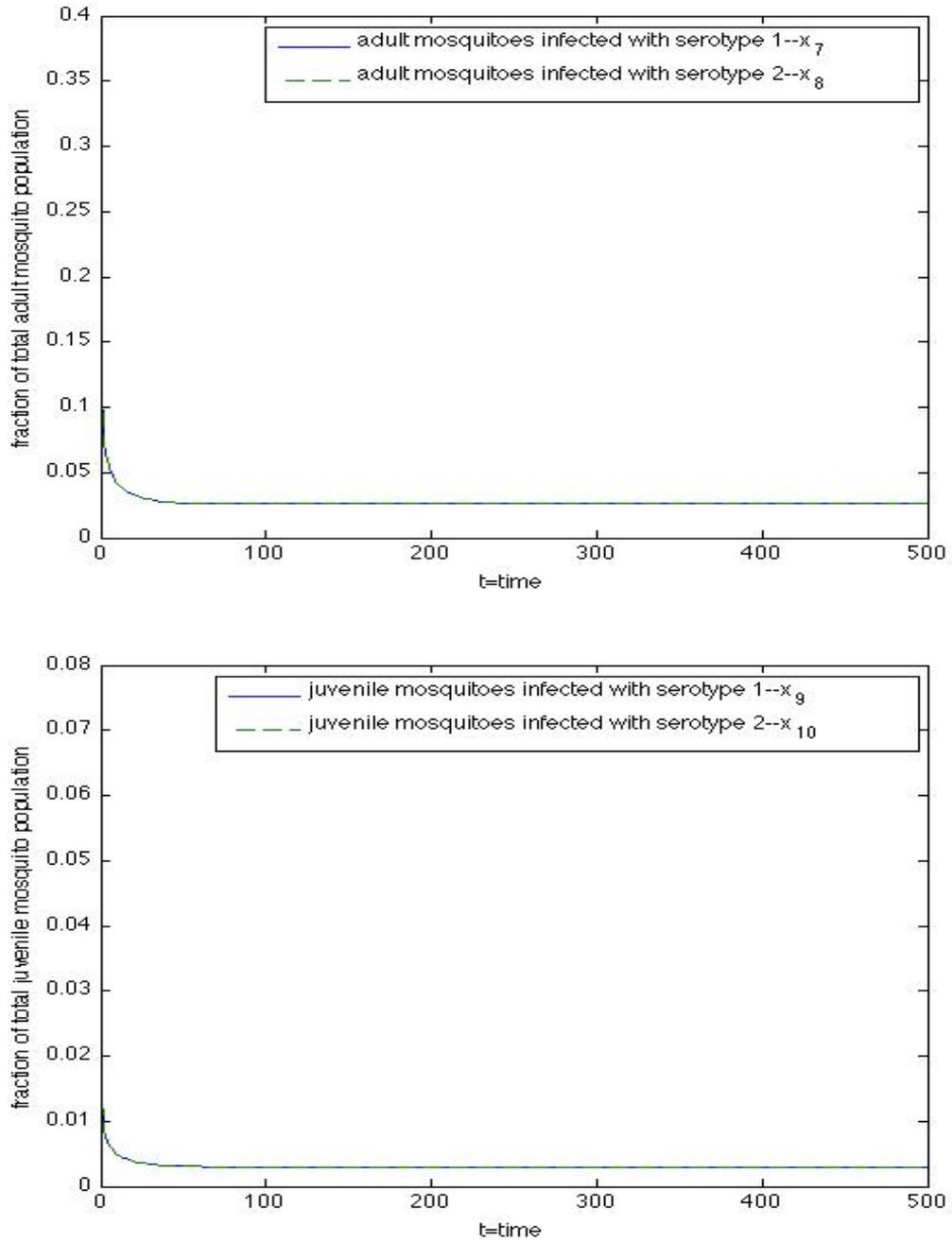


Figure 5.15: System (5.3.2) decouples when $\mathcal{R}_1 = 1.08$, $\mathcal{R}_2 = 1.08$, $\beta_1 = \beta_2 = .5$; other parameter values given in Table 5.2.

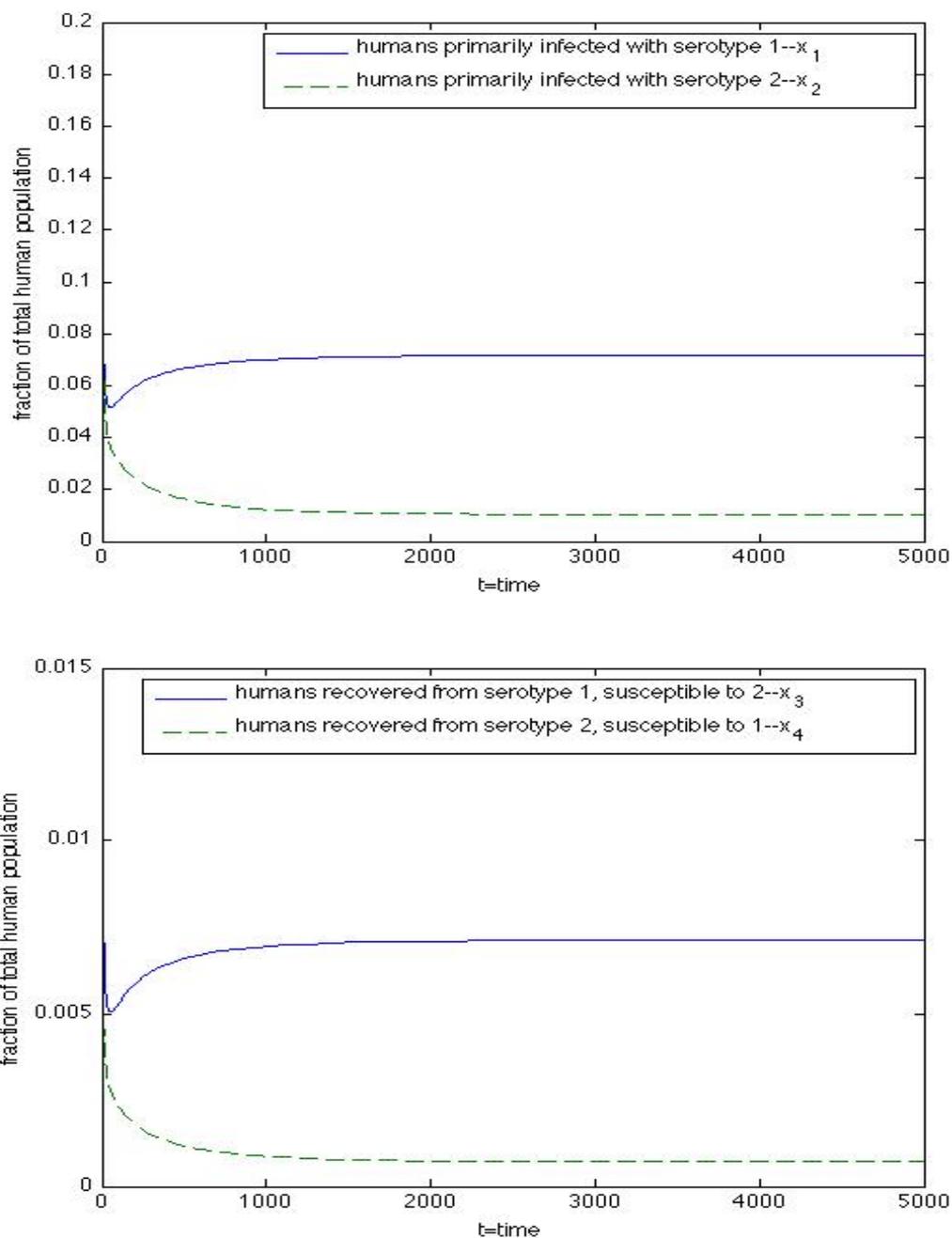


Figure 5.16: Solutions of system (5.3.2) converge to an endemic equilibrium when $\mathcal{R}_1 = 1.08$, $\mathcal{R}_2 = 1.08$, $\beta_1 = 5$, $\beta_2 = .5$; other parameter values given in Table 5.2.

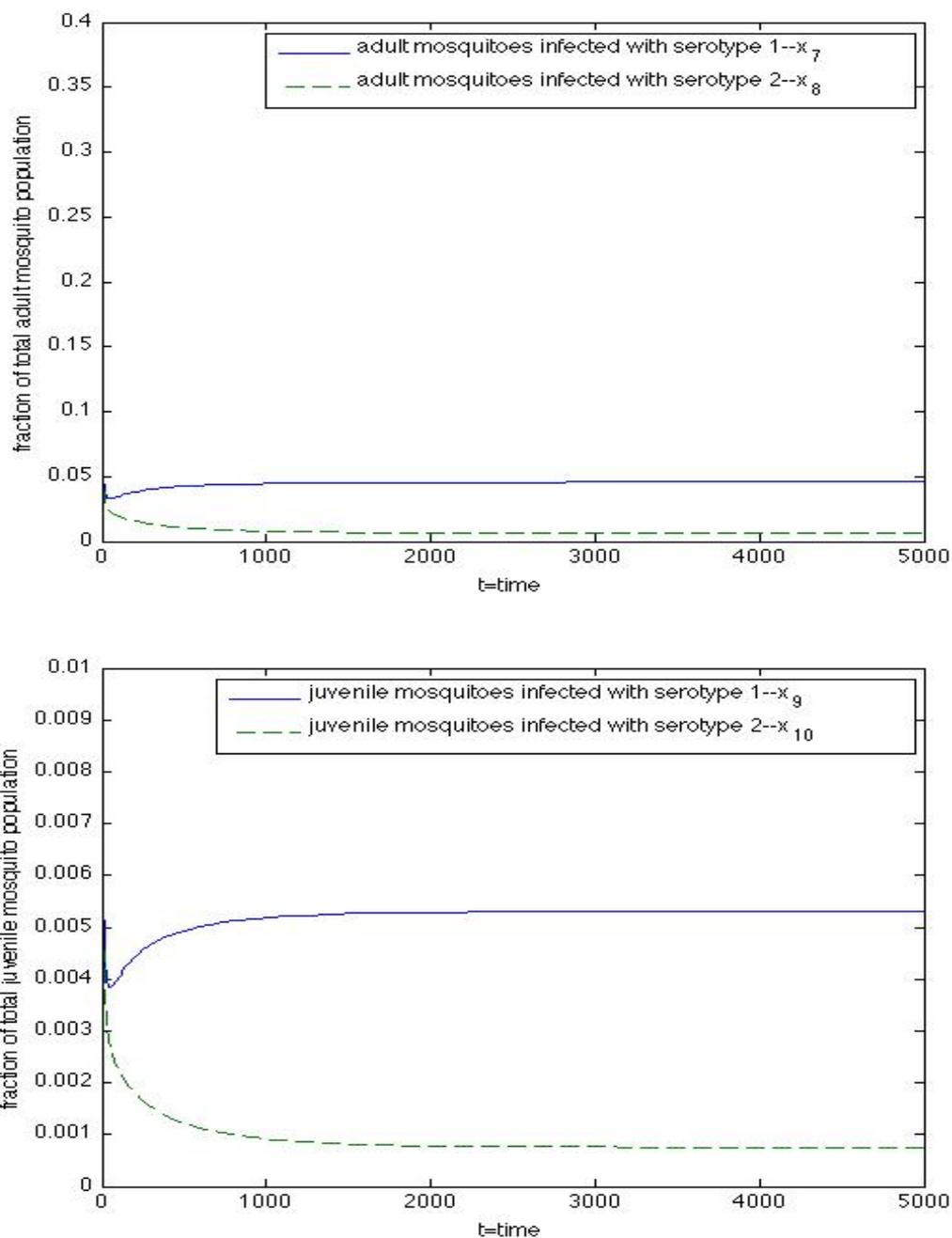


Figure 5.17: Solutions of system (5.3.2) converge to an endemic equilibrium when $\mathcal{R}_1 = 1.08$, $\mathcal{R}_2 = 1.08$, $\beta_1 = 5$, $\beta_2 = .5$; other parameter values given in Table 5.2.

Appendix I

The degree-four polynomial in the proof of Proposition 2.6 is given by:

$$f(x_4) =$$

$$(g^3 r^3 v_H y_H^2 \tau_1 \lambda_H + 2 g^3 r^3 v_H^2 y_H \tau_1 \lambda_H + g^3 r^3 v_H^3 \tau_1 \lambda_H) x_4^4 +$$

$$\begin{aligned} & g^2 (y_H + v_H) r^2 (r g p_1 v_H^3 + r v_H^2 g p_1 \lambda_H - 3 r v_H^2 g \tau_1 \lambda_H + r v_H^2 g y_H p_1 \\ & + r v_H g y_H p_1 \lambda_H - 3 r v_H g y_H \tau_1 \lambda_H + v_H^2 \tau_1 \lambda_H \lambda_v - v_H^2 \tau_1 \lambda_H p_1 \\ & + 2 v_H^2 \tau_1 \lambda_H u_m - v_H \lambda_v \lambda_H^2 \tau_1 - v_H \tau_1 \lambda_H y_H p_1 - v_H \tau_1 \lambda_H^2 p_1 + 2 v_H \tau_1 \lambda_H y_H u_m - \tau_1 \lambda_H^2 y_H p_1) x_4^3 + \end{aligned}$$

$$\begin{aligned} & (-6 g^3 r^3 v_H^2 y_H p_1 \lambda_H - 3 g^3 r^3 v_H y_H^2 p_1 \lambda_H + 2 \tau_1 \lambda_H^2 g^2 r^2 v_H^2 p_1 - r v_H g \lambda_v \lambda_H^2 \tau_1 u_m y_H + r v_H^2 g u_m y_H \tau_1 \lambda_H \lambda_v \\ & + 2 g^2 r^2 v_H \lambda_v \lambda_H^2 \tau_1 y_H - 2 g^2 r^2 v_H^2 y_H \tau_1 \lambda_H \lambda_v - g^2 r^2 v_H \lambda_v \lambda_H^2 p_1 y_H - g^2 r^2 v_H^2 \lambda_v \lambda_H p_1 y_H - \tau_1 \lambda_H^2 \lambda_v p_1 v_H g r y_H \\ & - v_H^2 \tau_1 \lambda_H \lambda_v p_1 g r y_H - \tau_1 \lambda_H^2 \lambda_v p_1 v_H^2 g r - r v_H^2 g \lambda_v \lambda_H^2 \tau_1 u_m + r g v_H^3 u_m \tau_1 \lambda_H \lambda_v - r v_H^2 g \lambda_v^2 \lambda_H^2 \tau_1 \\ & - 2 g^2 r^2 v_H^3 \tau_1 \lambda_H \lambda_v - g^2 r^2 v_H^2 \lambda_v \lambda_H^2 p_1 - g^2 r^2 v_H^3 \lambda_v \lambda_H p_1 - \tau_1 \lambda_H \lambda_v v_H^3 p_1 g r \\ & + 4 g^2 r^2 v_H^3 y_H p_1 u_m + 2 g^2 r^2 v_H^2 y_H^2 p_1 u_m - 6 g^3 r^3 v_H^3 y_H p_1 - 3 g^3 r^3 v_H^2 y_H^2 p_1 + 3 g^3 r^3 v_H y_H^2 \tau_1 \lambda_H \\ & + 2 g^2 r^2 v_H^2 \lambda_v \lambda_H^2 \tau_1 - 2 \tau_1 \lambda_H g r y_H^2 p_1 v_H u_m - 3 g^3 r^3 v_H^4 p_1 + 6 g^3 r^3 v_H^2 y_H \tau_1 \lambda_H + 3 g^3 r^3 v_H^3 \tau_1 \lambda_H \\ & + 4 \tau_1 \lambda_H^2 g^2 r^2 y_H p_1 v_H + 2 \tau_1 \lambda_H g^2 r^2 y_H^2 p_1 v_H + 4 \tau_1 \lambda_H g^2 r^2 y_H p_1 v_H^2 - 4 \tau_1 \lambda_H^2 g r y_H p_1 u_m v_H \\ & - 2 \tau_1 \lambda_H^2 g r y_H^2 p_1 u_m + 2 g^2 r^2 v_H y_H^2 p_1 \lambda_H u_m + 4 g^2 r^2 v_H^2 y_H p_1 \lambda_H u_m + 2 r v_H^2 g u_m^2 y_H \tau_1 \lambda_H \\ & - 4 g^2 r^2 v_H y_H^2 \tau_1 \lambda_H u_m - 8 g^2 r^2 v_H^2 y_H \tau_1 \lambda_H u_m + r v_H g u_m^2 y_H^2 \tau_1 \lambda_H - 4 \tau_1 \lambda_H g r y_H p_1 v_H^2 u_m \\ & + 2 \tau_1 \lambda_H^2 g^2 r^2 y_H^2 p_1 + 2 g^2 r^2 v_H^3 \tau_1 \lambda_H p_1 + 2 g^2 r^2 v_H^3 p_1 \lambda_H u_m + r g v_H^3 u_m^2 \tau_1 \lambda_H - 4 g^2 r^2 v_H^3 \tau_1 \lambda_H u_m \\ & - 2 \tau_1 \lambda_H g r v_H^3 p_1 u_m - 2 \tau_1 \lambda_H^2 g r v_H^2 p_1 u_m - 3 g^3 r^3 v_H^3 p_1 \lambda_H + 2 g^2 r^2 v_H^4 p_1 u_m) x_4^2 + \end{aligned}$$

$$\begin{aligned}
& (6g^3r^3v_H^2y_Hp_1\lambda_H + 3g^3r^3v_Hy_H^2p_1\lambda_H - \tau_1\lambda_H^2g^2r^2v_H^2p_1 + 2rv_H^2gu_m^2y_Hp_1\lambda_H + rv_Hgu_m^2y_H^2p_1\lambda_H \\
& - \tau_1\lambda_H^2u_m^2y_H^2p_1 - \tau_1\lambda_Hu_m^2y_H^2p_1v_H - 2\tau_1\lambda_Hu_m^2y_Hp_1v_H^2 + rgv_H^3u_m^2p_1\lambda_H - \tau_1\lambda_Hu_m^2v_H^3p_1 \\
& - \tau_1\lambda_H^2u_m^2v_H^2p_1 - 2\tau_1\lambda_H^2u_m^2y_Hp_1v_H + rv_Hg\lambda_v\lambda_H^2\tau_1u_m y_H - rv_H^2gu_m y_H\tau_1\lambda_H\lambda_v - g^2r^2v_H\lambda_v\lambda_H^2\tau_1y_H \\
& + g^2r^2v_H^2y_H\tau_1\lambda_H\lambda_v + 2g^2r^2v_H\lambda_v\lambda_H^2p_1y_H + 2g^2r^2v_H^2\lambda_v\lambda_Hp_1y_H + \tau_1\lambda_H^2\lambda_vp_1v_Hgr y_H \\
& + v_H^2\tau_1\lambda_H\lambda_vp_1gr y_H + \tau_1\lambda_H^2\lambda_vp_1v_H^2gr + rv_H^2g\lambda_v\lambda_H^2\tau_1u_m - rgv_H^3u_m\tau_1\lambda_H\lambda_v \\
& + rv_H^2g\lambda_v^2\lambda_H^2\tau_1 + g^2r^2v_H^3\tau_1\lambda_H\lambda_v + 2g^2r^2v_H^2\lambda_v\lambda_H^2p_1 + 2g^2r^2v_H^3\lambda_v\lambda_Hp_1 + \tau_1\lambda_H\lambda_vv_H^3p_1gr \\
& - rv_H^2g\lambda_v\lambda_Hp_1u_m y_H - rv_Hg\lambda_v\lambda_H^2p_1u_m y_H - \tau_1\lambda_H^2\lambda_vp_1v_Hu_m y_H - v_H^2\tau_1\lambda_H\lambda_vp_1u_m y_H - rv_H^2g\lambda_v\lambda_H^2p_1u_m \\
& - rgv_H^3\lambda_v\lambda_Hp_1u_m - \tau_1\lambda_H\lambda_vv_H^3p_1u_m - 8g^2r^2v_H^3y_Hp_1u_m - 4g^2r^2v_H^2y_H^2p_1u_m + 6g^3r^3v_H^3y_Hp_1 \\
& + 3g^3r^3v_H^2y_H^2p_1 + 2rgv_H^3u_m^2y_Hp_1 + rv_H^2gu_m^2y_H^2p_1 - g^3r^3v_Hy_H^2\tau_1\lambda_H - g^2r^2v_H^2\lambda_v\lambda_H^2\tau_1 \\
& + 2\tau_1\lambda_Hgr y_H^2p_1v_Hu_m + 3g^3r^3v_H^4p_1 - 2g^3r^3v_H^2y_H\tau_1\lambda_H - g^3r^3v_H^3\tau_1\lambda_H \\
& - 2\tau_1\lambda_H^2g^2r^2y_Hp_1v_H - \tau_1\lambda_Hg^2r^2y_H^2p_1v_H - 2\tau_1\lambda_Hg^2r^2y_Hp_1v_H^2 \\
& + 4\tau_1\lambda_H^2gr y_Hp_1u_m v_H + 2\tau_1\lambda_H^2gr y_H^2p_1u_m - 4g^2r^2v_Hy_H^2p_1\lambda_Hu_m - 8g^2r^2v_H^2y_Hp_1\lambda_Hu_m \\
& - 2rv_H^2gu_m^2y_H\tau_1\lambda_H + 2g^2r^2v_Hy_H^2\tau_1\lambda_Hu_m + 4g^2r^2v_H^2y_H\tau_1\lambda_Hu_m - rv_Hgu_m^2y_H^2\tau_1\lambda_H \\
& + 4\tau_1\lambda_Hgr y_Hp_1v_H^2u_m - \tau_1\lambda_H^2g^2r^2y_H^2p_1 - g^2r^2v_H^3\tau_1\lambda_Hp_1 - 4g^2r^2v_H^3p_1\lambda_Hu_m \\
& - rgv_H^3u_m^2\tau_1\lambda_H + 2g^2r^2v_H^3\tau_1\lambda_Hu_m + 2\tau_1\lambda_Hgr v_H^3p_1u_m \\
& + 2\tau_1\lambda_H^2gr v_H^2p_1u_m + 3g^3r^3v_H^3p_1\lambda_H - 4g^2r^2v_H^4p_1u_m + rgv_H^4u_m^2p_1 - \tau_1\lambda_H^2\lambda_vp_1v_H^2u_m)x_4 \\
& - rgp_1v_H(y_H + v_H)(\lambda_H + v_H)(rg - u_m)(rgy_H + rv_Hg + \lambda_v\lambda_H - u_my_H - v_Hu_m)
\end{aligned}$$

Bibliography

- [1] *Centers for Disease Control and Prevention*, <http://www.cdc.gov/Dengue>. [cited April 23, 2010].
- [2] *Dengue signs and clinical symptoms*, CBWInfo.com, <http://www.cbwinfo.com/Biological/Pathogens/DENV.html>. [cited April 23, 2010].
- [3] *Dengue Virus Net*, <http://www.denguevirusnet.com/signs-a-symptoms.html>. [cited April 23, 2010].
- [4] *World Health Organization*, <http://www.who.int/topics/dengue/en>. [cited April 23, 2010].
- [5] *Matrix theory and applications*, Proceedings of Symposia in Applied Mathematics, vol. 40, American Mathematical Society, Providence, RI, 1990. Lecture notes prepared for the American Mathematical Society Short Course held in Phoenix, Arizona, January 10–11, 1989, Edited by Charles R. Johnson, AMS Short Course Lecture Notes.
- [6] *Classification*, Medical Microbiology (1996), 213–261.
- [7] G. Butler, H.I. Freedman, and P. Waltman, *Uniformly persistent systems*, Proc. Amer. Math. Soc. **96** (1986), no. 3, 425–430.
- [8] F.A.B. Coutinho, M.N. Burattini, L.F. Lopez, and E. Massad, *Threshold conditions for a non-autonomous epidemic system describing the population dynamics of dengue*, Bull. Math. Biol. **68** (2006), no. 8, 2263–2282.
- [9] D.A.T. Cummings, R.A. Irizarry, N.E. Huang, T.P. Endy, A. Nisalak, K. Ungchusak, and D.S. Burke, *Travelling waves in the occurrence of dengue haemorrhagic fever in Thailand*, Nature **427** (2004), no. 6972, 344–347.
- [10] J.P. Cunha and M.C. Stoppler, *Dengue fever*, MedicineNet.com, http://www.medicinenet.com/dengue_fever/article.htm. [cited April 23, 2010].
- [11] L. Esteva and C. Vargas, *A model for dengue disease with variable human population*, J. Math. Biol. **38** (1999), no. 3, 220–240.
- [12] ———, *Coexistence of different serotypes of dengue virus*, J. Math. Biol. **46** (2003), no. 1, 31–47.
- [13] C. Favier, N. Degallier, M.A. Dubois, J.C. Boulanger, C.E. Menkes, L. Torres, et al., *Dengue epidemic modeling: stakes and pitfalls*, Asia Pacific Biotech News **9** (2005), no. No. 22, 1191–1194.
- [14] C. Favier, D. Schmit, C.D.M. Muller-Graf, B. Cazelles, N. Degallier, B. Mondet, and M.A. Dubois, *Influence of spatial heterogeneity on an emerging infectious disease: the case of dengue epidemics*, Proceedings of the Royal Society B: Biological Sciences **272** (2005), no. 1568, 1171–1177.

- [15] Z. Feng and J.X. Velasco-Hernandez, *Competitive exclusion in a vector-host model for the dengue fever*, J. Math. Biol. **35** (1997), no. 5, 523–544.
- [16] M. Fiedler, *Special matrices and their applications in numerical mathematics*, Springer, 1986.
- [17] R.A. Fisher and J.H. Bennett, *The genetical theory of natural selection: a complete variorum edition*, Oxford University Press, USA, 1999.
- [18] T. Fujimoto and R.R. Ranade, *Two characterizations of inverse-positive matrices: the Hawkins-Simon condition and the Le Chatelier-Braun principle*, Electronic Journal of Linear Algebra **11** (2004), 59–65.
- [19] D.O. Fuller, A. Troyo, and J.C. Beier, *El Niño Southern Oscillation and vegetation dynamics as predictors of dengue fever cases in Costa Rica*, Environmental Research Letters **4** (2009), 1–8.
- [20] D.J. Gubler, *Dengue*, The arboviruses: epidemiology and ecology **2** (1986), 213–261.
- [21] ———, *Dengue and dengue hemorrhagic fever*, Clinical microbiology reviews **11** (1998), no. 3, 480–496.
- [22] K.P. Hadeler and M.A. Lewis, *Spatial dynamics of the diffusive logistic equation with a sedentary compartment*, Canadian Appl. Math. Quart **10** (2002), 473–499.
- [23] J.K. Hale and H. Koçak, *Dynamics and bifurcations*, Texts in Applied Mathematics, vol. 3, Springer-Verlag, New York, 1991.
- [24] S.B. Halstead, D.J. Gubler, and G. Kuno, *Dengue and dengue hemorrhagic fever*, Handbook of Zoonoses (1994), 89–99.
- [25] D. Harper, *Online Etymology Dictionary*, <http://www.etymonline.com/index.php?search=dengue&searchmode=none>, 2001. [cited April 23, 2010].
- [26] M.W. Hirsch and H. Smith, *Monotone dynamical systems*, <http://math.cts.nthu.edu.tw/Mathematics/english/lecnotes/2006/MonotoneDynamics.pdf>, 2004.
- [27] P. Hochedez, S. Jaureguiberry, M. Debruyne, P. Bossi, P. Hausfater, G. Brucker, F. Bricaire, and E. Caumes, *Chikungunya infection in travelers*, Emerging infectious diseases **12** (2006), no. 10, 1565–1567.
- [28] R.A. Horn and C.R. Johnson, *Topics in matrix analysis*, Cambridge University Press, Cambridge, 1994. Corrected reprint of the 1991 original.
- [29] B. Kim, *Computing traveling-wave front solutions in a diffusive predator-prey model*, University of Michigan, REU Program, <http://www.math.lsa.umich.edu/undergrad/REU/ArchivedREUpapers/reu2004.pdf>, 2004.
- [30] M. Kot, *Elements of mathematical ecology*, Cambridge University Press, Cambridge, 2001.
- [31] M. Lewis, J. Renclawowicz, and P. van den Driessche, *Traveling waves and spread rates for a West Nile virus model*, Bull. Math. Biol. **68** (2006), no. 1, 3–23.
- [32] B. Li, H.F. Weinberger, and M.A. Lewis, *Spreading speeds as slowest wave speeds for cooperative systems*, Math. Biosci. **196** (2005), no. 1, 82–98.
- [33] Y. Lou and X.Q. Zhao, *A climate-based malaria transmission model with structured vector population*, SIAM Journal on Applied Mathematics **70** (2010), 2023–2044.

- [34] P. Magal, *Perturbation of a globally stable steady state and uniform persistence*, J. Dynam. Differential Equations **21** (2009), no. 1, 1–20.
- [35] P. Magal and X.Q. Zhao, *Global attractors and steady states for uniformly persistent dynamical systems*, SIAM J. Math. Anal. **37** (2005), no. 1.
- [36] N.A. Maida and H.M. Yang, *Describing the geographic spread of dengue disease by traveling waves*, Math. Biosci. **215** (2008), no. 1, 64–77.
- [37] CCC Newsdesk, *Brazil tunes in to climate change issues*, ClimateChangeCorp (March 2007).
- [38] L. Perko, *Differential equations and dynamical systems*, Third, Texts in Applied Mathematics, vol. 7, Springer-Verlag, New York, 2001.
- [39] A. Rivero, P. Agnew, S. Bedhomme, C. Sidobre, and Y. Michalakis, *Resource depletion in Aedes aegypti mosquitoes infected by the microsporidia Vavraia culicis*, Parasitology **134** (2007), no. 10, 1355–1362.
- [40] S. Ruan and J. Wu, *Modeling spatial spread of communicable diseases involving animal hosts*, Spatial Ecology (2009), 293–316.
- [41] K.J. Ryan, C.G. Ray, and J.C. Sherris, *Sherris medical microbiology: an introduction to infectious diseases*, McGraw-Hill Medical, 2004.
- [42] M. Schechter, *Principles of functional analysis*, Second, Graduate Studies in Mathematics, vol. 36, American Mathematical Society, Providence, RI, 2002.
- [43] R. Siegel, *Flavivirus*, www.stanford.edu/group/virus/1999/asb-flavi/overview.html. [cited April 23, 2010].
- [44] H. L. Smith, *Monotone dynamical systems*, Mathematical Surveys and Monographs, vol. 41, American Mathematical Society, Providence, RI, 1995. An introduction to the theory of competitive and cooperative systems.
- [45] R. V. Southcott, *Cleland, Sir John Burton (1878 - 1971)*, Australian Dictionary of Biography **8** (1981), 23–25.
- [46] M. Sriprom, P. Barbazan, and I. M. Tang, *Destabilizing effect of the host immune status on the sequential transmission dynamic of the dengue virus infection*, Math. Comput. Modelling **45** (2007), no. 9-10, 1053–1066.
- [47] L.T. Takahashi, N.A. Maida, W. Castro Ferreira Jr., P. Pulino, and H.M. Yang, *Mathematical models for the Aedes aegypti dispersal dynamics: travelling waves by wing and wind*, Bull. Math. Biol. **67** (2005), no. 3, 509–528.
- [48] K.B. Tan, H.L. Koh, A.M.I. Izani, and S.Y. (2008) Teh, *Modeling mosquito population with temperature effects*, Penang, Malaysia, 2008.
- [49] M.G. Teixeira, M.C.N. Costa, M.L.B. Lima, and E. Mota, *Dengue and dengue hemorrhagic fever epidemics in Brazil: what research is needed based on trends, surveillance, and control experiences?*, Cad. Saúde Pública **21** (2005), 1307–1315.
- [50] U. Thavara, A. Tawatsin, C. Chansang, W. K-ngamsuk, S. Paosriwong, J. B-Long, Y. Rongsriyam, and N. Komalamisra, *Larval occurrence, oviposition behavior and biting activity of potential mosquito vectors of dengue on Samui Island, Thailand*, J. Vect. Ecol. **26** (2001), 178–180.

- [51] K.M. Tomashek, *Dengue fever (DF) and dengue hemorrhagic fever (DHF)*, CDC Health Information for International Travel 2010 (2009).
- [52] P. van den Driessche and J. Watmough, *Reproduction numbers and sub-threshold endemic equilibria for compartmental models of disease transmission*, Math. Biosci. **180** (2002), 29–48. John A. Jacquez memorial volume.
- [53] A.I. Volpert, A. Vitaly Volpert, and A. Vladimir Volpert, *Traveling wave solutions of parabolic systems*, Translations of Mathematical Monographs, vol. 140, American Mathematical Society, Providence, RI, 1994. Translated from the Russian manuscript by James F. Heyda.
- [54] W. Wang and X.Q. Zhao, *Threshold dynamics for compartmental epidemic models in periodic environments*, J. Dynam. Differential Equations **20** (2008), no. 3, 699–717.
- [55] H/ F. Weinberger, Mark A. Lewis, and B. Li, *Analysis of linear determinacy for spread in cooperative models*, J. Math. Biol. **45** (2002), no. 3, 183–218.
- [56] E. W. Weisstein, *MathWorld—A Wolfram Web Resource*, Wolfram Research, Inc., <http://mathworld.wolfram.com/Resultant.html>. [cited April 23, 2010].
- [57] M. Whiteside, T.S. Willis, and P. G-Fort, *Dengue fever reemergence in Florida*, HIV CareLink, A Newsletter for HIV/AIDS Primary Care Provider **11** (March 2010), no. 1.
- [58] C. Zettel and P. Kaufman, *Featured Creatures*, University of Florida’s Institute of Food and Agricultural Sciences, <http://entnemdept.ufl.edu/creatures/aquatic/aedesaegypti>. [cited April 23, 2010].
- [59] F. Zhang and X.Q. Zhao, *A periodic epidemic model in a patchy environment*, J. Math. Anal. Appl. **325** (2007), no. 1, 496–516.
- [60] W. Zhang, S.Q. Shen, and Z.Z. Han, *Sufficient conditions for Hurwitz stability of matrices*, Latin American applied research **38** (2008), 253–258.
- [61] X.Q. Zhao, *Global asymptotic behavior in a periodic competitor-competitor-mutualist parabolic system*, Nonlinear Anal. **29** (1997), no. 5, 551–568.